MEASUREMENT AND PREDICTION OF FREEZING RATES

submitted by

PETER BARNES

In fulfilment of the requirements for a

DOCTORATE OF PHILOSOPHY

UNIVERSITY OF ASTON IN BIRMINGHAM

October 1977.

MEASUREMENT AND PREDICTION OF FREEZING RATES.

PETER BARNES DOCTORATE OF PHILOSPHY 1977.

SUMMARY.

This research has developed an experimental method to measure frozen phase thickness of liquids, based on the density differences between the frozen and unfrozen phases and compared experimental freezing rates with rates predicted by theoretical methods, including those of Planck, Neumann and Goodman.

Freezing rate experiments produced ice thicknesses from 6 mm to 30 mm of distilled water, grapefruit juice and 5 and 10 per cent sodium chloride solutions with initial temperatures between 3.5 and 25 C, coolant temperatures between -4 and -16 C and with heat transfer coefficient values of 2000, 1700, 900 and 56.8 W/m^2C. Accurate values of the heat transfer coefficient were determined by initial experimental work.

A literature survey, although revealing many theoretical methods for predicting freezing times of liquids, alloys and watery foodstuffs, found that only in a few cases had comparison between theoretical and experimental results been made and in these cases agreement was generally poor. The theoretical methods used restrictive assumptions to simplify the moving boundary and heat conduction equations and showed wide variations (e.g. 100%) in predicted freezing times which precluded the choice of any as obviously accurate.

A finite difference method of Vasil'ev and Uspenskii was modified to predict to within 8% the freezing times of distilled water.

The freezing rates of electrolyte solutions, under conditions of low freezing rates (0.0012 mm/s), were found to be less than those of distilled water due to the formation of a layer of high solute concentration adjacent to the interface which lowered the solution freezing point. Incorporation of this effect into the Vasil'ev and Uspenskii method predicted electrolyte solution freezing rates to within 15%.

Conduction, phase change, freezing, preservation.

ACKNOWLEDGEMENTS

The author would like to thank Dr. M. C. Jones for his advice and encouragement given throughout the duration of this work and Mrs. S. Shanks and Mrs. P. Barnes for typing the thesis.

CONTENTS.

LIST OF FIGURES.

Figures in main text.(Continued) Page.

Figures in Appendices. Page.

Figures in appendices (Continued) Page.

NOMENCLATURE.

Symbols used in main text.

Symbol	Term	Units.
TA	ambient temperature	C
TI	initial temperature	C
Tc	coolant temperature	C
Tm	freezing point temperature.	C
Ts	surface temperature	C
Ta	temperature at axis of symmetry.	C
H	heat transfer coefficient.	W/m^2C
HG	heat gain coefficient	W/m^2C
X	ice thickness	m
t	time	S
k	time step length	S
h	distance step length	m
C_1	thermal capacity of frozen phase.	J/kgC
C_2	thermal capacity of unfrozen phase.	J/kgC
K_1	thermal conductivity of frozen phase.	W/mC
K_2	thermal conductivity of unfrozen phase.	W/mC
α_1	thermal diffusivity of frozen phase.	m^2/s

Symbol.	Term.	Units.
α_2	thermal diffusivity of unfrozen phase.	m^2/s
ρ_1	frozen density.	kg/m^3
ρ_2	unfrozen density.	kg/m^3
D	thermal diffusivity of NaCl.	m^2/s
L	latent heat.	J/kg

Symbols used in specific sections.

Chapter 7.		Units.
$\bar{C}\infty$	Bulk liquid solute concentration.	$kmol/m^3$
$\bar{C}i$	Liquid solute interface concentration.	"
$\bar{C}_1$	Frozen phase solute concentration.	"
$\bar{C}_2$	Liquid phase solute concentration.	"

Appendix 3.		
TD	Steady state heat transfer disc temperature.	C
TB	Final offset temperature of aluminium bar.	C
Cp	Specific heat of aluminium.	

Appendix 4-4 (Vasil'ev and Uspenskii method).		
V	Temperature in unfrozen phase.	C
W	Temperature in frozen phase.	C

CHAPTER 1

INTRODUCTION

The aim of the research described in this thesis was to establish a practical working formula to predict accurately the position of the freezing interface in a pure liquid or electrolyte solution undergoing solidification. This involved solution of the transient heat transfer equations describing freezing, and comparison with experiments. The analysis required prediction of the temperature profiles in the frozen and liquid phases, and, in the case of freezing electrolytes, knowledge of concentration profiles set up by the advancing interface.

Practical cases involving heat transfer with a phase change include the casting of metals, freezing and thawing of soil, preservation of blood and freezing of aqueous solutions and foodstuffs which this research concentrates on.

Accurate knowledge about the freezing of foodstuffs is important to the food industry because the quality of the frozen product is effected by the rate of freezing (it is generally agreed that the faster the rate of freezing the better the quality (86-88) and, freezing installations of optimum sizes can only be built with accurate knowledge of freezing rates. (44)

The overall freezing operation which involves reducing the initial temperature of the material to its frozen storage temperature can be split into four stages:- (see figure 1-1)

(1) Precooling.

(2) Subcooling (sometimes referred to as supercooling in literature (70).

(3) Freezing.

(4) Tempering.

During the precooling period the temperature of the material is reduced until its surface temperature is at its freezing point. The rate of heat transfer depends on the heat transfer coefficient, area exposed, temperature difference and time. The precooling stage, like the subcooling stage, usually occupies only a small part (1-2%) of the overall freezing time. Subcooling of the liquid phase below its freezing point occurs to some degree in all materials and is related to, among other factors, the rate of crystallisation. The effect of subcooling is usually neglected in analysis of freezing problems. (86). Studies of subcooling and nucleation are given in references (73, 74, 100-103).

Figure 1-1
Typical time - temperature curves for:
(a) Water
(b) Aqueous solutions

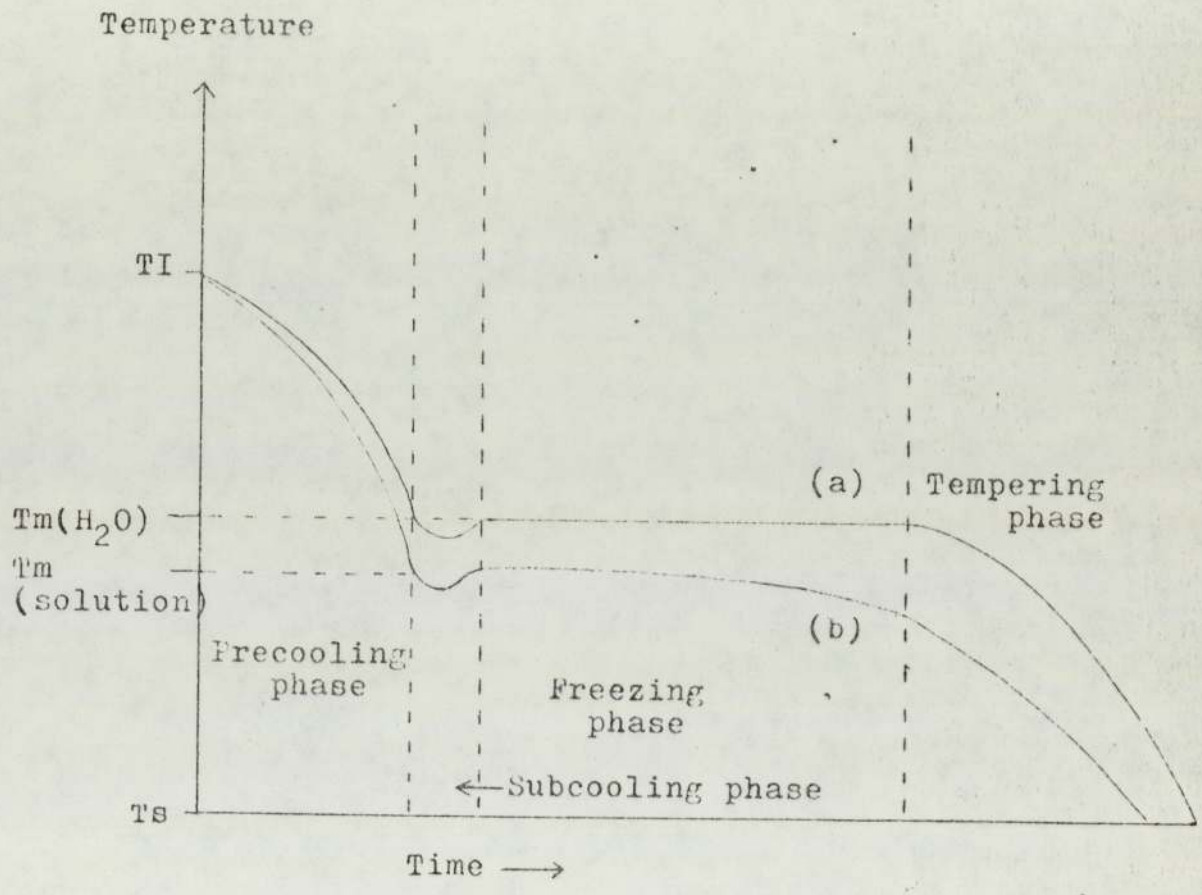

Schematic diagram only - time scales are different for two curves (a) & (b)

Due to the high value of the latent heat of fusion of water compared to the specific heats of water and ice the freezing stage occupies the vast majority of the process time in the overall freezing operation.

The freezing stage is represented by a plateau on the freezing curve. It is during this stage that the frozen-unfrozen interface traverses the body being frozen and the latent heat of fusion released at the interface is conducted to the coolant across an increasing thickness of frozen product. (86). The rate at which the latent heat can be conducted across the frozen phase is usually the rate controlling step in commercial food freezing systems. (88).

The tempering stage reduces the body to the storage temperature. For foodmaterials the storage temperature is generally -18 C to -20 C. (89). (Details of problems encountered with the freezing preservation of foods are given in appendix 7).

In general a pure liquid freezes at a constant temperature whilst aqueous solutions and liquid mixtures freeze over a range of temperatures (see figure 1-1) giving solid and liquid phases of different compositions. With most foods 90% of the water is frozen by -5 C. (90).

Freezing occurs at different rates at different positions in a body (4). The point cooling most slowly is referred to as the 'thermal centre' of the body. The thermal centre is used by food technologists to define freezing time as the time for the thermal centre to fall through the zone of maximum crystal formation (0 to -5 C) (88). If this time is less than two hours, then the term 'commercially quick frozen' is used

The requirements of a practically useful predictive freezing method for estimating freezing times are that the method should :

1. Be quick and practical.
2. Include the effect of the heat transfer coefficient between the coolant and material being frozen.
3. Be able to handle freezing from well above the freezing point.
4. Be supported by experimental results.
5. Be applicable to materials that exhibit a freezing point range.
6. Predict the time for the total freezing operation (i.e. time from initial temperature to storage temperature).
7. Apply to irregular-shaped materials.

Predictive methods for estimating freezing times have been studied by many workers (1 - 80) generally the methods assume the following conditions:

1. Initial uniform temperature of material being frozen.
2. Constant coolant temperature. .
3. Material has constant thermal conductivity and specific heat (different for the two phases).
4. A density which does not vary with temperature or alter during the freezing process.
5. A definite freezing point at which latent heat is liberated.
6. Heat transfer is in one direction only.
7. Heat transfer within the watery solid is by conduction with a convective boundary condition. (Convective heat transfer in the body is neglected).

With the above assumptions we obtain the following governing equations for a freezing model in which the subscripts 1 and 2 refer to the frozen and unfrozen phases respectively.

(The model is diagramatically shown in figure 1-2 and derived in appendix 6).

Conduction equations:-

Phase 1
$$\frac{\partial T_1}{\partial t} = \alpha_1 \frac{\partial^2 T_1}{\partial x^2} \qquad (1\text{-}1)$$

Phase 2
$$\frac{\partial T_2}{\partial t} = \alpha_2 \frac{\partial^2 T_2}{\partial x^2} \qquad (1\text{-}2)$$

Boundary conditions: at frozen-unfrozen interface x=X(t)

$$-L\rho \frac{dX}{dt} = -K_1 \left(\frac{\partial T_1}{\partial x}\right)_X + K_2 \left(\frac{\partial T_2}{\partial x}\right)_X \qquad (1\text{-}3)$$

$$T_1 = T_2 = Tm \qquad (1\text{-}4)$$

: at coolant surface x = o

$$H(Tc - Ts) = -K_1 \left(\frac{\partial T_1}{\partial x}\right)_{x=o} \qquad (1\text{-}5)$$

: at the axis of symmetry

$$\left(\frac{\partial T_2}{\partial x}\right) = 0 \quad \text{at } x = a \qquad (1\text{-}6)$$

Figure 1 - 2 1 - Dimensional Freezing.

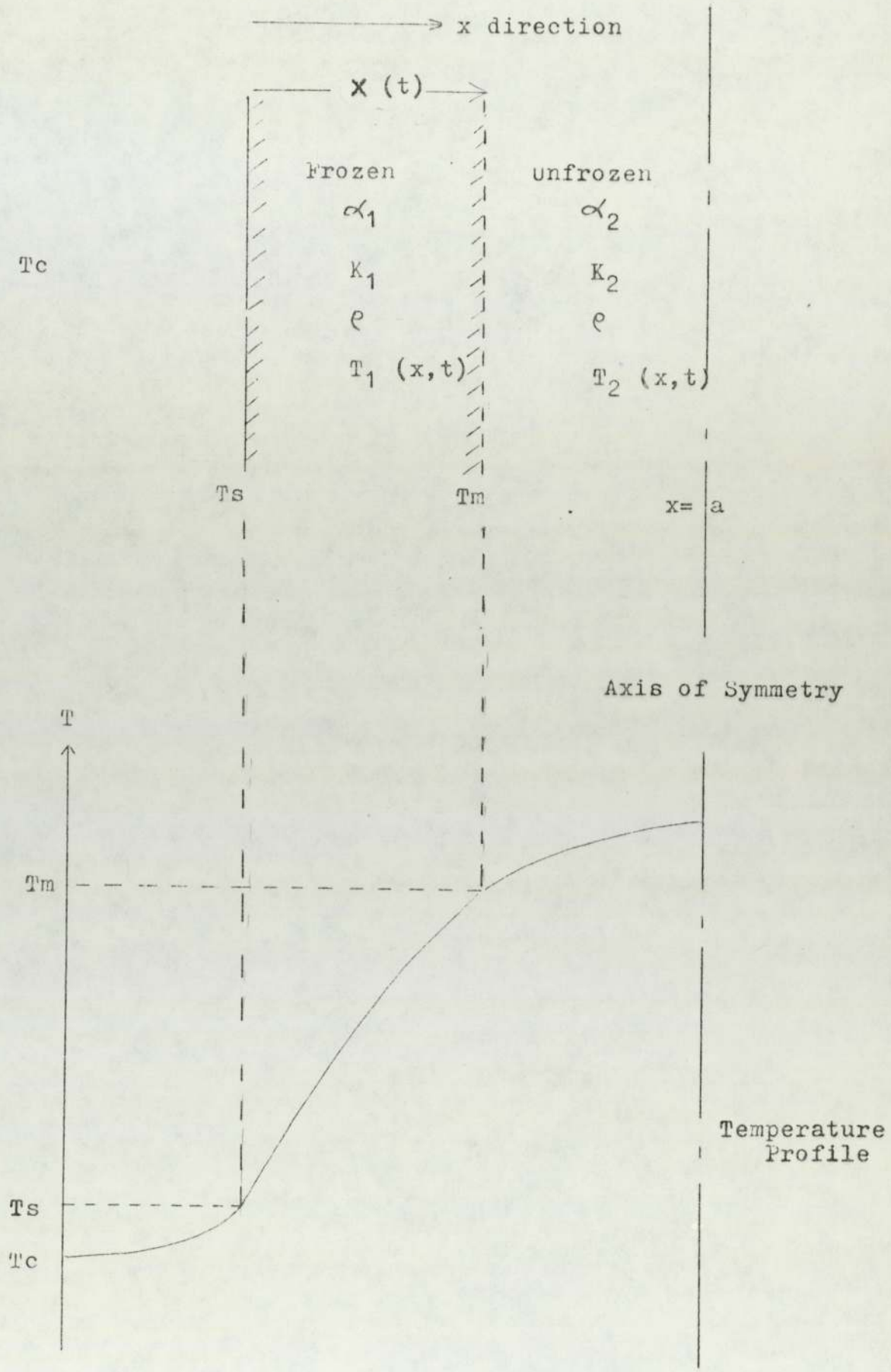

Initial conditions are:

$$X(t) = o \quad \text{at} \quad t = o \tag{1-7}$$

$$T_2 = f(x) \quad \text{at} \quad t = o \tag{1-8}$$

The set of equations (1-1) to (1-8) has no general solution, and thus, there is no single analytical formula that can be used to calculate freezing rates in all cases. Practical freezing problems may be more complicated than equations (1-1) to (1-8) due to the simplifying assumptions given on page 6.

Since there is no exact analytical solution to the simplest freezing problems, we are forced to consider approximate solutions. The approximations can be split into analytical solutions, in which temperature profiles in one or both phases are assumed, and numerical methods which usually require solution by digital computer.

Chemical Engineering (90,91) and Foodscience textbooks (92-99) only evaluate the simpler analytical formulas and generally do not compare predicted freezing times with experimental results.

This research fills this gap in knowledge by:

(1) Evaluation of experimental freezing rate experiments concentrating on conditions to promote quick freezing since these conditions are desirable in the food industry. The experimental side of the research is described in Chapter 3.

(2) Evaluation and comparison of theoretical formulas from the literature.
A literature review of a wide range of approximate solutions to the heat transfer problem with a phase change is given in chapter 2. Theoretical freezing methods studied in detail are discussed in chapter 4 and appendix 4.

(3) Comparison of theoretical and experimental freezing times of distilled water. This work is given in chapter 5 along with the determination of the most accurate predictive theoretical formula.

(4) Study of the freezing of electrolyte solutions. This work is discussed, both theoretically and experimentally in chapter 6.

(5) Comparison of theoretical results with other worker's experimental work (comparison and discussion given in chapter 6 and appendix 2).

(6) Development of the most accurate freezing formula into a simplified formula by the use of dimensionless groups (this work is discussed in chapter 7).

CHAPTER 2.

LITERATURE SURVEY.

2-1 INTRODUCTION.

The aim of the literature survey is to review and classify published theoretical and experimental studies in the field of heat transfer with a phase change.

Several general surveys of methods predicting rates of freezing and melting exist, including Muehlbauer and Sunderland (1), Bankoff (2) and Kinder and Lamb (3) on methods specifically developed for the freezing of foods. There was however little evidence of any critical review of a range of theoretical methods predicting freezing times with corroborative comparison of experimental results.

Temperature distributions during freezing and thawing processes have been studied by Ede (4) and Malton (5).

Initial study generally revealed a lack of recorded experimental work, although workers including London and Seban (25), Charm (6), Komari and Hirae (32), Earle (7) and Bakal (8) did compare their theoretically predicted freezing times with results from their own experiments. Experimental results when published often gave

insufficient physical properties or system data for comparison with theory.

This survey classifies the theoretical freezing rate methods according to whether they include or exclude the criteria given for a useful predictive method on page 5 of the introduction. Five classes of methods were used. (1) Methods based on neglecting the heat transfer coefficient (section 2-2). (2) Methods based on neglecting the initial material temperature (section 2-3). (3) Methods calculating time for the freezing stage only (section 2-4). (4) Methods calculating complete freezing time with constant freezing point (section 2-5) and (5) Methods calculating complete freezing time with variable freezing point (section 2-6).

This classification is shown in table 2-1 which also indicates whether the method produces an expression from which freezing times may be obtained readily (i.e. by hand calculator).

The requirement that the theoretical method should account for freezing times of irregularly shaped objects is mentioned in recommendations for further work (Chapter 8).

Section 2-7 at the end of the literature survey briefly discusses the various experimental techniques used to measure solidified layers, by other workers, in the field of heat transfer with a phase change.

Table 2-1.

Classification of the most important freezing rate methods.

Criteria in table shows if the methods allow for :

(1) A finite heat transfer coefficient.

(2) Calculation of freezing stage time with TI=Tm only.

(3) Calculation of freezing stage time with TI $\geqslant$ Tm.

(4) Calculation of total freezing time (precooling stage + freezing stage + tempering stage) with constant Tm, with TI > Tm.

(5) Calculation of total freezing time, with variable Tm, with TI > Tm.

(6) Simple evaluation e.g. by hand calculator.

Method	Criteria of method						Section Classified in
ANALYTICAL	1	2	3	4	5	6	
Neumann			Y				2-2
Planck	Y	Y				Y	2-3
Modified Planck.	Y		Y			Y	2-4
Rutov, Nagaoka.	Y		Y	?		Y	2-4
London and Seban 1.	Y		Y			Y	2-3
London and Seban 2.	Y		Y			Y	2-4
Goodman	Y		Y				2-3
Bakal	Y		Y	Y	Y		2-6
FINITE DIFFERENCE.							
Vasil'ev & Uspenskii.	Y		Y				2-4
Murray & Landis	Y		Y				2-4
Earle & Earle	Y		Y	Y			2-5
Charm	Y		Y	Y			2-5

Y indicates Yes.

Blank spaces indicates No.

2-2 METHODS BASED ON NEGLECTING THE HEAT TRANSFER COEFFICIENT.

The first important solution to the freezing problem was presented by Neumann in lectures in the 1860's, however publication (9) of the lectures was not until 1912. Neumann's solution was applied to a semiinfinite slab with the face at x = 0 maintained at a constant temperature. With this latter condition of an infinite heat transfer coefficient between the coolant and the surface of the body, the heat flux boundary condition, equation (1-5) of the mathematical model is reduced from :

$$H(Tc-Ts) = -K_1 \left(\frac{\partial T_1}{\partial x} \right)_{x = 0} \qquad (1-5)$$

to $Tc = Ts$.

The Neumann solution together with the Planck method, first published in 1913, and discussed in section 2-3, have become the two best known and most widely used freezing rate methods. However both, as will be shown, have serious limitations to their practical applications.

The practical applications of Neumann's solution are severely limited since generally commercial freezing

systems achieve only a relatively low heat transfer coefficient; the result of this is that the Neumann method underestimates freezing times. However, for systems involving very rapid freezing of thin ice layers (e.g. the case hardening of foodstuffs for packaging before complete freezing using liquid nitrogen) the Neumann solution may be applicable.

Further work with infinite heat transfer coefficients has been undertaken by Luikov (11) for both infinite cylinders and slabs, while Carslaw and Jaeger (10) gives an extensive review of Neumann solutions.

2-3 THEORETICAL METHODS WITH INITIAL TEMPERATURE EQUAL TO THE FREEZING POINT (i.e. TI=Tm)

This group of theoretical methods by assuming that the initial material is equal to the freezing temperature excludes the precooling time and the effect of the thermal capacity of water on the freezing time. The boundary condition at the frozen-unfrozen interface (1-3) is reduced to :

$$-L\rho \frac{dX}{dt} = -K_1 \left(\frac{\partial T_1}{\partial x} \right)_X$$

due to no heat flow from the unfrozen phase. Methods of this type are sometimes referred to as 'Stefan' methods after one of the earliest workers in the field (12).

The effect of omitting the precooling time results is an under-estimation of the overall freezing time by the amount of the precooling time (with water based materials however the precooling stage is very small compared to the actual freezing stage). Neglecting the thermal capacity of water leads to serious under-estimation of the freezing time when the initial temperature is well above the freezing point. (i.e. when the effect of neglecting the thermal capacity is greatest).

The inclusion, in Neumanns solution, of a convective boundary condition at the surface of the body together with the assumption that the rate of freezing is slow in comparison to the rate at which the temperature can equilibriate in the frozen material, (so that a linear temperature profile exists in the ice) produces the solution independently obtained in 1913 by Planck (13).

Goodman (14 and 15) studying the melting of a semi infinite solid assumed constant uniform temperature beyond the ice interface. The assumption is analogous

to the constant velocity or temperature assumptions outside the boundary layer of boundary layer analysis. Goodman then used the integral method of boundary layer analysis to reduce the partial differential heat equation to an ordinary differential equation as done in boundary layer analysis by Pohlhausen (16).

The resulting integral quantity, which is proportional to the total sensible heat of the region, was referred to as the heat balance integral.

The main disadvantage of the method was the complicated algebra involved which was increased further in complexity by Goodman and Shea in considering melting of slabs initially below the melting temperature (17). Further applications of integral methods are given (18-24).

The methods of Goodman, Planck and Neumann are evaluated (chapter 4, and appendix 4) in detail and compared with experimental results from freezing distilled water in chapter 5.

London and Seban (25)used two idealised systems (see figure 2-1) in which (1) the thermal capacity was neglected and (2) the capacitance $C = C_1X$, dependent on the ice thickness, was assumed to be lumped at the centre of the ice layer.

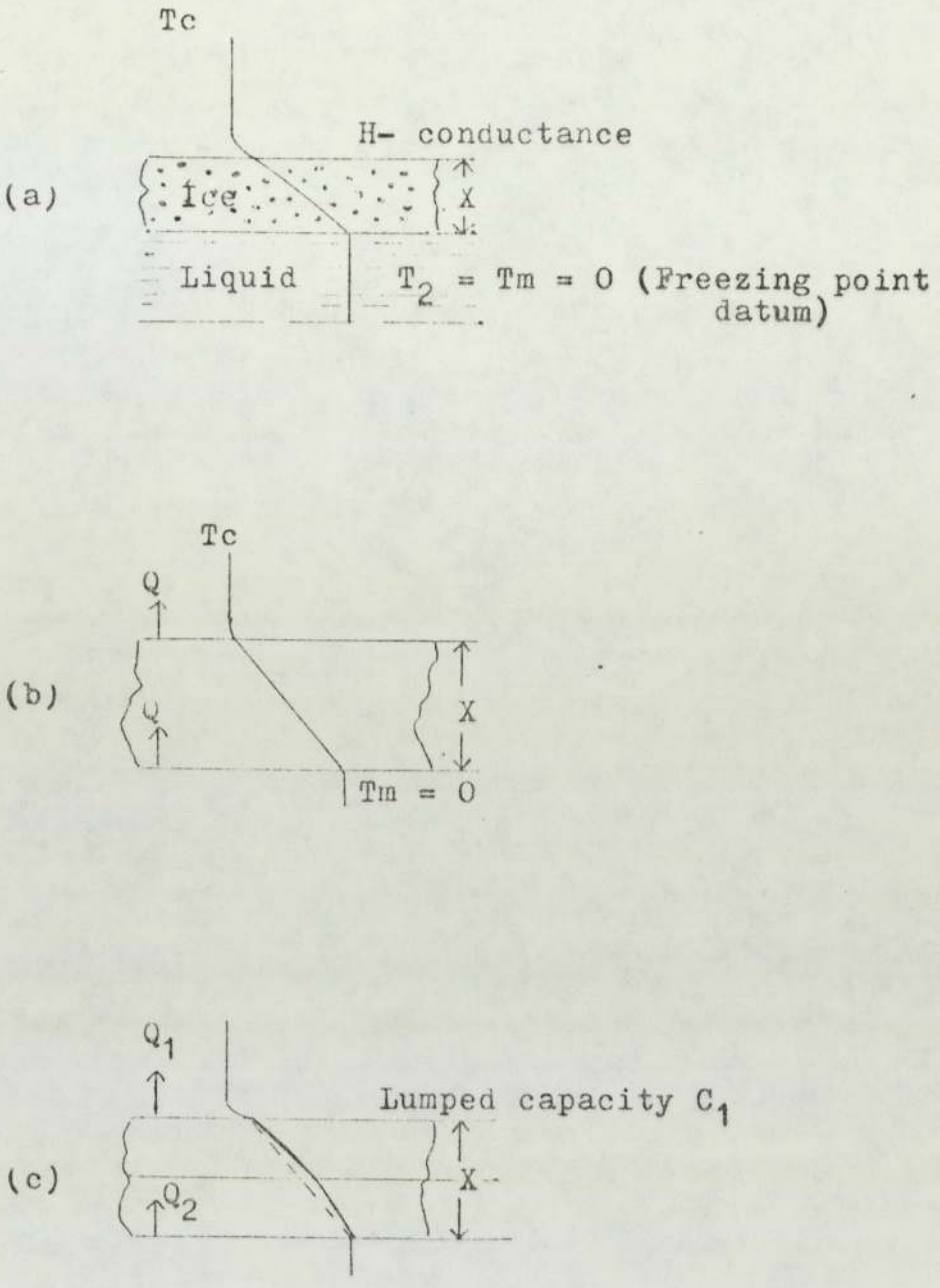

Temp. distribution for first system

Figure 2-1 Idealised systems of Ice formation (London & Seban)

(a) Temperature conditions during ice formation

(b) First idealised system

(c) Second idealised system

Comparison of solutions for the two idealised systems with (Tm-Tc) up to 30 C gave differences in freezing times between the two systems of 5 per cent or less for all ice thickness.

Krieth and Romie (26), using an electrical analogue, confirmed the work of London and Seban for systems where L/C_1 (Tm-Tc) $>>1$. Cochran (27) and Robertson and Schenck (28) modified the London and Seban equation for cases when L/C_1 (Tm-Tc) approached 1 when they stated that the London and Seban method overestimated the thickness of the solidified layer by up to 13 per cent. Robertson and Schenck introduced a theoretical corrective solidified layer calculated for a computer program which utilized the 'fictive specific heat' (i.e. variable specific heat) method of handling solidification at constant temperature (29).

Cowell (30) produced formulae based on Neumann's solution, but assuming that TI was equal to Tm, for infinite heat transfer coefficients and Planck's method for finite heat transfer coefficients for predicting freezing stage times (t_f) and analytical formula (Carslaw and Jaeger) for predicting tempering times, (t_t).

Cowell incorporated the predicted times into the following expression:

$$T_{total} = A(t_f + t_t)$$

where A is a factor for the precooling time. Since no details of the method of evaluation or numerical value of A were given and since both the Planck and Neumann methods employ restrictive assumptions the method was not studied further.

2-4 METHODS PREDICTING TIME FOR FREEZING STAGE ONLY

These methods calculate the time for the frozen-unfrozen interface to traverse the body being frozen, they take no account of precooling or tempering stage times but include the effect of the thermal capacity of water. For freezing of aqueous solutions in which the freezing stage is much larger than the precooling and tempering stages the exclusion of the precooling and tempering stages is probably justified.

Extension of Neumann's solution (10) has centered on incorporating a convective heat transfer boundary condition at x = 0 which produces a time-dependent surface temperature. Charm and Slavin (31) and Komori and Hirai (32) have both produced methods with this extension but their methods have had no corroborative experimental comparison.

Planck (33) modified his original formula to include the sensible heat of both phases in the total heat that must be transferred to the coolant whilst retaining the linear temperature profiles. Extensions of this work to include the effect of precooling based on experimental results has been undertaken by Rutov (34), Nagaoka (35) and others (30, 36-39). The modified method of Planck together with the extensions due to Rutov and Nagaoka are developed in chapter 4.

London and Seban (40) gave experimental confirmation of their lumped parameter method for infinite cylinders. (see figure 2-1(c) - the capacity is lumped at the centre of the ice layer). Good agreement (differences of 10 per cent or less) between theory and experimental results was obtained with water but, with foods less accuracy (20 per cent error) was achieved. The reasons given for the reduced accuracy in predicting the freezing rates of foods were inaccuracies in thermal properties and changes in the freezing point as the interface moved.

Other approximate analytical methods and papers considering the change of phase heat conduction problem are given (41-48 & 76-80).

An alternative to analytical methods for approximating the heat conduction problem with a phase change is the use of finite difference techniques.

The finite difference method divides the body being frozen into discrete intervals (of equal or variable length). The capacity of each section is lumped at its centre or nodal point, and considered to be uniform over the section at each instant of time.

The main advantage of finite difference procedures is that they are able to overcome some of the restrictive assumptions used in the analytical methods, for example, the need to assume a given form of temperature profile and the need for a constant initial material temperature.

The main problem of the finite difference procedures is to represent the method in a convergent form. The disadvantage of requiring small nodal spacing and time intervals in order to attain sufficient accuracy, which leads to many calculations being necessary for each time step length, is largely overcome by the speed of operation of computers. An added disadvantage of most of the finite difference methods is that they have not been developed into convenient usable forms.

Essentially the finite difference method calculates the time for the frozen-unfrozen interface to advance from a given node to the next, (i.e. from node 3 to node 4 in figures 2-2 and 2-3). Methods may use either constant inter-node step lengths or variable step lengths.

Vasil'ev and Uspenskii (49) developed an implicit finite difference scheme using constant step lengths. This method, although sometimes found to predict negative freezing times for the interface to traverse one nodal point, was thought to be the simplest and most adaptable of the finite difference methods and was therefore studied further and modified, (see chapters 4,5 and 7 and appendix 4).

Other workers using finite difference methods with constant step lengths include, Ehrlich (50) who used the Crank-Nicolson (51) finite difference procedure with a three point approximation of the space derivative on either side of the moving boundary. Dusinberre (52) used an 'enthalpy-flow temperature' method due originally to Eyres (53). This method took into account the latent heat effect to give an additional specific heat at the fusion temperature. Price and Slack (54) determined the effect of latent heat on the stability and accuracy of the solution of transient heat conduction problems with a moving boundary.

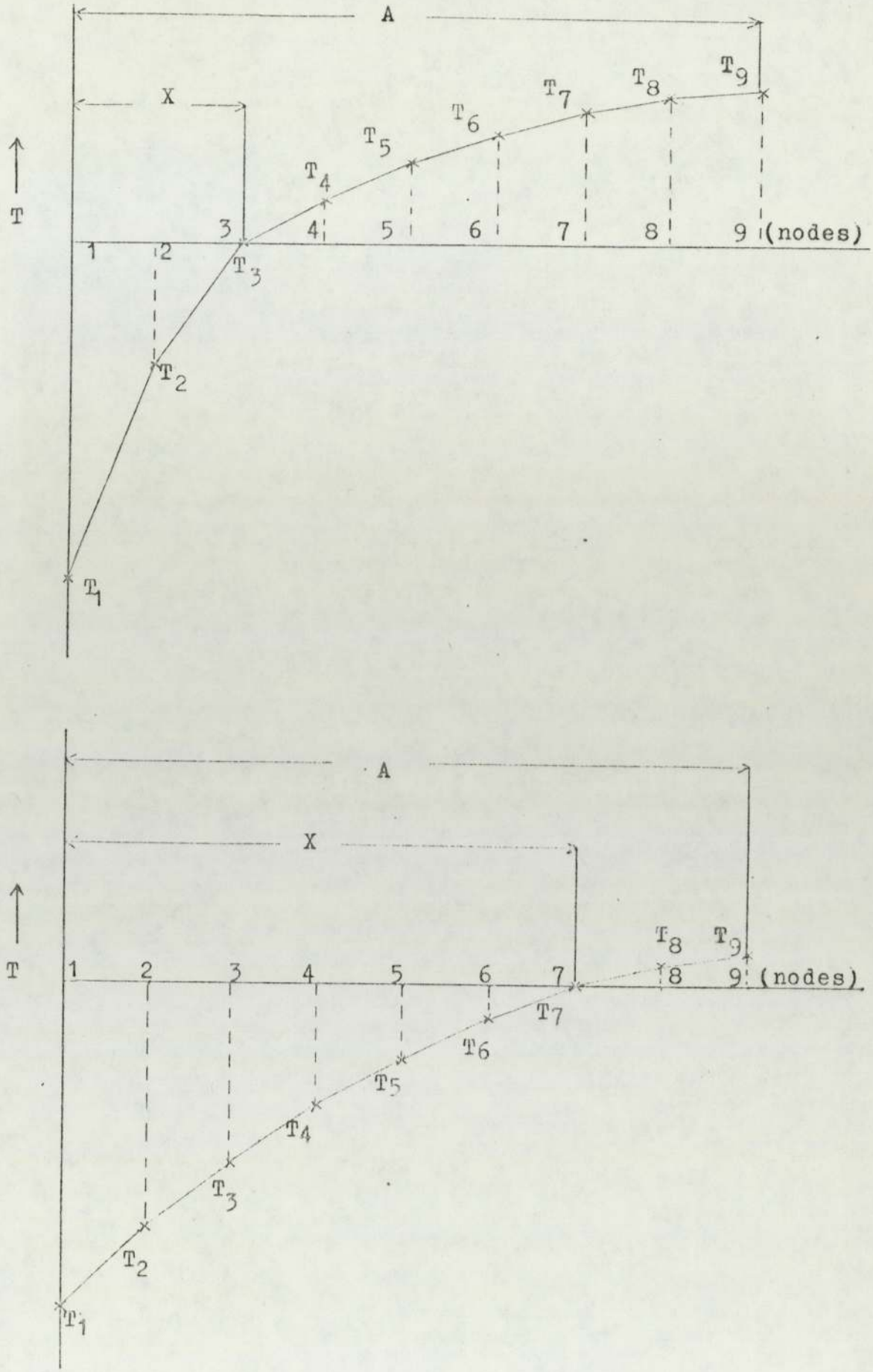

Figure 2-2 Constant spaced finite difference temperature profiles (Vasil'ev and Uspenskii)

Murray and Landis (55) used variable step lengths in both phases to imobilise the moving interface with respect to the difference scheme (i.e. the position of the interface is always known). This procedure was first used by Landau (47) for melting finite slabs where the liquid formed was immediately removed. The method of Murray and Landis is represented on figure 2-3.

One disadvantage of the method was that two phases must always be present. This led to initial errors in estimating freezing times and the inability to account for tempering time to reduce the frozen body to its storage temperature. However, independent analytical formula, for example from Carslaw and Jaeger (10) or Rutov (56), could be incorporated into the method to calculate the tempering and/or precooling time.

As can be seen from figure 2-3 the method initially involved very small solid step lengths and correspondingly large liquid step length. The reverse applied near the end of the freezing. Lotkin (57,58) devised a numerical integration scheme with unequal subdivisions in both the space and time variables and found greater accuracy with smaller step lengths in both phases near the interface.

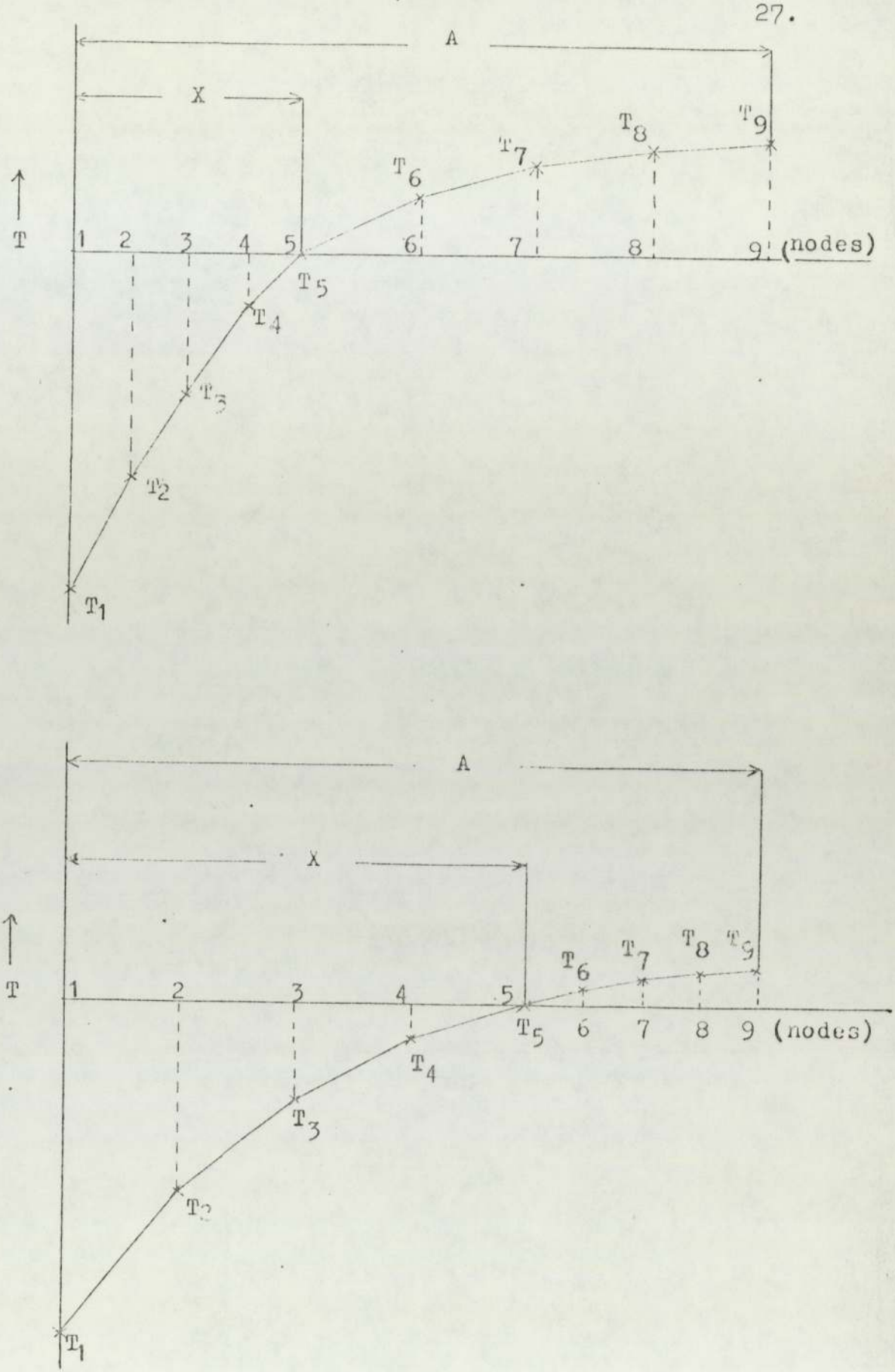

Figure 2-3 Variable spaced finite difference temperature profiles (Murray & Landis)

Further references to finite difference methods are given (59-64).

2-5. METHODS THAT PREDICT TIME FOR THE COMPLETE FREEZING PROCESS WITH A CONSTANT FREEZING POINT

Methods in this category predict the time to cool a body from its initial temperature to its storage temperature and so estimate the precooling time, freezing time and the tempering time. The methods are more complicated than other methods previously described since they contain formulas to calculate time for the three stages in the overall freezing process.

Charm (6) divided finite slabs and cylinders into sections and calculated the time for the interface to travel across each section in turn, and formulae to estimate precooling and tempering times.

The results predicted by the Charm method were compared with experimental fish freezing results and showed an underestimation (up to 30%) of experimental freezing times throughout the process. Charm stated that the discrepancies were due to uncertainties in the thermal properties of fish.

A similar method was evaluated by Earle and Earle (7) for spherical and three-dimensional plane boundaries incorporating variable specific heat and thermal conductivity. The method as presented was complicated and there seems little point in accounting for the variation in thermal properties when other workers (London and Seban (40) and Charm (6)) conclude that discrepancies between theoretical and experimental freezing times were due to lack of knowledge of the true values of thermal properties.

Lockwood (65) working on fire proofed enclosures described a numerical method in which the physical property variation with temperature was again accounted for. The procedure involved the use of the explicit finite difference technique, in conjunction with two integral transformations, based on the methods by Eyres (53) for variations in physical properties and Price and Slack (54) for phase change. The method suffered from the numerical instability associated with explicit finite difference procedures.

Methods described in section 2-4 could be used to predict overall freezing times if independent analytical or finite-difference schemes are incorporated to estimate precooling and tempering times, into the method.

The finite-difference methods seem to offer the best opportunity to predict accurately freezing rates in comparison to the analytical methods which contain rather restrictive assumptions.

2-6. METHODS THAT PREDICT TIME FOR THE COMPLETE FREEZING PROCESS WITH A VARIABLE FREEZING POINT

The methods surveyed here differ from the methods in the previous section only by accounting for a variable freezing point. The methods in this section lend themselves to estimating the freezing times of aqueous solutions, in which rejection of the solute from the frozen phase increases its concentration in the liquid and hence changes the freezing point.

Tein and Geiger (24) working on the melting of alloys replaced the frozen-unfrozen interface by a 'freezing zone' or a 'mixed zone' separating the solid phase from the liquid phase. They introduced two freezing points, an initial freezing point (Tm_1, at which temperature solidification starts) and a final freezing point (Tm_2, at which temperature the latent heat becomes insignificant compared to the specific heat), between these freezing points the 'mixed' phase exists.

Initial work on systems when the initial temperature was equal to Tm_1 and having an infinite heat transfer coefficient assumed that there was instantaneous formation of the three phases, solid, mixed and liquid. Using Goodman's heat balance integral method temperature distributions in the three phases were obtained. The work was extended by Tein and Koump (66) to include a finite heat transfer coefficient. Further studies on alloy solidification exist (67-69).

Extension of the above work by Bakal and Hayawaka (8) for foodstuffs with initial temperature above Tm_2 produced the series of conditions shown in figure 2-4 that could exist during freezing operations. The significance of their analysis was that under rapid freezing conditions two interfaces and three phases could exist at one time (figure 2-4 (f)). Comparison of this work with experimental results showed poor relationships for the freezing phase, but more accurate predictions for the other phases. The reason for poor accuracy during the freezing stage was probably the lack of knowledge of the thermal properties in the mixed phase. Problems were also encountered in determining the end of the freezing stage and the start of the tempering stage due to the variation in the freezing point during freezing.

Figure 2-4 Cooling-freezing-tempering phases (Bakal)

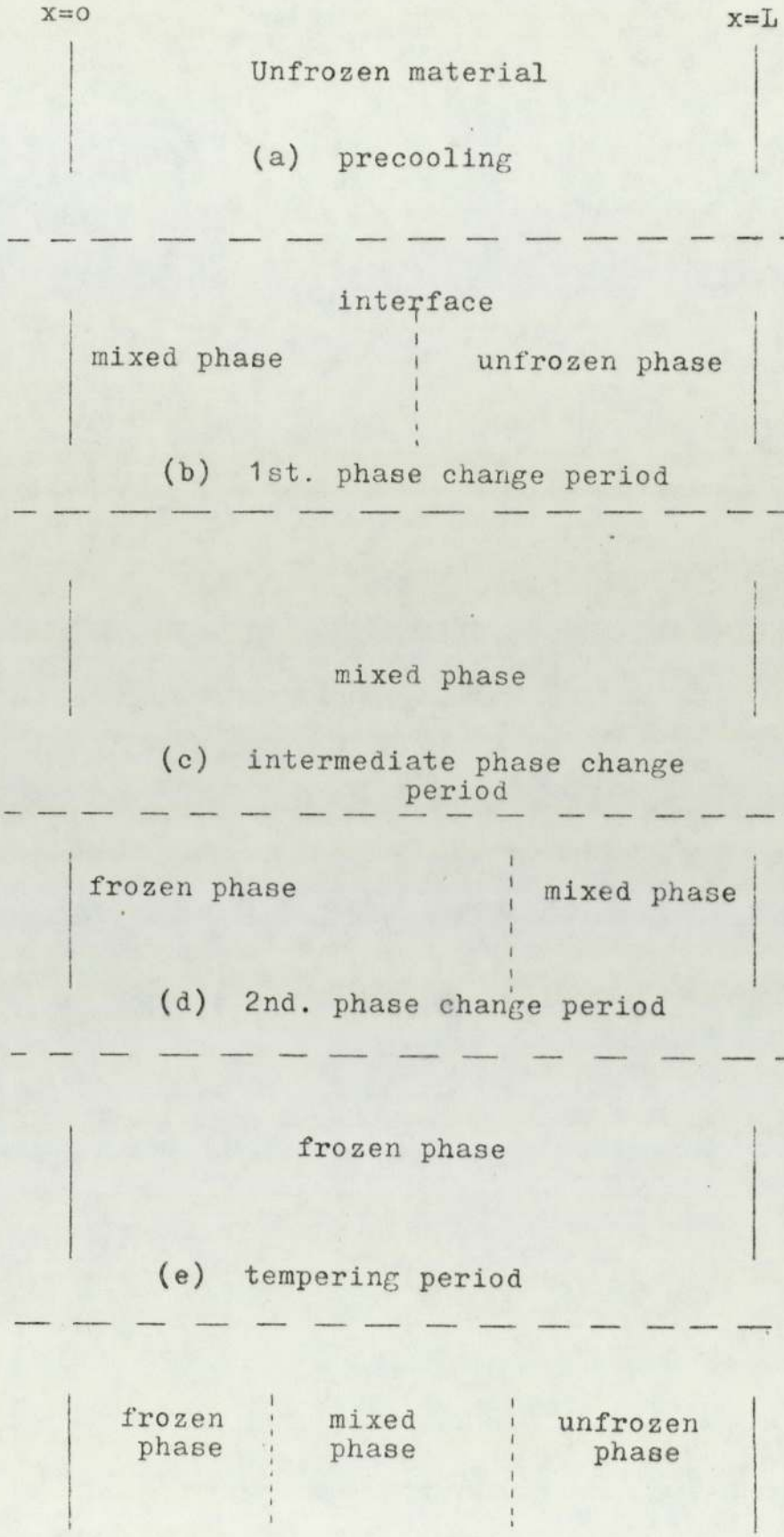

Quantitative comparison of Bakal and Hayawaka's method with experiment appears to be unprofitable with our present inadequate knowledge of the thermophysical properties of foodstuffs, and whilst the simple predictive methods remain largely untested.

Terwilliger and Dizio (70) and Grange et al (71) studied solute rejection with finite and semi-infinite systems of sodium chloride solutions respectively. They concluded independently that although only a small proportion (up to 10%) of the solute was rejected by the frozen phase, the rejected solute formed a high concentration layer at the frozen-unfrozen interface which could, especially under conditions of slow freezing, significantly alter the freezing temperature of the solution. Other work incorporated by Terwilliger and Grange is given (72-75).

Chapter 6 discusses the problem of electrolyte freezing in more detail.

2.7 EXPERIMENTAL TECHNIQUES FOR MEASURING SOLIDIFIED LAYERS.

In the field of metallic solidification, techniques employed to study rates of solidification include pour-out,

thermocouple, dip-stick, tracer, optical and acoustic methods (81-84).

The pour-out technique which involved removing the unfrozen phase to leave the solidified layer proved tedious due to the restriction of obtaining only one measurement for each experimental run. The optical technique, developed by Thomas and Westwater (84) was used for systems where the test material had a translucent solid phase and a transparent liquid phase. The use of acoustics is well established in the field of non-destructive testing where internal defects in a metallic component may be detected from the reflection or scattering of the incident sound energy. Bailey and Dula (81) developed an acoustic method for following the motion of the solid-liquid interface during the freezing of water where the heat transfer is undirectional. They state that the relationship, $X = m\sqrt{t} + a$, where m and a are constant holds for the freezing of water.

The use of thermocouples for measuring solidification rates has been extensively used in food research (4, 6, 7, 25, 26, 32 and 34) as well as in the field of metallic solidification. The thermocouple technique measures the position of the solid-liquid interface by the thermal arrest due to the liberation of latent heat on the recorded time - temperature profiles.

This thermal arrest is most significant in, and the technique most suitable to, systems where the latent heat is much greater than the specific heats of the material under test (e.g. foodstuffs). The disadvantage with the thermocouple technique is that several thermocouples must be used in each experiment to record the process of the solid-liquid interface, the introduction of these thermocouples into the system can lead to excessive heat loss via the thermocouple wires.

Dip-stick methods have been employed with the freezing of liquid materials. The technique is simple and gives direct readings, but suffers the major disadvantage of disturbing the system when each measurement is taken (85).

The type of experimental method for measuring the solidified layers of liquids in the experiments carried out in this research was chosen by considering the requirements that the apparatus should be inexpensive, reliable, give direct continuous readings if possible and not disturb the system when taking the measurements.

The physical properties of the liquids to be frozen were studied in order to find a property that varied

greatly between the solid and liquid phases but remained comparatively constant in each phase over the temperature range used in the experiments, and was easily measured. The density was chosen as the property to be measured since it has a variation of 9% between the two phases but remains constant in each phase. (See appendix V).
An experimental apparatus was designed (see chapter 3) based on the dilatometry principle in which the variation of volume due to ice formation was directly converted into ice thickness.

CHAPTER 3.

EXPERIMENTAL WORK.

The experimental side of the research involved :

1. The design, construction and commissioning of a laboratory scale apparatus enabling accurate determination of freezing rates of liquids for a range of known coolant temperatures and heat transfer coefficients between the coolant and the freezing liquids.

2. Freezing rate experiments with distilled water, aqueous solutions of sodium chloride and fruit juice to provide experimental data for comparison with theoretical results from the methods described in Chapter 4.

3.1 EXPERIMENTAL APPARATUS.

In order to supply the coolant under given conditions and to accurately measure frozen thicknesses of ice the apparatus consisted of the following items : (see figure 3-1).

a) Coolant tank (capacity approx. 20 litres).

b) Coolant pump.

c) Three cooling units.

d) Heater (2 kilowatts), contact thermometer and relay switch.

e) Temperature recorder, (Honeywell type Electronik 15), and copper constantin thermocouples.

f) Stirrer.

g) Rotameter.

h) 16 cm. diameter Dewar flask.

i) Clock.

j) Travelling telescope (Precision Tool and Instrument Co.).

k) Freezing apparatus-freezing vessel, heat transfer discs and coolant reservoir.

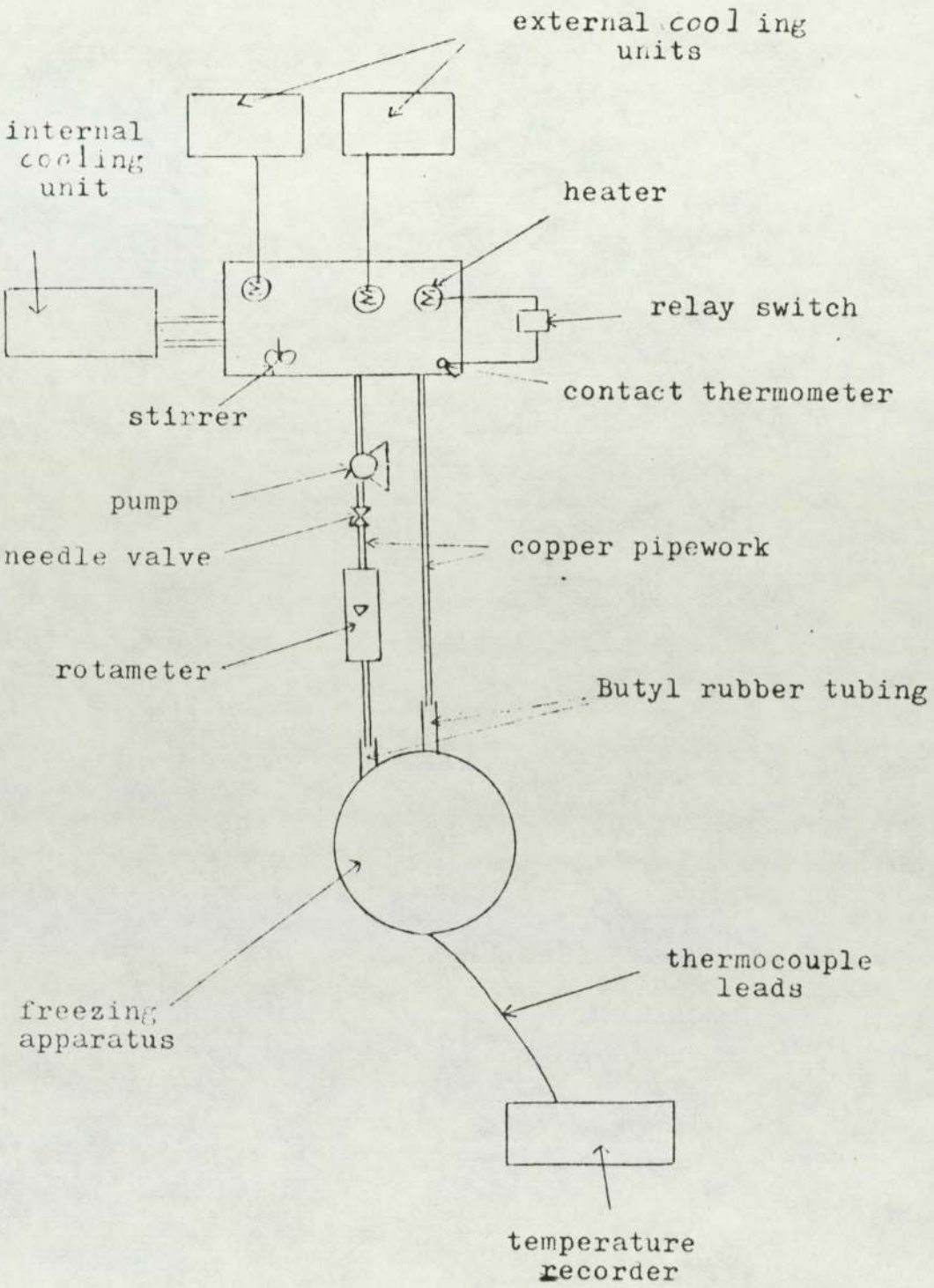

Figure 3-1 Plan layout of equipment.

The coolant used was a 50% wt. solution of methanol (freezing point -55 C). Due to the poisonous nature of methanol vapour, the apparatus was designed to fit inside a fume cabinet.

Copper pipework was used to transport the coolant around the apparatus. The pipework was heavily lagged with asbestos fibre. Two short butyl rubber tubes connected the heat transfer equipment to the copper pipework to absorb vibration from the coolant pump carried along the copper pipe.

3.1.1. Heat Transfer Apparatus.

The heart of the apparatus was the freezing equipment which consisted of a coolant reservoir, heat transfer disc and freezing vessel arranged as shown in figure 3-2. In experiments the freezing equipment was enclosed in a Dewar flask and all external surfaces were lagged to reduce heat gain from the surroundings, (see figure 3-3). The heat transfer equipment permitted a heat flow from the freezing vessel to the coolant, via the heat transfer disc. The coolant surfaces of the heat transfer discs and freezing vessel are machine smoothed to help achieve good contact.

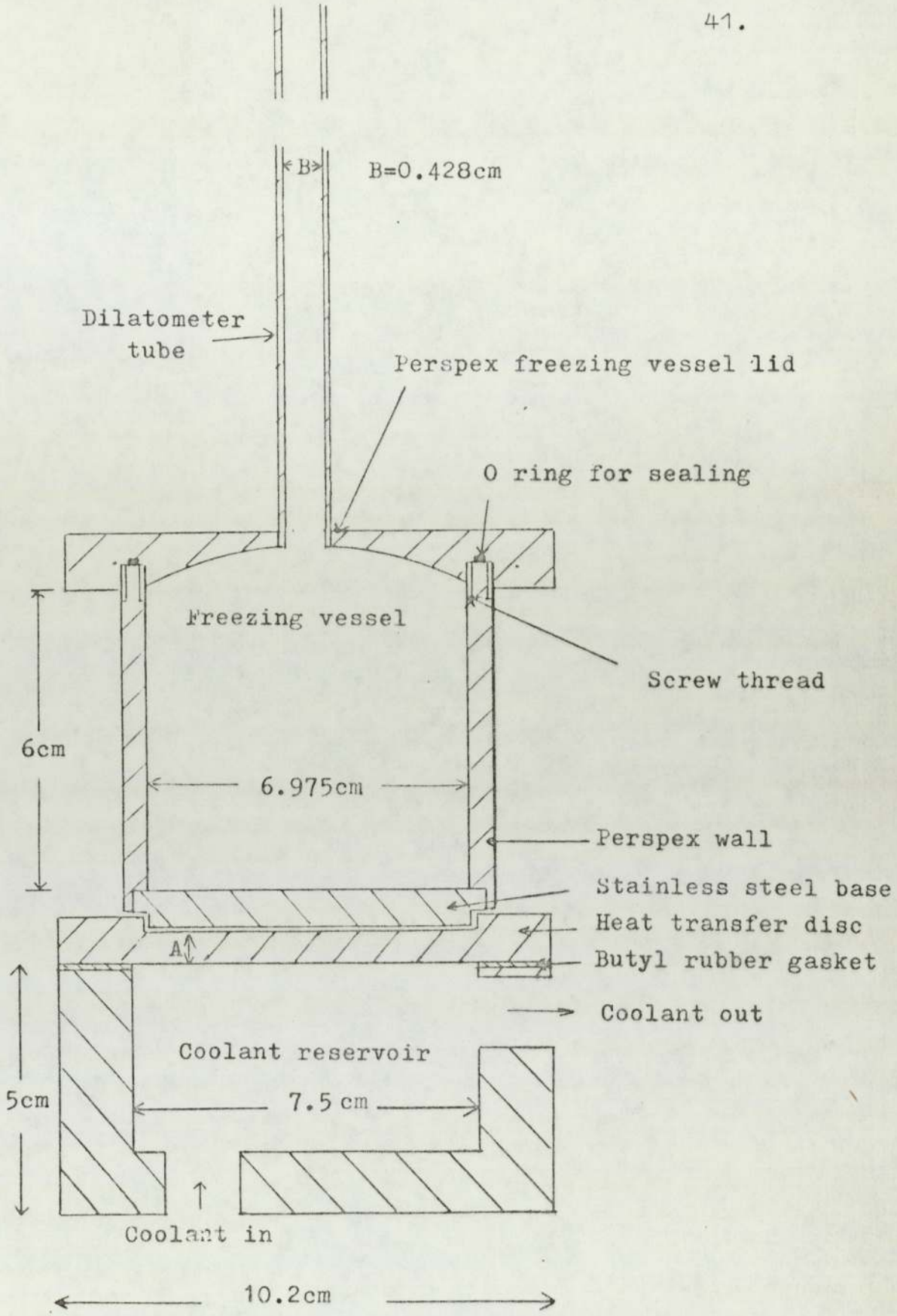

Figure 3-2 Freezing apparatus in position (lagging omitted)

Five interchangeable discs made of copper, brass, stainless steel, copper plus polythene and perpex were used to provide a range of resistances to the heat flow between the freezing chamber and the coolant.

The dimensions of the discs and coolant reservoir are shown in figure 3-2. A thermocouple was positioned in the reservoir to monitor bulk coolant temperature.

The contact surfaces of the freezing chamber and heat transfer discs were machine smoothed (to achieve good surface contact) and tested for flatness. The thicknesses of the discs after machine smoothing are given in table 3-1.

TABLE 3-1.

Heat Transfer Disc.	Thickness of Disc (A in fig. 3-2) (mm)	Heat Transfer Coefficient (W/m^2 C)
Copper	4.22	2000.0
Brass	11.15	1700.0
Stainless Steel	10.79	900.0
Copper + Polythene	4.22 (C) + 0.96 (p)	350.0
Perpex	3.25	56.8

The principle of the method of determining ice thickness in the freezing chamber was based on dilatometry. The concave design of the freezing chamber top (figure 3-2) ensured that when the chamber was filled with liquid and the top screwed up tightly the liquid was forced up the dilatometer tube (figure 3-2). As freezing started at the chamber base, the volume increased due to phase change (the frozen phase formed was always less dense than the liquid phases for all liquids frozen, with water there was approximately a 9% increase in volume on freezing) forced the liquid further up the dilatometer tube. The liquid height was directly related to the ice thickness. However the change in height in the dilatometer tube for a given thickness of ice depended on the difference in phase densities. The density difference was dependent on the solute and its concentration, the freezing chamber had therefore to be calibrated for solutions of different concentrations. Details of the calibration of the freezing chamber are given, along with further details of the operation of the apparatus for accurate measurement of the ice thickness, in appendix 9.

3.2 DETERMINATION OF A HEAT TRANSFER COEFFICIENT.

Theoretical methods (except those based on Neumanns'exact' solution, see chapter 2, section 2.1) contain the heat transfer coefficient between the coolant and the freezing liquid. Determination of numerical values for this coefficient was therefore required for evaluation of these formulas. In our equipment this coefficient was variable according to the freezing chamber base used.

The method of determination of the coefficient under experimental freezing rate conditions (see table 3-2) for all five heat transfer discs is given in appendix 3. The results of the determination are given in table 3-1.

3.3 EXPERIMENTAL PROCEDURE FOR FREEZING LIQUIDS.

Constant temperature was attained in the coolant reservoir of the heat transfer equipment (monitored by thermocouple). A thin layer of oil was smeared over the contact surface of the heat transfer disc. Good contact was made between the dilatometer vessel and heat transfer disc, the stop clock started, and the liquid miniscus height in the dilatometer

tube measured by the travelling telescope to an accuracy of 0.05 mm (see figure 3.3). Height measurements of the liquid in the dilatometer tube were read at frequent intervals until the desired frozen layer thickness had formed. (Appendix 9 contains details of the conversion of dilatometer readings to ice thickness).

TABLE 3-2. EXPERIMENTAL SYSTEM CONDITIONS.

Heat Transfer Coefficient (W/m^2 C)	Coolant Temperature (C)	Initial Liquid Temperature (C)
2000, 1700, 900, 350 & 56.8	between -4 and -16	between 3 and 25

3.4 EXPERIMENTAL RESULTS.

Reproducible results were obtained for all the liquids frozen under the range of experimental conditions given in table 3-2. A full list of results is given in Appendix 1.

Comparison of experimental results and theoretical predictions of freezing rates is given in Chapters 5, 6 and 7 and Appendices 8 and 10.

Figure 3-3 Measurement of ice thickness.

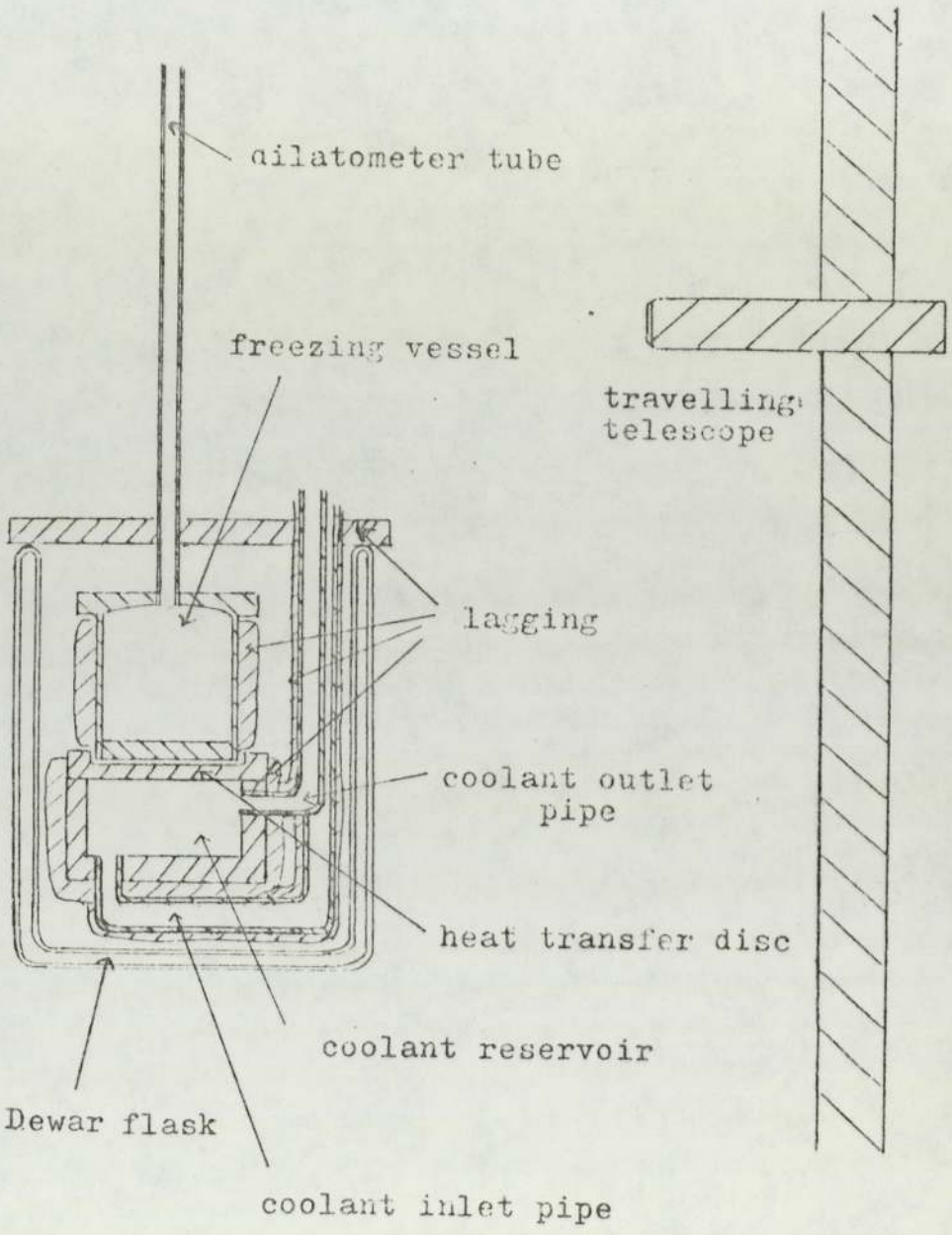

CHAPTER 4

ANALYTICAL AND NUMERICAL SOLUTIONS OF FREEZING PROBLEMS STUDIED IN DETAIL

The solutions studied are the analytical approximations of Planck (13,33), Goodman (14,15) and Neumann (10) in which the temperature profiles in the solid and liquid phases are represented by linear expressions (Planck), polynomials (Goodman) and error functions (Neumann), and the finite difference method of Vasil'ev and Uspenskii (49) The methods were chosen as being the most important theoretical methods developed for solving the heat transfer problem. Derivation of the equations given in this chapter are shown in appendix 4.

4-1 Planck's Methods

4-1.1 Planck's Original Method

This is the simplest and most widely used freezing formula.

The method assumes that the thermal capacities of the frozen and unfrozen phases are negligible and therefore that $\partial T/\partial X$ is constant in each phase, since from equation (1-1) :-

Figure 4-1 Assumed temperature profile of Plancks method.

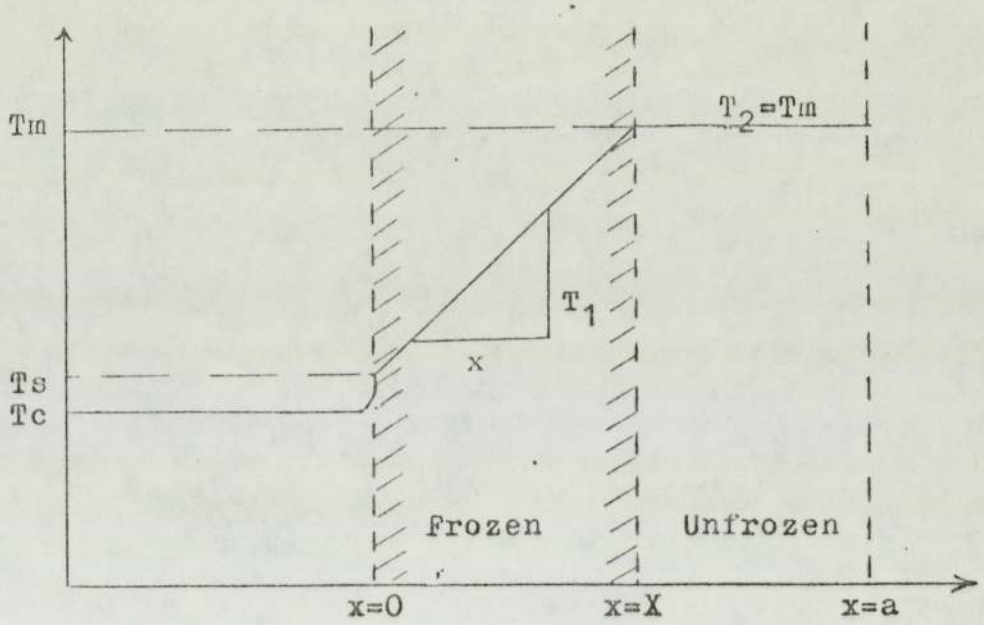

$$\frac{\partial T_1}{\partial t} = \alpha_1 \frac{\partial^2 T_1}{\partial X^2} \qquad (1\text{-}1)$$

If $C_1 \rightarrow 0$ then $\alpha_1 \rightarrow \infty$

then $\frac{\partial^2 T_1}{\partial x^2} \rightarrow 0$

With the further restriction of the unfrozen phase temperature initially being equal to the freezing temperature the resulting formula representing the time (t) to freeze a thickness (X) of material is:

$$t = \frac{L\rho\,(2K_1X + HX^2)}{2K_1\,H\,(Tm-Tc)} \qquad (4\text{-}2)$$

(the assumed temperature profile is shown in figure 4-1).

4-1.2 Planck's Modified Method

Planck, retaining linear temperature profiles (see figure 4-2), extended his original method to include the sensible heat of both phases in the total heat that must be transferred from the frozen-unfrozen interface to the coolant.

Figure 4-2 Assumed temperature profile of the modified Planck method

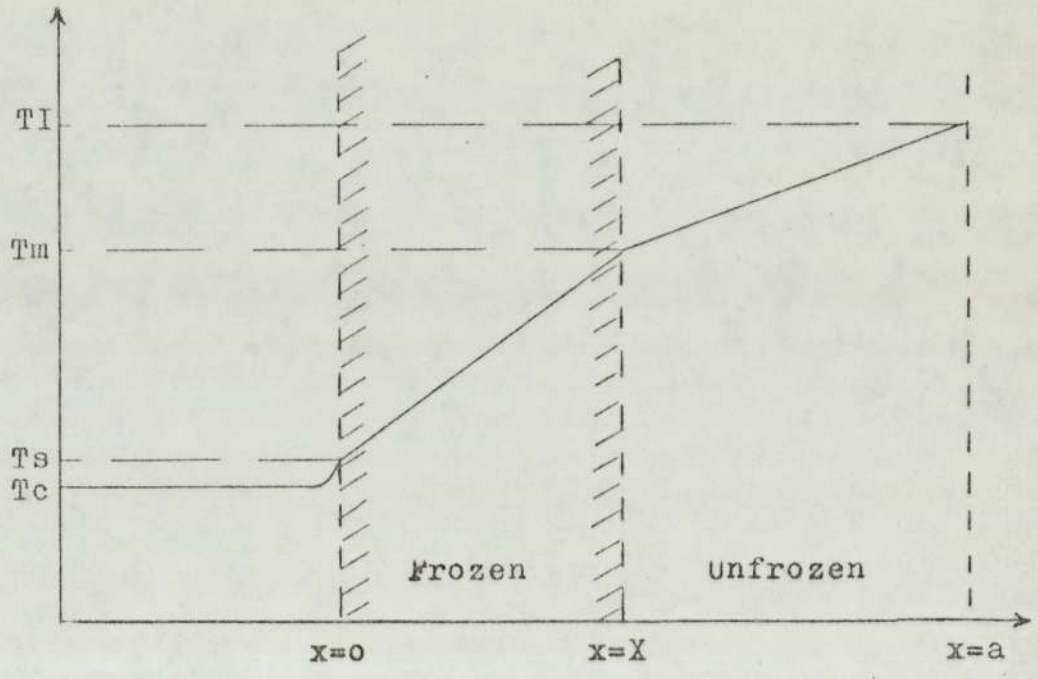

The specific heat is assumed to be concentrated at the interface. The heat flux to freeze unit mass of material changes from L (neglecting specific heats) to the total enthalpy term; C_1 (Tm-Ts)/2+L+C_2(TI-Tm)/2 when the specific heats C_1 and C_2 are included.

The dependence of t on X for this method is derived to be:

$$t = \frac{L\rho X^2}{2K_1(Tm-Tc)}\left[\left(C_1\frac{(Tm-Tc)}{2} + \frac{2K_1+1}{HX}\right)\left(1+C_2\frac{(TI-Tm)}{2}\right)\right] \quad (4-3)$$

4-1.3 Nagaoka & Rutov Extensions to Plancks Method.

Nagaoka (35) and Rutov (34) independently proposed further modifications to Planck's equation (4-3) to take into account precooling time. Their modifications (essentially heuristic) take the form:

$$t_T = t_p \ (1 + A \ (TI-Tm)) \quad (4-4)$$

where t_p = freezing time predicted by equation 4-3

t_p = total freezing time, i.e. for precooling plus freezing time.

A = constant :- 0.008 according to Nagaoka and 0.0053 according to Rutov.

4-2 Goodman's Integral Method

This method assumes a polynomial form of the temperature distribution in the frozen phase, see figure 4-3, which uses a quadratic function and uniform temperature in the liquid phase. In the derivation (appendix 4) the unfrozen phase temperature is taken as being equal to the freezing temperature to simplify otherwise very complicated equations, Goodman (15,17). The temperature variation in the cooling mass is therefore confined to a distance $\delta(t)$.

The method with the above assumptions has the same restrictive assumptions as the Original Planck method and involves more complicated calculation but attempts to account for the specific heat of water by the curved temperature profile in the frozen phase.

The method consists of determining the constants a and b in:

$$T_1(x,t) = a(x-\delta) + b(x-\delta)^2 \qquad (4-5)$$

from the boundary conditions of the problem.

The resulting equation for t in terms of X is:

$$t = \frac{K_1}{\alpha_1 H} \int_o^m \left[\frac{K_1}{H} \left(\frac{m}{2} + \frac{m^2}{6b} \frac{db}{dB} - \frac{a}{2b} - \frac{m}{4b} \frac{da}{dm} \right) \right] dm \qquad (4-6)$$

t is determined by numerical integration after evaluation of B, b, m and a.

Figure 4-3 Assumed temperature profile of Goodmans integral method.

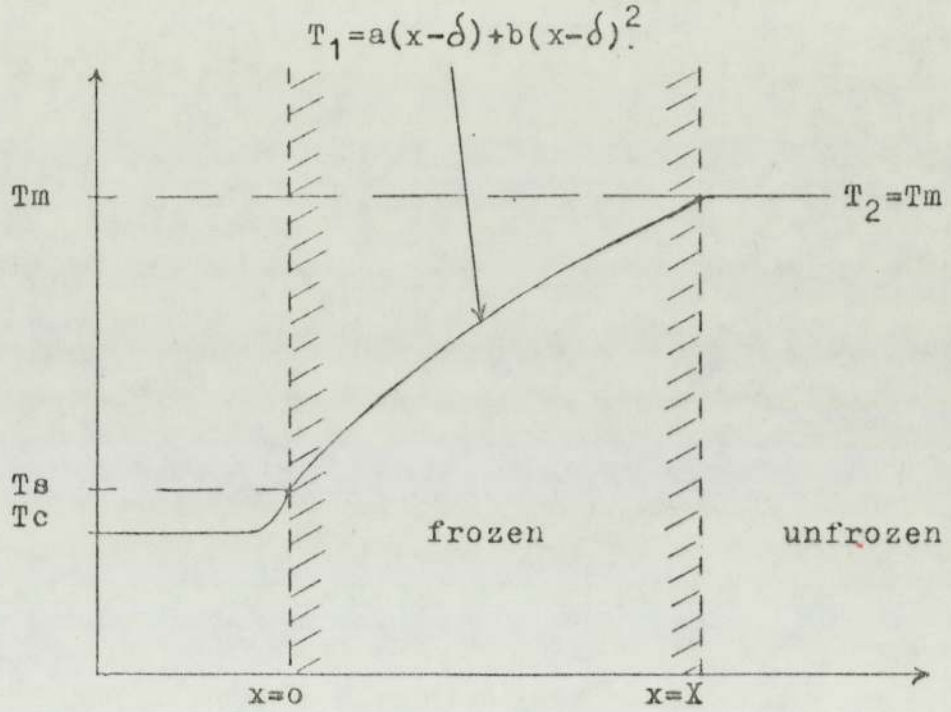

4-3 Neumann's Solution

An analytical solution can be obtained if we assume (1) that Ts is constant, which corresponds in practical cases to the assumption of a very high heat transfer coefficient i.e. Ts=Tc, and (2) that the unfrozen region is large compared to the frozen region for all times of interest, so that we may write:

$$T_2 \rightarrow TI \quad \text{as } x \rightarrow \infty$$

The solution for X as a function of t is then:

$$X = 2\lambda(\alpha_1 t)^{1/2} \tag{4-7}$$

Where λ is defined by the equation:

$$\frac{\exp(-\lambda^2)}{\operatorname{erf}\lambda} - \left(\frac{K_2^2\alpha_1}{K_1^2\alpha_2}\right)^2 \frac{TI-Tm}{Tm-Ts} \frac{\exp(\alpha_1\lambda^2/\alpha_2)}{\operatorname{erfc}(\lambda^2\alpha_1/\alpha_2)^{\frac{1}{2}}} = \frac{\lambda L\pi^{1/2}}{C_1(Tm-Ts)} \tag{4-8}$$

The temperatures and physical properties are substituted into (4-8), and λ found by trial and error.

This method predicts the thickness of the frozen layer to be proportional to the square root of time. By contrast Plonck's equation (4-2) requires that X is proportional to the square root of time only if $HX^2 >> K_1 X$ i.e. for large X or high H values.

4-4 Vasil'ev and Uspenskii Finite Difference Method

The method used is an implicit, fixed distance step length and variable time - step approximation based on that discribed by Vasil'ev and Uspenskii.

The basis of the method involves substituting finite difference operators into the heat conduction equations (1-1) and (1-2) to evaluate temperatures at each step length (see figure 4-4).

The temperatures calculated at nodes n-1 and n + 1, $T_{n-1,n}$ and $T_{n+1,n}$ are then used to predict the time, t , for the interface to advance from node n-1 to node n by the equation:

$$t = -L\rho h^2/(K_1 T_{n-1,n} + K_2 T_{n+1,n}) \qquad (4\text{-}9)$$

Equation (4-9) results from direct finite difference substitution into equation 1-3, the heat balance boundary conditions at the interface.

Two additional implicit finite difference schemes are incorporated into the method to account for preccoling and tempering times.

Figure 4-4 Assumed temperature profiles of Vasil'ev & Uspenskii finite difference method

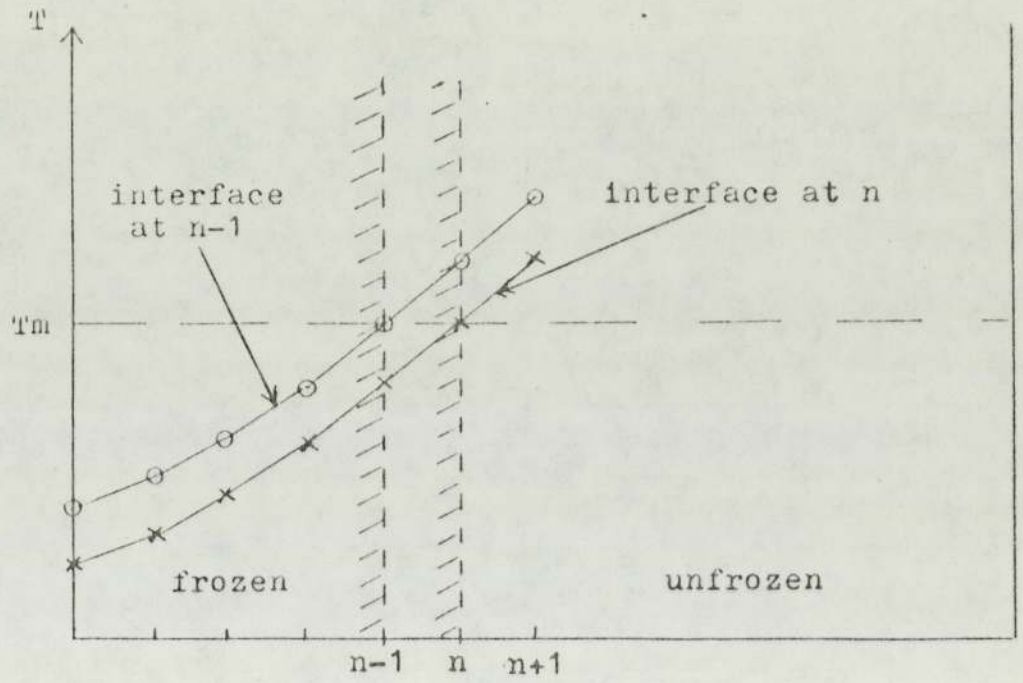

CHAPTER 5

DISCUSSION OF RESULTS FOR DISTILLED WATER

The theoretical freezing rate methods discussed in chapter 4 are evaluated and found to differ in their predicted freezing times. The theoretical results are then compared with experimental results obtained from experiments performed using the procedure described in chapter 3, with the following range of system variables:

System Variable	Range of System Variables
Heat transfer coefficient(H)	2000, 1700, 900 & 56.8 W/m^2C
Initial temperature (TI)	between 3 & 25 C.
Coolant temperature (Tc)	between-4 & -16 C.

Only the Vasil'ev and Uspenskii finite difference method and the Goodman integral method (if the initial temperature is near the freezing temperature) show reasonable comparison with experimental results.

The coolant temperature is shown to be the most important factor effecting freezing rates although the thermal capacity of ice is found to be relatively unimportant. However the thermal capacity of water and the heat transfer coefficient play significant roles in determining freezing rates and should be included in theoretical methods predicting freezing rates. The requirement of including these latter two factors into freezing rate formulas seriously limit the applicability of the Original Planck and Neumann methods. Modifications to Planck's method fail to accurately predict freezing rates due to their assumption of linear temperature profiles in the liquid phase.

Comparison of temperature profiles obtained by the Vasil'ev and Uspenskii method and by experiments reveal that the assumption of neglecting convection effects in the transfer of heat through the body being frozen is supported and that the vast majority of the overall freezing time is occupied by the freezing stage.

5-1 Comparison of theory and experiment

In chapter 4 a range of methods for predicting freezing rates was discussed. Table 5-1 compares the predicted times to freeze a 10 mm layer of water initially at 20 C with a coolant at -10 C through a surface heat transfer coefficient of 2000 W/m^2C.

TABLE 5-1

Predictive Method	Formulation	Freezing Time	% Deviation from Vasil'ev & Uspenskii
Planck	$t=.11x10^5X+.48x10^7X^2$	911	-41
Modified Planck	$t=.12x10^5X+.56x10^7X^2$	1050	-32
Rutov	$t=.13x10^5X+.62x10^7X^2$	1161	-25
Nagoaka	$t=.14x10^5X+.65x10^7X^2$	1218	-21
Neumann	$t=.83x10^6X^2$	431	-72
Goodman	computed value	1256	-19
Vasil'ev & Uspenskii	computed value	1550	(-)

The wide differences of predicted freezing times result from the distinct assumptions of the several methods, and preclude the choice of any of the methods as obviously accurate.

In order to establish the accuracy of the methods comparison with experimental freezing results was needed. The experiments carried out were described in chapter 3.

As discussed in chapter 3 the important experimental variables were; heat transfer coefficient (H), coolant temperature (Tc), and initial material temperature (TI).

Graphs 5-1 to 5-6 show experimental freezing curves and corresponding predicted freezing curves by the following methods. (a) Neumann, (b) Planck, (c) Modified Planck, (d) Rutov, (e) Goodman and (f) Vasil'ev and Uspenskii for the experimental conditions in table 5-2.

TABLE 5-2

Graph	System	Heat Transfer Coefficient	Initial Temperature	Coolant Temperature
		W/m^2C	C	C
5-1	1	2000	3.5	-10.0
5-2	2	2000	20.0	-10.0
5-3	3	2000	25.0	-10.0
5-4	4	2000	20.0	-15.0
5-5	5	900	20.0	-10.0
5-6	6	900	20.0	-15.0

Freezing of Distilled Water

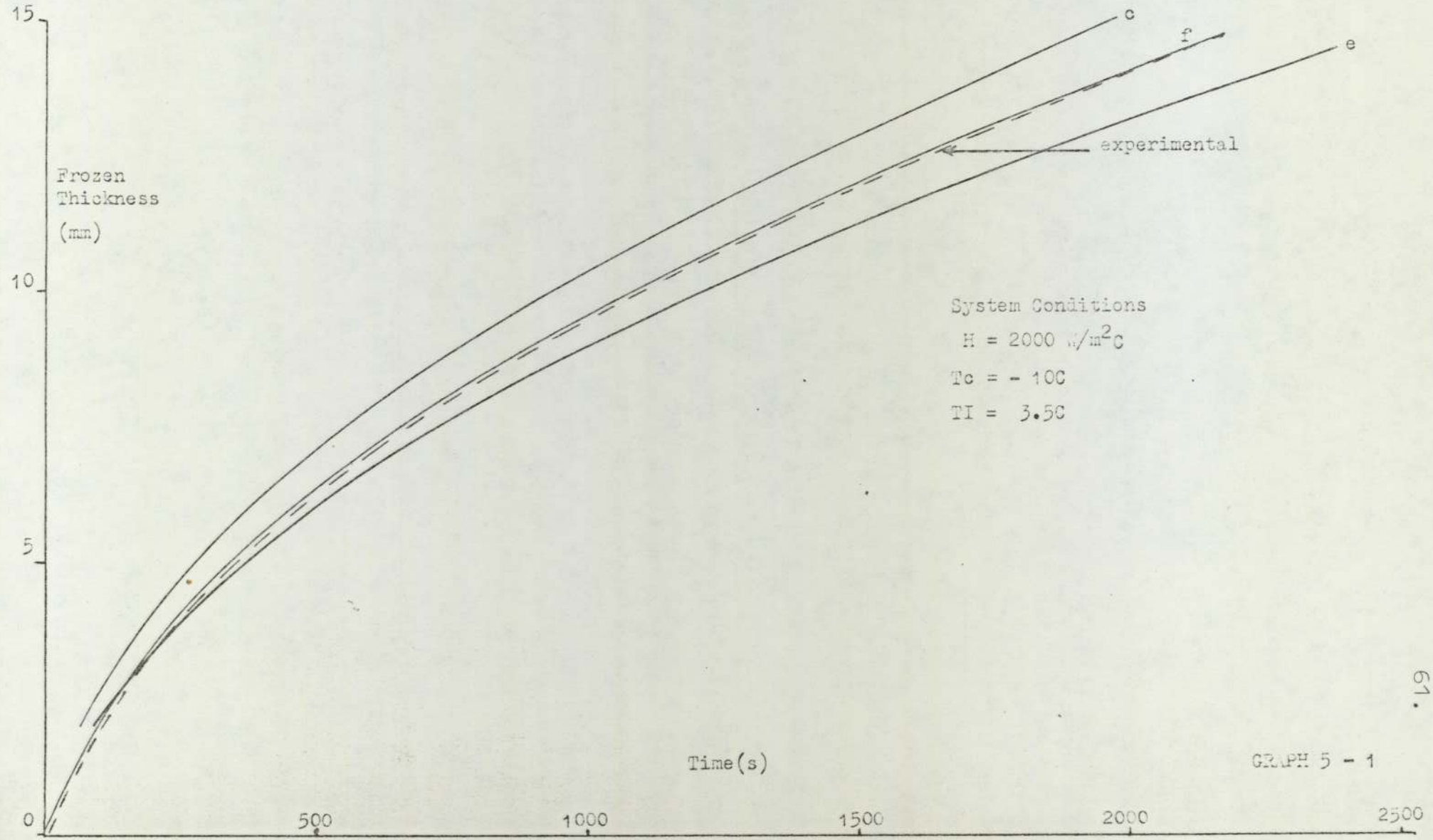

GRAPH 5 - 1

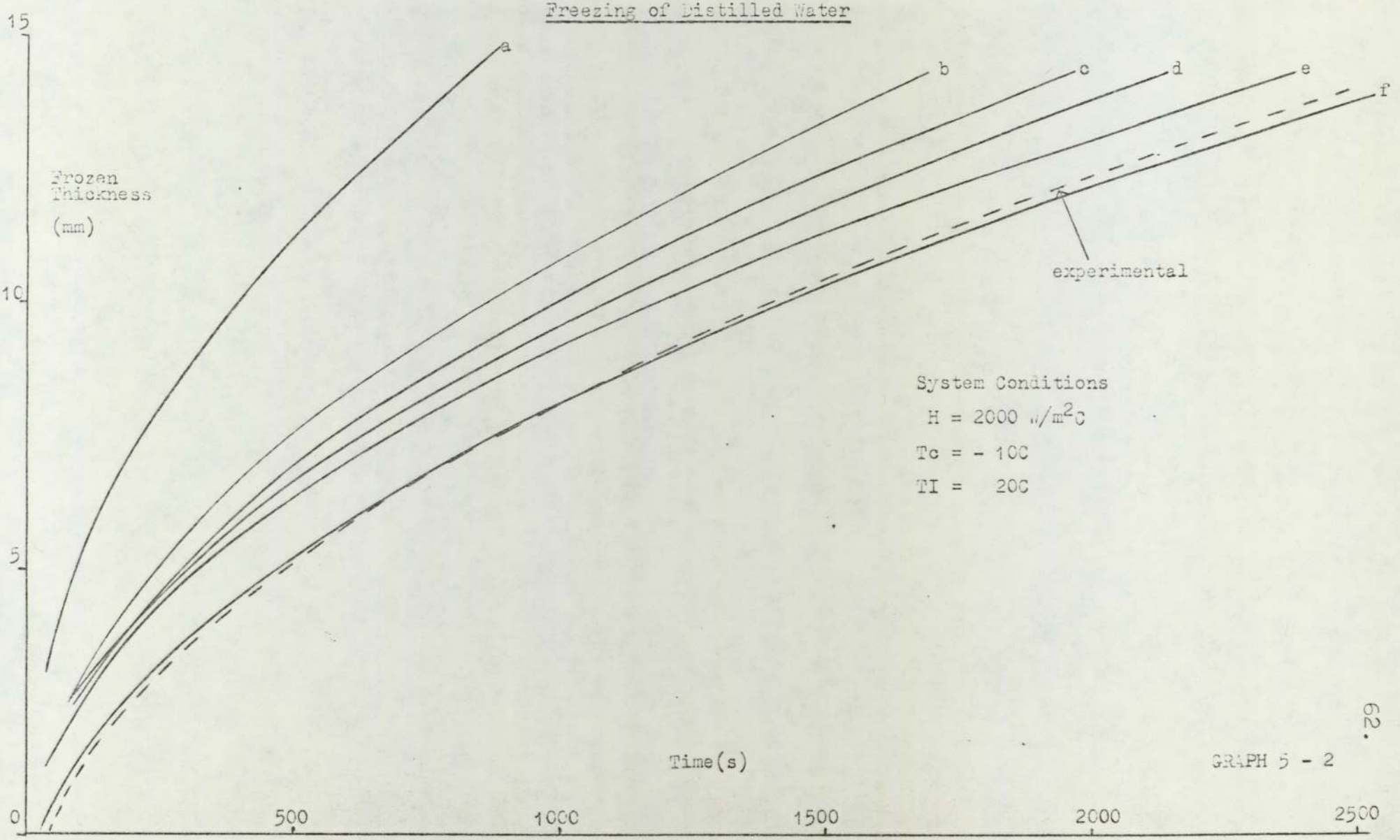
Freezing of Distilled Water
15
10
5
0
Frozen Thickness (mm)
a
b
c
d
e
f
experimental
System Conditions
H = 2000 w/m²C
Tc = - 10C
TI = 20C
Time(s)
500
1000
1500
2000
2500

GRAPH 5 - 2

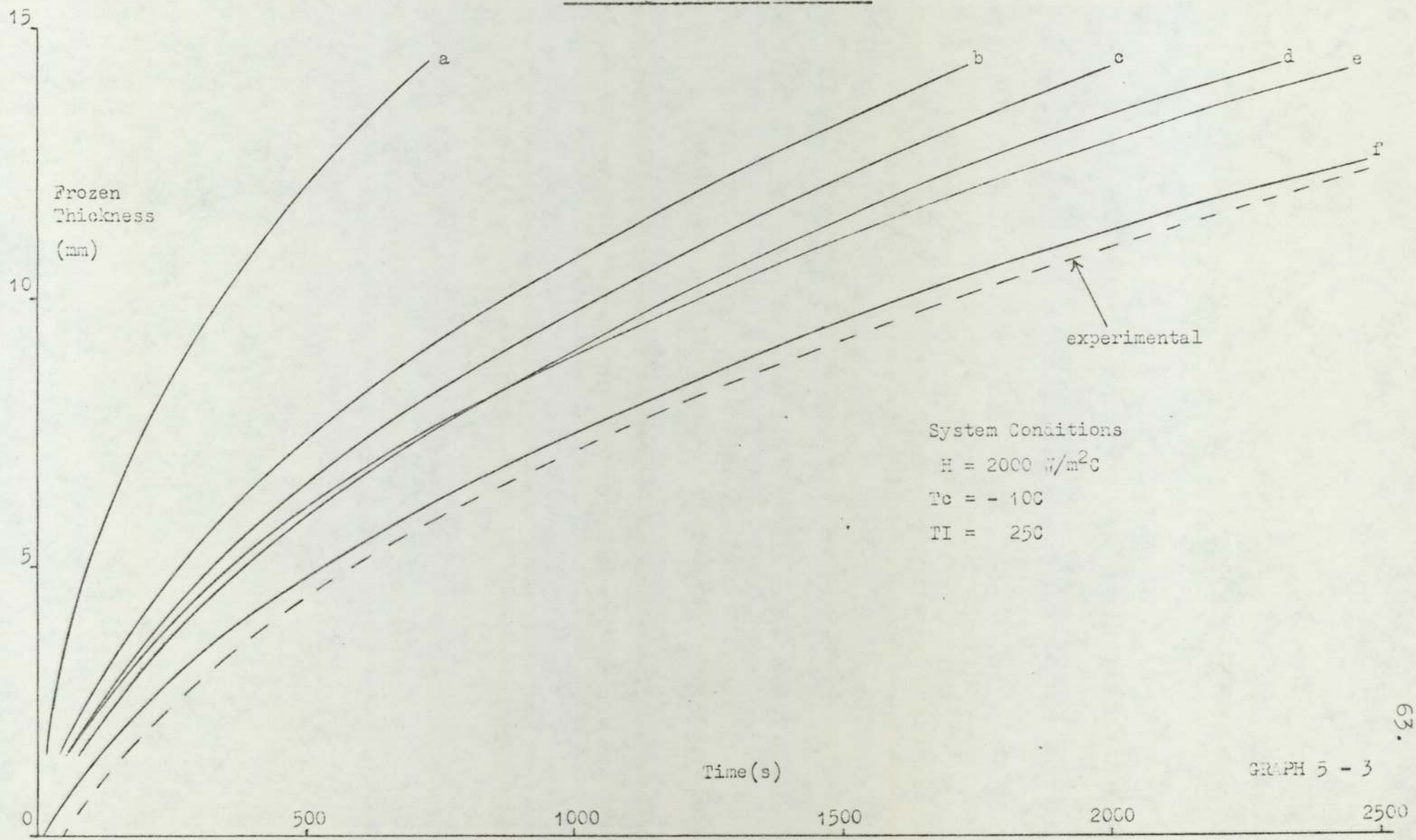
Freezing of Distilled Water
15
10
5
0
Frozen
Thickness
(mm)
a
b
c
d
e
f
experimental
System Conditions
H = 2000 W/m²C
Tc = - 10C
TI = 25C
Time(s)
500
1000
1500
2000
2500

GRAPH 5 - 3

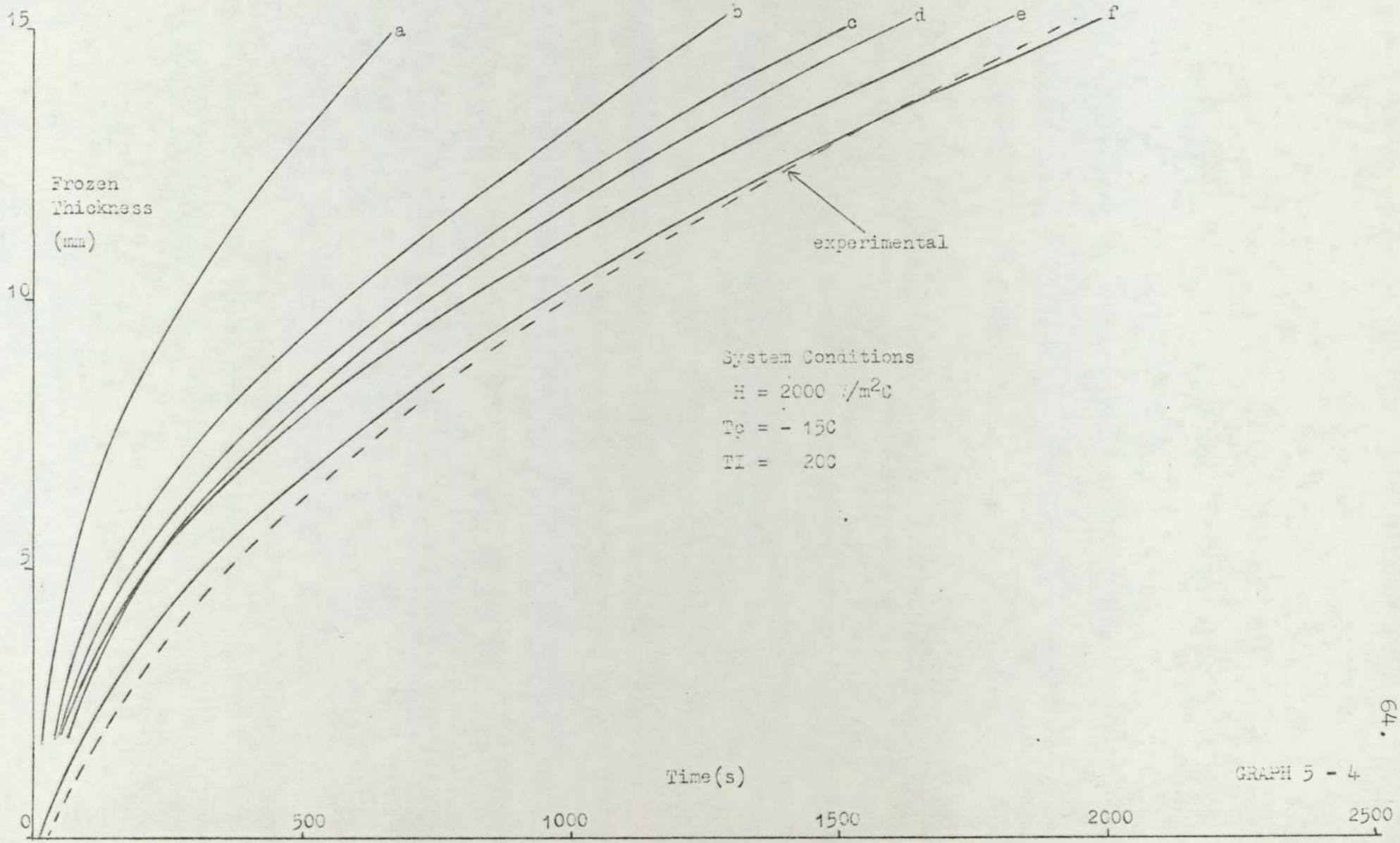
Freezing of Distilled Water
15
10
5
0
Frozen Thickness (mm)
a
b
c
d
e
f
experimental
System Conditions
H = 2000 W/m²C
Tp = - 15C
TI = 20C
500
1000
1500
2000
2500
Time(s)

GRAPH 5 - 4

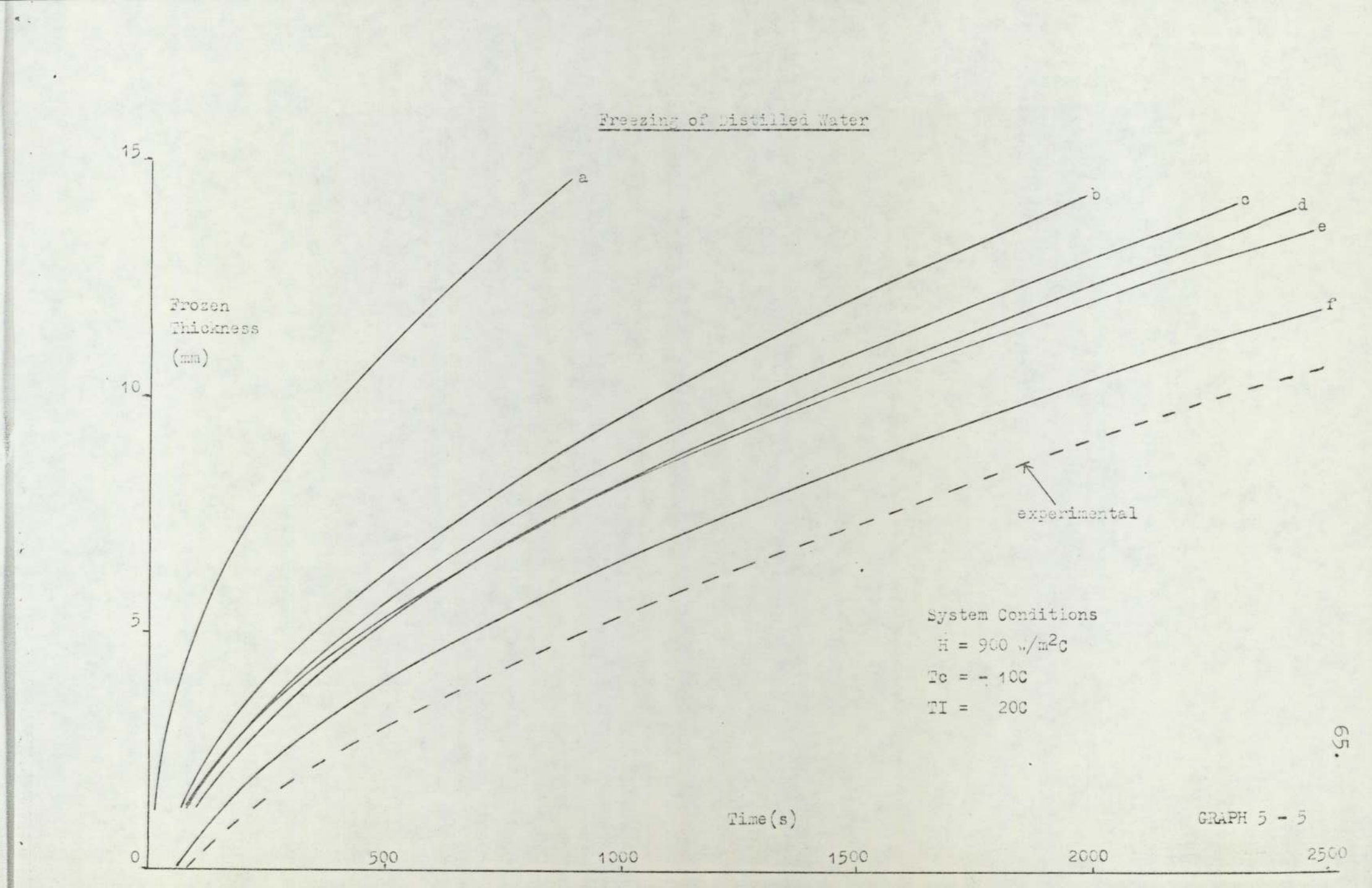
Freezing of Distilled Water
15
10
5
0
Frozen
Thickness
(mm)
a
b
c
d
e
f
experimental
System Conditions
H = 900 w/m²C
Tc = - 10C
TI = 20C
Time(s)
500
1000
1500
2000
2500

GRAPH 5 - 5

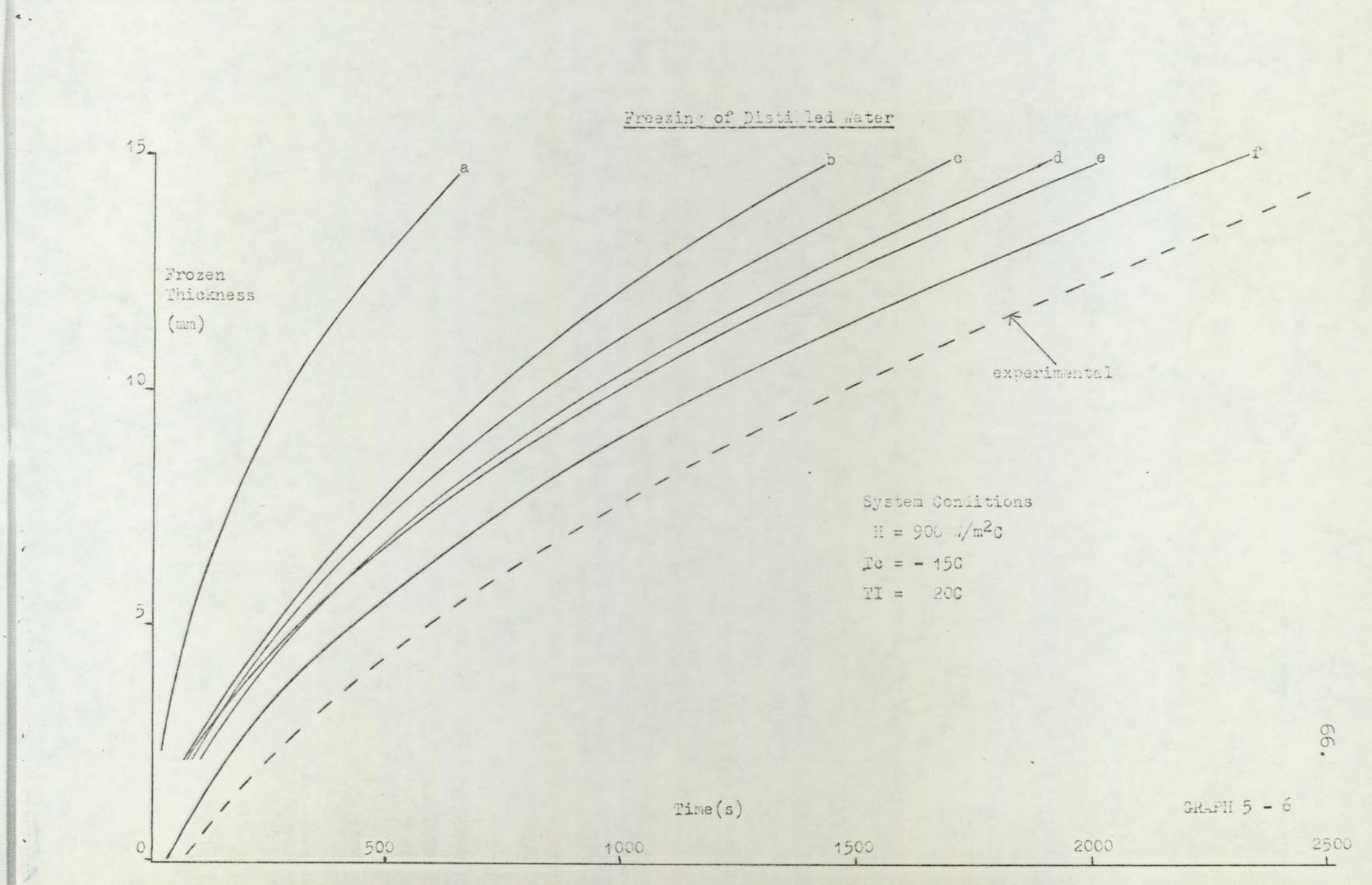
Freezing of Distilled Water
15
10
5
0
Frozen Thickness (mm)
a
b
c
d
e
f
experimental
System Conditions
H = 900 W/m²C
Tc = - 15C
TI = 20C
Time(s)
500
1000
1500
2000
2500

GRAPH 5 - 6

Graphs 5-1, 5-2 and 5-3 show variations in freezing times due solely to changes in TI, graphs 5-3 & 5-4, 5-5 and 5-6 show variations in freezing times due to changing Tc. Changes in freezing times due to altering H are shown by graphs 5-2 & 5-5, 5-4 and 5-6. (Tabulated values for these experimental conditions are given in Appendix 8).

Graphs 5-1 to 5-6 show that theoretical methods, with the exception of the Vasil'ev and Uspenskii method and in one case the Goodman method, under-estimate freezing times. Table 5-3 shows the percentage variation between the experimental and theoretical freezing times in freezing 10 mm of ice for the six system conditions in Table 5-2.

TABLE 5-3

	% Range between experimental and theoretical freezing times using					
SYSTEM	(a) Neumann	(b) Planck	(c) Modified Planck	(d) Rutov	(e) Goodman	(f) Vasil'ev & Uspenskii
1	- 67	- 22	-17	-14	+12	+ 2
2	-235	- 62	-40	-21	-17	+ 2
3	-386	- 97	-67	-28	-43	- 8
4	-242	- 70	-45	-25	-20	- 7
5	-400	-102	-76	-54	-52	-22
6	-390	-102	-75	-51	-50	-27

(minus sign indicates theoretical under-estimation

of experimental freezing times and positive sign overestimation).

The results obtained from Nagaoka's method (see p51) are not shown since they always lie between the freezing times of Modified Planck and Rutov, both of which always underestimate experimental freezing times.

Graphs 5-7, 5-8 and 5-9 show further comparison between experimental and theoretical Vasil'ev and Uspenskii freezing times for different values of H. From the graphs 5-1 to 5-9 and table A8-1 in appendix 8, the most accurate theoretical method can be seen to be that of Vasil'ev and Uspenskii.

A discussion of the effects of the system variables H, TI and Tc along with the determination of temperature profiles, subcooling effects and division of the overall cooling process into the various stages in the overall freezing process follows.

5-2 Effect of Heat Transfer Coefficient (H)

In all experiments undertaken the heat transfer coefficients have finite values (see table 3-1 p42)

Freezing of Distilled Water

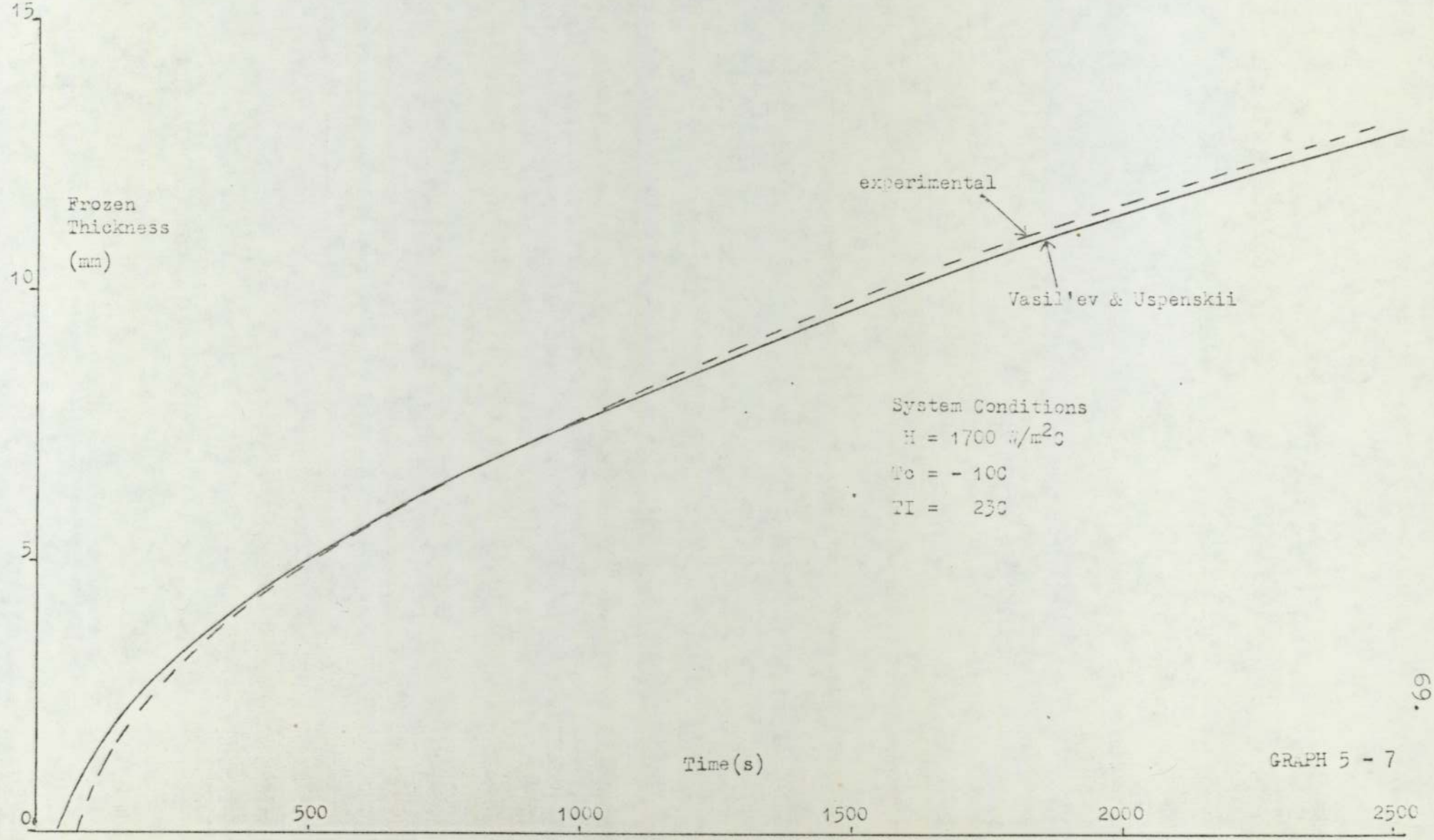

GRAPH 5 - 7

Freezing of Distilled Water

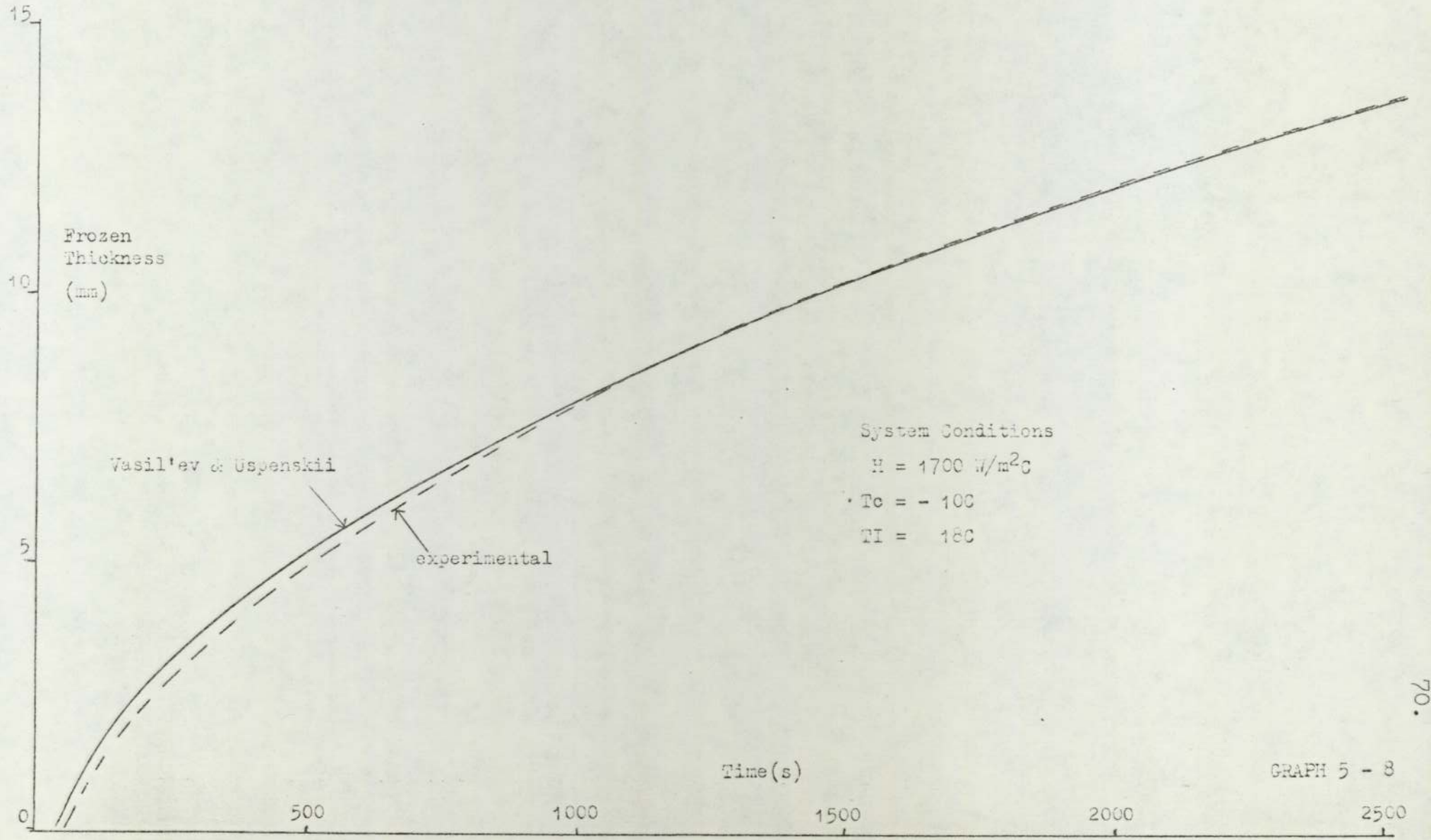

GRAPH 5 - 8

Freezing of Distilled Water

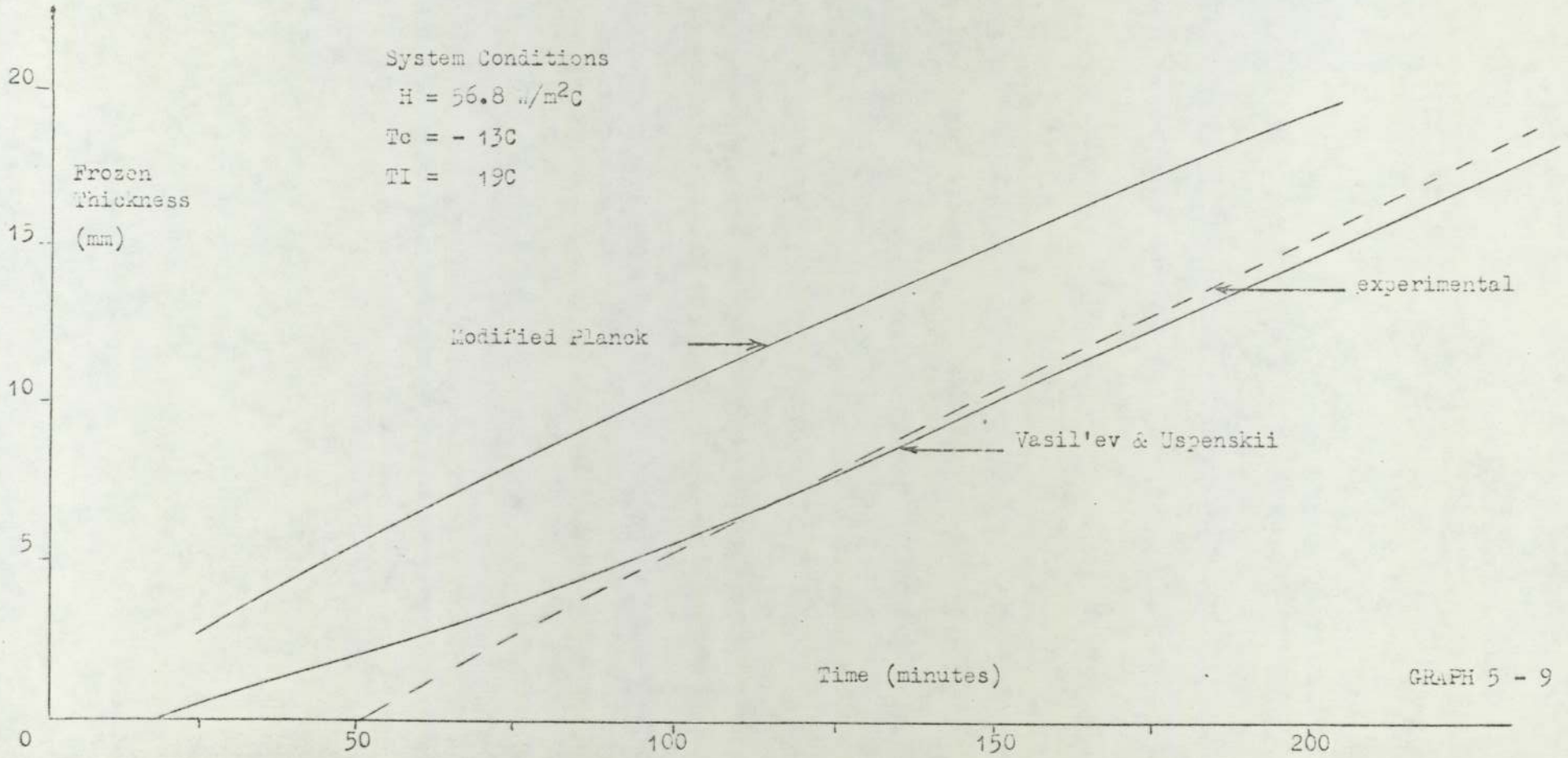

GRAPH 5 - 9

The lower the value of H, the greater the error in the predicted freezing times by Neumanns method (see table 5-3). Accurate knowledge of numerical values of H becomes increasingly important the lower the value of H. This can be illustrated by the following example.

Using the Modified Planck formula, a 100 per cent decrease in the value of H between the values 1700 and 850 W/m^2C increases the freezing time for 10 mm of ice by 450 s. or nearly 5%. In contrast, with the same Tc and TI, varying H between 500 and 250 W/m^2C increases the corresponding freezing time by 1000 s. or 27%.

This effect is seen because at low H values the major resistance to heat transfer (i.e. 1/H) is between the freezing vessel and the coolant whereas at higher H values the resistance of the ice layer predominates. Any change in the major resistance or rate controlling resistance, will be more significant than in a non rate controlling resistance.

5-3 Effect of Initial Temperature (TI)

If the heat transfer coefficient (H) and the coolant temperature (Tc) remain constant, the freezing rate of water decreases with increasing liquid temperature.

The effect of neglecting the thermal capacity of water can be shown by calculating the heat load to reduce the initial temperature of the water to 0 C and then freeze it. When the thermal capacity (C_2) is neglected only the latent heat (L) needs to be removed, however, inclusion of C_2 changes the heat load to (L + C_2 (TI-Tm)). Table 5-4 tabulates heat loads for the two cases with TI = 25 and 3.5 C.

TABLE 5-4 Calculation of heat loads to reduce water temperature.

Heat load required to reduce 1 kg of water from its initial temperature to 0 C, and freeze it (J)	(TI-Tm) 25 C	(TI-Tm) 3.5 C	% change in heat load due to variation in (TI-Tm)
Including thermal capacity	$.54 \times 10^6$	$.34 \times 10^6$	56
Excluding thermal capacity	$.33 \times 10^6$	$.33 \times 10^6$	0
% change in heat load due to inclusion of thermalcapacity	63	4	

The results from table 5-4 show the importance of TI and C_2 in determining the heat load and the errors in predictive methods that ignore TI and C_2 can be seen in table 5-5.

TABLE 5-5 Effect of TI on predicted freezing times.

Method	Freezing Times (s) TI=25.0C	TI=20.0C	TI=3.5C	% Difference due to ΔTI (25-3.5C)
Experimental	1800	1475	1115	61
Vasil'ev & Uspenskii	1715	1507	1099	57
Modified Planck	1078	1050	954	13
Nagaoka	1294	1250	981	24
Rutov	1143	1192	967	18
Planck	911	911	911	0
Goodman	1256	1256	1256	0
% Range in Freezing Times	88	65	18	

Table 5-5 shows that the smaller the temperature difference between initial and freezing (Tm) temperatures is, the more the experimental and theoretical freezing times agree. This is because the error caused by excluding the thermal capacity of water is reduced. Since most freezing operations involve a temperature difference between TI and Tm of at least 15 C inclusion of the thermal capacity of water is required to accurately predict freezing times. With this requirement the Original Planck and Goodman methods became inapplicable. However it should be noted that the Goodman method shows reasonably accurate prediction of freezing times when TI-Tm is small (see table 5-3 system 1 and Graph 5-1).

Goodmans method can therefore be used when the effect of the thermal capacity of water is small. Table 5-5 also shows only small changes (13-24%) in freezing times due to alteration of TI for the Planck, Modified Planck, Nagaoka and Rutov method compared to 61% change in experimental freezing times indicating that the assumption of linear temperature profiles in the unfrozen phase is inadequate (see section 5-5.1 for further discussion on this). Only the Vasil'ev and Uspenskii method predicts the experimental variation of freezing time with TI.

5-4 Effect of Coolant Temperature (Tc)

The most important factor affecting freezing rates is the coolant temperature driving force (Tm-Tc). Table 5-6 shows the effect on experimental freezing times of increasing Tm-Tc by 50% for two values of the heat transfer coefficient.

TABLE 5-6 Variation in freezing times by changing Tc.

Temperature Driving Force Tm-Tc	Experimental Freezing Times (s)	
	H = 2000 W/m^{2}C TI= 20.0 C	H = 900 W/m^{2}C TI= 20.0 C
10	1475	2040
15	1030	1500
% decrease in freezing times	43	36

All freezing methods take into account the coolant temperature and, except the original Planck method, include terms for the thermal capacity of ice. Table 5-7 shows the time to generate 10 mm. of ice for a range of Tc and H values.

TABLE 5-7

METHOD	H=900 W/m^{2}C TI = 20 C Tc (C): - 10	- 15	% difference.	H=2000W/m^{2}C TI=20C Tc (C): - 10	- 15	% difference.
	Freezing Times			Freezing Times		
Modified Planck	1277	859	48	1050	708	48
Goodman	1470	997	47	1256	853	47
Vasil'ev & Uspenskii	1843	1174	56	1507	961	56
Planck	1113	742	50	911	607	50
Experimental	2040	1500	36	1475	1030	43

In table 5-7 the calculated change in freezing time resulting from the change in Tc agrees fairly well with the experimental change, even for Plancks original method. The relative unimportance of the ice thermal capacity compared to the latent heat appears in table 5-8 which gives the specific enthalpy of water measured from a datum temperature of -25 C.

TABLE 5-8

	Water Enthalpy measure from -25 C								
Temperature	-25	-20	-15	-10	-5	0	5	10	15
Specific Enthalpy	0	10.5	21	31.5	42	387	392	397	402

The table shows that the ice thermal capacity contributes only (52.5-21) / (397-21) or 8% of the total enthalpy removed in freezing water from 10 C to -15 C.

5-5 TEMPERATURE PROFILES.

Two thermocouples were positioned in the freezing vessel, one at the coolant surface, to measure the degree of subcooling, and the other 15 mm from the coolant surface, to obtain temperature profiles within the body of the fluid being frozen. Both thermocouples were connected to the Honeywell temperature recorder.

5-5.1 Temperature profiles within the body being frozen.

Table 5-9 compares experimental and theoretical

(Vasil'ev and Uspenskii method) times for the temperature, at a distance 15 mm from the coolant surface, to be reduced to 15, 10, 5 and 0 C for three system conditions.

TABLE 5-9.

METHOD	SYSTEM CONDITIONS	TIME (S) FOR LIQUID TO REACH			
		15 C	10 C	5 C	0 C
Vasil'ev & Uspenskii	H = 2000 W/m^2C	550	1000	1710	3065
Experimental	TI=20 C TC=-10 C	480	940	1720	3100
Vasil'ev & Uspenskii	H = 2000 W/m^2C	500	810	1280	1982
Experimental	TI=20 C TC=-15 C	420	720	1180	1980
Vasil'ev & Uspenskii	H = 2000 W/m^2C	880	1300	2050	3350
Experimental	TI=25 C TC=-10 C	720	1100	1850	3250

Table 5-9 shows fair agreement between experimental and theoretical cooling times. Since the Vasil'ev and Uspenskii method is based solely on conduction heat

transfer through the body of the water the assumption of neglecting convection, as assumed by all the predictive methods, is supported. The applicability of the Vasil'ev and Uspenskii method to provide fairly accurate temperature profiles is also shown.

Figure 5-1 is a comparison of temperatures predicted throughout a body (40 mm in length, 10 mm frozen) using the Modified Planck and Vasil'ev and Uspenskii methods. The figure shows close agreement with linear temperature profiles in the frozen phase but no agreement in the predicted unfrozen temperature profiles. The result of the variation in the temperature profiles is that in equation (1-3)

$$L\rho\frac{dx}{dt} = K_1\left(\frac{\partial T_1}{\partial x}\right) - K_2\left(\frac{\partial T_2}{\partial x}\right) \qquad (1\text{-}3)$$

the term $-K_2\left(\frac{\partial T_2}{\partial x}\right)$ calculated by the Vasil'ev and Uspenskii method is much larger than the value obtained by the modified Planck method using the linear temperature profile. If $-K_2\left(\frac{\partial T_2}{\partial x}\right)$ is too small with the Planck method then $\frac{dx}{dt}$ is too large and hence t, the freezing time too small (from equation 1-3).

Figure 5 - 1 Temperature Profiles Assumed by the Modified Planck Method and Calculated by the Vasil'ev and Uspenskii Method

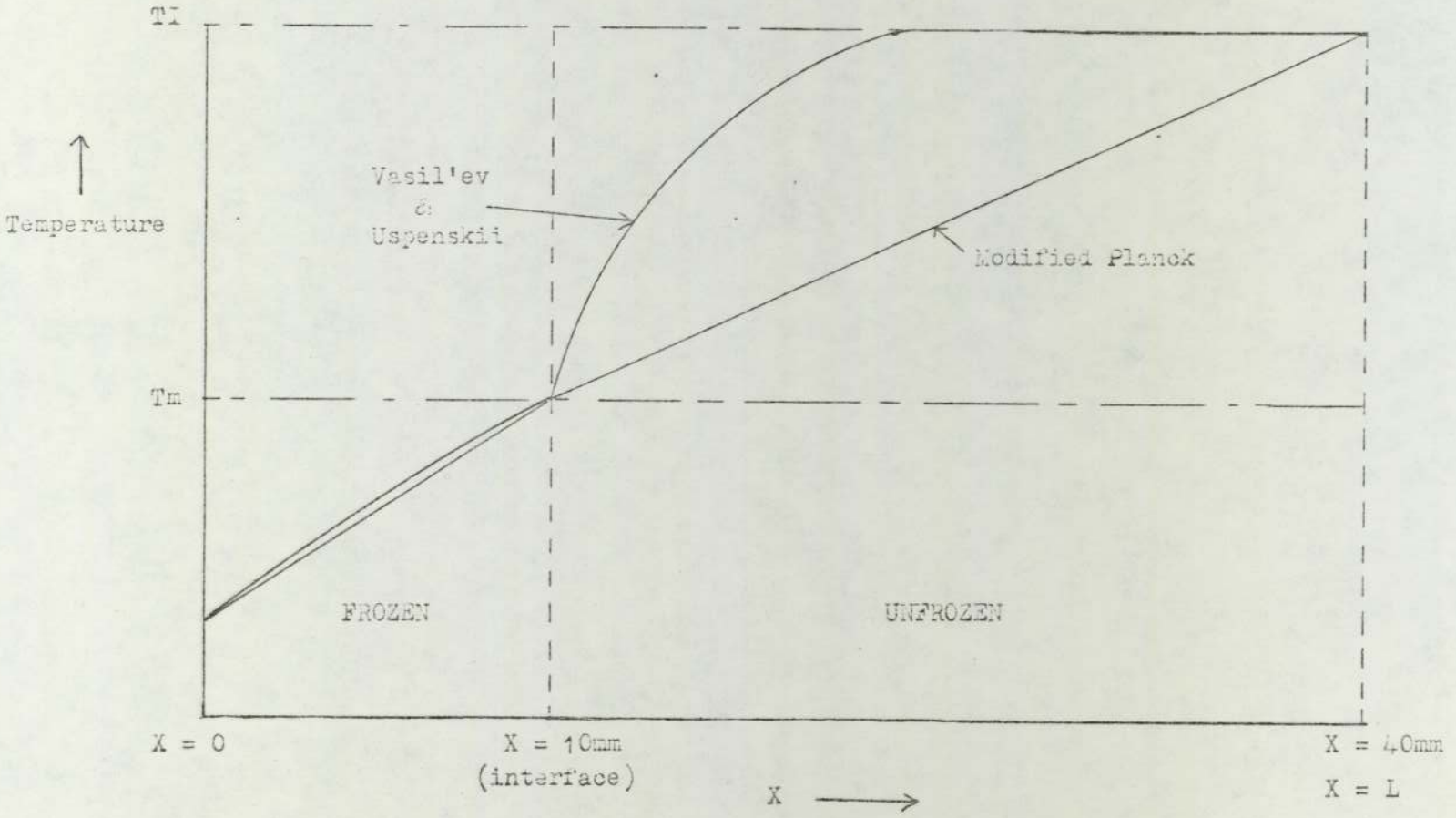

The authors by comparing their own experimental and theoretical freezing times attempted to fit their own correction factor to the Modified Planck method on the same basis as Rutov and Nagaoka but found that no one value could be used for all the experiments performed. This was due to increased inaccuracy with high TI values caused by the assumption of linear temperature profiles. Table 5-10 compares experimental and theoretical results from the Modified Planck method for freezing 10 mm ice by varying TI but maintaining Tc and H constant.

TABLE 5-10

	TI (C)	Experimental Freezing Times (s).	Modified Planck Freezing Times (s)	% Error
Tc = -10 C	3.5	1115	954	-17
H=2000 W/m^{2}C	20.0	1475	1050	-40
	25.0	1800	1078	-67

From these results a correction factor in the formula:

$$t_T = t_p (1 + A(TI - Tm) \qquad (4-4)$$

would have values ranging between 0.048 and 0.0268. Apart from the range of values of A needed these values are greater than the values postulated by Rutov and Nagaoka by a factor of 4 to 10.

5-5.2 Effect of Subcooling.

Experimental subcooling and precooling times were found to be approximately equal (see table 5-11). The degree of subcooling, although generally small, was found to increase with slower freezing rates. Table 5-11 shows a greater degree of subcooling for the system with the low heat transfer coefficient and low overall freezing driving force.

TABLE 5-11 Precooling and Subcooling Stages.

System Conditions	H = 900 W/m^2C Tc = -10 C TI = 20 C	H = 56.8 W/m^2C Tc = -13 C TI = 20 C
Precooling time	40 s	1920 s
Subcooling time	30 s	1440 s
Degree of Subcooling	-2.0 C	-3.4 C

Figure 5-2 is a qualitative comparison of experimental freezing rates, including the precooling and subcooling periods, with the curves predicted by Vasil'ev and Uspenskii method. The figure shows that the Vasil'ev and Uspenskii method (along with the other theoretical methods) does not include the subcooling effect adequately. The describing equations (1-1 to 1-8, Chapter 1) do not take the effect into account. The result of this was that the theoretical freezing stage commenced earlier than the experimental freezing stage. With experiments all the experimental freezing times, except when the stainless steel heat transfer disc was used, converged and crossed the theoretically predicted freezing times of the Vasil'ev and Uspenskii method. The important factor was the total enthalpy removed from the system. The absence of crossover with the stainless steel disc was unexplained.

However as can be seen from table 5-11 the precooling and subcooling stages together occupy only a very small proportion of the overall freezing time.

5-5.3 Division of overall freezing operation into stages.

Table 5-12 compares the experimental and theoretical (Vasil'ev and Uspenskii) times for the precooling and

Figure 5 - 2 Qualitative Comparison of Experimental and Theoretical Freezing Rates

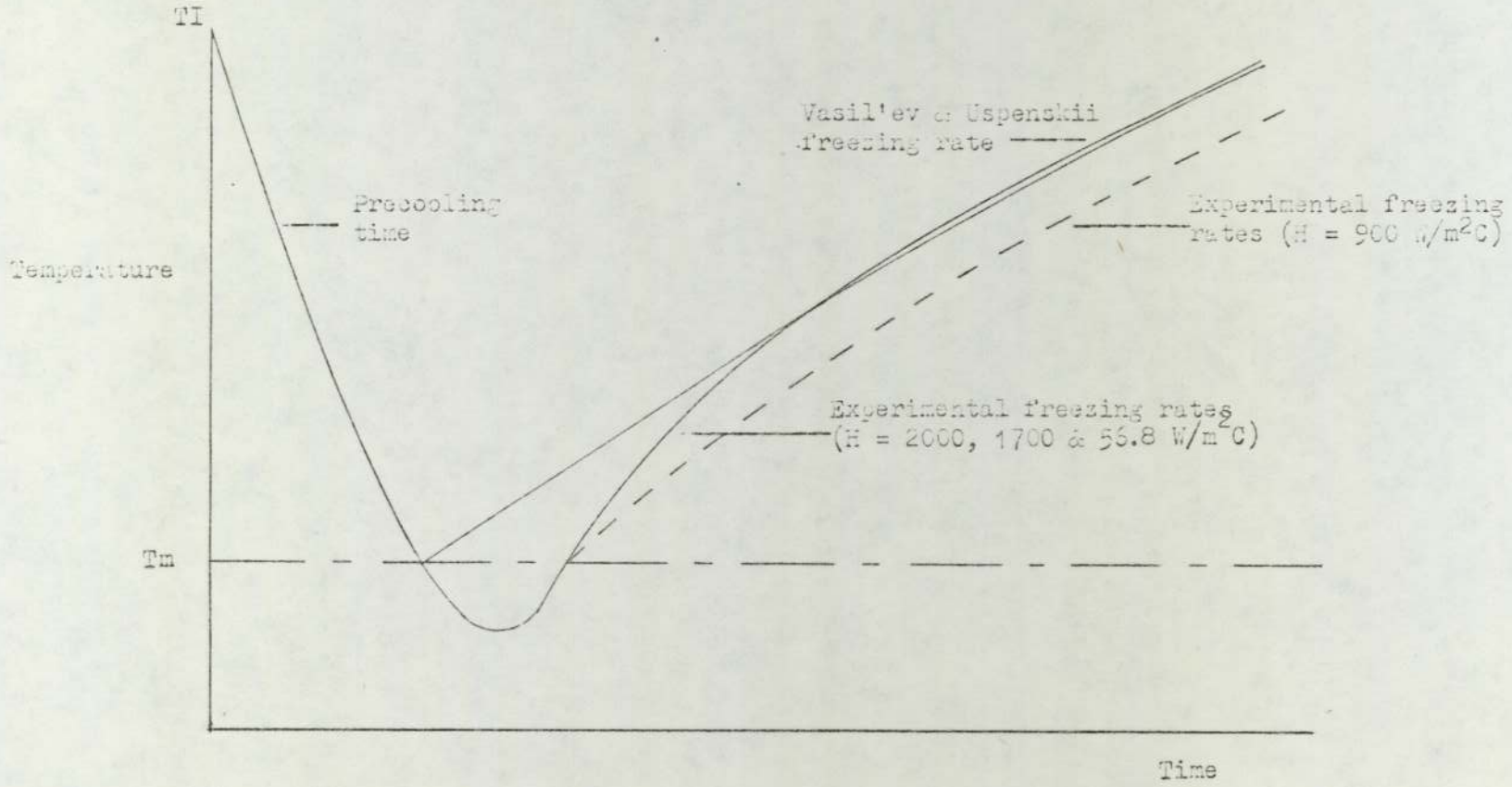

subcooling and freezing stages for two systems. The table shows underestimation of the experimental precooling and subcooling stage by the Vasil'ev and Uspenskii method and slight overestimation of the experimental freezing stage. The variation in the time occupied by the various stages is very marked.

Table 5-12 Comparison of theoretical and experimental precooling and subcooling stages.

System Conditions	Stage	Time (s) Experimental	Time (s) Theoretical
$H=2000\ W/m^2C$ $TI = 25\ C$ $Tc = -10\ C$ Ice thickness = 14 mm.	Precooling & Subcooling	75	49
	Freezing	3050	2967
$H=56.8\ W/m^2C$ $TI = 19\ C$ $Tc = -13\ C$ Ice thickness = 20 mm.	Precooling & Subcooling	3000	1069
	Freezing	14760	15322

Comparison of the overall freezing time (from initial temperature to storage temperature) between theoretical and experimental results was not possible since experimental measurements did not record tempering times. The Vasil'ev and Uspenskii method, however, for all the experiments carried out predicted that the freezing stage occupied about 95% of the overall time and the tempering stage about 3%.

5-6 Conclusions.

1. Heat transfer in the body being frozen is by conduction, convection can be neglected (section 5-5a).

2. The heat capacity of ice can be neglected (it represents only 8% of the total enthalpy removed in freezing water between 15 C and -10 C). Temperature profiles in the frozen phase can be taken to be linear (section 5-4).

3. The heat capacity of water should be included in theoretical formulas (section 5-3). Thus the original Planck and Goodman

methods incur serious errors when TI-Tm is large. The Goodman method however, shows good agreement with experimental result when TI-Tm is small (see graph 5-1).

4. Temperature profiles in the frozen phase are not linear. This leads to inaccuracies in predicted freezing times from the Modified Planck method and the Nagaoka and Rutov extensions to the Modified Planck method since these formulas assume linear unfrozen temperature profiles (section 5-5.1).

5. The heat transfer coefficient in all experiments has a finite value. This leads to very large errors in the freezing times predicted by Newman's solution (section 5-2 and graphs 5-2 to 5-6).

6. The vast majority of the overall freezing time (about 95%) is taken up by the freezing zone (section 5-5.3). The subcooling phase plays little part in the overall freezing time (about 1-2%) and although underestimated can be accounted for by the Vasil'ev and Uspenskii method, (sections 5-5.2 and 5-5.3).

7. The Vasil'ev and Uspenskii method is the most accurate theoretical formula and is the only predictive method to :

   a) Be supported by experimental results in predicting freezing rates of distilled water.

   b) Accurately predict temperature profiles of distilled water.

   The method can be applied to systems :

   a) Involving freezing from high initial temperatures (25 C) to low coolant temperatures (-15 C).

   b) With a wide range of heat transfer coefficients (2000 to 56.8 W/m^2 C).

In chapter 6 comparison is made between the experimental freezing times of aqueous solutions and theoretical predictions mainly using the Vasil'ev and Uspenskii method (as modified by the author, see Appendix 4) since this method is the most accurate in predicting experimental distilled water freezing times.

In Chapter 7 an attempt is made to produce a simple formula representing predictions.

DISCUSSION OF RESULTS FOR AQUEOUS SOLUTIONS.

6-1 INTRODUCTION.

The aim of this chapter is to compare the freezing characteristics of aqueous solutions with those of distilled water and if necessary to extend predictive methods to account for the freezing of aqueous solutions.

The freezing temperature of an aqueous solution is dependent on the liquid interface solute concentration which may steadily increase during freezing due to solute rejection from the solid
The increase in liquid solute concentration will lower the freezing point of the remaining liquid solution resulting in the solution freezing over a temperature range.

Experimental freezing experiments on solutions of different concentrations namely, grapefruit juice, 5 per cent sodium chloride and 10 per cent sodium chloride were carried out under varying system conditions (H, Tc and TI) to determine whether the solute rejection

significantly changed the freezing rate.

Measurements of solute concentrations in both liquid and frozen phases were carried out to determine the actual amount of solute rejected.

The experimental studies were accompanied by an attempt to make a theoretical allowance for the freezing point variation caused by the solute concentration profile set up in the liquid phase by the rejection phenomenon, and to include this freezing point correction factor in the Vasil'ev and Uspenskii prediction of freezing rates.

The effect of heat gain on the freezing rates of the aqueous solutions was considered but found not to alter the freezing times significantly. The effect is briefly discussed at the end of the chapter.

The subcooling effect, although slightly greater with aqueous solutions than with distilled water, was ignored since it represented only a minor proportion of the overall freezing time. The freezing stage occupied the vast majority of the overall freezing time (as for distilled water).

6-2 COMPARISON OF EXPERIMENTAL AND THEORETICAL FREEZING RESULTS FOR AQUEOUS SOLUTIONS.

6-2.1 FREEZING OF GRAPEFRUIT JUICE.

The experimental freezing results of grapefruit juice (origin 104) were found to be very similar to distilled water results with the same system conditions (Tc, TI and H).

The grapefruit freezing point was measured to be -1.0C, the ionic concentration to be equivalent to 1% sodium chloride and the density equivalent to 5% sodium chloride. The other physical properties of grapefruit were taken to be those of distilled water.

Experimental freezing results were compared with the Vasil'ev and Uspenskii and the Modified Planck methods. The results are shown on graphs 6-1 and 6-2 and tabulated in appendix 8, table A8-2.

The results show that the Modified Planck method underestimates freezing times. For the results presented, for freezing 10 mm of frozen layer, the underestimation ranges between 10 and 100%. The Vasil'ev and Uspenskii method has its temperature scales, in both phases, adjusted by 1C to bring the freezing

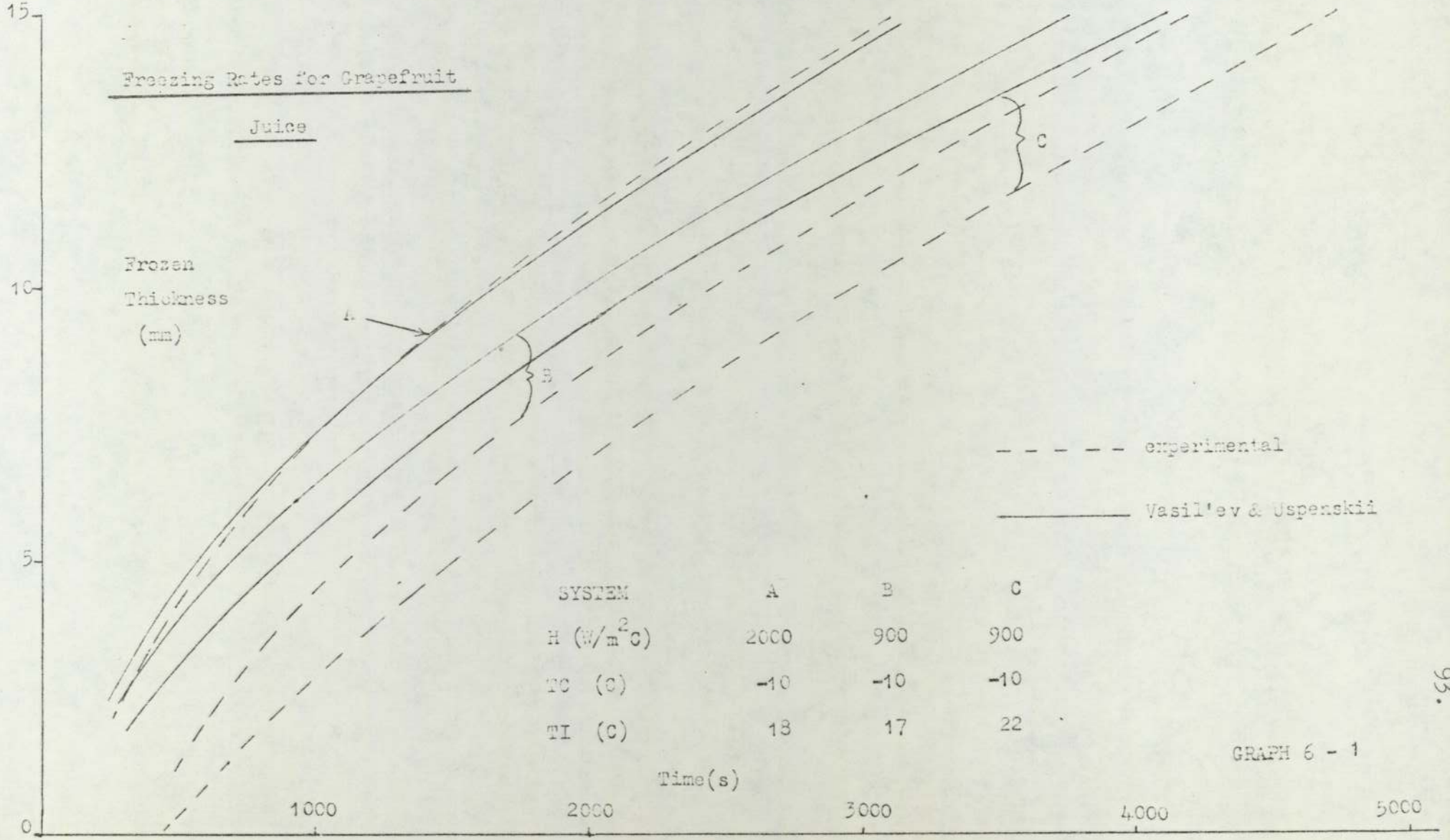

SYSTEM	A	B	C
H (W/m^2C)	2000	900	900
TC (C)	-10	-10	-10
TI (C)	18	17	22

GRAPH 6 - 1

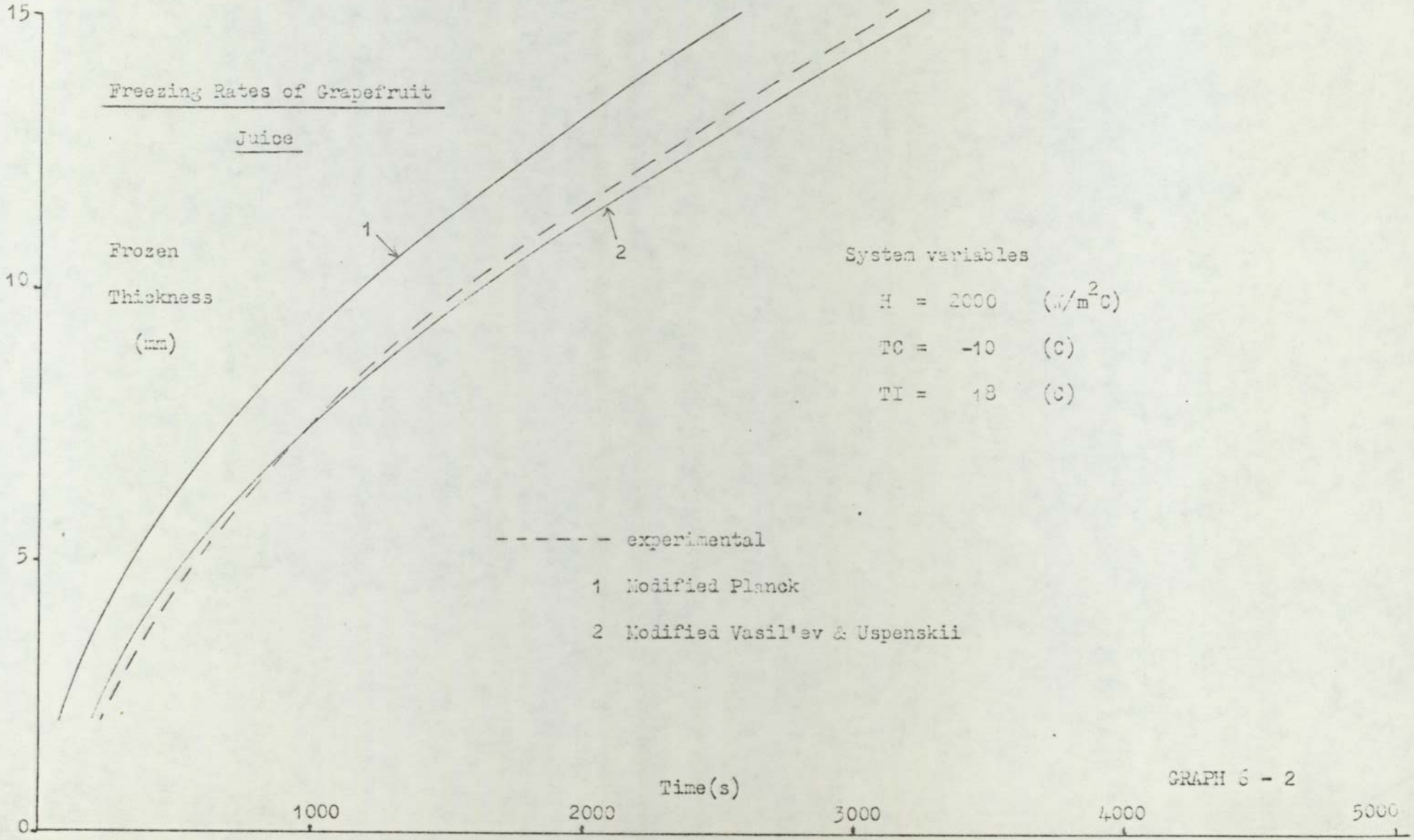
Freezing Rates of Grapefruit
Juice
Frozen
Thickness
(mm)
15
10
5
0
1
2
System variables
H = 2000 (W/m²C)
TC = -10 (C)
TI = 18 (C)
experimental
1 Modified Planck
2 Modified Vasil'ev & Uspenskii
Time(s)
1000
2000
3000
4000
5000

GRAPH 6 - 2

point back to 0C.

Comparison of experimental and Vasil'ev and Uspenskii results show good agreement (see table 6-1).

TABLE 6-1 FREEZING OF GRAPEFRUIT JUICE.

SYSTEM	Experimental Freezing Time (s)	Modified Planck (s)	% error	Vasil'ev and Uspenskii (s)	% error
Tc=-11C, TI=15 C H=900 W/m^2 C	1740	1249	-39	1711	-2
Tc=10 C, TI=-16C H=2000 W/m^2C	1182	1074	-10	1278	+8

There is the same convergence and crossover of the experimental and theoretical freezing curves as experienced with distilled water with H=2000 W/m^2C while with H=900 W/m^2C the theoretical predictions slightly underestimate freezing times.

For the grapefruit juice it can be concluded that the effect of reducing the freezing temperature by a constant value of -1.0 C can adequately account for its freezing times for all experiments.

6-2.2 FREEZING OF 5% AND 10% SODIUM CHLORIDE SOLUTIONS AND SOY BEAN CURD.

Comparison of experimental and theoretical results from the Modified Planck and Vasil'ev and Uspenskii methods are given in graphs 6-3 and 6-4 and tabulated in appendix 8, tables A8-3 and A8-4.

In the Vasil'ev and Uspenskii method adjusted temperature scales are used in order to maintain the freezing temperature at 0 C. (For example for 5% NaCl the initial and coolant temperatures are defined as TI = TI + 3.0 and Tc = Tc + 3.0 since -3.0 C is the freezing point of 5% NaCl. For 10% NaCl the temperature scale is changed by 6.6 C).

Analysis of these results shows a marked difference in the degree of agreement between the experimental and theoretical results depending on the rate of freezing.

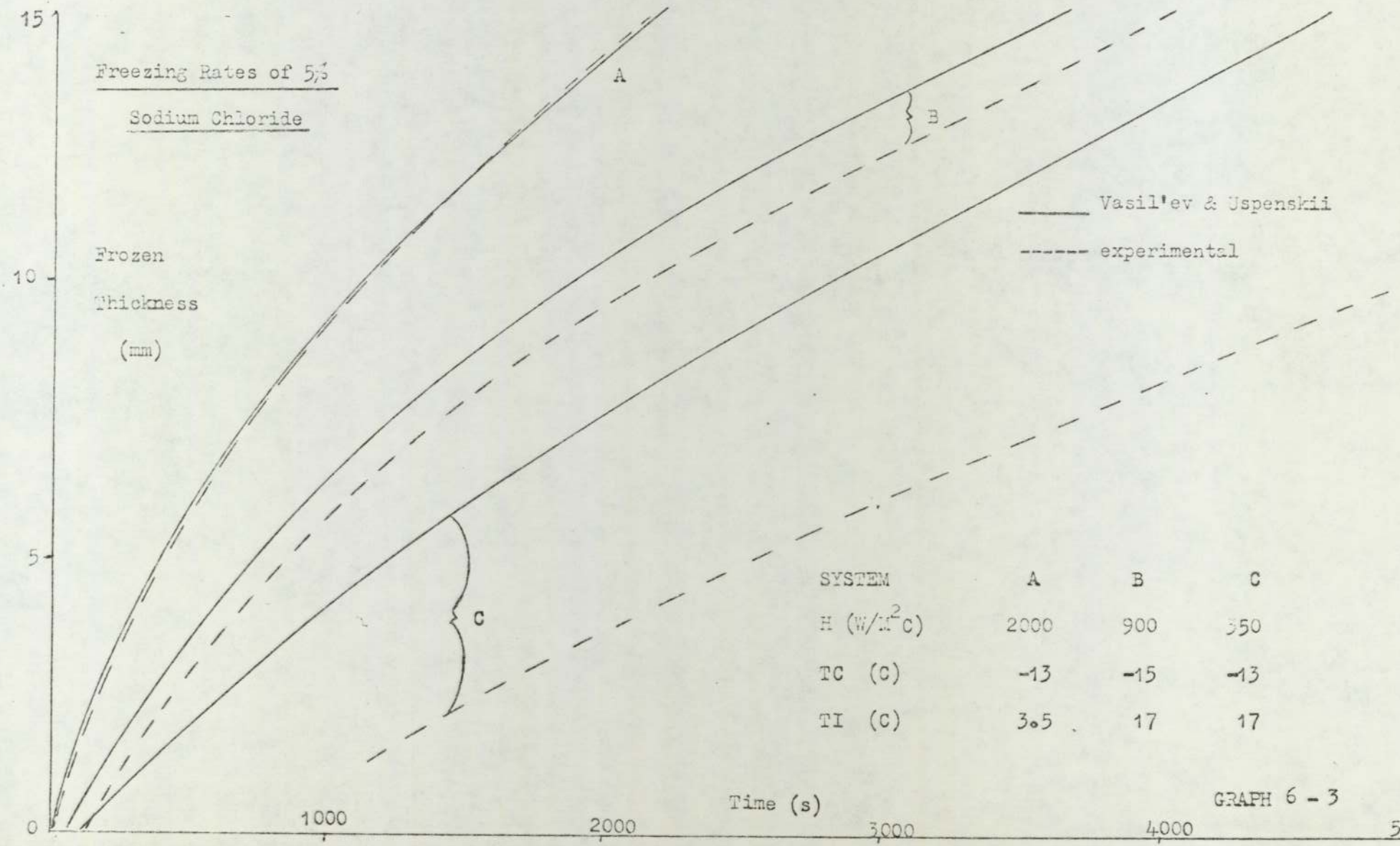
Freezing Rates of 5% Sodium Chloride
Frozen Thickness (mm)
15
10
5
0
1000
2000
3000
4000
5000
Time (s)
A
B
C
Vasil'ev & Uspenskii
experimental
SYSTEM A B C
H (W/M²C) 2000 900 350
TC (C) -13 -15 -13
TI (C) 3.5 17 17

GRAPH 6 - 3

Freezing Rates of 10% Sodium Chloride

---------- experimental

_____Vasil'ev & Uspenskii

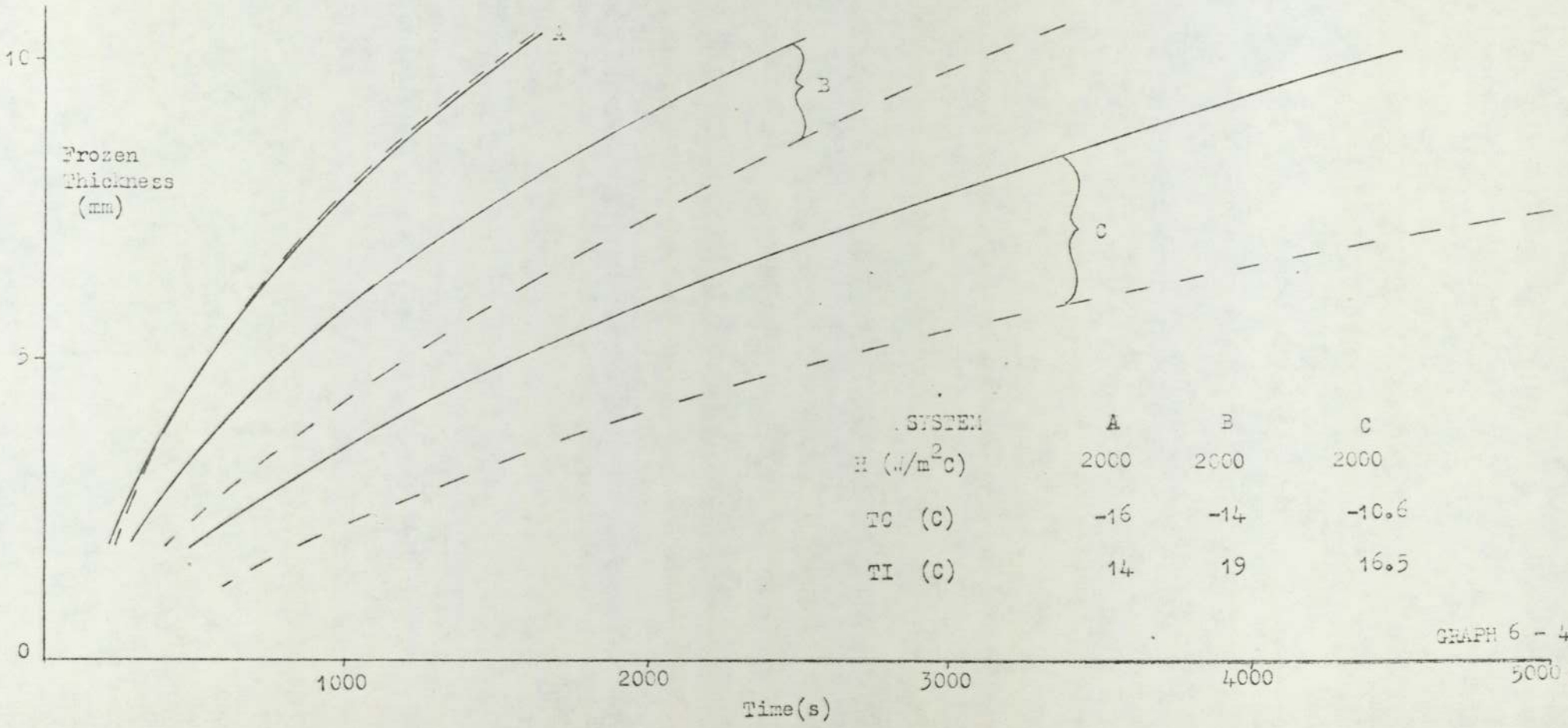

SYSTEM	A	B	C
H (W/m^2C)	2000	2000	2000
TC (C)	-16	-14	-10.6
TI (C)	14	19	16.5

GRAPH 6 - 4

One group of experiments compared the freezing times of distilled water, 5 per cent sodium chloride and 10 percent sodium chloride under conditions of identical temperature differences. This entailed adjusting the initial and coolant temperatures so (Tm-Tc) and (TI-Tm) were the same for the three liquids.

Table 6-2 shows the initial and coolant temperatures used for the three liquids in order to obtain the temperature differences (Tm-Tc) equal to 10 C and (TI-Tm) equal to 20 C.

Under these identical temperature driving forces (Tm-Tc and TI-Tm) with system conditions for a fast freezing rate of .005 mm/s distilled water, 5% NaCl and 10% NaCl froze at the same rate (see table 6-2 and graphs 6-5 and 6-6).

TABLE 6-2.

SYSTEM CONDITIONS	SOLUTION		
	DISTILLED WATER	5% NaCl	10% NaCl
H (W/m^2 C)	2000	2000	2000
Tc (C)	-10.0	-13.0	-16.5
(Tm-Tc) (C)	10.0	10.0	10.0
TI (C)	20.0	17.0	13.5
(TI-Tm) (C)	20.0	20.0	20.0
ICE THICKNESS (mm)	FREEZING TIME (S)		
2.0	182	189	192
6.0	690	700	710
10.0	1475	1470	1500

Comparison of Experimental Freezing Curves for Distilled Water, 5% and 10% NaCl Solutions

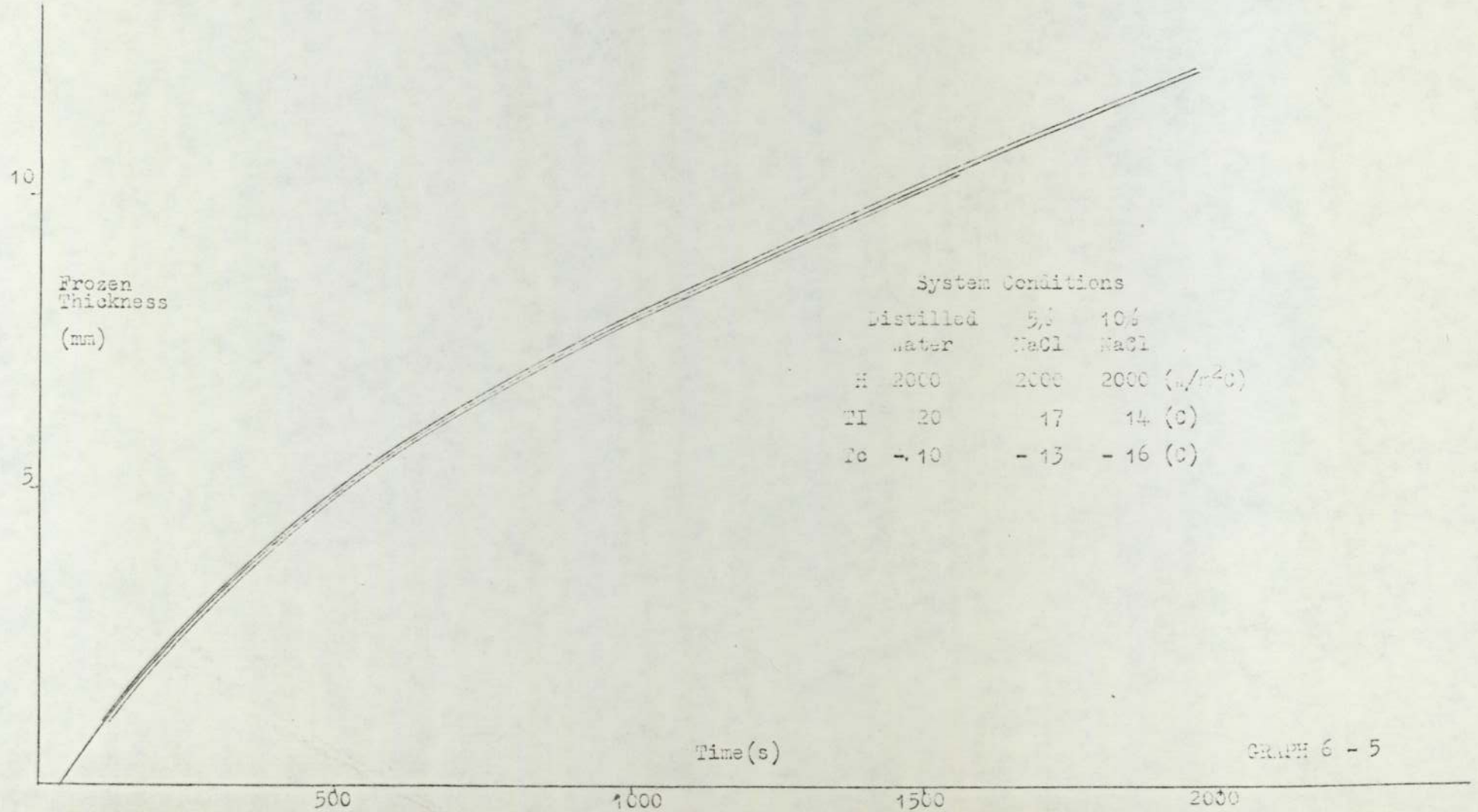

GRAPH 6 - 5

Comparison of Experimental Freezing Results for 5% NaCl Solution
and Modified Planck and Vasil'ev and Uspenskii Theoretical Methods

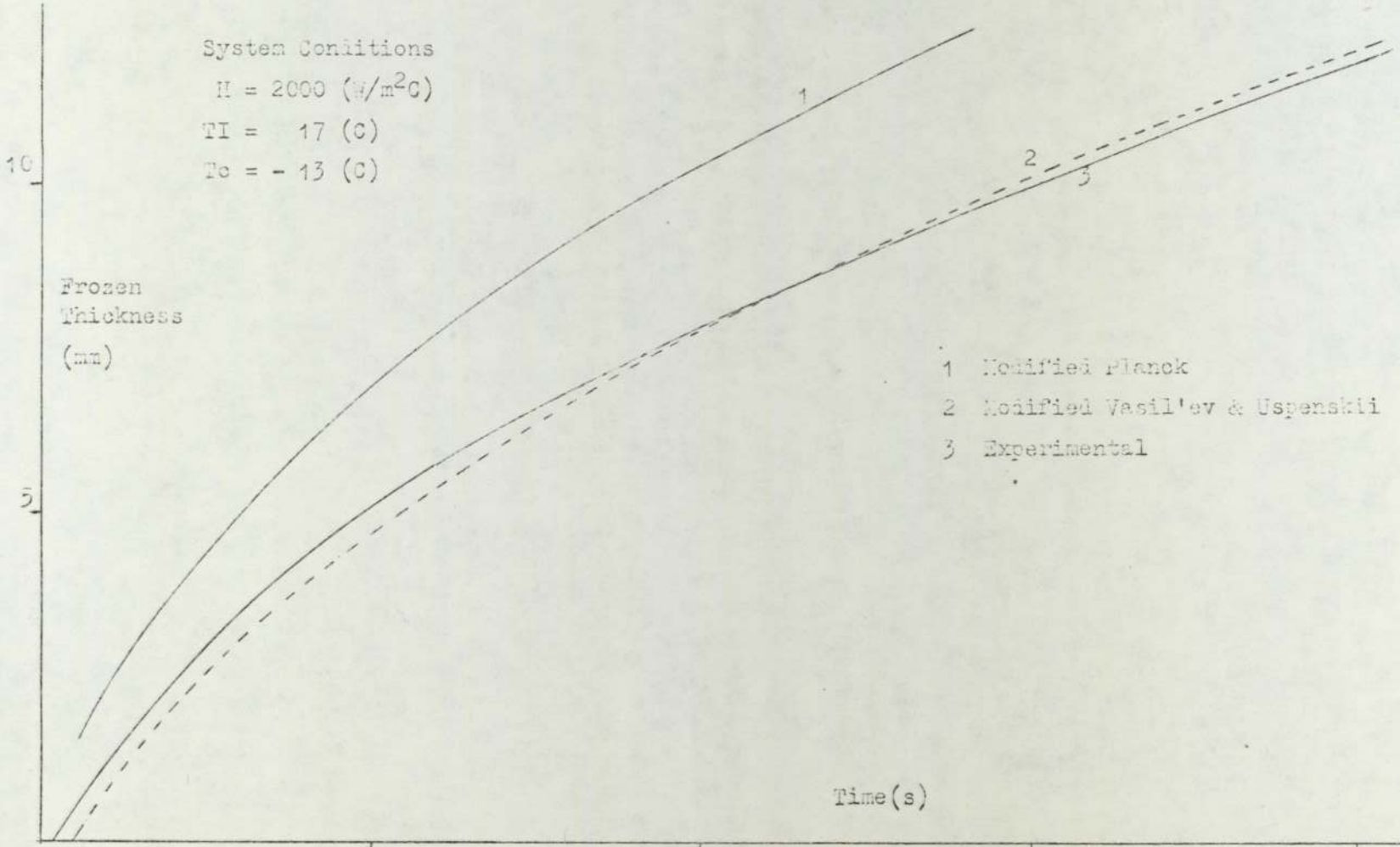

GRAPH 6 - 6

Under these freezing rates agreement between theoretical and experimental results was of the same order as with distilled water and grapefruit juice and the Vasil'ev and Uspenskii method can be said to predict the solution freezing rate adequately by adjustment of temperature scales.

When the sodium chloride solutions were frozen at a slow freezing rate of .0012 mm/s the Vasil'ev and Uspenskii method significantly underestimated (up to 40%) freezing times (see graphs 6-3 and 6-4) and adjustment of temperature scales no longer was sufficient to account for the freezing of the aqueous solutions.

A comparison was made between the experimentally determined freezing rates of Soy Bean Curd, published by Komari (32), and the theoretically predicted freezing times calculated by the Goodman, Modified Planck, Nagaoka and Vasil'ev and Uspenskii methods, The results are tabulated, for two systems in Appendix 2. The results show that all the theoretical methods underestimate the experimental freezing times with the Goodman and Vasil'ev and Uspenskii methods being the least inaccurate of the predictive methods. (It should be noted that the initial temperature of the soy bean curd in the experiments performed was equal to the freezing

point or 4 C above the soy bean curd freezing point). The freezing point of the soy bean curd was quoted as O C by Komari.

The discrepancies between experimental and theoretical freezing times for the electrolyte solutions and soy bean curd may have been due to the watery solutions freezing over a range of temperatures.

Experiments to show the amount of solute rejected are given in the next section. Theoretical work on the effect of solute migration in the freezing of electrolyte solutions is then discussed in section 6-4.

6-3 EXPERIMENTAL DETERMINATION OF SOLUTE REJECTED FROM FROZEN PHASE ON FREEZING.

A conductivity bridge was used to determine solute concentrations of the initial solution and frozen phase. (After an experimental run the unfrozen phase was poured off, the frozen phase allowed to thaw and its conductivity then measured). Calibration of the conductivity bridge permitted direct conversion of the readings in mmho/cm to concentrations (moles/litre). Table 6-3 shows concentration results from

experiments using heat transfer coefficients of 2000 and 350 W/m^2 C, with TI = 17.0 C and Tc = -13.0 for 5% NaCl.

TABLE 6-3.

Heat Transfer Coefficient	Bulk Initial conc. (C_∞). kmol/m^3.	Frozen Phase conc. (C_1) kmol/m^3.	$C_\infty - C_1$ kmol/m^3	Ice thickness X_1 (mm)
350	.72	.62	.10	10
350	.74	.65	.09	12
350	.81	.74	.07	13
2000	.82	.79	.03	20
2000	.84	.81	.03	15

The results from table 6-3 show that the amount of rejected solute was small in all experiments but the amount was greater the slower the solution froze (i.e. H = 350 W/m^2 C). The amount of solute rejected seemed to be independent of the ice thickness. The range of values of $\bar{C}_\infty - \bar{C}_1$ from table 6-3 (0.1-0.03 kmol/m^3) may be compared with the figure of 0.085 kmol/m^3 for $\bar{C}_\infty - \bar{C}_1$, when

$\bar{C}_{\infty}$ = 1.0 kmol/m^3 and $\bar{C}_1$ = 0.915 kmol/m^3, given by Grange etal, see section 6-4.3.

6-4 THEORY OF FREEZING OF ELECTROLYTE SOLUTIONS.

6-4.1 Introduction.

A solution originally containing a homogeneous distribution of a solute, experiences a redistribution of this solute on solidification resulting from the difference in solubility of the solute in the solid and liquid phases.

Rejected solute will distribute itself completely throughout the unfrozen phase if the thermal driving force is small enough to allow equilibrium solidification to occur. However, in practice, true equilibrium solidification is seldom approached. This is due to the thermal diffusivities of water and ice being respectively approximately 100 and 1000 times greater than the diffusion coefficient of NaCl in water. As a result, solute rejected at the advancing frozen-unfrozen interface cannot undergo infinite diffusion into the bulk unfrozen phase, but forms a solute-rich region of layer in the unfrozen phase adjacent to the interface. The existence of a solute rich layer has been reported by Grange, Viskanta and Stevenson (70) and Terwilliger and Dizio (71) for freezing of finite and semi-infinite systems respectively of sodium chloride solutions.

The conclusions to be drawn from both studies are :

1. A small proportion only of the solute is rejected by the frozen phase. Solute remains in the frozen phase due to bulk entrapment.

2. The solute rich liquid layer, X_3 is very small, its thickness being inversely related to the thermal driving force and directly related to the frozen layer thickness, X_1.

3. The freezing temperature is dependent on the liquid interface solute concentration, $\bar{C}i$. Since $X_1 \gg X_3$ a small decrease in the solid solute concentration can greatly affect $\bar{C}i$.

4. The concentration gradient in X_3 is very steep and can be represented by an exponential curve.

5. Solute concentration in the frozen layer was found to be constant for semi-infinite systems but variable for finite systems.

6-4.2 Work on Semi-Infinite Systems (Terwilliger & Dizio).

Terwilliger and Dizio state that the enriched solute boundary layer may lead to supercooling. The phenomenon of supercooling was first described by Rutter and Chalmers (105) to explain the solidification of alloys when an impurity was present.

Owing to the very steep concentration gradient in the melt at the interface, the solidification temperature of the melt increases sharply from a value corresponding to the interface concentration $\bar{C}i$, to one corresponding to the bulk concentration, $\bar{C}\infty$. Within this region however, the actual temperature distribution may lie below the solidification temperature profile and account for supercooling, (see figure 6-1).

If supercooling occurs, an unstable situation may develop. Tiller etal (106) concluded that the interface crystal morphology changed to reduce supercooling. This principle was extended by Terwilliger and Dizio who produced the following expression for the critical interface concentration, $\bar{C}i^*$, above which supercooling will occur :

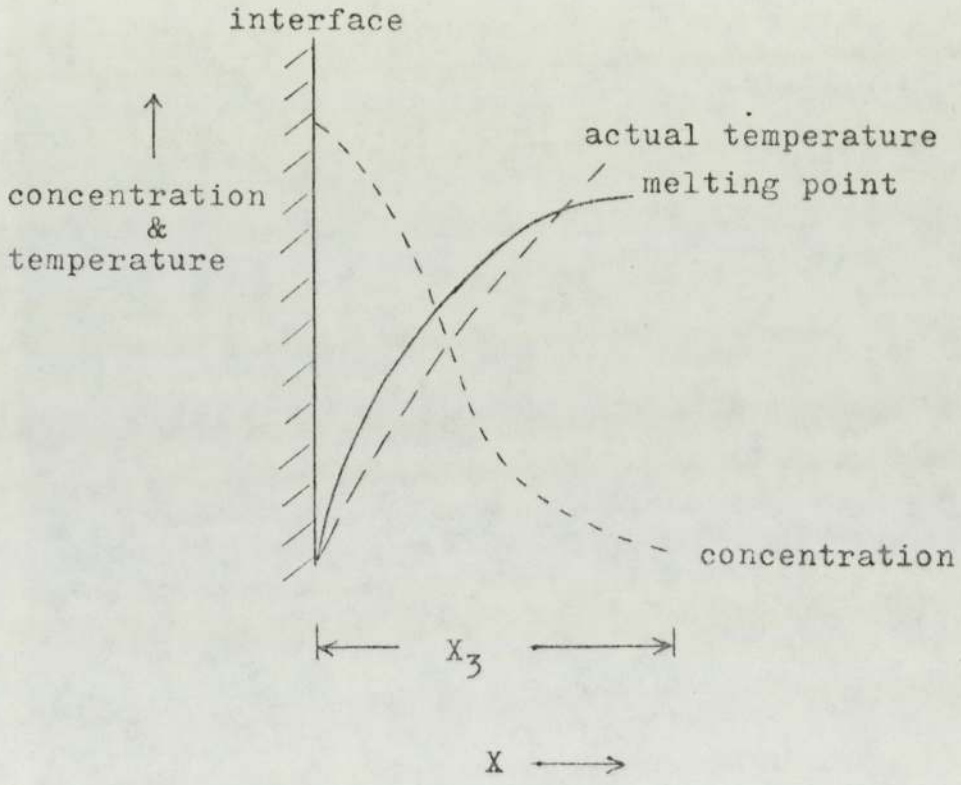

Figure 6-1 Supercooling effect
(Subcooling)

$$\bar{C}i \geq \bar{C}\infty + \frac{\sqrt{\frac{\gamma}{2\alpha_2 \pi}}\, e^{\left(\frac{-\gamma(1-w)^2}{2\alpha_2}\right)} (TI-Ti)}{(1-w)\frac{\gamma}{2D}\, m\, erfc\left(\frac{\gamma}{2\alpha_2}(1-w)\right)} \qquad (6-1)$$

(The term w in equation 6-1 is a dimensionless density correction factor $1-\rho_1/\rho_2$).

Terwilliger and Dizio state that the system will always try to return to the stable situation of $\bar{C}i^*$. Evaluation of equation 6-1 involves substitution of the interfacial temperature Ti by $Tm-m\bar{C}i$ and determination of the unknown constant γ. γ is determined from a Neumann type expression relating the ice thickness and time as :

$$X_1(t) = \sqrt{2\,\gamma\, t} \qquad (6-2)$$

Terwilliger and Dizio define an effective distribution coefficient, $Ke = \bar{C}s/\bar{C}\infty$ to describe solute redistribution. There is considerable disagreement about Ke being a function of freezing rate. Johnson (107) found Ke to be a constant for all runs. Adams (108) found Ke to be directly proportional to freezing rate in the freezing of sea water, while Weeks (109) reports the quantity ln ((1/Ke)-1) to be directly

proportional to the freezing rate. Terwilliger and Dizio conclude from their own experiments that Ke is only an indirect function of the freezing rate and can be taken to be constant. They also state that there is greater purification at low thermal driving forces than at high thermal driving forces.

The explanation of greater purification with slow thermal driving rates can be shown by the following example. Consider two solutions, having the same initial concentration and temperature, being frozen at different thermal driving forces. At a given freezing rate, the boundary layer thickness will be uniquely determined.

If the same value of $\bar{C}i$ is present in both systems, (assumed from equation 6-1) the same amount of excess solute will be contained in the two boundary layers at a freezing rate common to both systems. But the amount of ice already formed when the interface reaches the same particular velocity will be less at the lower driving force. Consequently, the solid phase depletion must necessarily be greater. Figure 6-2 illustrates this principle.

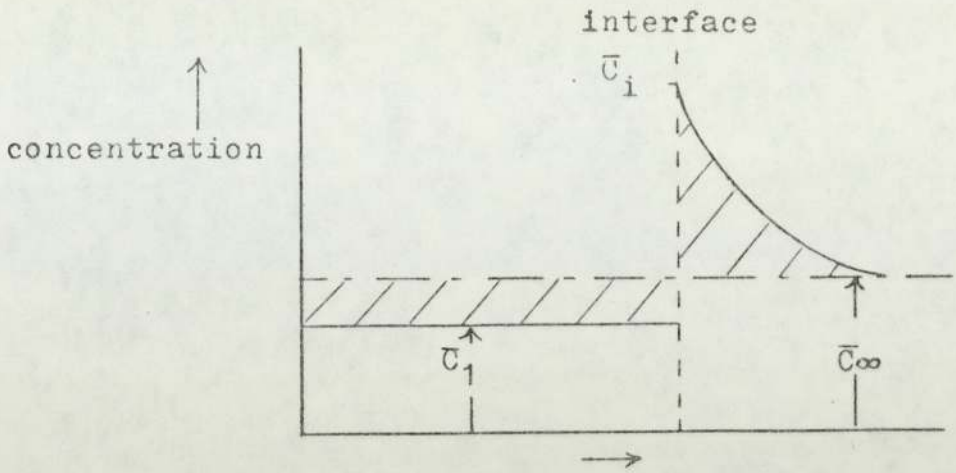

6-2a Theoretical solute distribution at high solidification driving force

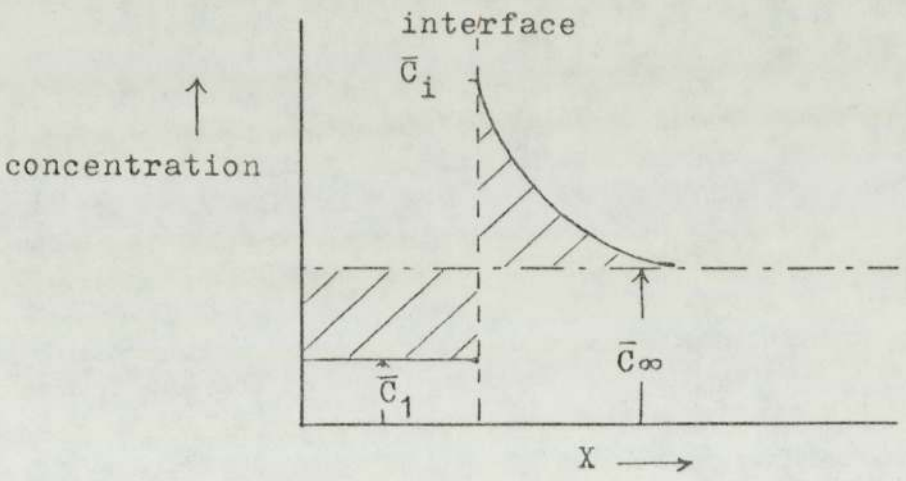

6-2b Theoretical solute distribution at low solidification driving force

Figure 6-2 Effect of rate of solidification on solute redistribution (Terwilliger & Dizio)

Figure 6-2(a) shows the solute distribution for the system being frozen at the higher driving force. Figure 6-2(b) represents the same for the lower driving force. In both systems, the interface is moving at the same velocity. All four cross-hatched regions, then, are equal. But since less ice has been formed in the system represented by figure 6-2(b), the solid phase concentration is also lower.

Terwilliger and Dizio conclude that the values $\bar{C}i^*$ and δ (dependent on thermal driving force) are the two main factors controlling redistribution.

The calculation of the constant δ in equation 6-2 can be made experimentally from the slope of the graph of frozen thickness against time. Graphs 6-7 and 6-8 show that linear relationship between X and $\sqrt{t}$ exist for 5% and 10% sodium chloride. (Similar relationships were found to exist for distilled water and grapefruit juice). The values of δ obtained from the four systems of 10% sodium chloride are shown in table 6-4.

Evaluation of γ for Freezing of 5% Sodium Chloride

System	H (W/m^2C)	TI (C)	Tc (C)	γ (mm^2/s)
1	2000	3.5	- 13	1.85
2	2000	17	- 13	1.81
3	900	17	- 13	1.82
4	2000	17	- 13	1.25

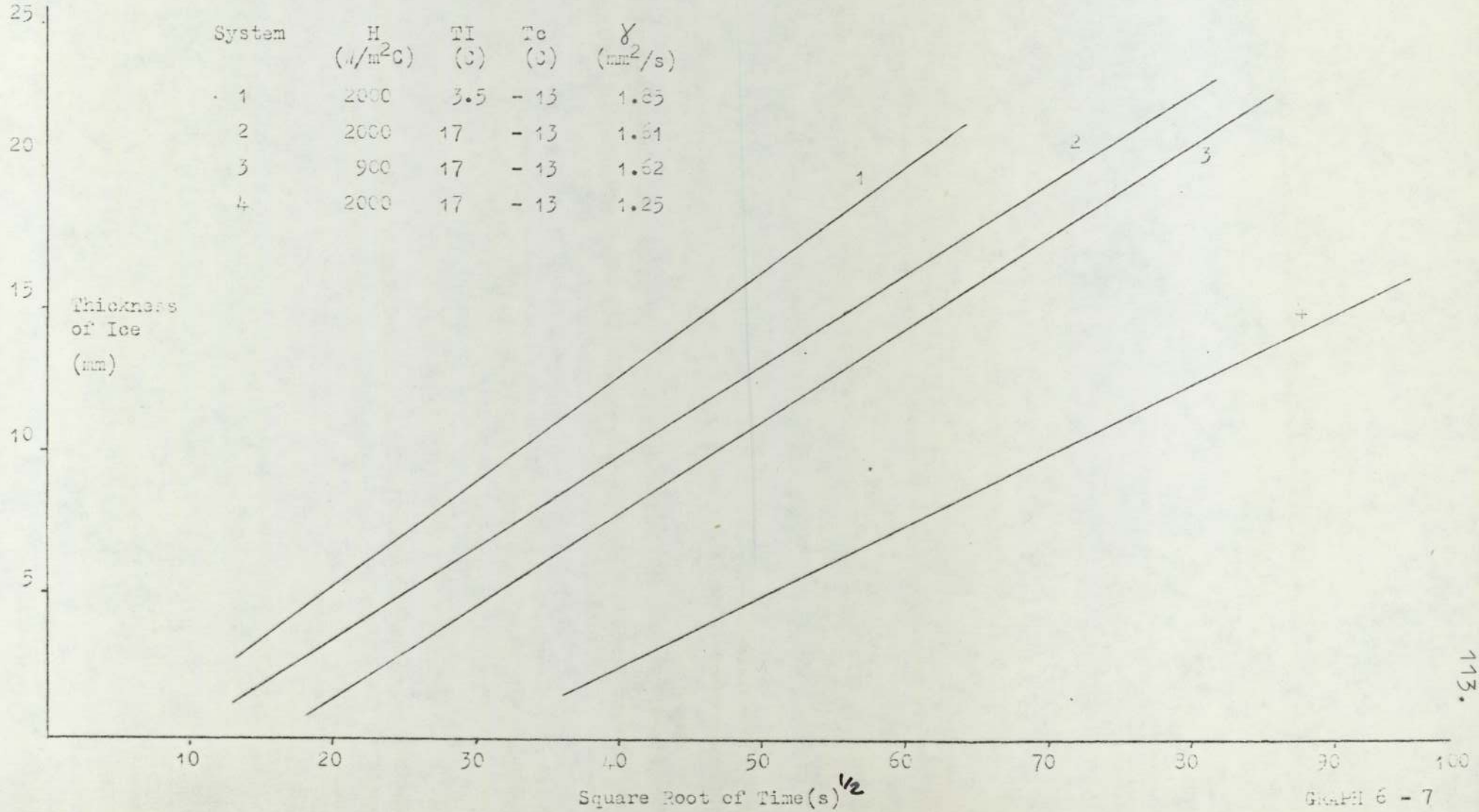

GRAPH 6 - 7

Evaluation of γ. Freezing of 10% Sodium Chloride

System	H (W/m^2C)	TI (C)	Tc (C)	γ (mm/s)
1	2000	14	- 16	1.67
2	2000	19	- 14	1.09
3	900	21	- 15	1.16
4	2000	16.5	- 10.5	0.76

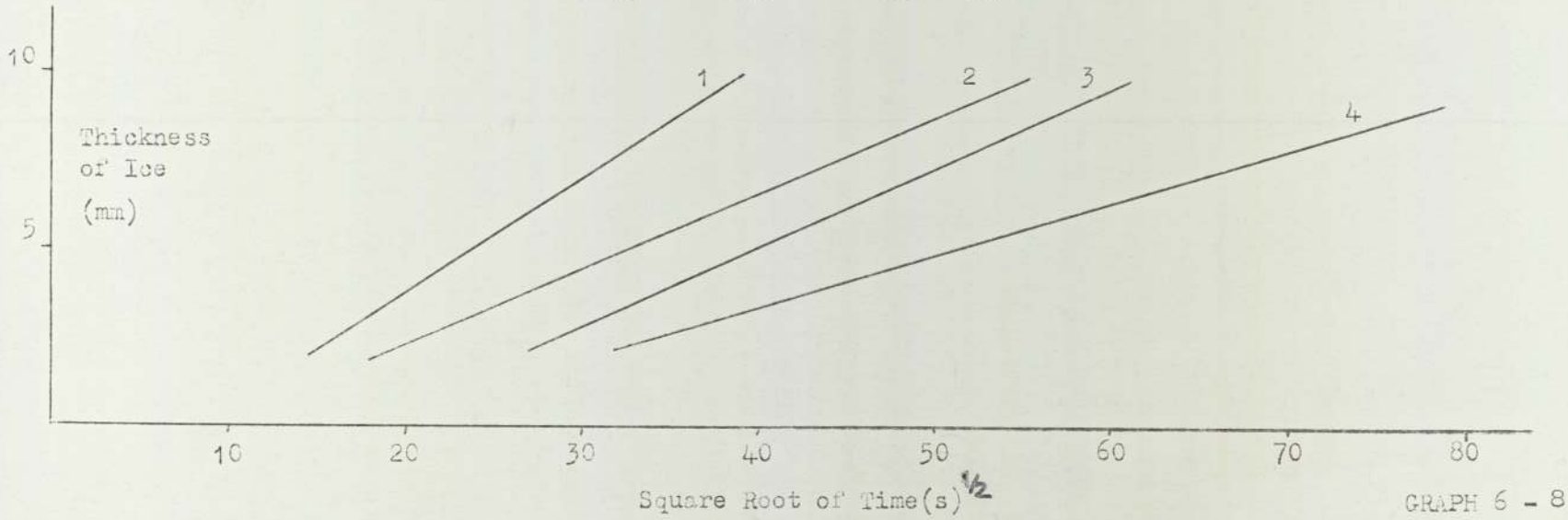

GRAPH 6 - 8

TABLE 6-4 *Freezing rates of 10% NaCl*

SYSTEM	γ (mm^2/s)	Freezing rate (mm/s)
(1) Tc=-16 C TI= 14 C H= 2000 W/m^2C	1.67	.005
(2) Tc=-14 C TI= 19 C H= 2000 W/m^2C	1.09	.009
(3) Tc=-15 C TI= 21 C H= 900 W/m^2C	1.16	.008
(4) Tc=-10.6 TI= 16.5 C H=2000 W/m^2C	0.76	.012

The values of γ for systems (1) and (4) in table 6-4 compare reasonably with Terwilliger and Dizio values of γ = .0106 mm/s for freezing rates of 4.0 to 0.8 mm/s and γ = .0036 mm/s for freezing rates of 0.4 to 1.2 mm/s.

For the system H = 2000 W/m^2C, TI = 16.5 C and Tc = -10.6 C for 10% NaCl the value of γ = 0.76 mm/s was substituted into equation 6-1 :

$$\bar{C}i \geq \bar{C}\infty + \frac{\sqrt{\frac{\gamma}{2\alpha_2 \pi}}\, e^{\left(\frac{-\gamma(1-w)^2}{2\alpha_2}\right)} (TI-Ti)}{(1-w)\,\frac{\gamma}{2D}\, m\, erfc\left(\frac{\gamma}{2\alpha_2}(1-w)\right)} \quad ; \quad (6-1)$$

(1-w) = .083

to evaluate $\bar{C}i^*$ as :

$\bar{C}i^* = \bar{C}\infty + .0094\ (TI-Ti)$

substituting $\bar{T}i$ by $Tm - m\,\bar{C}i$

and letting R = .0094

$$\bar{C}i^* = \frac{\bar{C}\infty}{(1-Rm)} + \frac{RTI}{(1-Rm)} - \frac{RTm}{(1-Rm)}$$

$$\bar{C}i^* = 1.79 + .17 + .08$$

$$\therefore \bar{C}i^* = 2.04 \text{ mol/litre } (kmol/m^3).$$

and the interface freezing temperature = -7.7 C.

This calculation shows a constant depression of the freezing point of 10 per cent sodium chloride of 1.1 C (i.e. 7.7 -6.6 C).

A similar calculation for the faster freezing rate system of 10 per cent sodium chloride (H=2000 W/m^2C, TI = 14 C and Tc = -16 C), on substituting α = 1.67 mm^2/s into equation 6-1, produces a freezing point of -6.9 C. The depression of freezing point in this case being 0.3 C (6.9 C - 6.6 C).

The two calculations indicate greater freezing point depression the slower the rate of freezing and support the theory diagramatically shown in figure 6-2.

6-2.2 Work on Finite Systems (Grange et al).

Grange, Viskanta and Stevenson used the physical

model shown in figure 6-3 for the study of finite systems. In their procedure the temperature and liquid concentration distributions are approximated by polynomials with coefficients which are functions of time using the integral method of Goodman. The solid concentration being a function of solidification rate and interface morphology had to be specified from experimental data. They derive the following expression for the high solute concentration layer (here the difference in the phase densities has been omitted) :

$$X_3 = 3D/\frac{dX_1}{dt} \qquad (6\text{-}3)$$

This expression supports the statement of Terwilliger and Dizio that at a given freezing rate, the boundary layer thickness is uniquely determined.

Verification of equation 6-3 can be made by predicting theoretical X_3 thicknesses from the equation and comparing the results with experimental X_3 thicknesses published by Terwilligo and Dizio (70). Table 6-5 compares the results.

Figure 6-3 Temperature and concentration profiles used by Grange.

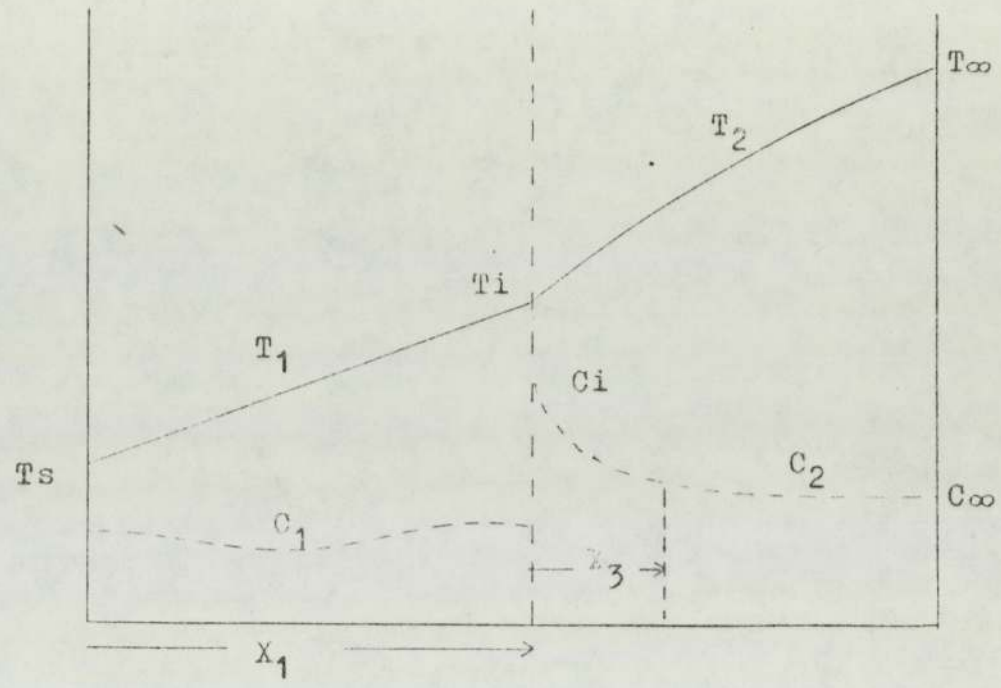

TABLE 6-5.

Theoretical Results	Experimental Results				
X_3 (mm)	X_3 (mm)	$\frac{dX_1}{dt} \times 10^3$ (mm/s)	X_1 (mm)	X_1/X_3	$C\infty$ (kmol/m^3)
.066	.090	40.6	26.8	298	.005
.362	.350	7.5	116.9	334	.005
.062	.060	43.9	27.1	452	.105
.338	.300	8.0	117.1	390	.105
.214	.200	12.6	31.9	159	.005
.718	.680	3.7	81.0	119	.005
.203	.190	13.3	30.3	159	.105
.690	.580	3.9	80.6	139	.105

The results from table 6-5 show (a) Good agreement between experimental and theoretical X_3 thicknesses and so verifies equation 6-3 as being able to accurately predict the thickness of the high solute concentration layer and (b) The thickness of X_3 is very small compared to the frozen thickness X_1.

However their derivation of an expression for the interface temperature is mathematically wrong since their basic equation expressed as :

$$Ti = Tm\ (1-m\bar{C}i)$$

should be of the form :

$$Ti = Tm-m\bar{C}i \text{ (used by Terwilliger)} \quad (6-4)$$

The resulting expression for Ti taking into account solute rejection should be : (assuming $\rho_1 = \rho_2$)

$$Ti = Tm - m\bar{C}\infty - \frac{4}{3}\cdot\frac{m}{D}\cdot X_1 \cdot \frac{dX_1}{dt}\cdot(\bar{C}\infty - \bar{C}_1) \quad (6-5)$$

and not as printed (110)

$$Ti = Tm\ (1-m\bar{C}\infty - \frac{4}{3}\frac{m}{D}\cdot X_1 \cdot \frac{dX_1}{dt}\cdot(\bar{C}\infty - \bar{C}_1)\ )$$

As can be seen from equation 6-5 the freezing temperature, Ti, is calculated from the following three terms :

(1) Tm. By equation 6-4, Tm, for aqueous solutions is defined as being equal to 0 C.

(2) $m\bar{C}\infty$. This term represents the depression of the freezing point due to the original bulk solute concentration ($\bar{C}\infty$) and the molar freezing point depression constant (m).

(3) $-\frac{4}{3}\cdot\frac{m}{D}\cdot X_1\cdot\frac{dX_1}{dt}\cdot(\bar{C}\infty-\bar{C}_1)$.

This term represent the depression of the freezing point due to migration of solute.

Grange etal conclude that the main differences between the salt rejection phenomena in finite and semi-infinite systems is that in finite systems, (a) the liquid interface concentration is not constant but increases with time due to increased solute rejection and (b) the assumption of a constant solute distribution coefficient, Ke, utilised in semi-infinite domains is invalid for freezing in finite regions.

6-4.4 Incorporation of the work of Grange, Viskanta and Stevenson into the Computer Program of Vasil'ev and Uspenskii.

The effect of the solute rejection was incorporated into the Vasil'ev and Uspenskii program in a subroutine. This involved correcting the freezing point by the equation :

$$Ti = Tm - m\bar{C}\infty - \frac{4}{3} \cdot \frac{m}{D} \cdot X_1 \cdot \frac{dX_1}{dt} \cdot (\bar{C}\infty - \bar{C}_1) \qquad (6\text{-}5)$$

In the computer program for the freezing of solutions the temperature scale has already been re-adjusted in the main program so that $m\bar{C}\infty \equiv 0$ (see section 6-4.6). The evaluation of equation 6-5 produced a value of Ti which varied for each step length and therefore the temperature scale had to be readjusted (by the value of Ti) for each step in order to bring Ti back to 0.

This process was achieved by the variable WT in the program. The freezing temperature over the first step length was taken to be the stated literature value for the concentration of solution used, i.e. WT=0. From the freezing rate predicted over this first step length (dX_1/dt), the frozen thickness (X_1), and using an

arbitary value of ($\bar{C}\infty - \bar{C}_1$) within the range 0.01 and 0.09 kmol/m^3 the value of Ti was evaluated. Wt was made equal to Ti and the temperature readjusted so that Tc = Tc + WT and TI = TI - WT. This temperature scale was used for freezing over the second step length.

Once dX_1/dt had been determined for the second step length Ti was re-evaluated according to the new freezing conditions and the temperature scale again readjusted with WT being equal to the new Ti. This process was continued over the whole length of the body being frozen.

The program was run for values of ($\bar{C}\infty - \bar{C}_1$) ranging from 0.01 to 0.09 kmol/m^3 in increments of 0.01 kmol/m^3. The results of this work for $\bar{C}\infty - \bar{C}_1$ equal to 0.01, 0.02 and 0.03 kmol/m^3 along with the corresponding changes in freezing temperatures are given in table 6-6, *(p 128)*.

In conclusion this modification can approximately account for the freezing of electrolytes at low freezing rates but has the disadvantage that ($\bar{C}\infty - \bar{C}_1$) must be arbitrarily chosen and have a constant value although the work suggests $\bar{C}_1$ to be a variable quantity.

6-4.5 Incorporation of the Work of Terwilliger and Dizio into the Computer Program of Vasil' ev and Uspenskii.

As with the work of Grange et al the effect of solute rejection described by Terwilliger and Dizio was incorporated into the Vasil'ev and Uspenskii program in a subroutine. However, unlike the work of Grange et al, the freezing temperature was reduced to a constant value, calculated from equation 6-1 :

$$\bar{C}i^* \geqslant \bar{C}\infty + \frac{\sqrt{\frac{\gamma}{2\alpha_2\pi}}\, e^{\left(-\frac{\gamma(1-W)^2}{2\alpha_2}\right)} (TI-Ti)}{(1-W)\cdot\frac{\gamma}{2D}\cdot m.\mathrm{erfc}\left[\sqrt{\frac{\gamma}{2\alpha_2}}(1-W)\right]} \qquad (6\text{-}1)$$

and therefore the temperature scale only had to be adjusted once.

The value of γ used for the system freezing 10 per cent NaCl with H = 2000 W/m^2C, TI = 16.5 C and Tc = -10.6 C was taken from table 6-4, the results are given in table 6-6.

6-4.6 Vasil'ev and Uspenskii Computer Program for Freezing of Electrolyte Solutions.

The listing of the Vasil'ev and Uspenskii program for predicting freezing rates of distilled water is given in appendix 4-4. The additional steps to incorporate the effect of solute rejection by Grange et al are given in the listing on p.*126*

The listing shows that the freezing point of the solution, TF (equivalent to $m\bar{C}_{\infty}$), is inputted into the program as a positive value and that WT is also calculated as a positive term. The use of positive values for these terms which appear as negative terms in equation 6-5 in order to allow easy adjustment of the temperature scales.

The temperature scale is adjusted in the main program for freezing over the first step length by the value TF.

Subroutine SOLUTE shows that the temperature scale is adjusted independently to account for solute rejection at each step length, hence the preceeding value of WT

Listing of Additional Steps for Electrolyte Freezing to Vasil'ev and Uspenskii Program (Grange etal)

In the main program

```
C    HH = DISTANCE STEP LENGTH
C    CC2= INITIAL SOLUTE CONCENTRATION
C    CC1= SOLID SOLUTE CONCENTRATION
C    XM = MOLAR FREEZING POINT DEPRESSION CONSTANT
C    DD = DIFFUSIVITY COEFFICIENT
C    TF = FREEZING POINT OF AQUEOUS SOLUTION
C    HH1= THICKNESS OF ICE LAYER
C    WT = CONSTANT
C
     WT =0
     HH1=HH
C    ADJUSTMENT OF TEMPERATURE SCALE OVER
C    FIRST STEP LENGTH
     TI = TI + TF
     TC = TC + TF
```

In Subroutine Solute

```
     SUBROUTINE SOLUTE
     COMMON TF, D, XM, TF, CC1, CC2
     COMMON ZNEW, HH, NMAX, HH1
C
     DO   5I = 1,NMAX
5    T(I)= T(I) - WT
     TC  = TC -WT
C
C    CALCULATION OF FREEZING POINT DEPRESSION FOR
C    NEXT STEP LENGTH
C
     WT  =(4./3.)*(XM/DD)*(HH1 HH/ZNEW)*(CC2-CC1)
     HH1 = HH1+HH
C    ADJUSTMENT OF TEMPERATURE SCALE OVER
C    NEXT STEP LENGTH
     DO  6I =1,NMAX
6    T(I)   =T(I) + WT
     TC     =TC   + WT

     RETURN
     END
```

is subtracted from the temperatures before the addition of the new value of WT calculated for the freezing over the next step length.

With the solute rejection phenomenon described by Terwilliger and Dizio the interface concentration is calculated from equation 6-1, and hence the interface temperature TF is obtained. The temperature scale is then adjusted once in the program by the statements :

```
      DO 5 I = 1, NMAX
    5 T(I) = T(I) + TF
      TC = TC + TF
```

Results from the Vasil'ev and Uspenskii programs incorporated the work of Grange and Terwilliger are given in table 6-6 and graph 6-9.

6-5 RESULTS.

Table 6-6 and graph 6-9 show that there is reasonable agreement between experimental and theoretical times for the semi-infinite systems and for the finite systems using an arbitrary figure for $\bar{C}_\infty - \bar{C}_1$ of 0.03 kmol/m^3.

Table 6-6 Freezing of 10% NaCl. System conditions H = 2000 W/m^2C, TI = 16.5 C and Tc = -10.6 C.

THEORETICAL RESULTS Grange				Terwilliger	EXPERIMENTAL RESULTS.	ICE THICKNESS
FINITE SYSTEMS ($C\infty - C_1$ $kmol/m^3$)				SEMI INFINITE SYSTEM		
$C\infty - C_1$ = 0.01 ΔTm (C)	Freezing Time (s)	$C\infty - C_1$ = 0.02 ΔTm (C)	Freezing Time (s)	$C\infty - C_1$ = 0.03 ΔTm (C)	Freezing Time (s)	ΔTm = 1.2 C Freezing Time (s)	Freezing Time (s)	(mm)
.48	540	.70	608	1.0	721	800	882	2
.49	1324	.80	1541	1.0	1836	2010	2268	4
.50	2528	.80	3004	1.0	3536	3540	3780	6
.51	4136	.85	4964	1.1	5814	5200	5400	8
.54	6076	.95	7322	1.3	8529	6800	6800	10
ΔTm at 40 mm = 0.9 C		ΔTm at 40 mm = 1.4 C		ΔTm at 40 mm = 1.73C		ΔTm at 40mm = 1.2 C		

Freezing of 10% Sodium Chloride

System Conditions

H (w/m^2C) = 2000

To (C) = - 10.6

TI (C) = 16.5

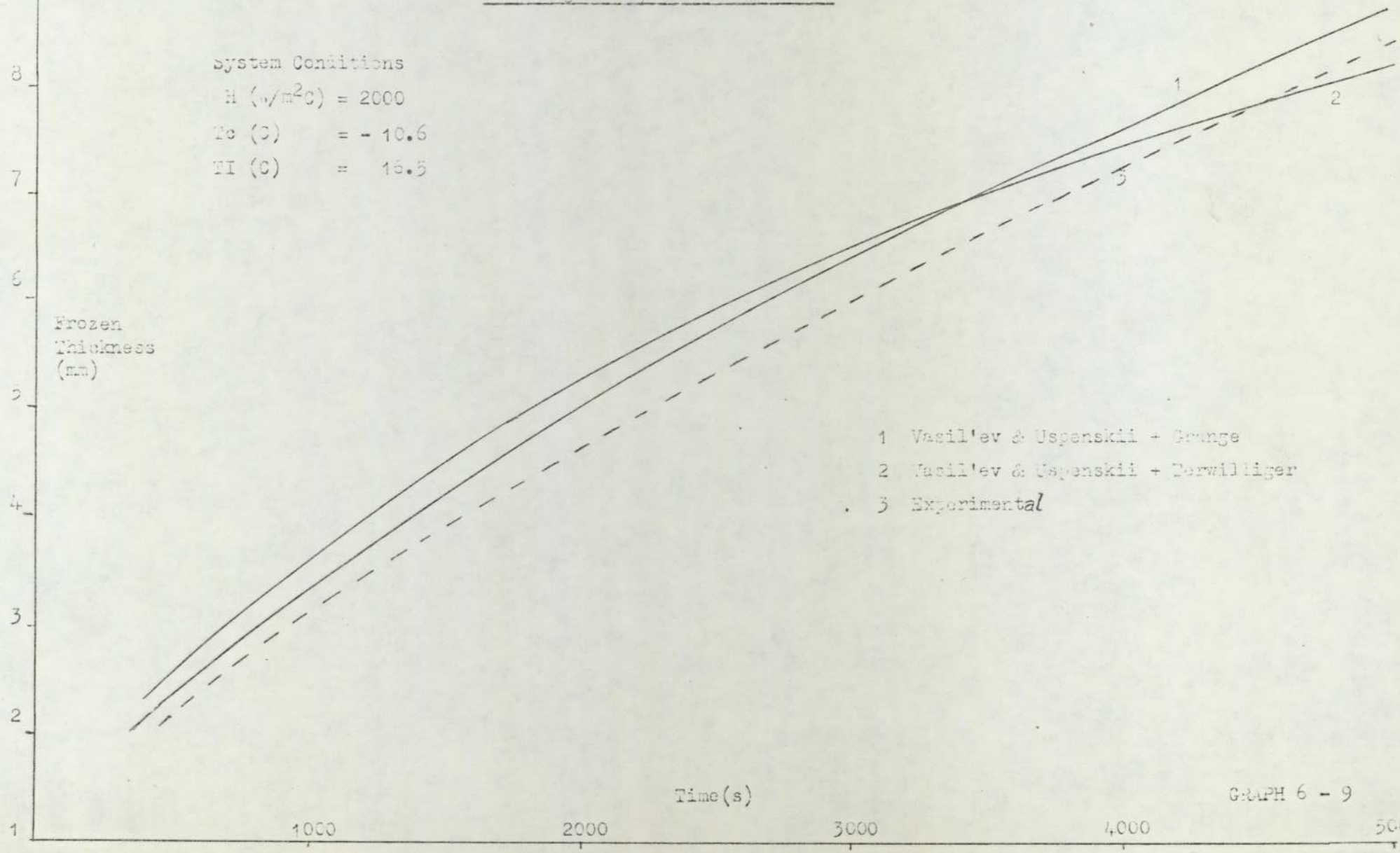

GRAPH 6 - 9

The table also shows what the theoretical freezing points would be at 40 mm of frozen thickness. It can be seen from these temperatures that the greater the ice thickness the larger the freezing point depression is for the finite system.

The value of $\bar{C}_\infty - \bar{C}_1 = 0.03$ kmol/m^3 is well within the range of experimental values obtained for solute rejection, (see table 6-3).

It can be concluded that solute rejection can account for the increase in freezing times for electrolyte solutions compared with distilled water. The precise mechanism of how the solute rejection phenomenon works however, is still not completely understood. The effects of concentration, temperature gradients and crystal morphology must be fully studied before the solute rejection phenomenon at the interface can be explained.

6-6 Effect of Heat Gain on Freezing Rates.

A second reason for longer freezing times of solution compared with distilled water was thought to be heat gain to the system. Heat gain to a system will be more

pronounced when the coolant temperature driving force (Tm-Tc) is small. The conditions of a small coolant temperature driving force are more commonly met with aqueous solutions than distilled water because Tm decreases with ionic concentration. The heat gain effect on the system will be proportionally greater the smaller the factor (Tm-Tc)/(TA-Tm) becomes (TA=ambient temperature).

Table 6-7 gives both theoretical and actual experimental temperature differences to illustrate the above point.

TABLE 6-7. Temperature driving forces.

Solution	TA (C)	Tc (C)	Tm (C)	TA-Tc (C)	Tm - Tc (C)	$\frac{Tm - Tc}{TA - Tc}$
		Theoretical Systems				
Distilled Water	20	-10	0	20	10	.50
5% NaCl	20	-10	-3	23	7	.30
10% NaCl	20	-10	-6.5	26.5	3.5	.13
		Actual Freezing System				
10% NaCl	16.5	-10.5	-6.5	23	4	.17
10% NaCl	14	-16	-6.5	30	9.5	.32

Table 6-8 compares the theoretical freezing times of both the Vasil'ev and Uspenskii programs for no heat gain and heat gain at x = L. The value of the heat gain coefficient (HG) incorporated into the program to account for heat gain was that evaluated in Appendix 3 for the heat transfer coefficient. (In this case HG = 9.6 W/m^2 C since this value corresponds to a value of H = 2000 W/m^2 C). The percentage increase in theoretical freezing times due to the incorporation of heat gain compared to no heat gain was only 5 per cent for freezing 10 mm of NaCl. The theoretical freezing times still underestimated experimental freezing times and heat gain alone cannot account for the freezing of electrolyte solutions.

TABLE 6-8.

SYSTEM CONDITIONS H = 2000 W/m^2 C Tc = -10.6 C
TI = 16.5 C.

Vasil'ev & Uspenskii Freezing Times		Experimental Freezing Times	Ice Thickness (mm)
No Heat Gain	Heat Gain at x = L		
477	501	882	2
1083	1151	2268	4
1974	2113	3780	6
3108	3311	5400	8
4411	4621	7100	10

CHAPTER 7.

ATTEMPT TO REPRESENT EXPERIMENTAL AND VASIL'EV AND USPENSKII FREEZING RATE DATA AS SIMPLE CORRELATION.

7-1 THE METHOD.

The method consisted of four stages :

(1) Representation of data from experiments as $X(t)$ vs $\sqrt{t}$.

(2) Derivation of parameters m and a in the expression :

$$X(t) = m\sqrt{t} + a \qquad (7\text{-}1)$$

(3) Examination of the accuracy of this expression of experimental results.

(4) Comparison of equation (7-1) with computed values.

7-2 EXPERIMENTAL DATA PLOTTED AS X(t) VS $\sqrt{t}$.

Appendix 10-1 shows the experimental data for H = 2000, 1700, 900 and 56.8 W/m^2C.

Graph 7-1 shows X(t) vs $\sqrt{t}$ for most of the results in appendix 10-1. As can be seen from graph 7-1 reasonable straight lines result.

Table 7-1 gives the least squares values* of m and a in equation 7-1 for all data sets in appendix 10-1.

Found by CBM SR 5190 R preprogrammed function.

TABLE 7-1

SET	1	2	3	4	5	6	7	8	9
Symbol on graphs	×	⊙		⊗	ϕ		△	+	•
H	2000	2000	2000	2000	1700	1700	900	900	56.8
TI	20	20	3.5	25	23	18	20	20	19
-Tc	15	10	10	10	10	10	15	10	13
m	0.403	0.323	0.356	0.297	0.303	0.314	0.368	0.301	0.341
a	-2.91	-2.39	-1.90	-2.50	-2.02	-2.08	-3.97	-4.08	-21.41

Experimental & Vasil'ev & Uspenskii (marked) values of values of X vs $\sqrt{t}$

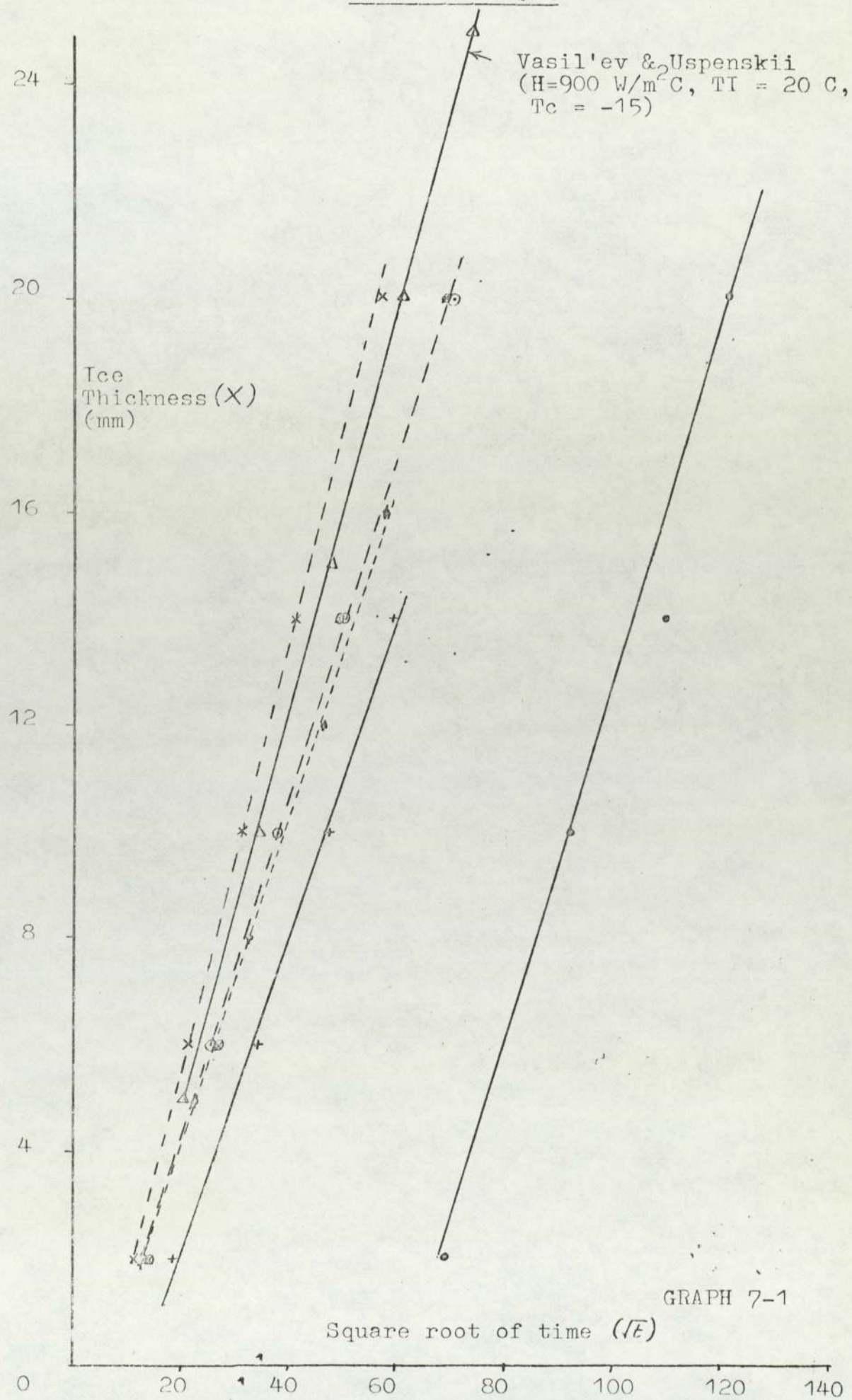

GRAPH 7-1

7-3 PARAMETERS m and a in terms of H, TI and (-Tc).

7-3.1 Parameter m.

$$\text{If } X(t) = m\sqrt{t} + a$$

$$t = \frac{(X(t)-a)^2}{m^2}$$

Comparison with Planck

$$t = L\rho\,(X/H + X^2/2K_1)/(Tm-Tc)$$

(rearranged equat. 4-2).

suggests that $m \propto \sqrt{-Tc}$ with $Tm = 0$

From table 7.1 taking sets 1 and 2 :

$$\left.\begin{array}{l} m = 0.403 \text{ with } -Tc = 15 \\ m = 0.323 \text{ with } -Tc = 10 \end{array}\right\} = m \propto (-Tc)^{.55}$$

set 7 and 8

$$\left.\begin{array}{l} m = 0.368 \text{ with } -Tc = 15 \\ m = 0.301 \text{ with } -Tc = 10 \end{array}\right\} = m \propto (-Tc)^{.495}$$

Thus, we assume that $m \propto \sqrt{-Tc}$.

The effect of TI on m is small. Take $m = c\sqrt{-Tc/TI^k}$. From table 7.1;

Sets 2, 3 and 4 → TI = 20, m = 0.323
TI = 3.5, m = 0.356
TI = 25, m = 0.297
} $m \propto TI^{-0.078}$

Sets 5 and 6 → TI = 23, m = 0.303
TI = 18, m = 0.314
} $m \propto TI^{-0.145}$

Take k = 0.1 (for small values, accuracy not vital).

The effect of H on m is probably negligible, as table 7-2 shows.

TABLE 7-2

SET	1	2	3	4	5	6	7	8	9
H	2000	2000	2000	2000	1700	1700	900	900	56.8
TI	20	20	3.5	25	23	18	20	20	19
-Tc	15	10	10	10	10	10	15	10	13
$\frac{mTI^{0.1}}{\sqrt{-Tc}}$	0.140	0.138	0.128	0.130	0.131	0.133	0.128	0.128	0.127

Table 7-2 shows m $TI^{0.1}/\sqrt{-Tc}$ to be substantially constant. A least squares fit of ln (H) versus (n m $TI^{0.1}/\sqrt{-Tc}$ gives a slope of 0.014, taken to be negligible.

$$\text{Thus } m = 0.13\ (1)\ (-Tc)^{\frac{1}{2}}\ (TI)^{-1/10} \qquad (7\text{-}2)$$

7-3.2 Parameter a

Parameter a is the extrapolated intercept of the X(t) versus $\sqrt{t}$ least squares fit, and is subject to greater error than m, particularly for H = 56.8 W/m^2C.

Examination of a values in table 7-1 shows (1) no clear effect of TI or Tc on a, (2) H = 1700 W/m^2C values may be anomolous.

Graph 7-2 shows ln (-a) versus ln (H), where (-a) is the arithmetic average for each H value. Ignoring H = 1700 W/m^2C the expression :

$$a = -250H^{-0.609} \qquad (7\text{-}3)$$

results, and expression (7-1) becomes :

GRAPH 7-2 ln (-a) vs ln (H)

Slope = -0.609

$-a = 250\ H^{-0.609}$

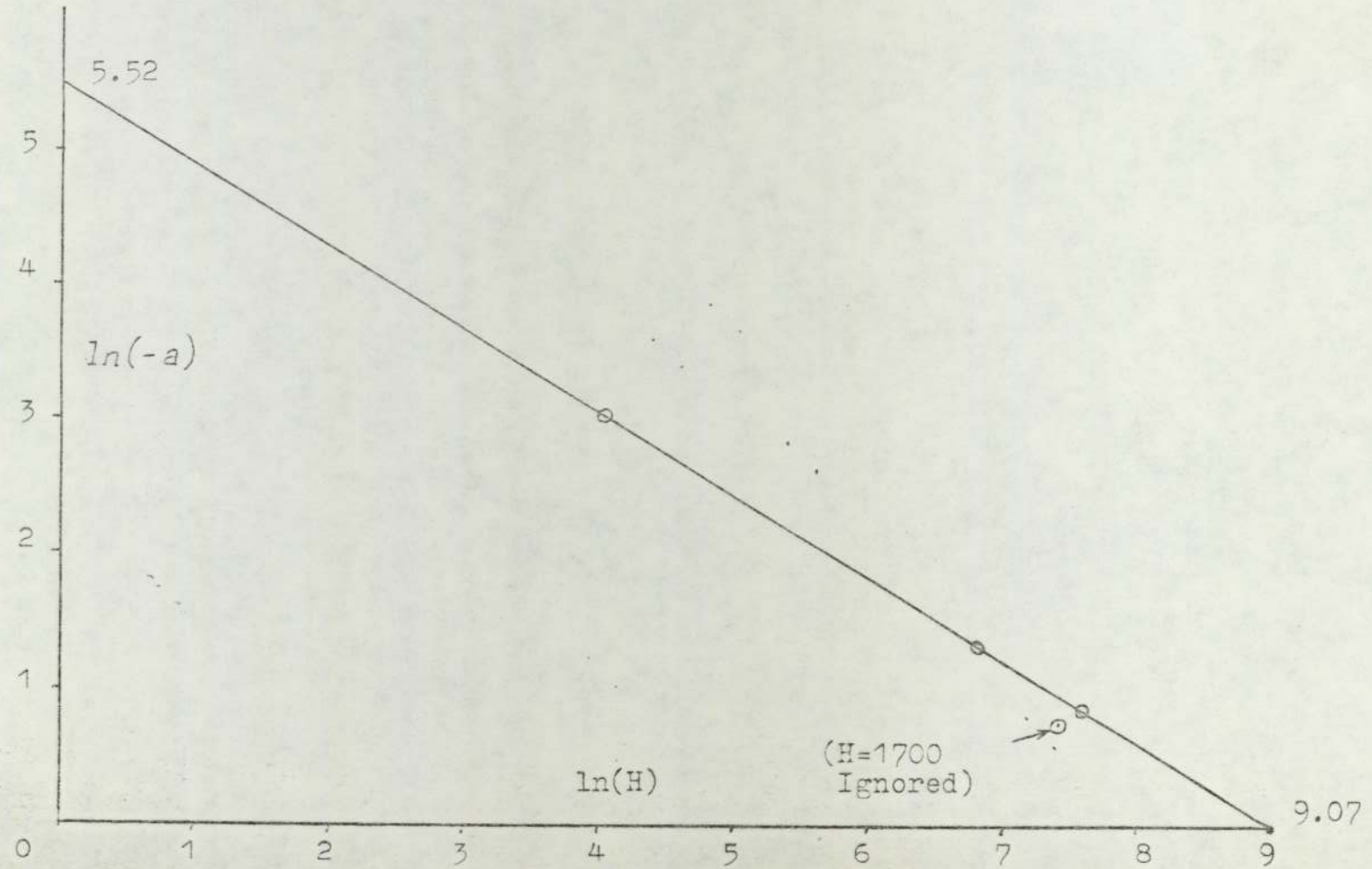

$$X(t) = 0.13 \sqrt{-Tc}\ (TI)^{-0.1} - 250H^{-0.61} \qquad (7\text{-}4)$$

7-4 COMPARISON OF EXPRESSION (7-4) WITH ARBITRARILY SELECTED EXPERIMENTAL SETS.

TABLE 7-3.

	H	TI, Tc		X = 2	6	10	14	20
SET 2	2000	20	Expt t=	182	680	1475	2570	-
		-10	(7-4)t=	208	753	1637	2862	5335
SET 6	1700	18	Expt t=	170	660	1480	2640	-
		-10	(7-4)t=	227	782	1669	2889	5341
SET 7	900	20	Expt t=	245	730	1500	2425	4150
		-15	(7-4)t=	250	699	1374	2277	4054

Table 7-3 shows a fair agreement ($\pm$ 20%, improving as X increases) between predicted and experimental times.

Comparison of Expression (7-4) with Vasil'ev and Uspenskii Computations.

Appendix 10-2 summarises the available X(t) versus t data produced by the Vasil'ev and Uspenskii program for distilled water, and includes comparisons with equation (7-4) for some data sets.

The comparisons show that equation (7-4) usually predicts a higher t value than computed, with largest differences for small X(t) values and low H value (up to 40% difference), but usually the difference is below 10%. A difference in shape of the formula and computed X(t) curves is evident from the variation of error with X(t).

CHAPTER 8.

CONCLUSIONS AND RECOMMENDATIONS FOR FUTURE WORK.

8-1 CONCLUSIONS.

8-1.1 Freezing of Distilled Water.

1. Comparison of the theoretically predicted and experimental freezing times has shown that :

   (a) The most accurate theoretical freezing rate method over the range of experimental variables used was the modified Vasil'ev and Uspenskii method, with a maximum divergence of 27% for all experiments and 8% error if results with H = 900 W/m^2C were neglected.

   (b) The results from the integral method of Goodman showed good agreement with experimental freezing times when the initial water temperature was near 0 C.

(c) The commonly used methods of Neumann and Planck together with their various modifications all underestimated the experimental freezing times by 22% to 400%.

2. Experimental work has shown that :

(a) The experimental procedure provided a simple, inexpensive and accurate method for the determination of planar ice thickness in liquid materials.

(b) A linear relationship existed between ice thickness and the square root of time, this expression also held for the freezing of electrolyte solutions. The expression $X(t) = m\sqrt{t} + a$ for the freezing of distilled water was evaluated as :
$X(t) = 0.13\ \sqrt{-Tc}\ (TI)^{-0.1} - 250H^{-0.61}$

(c) Three system variables; the heat transfer coefficient, coolant

temperature and initial liquid temperature significantly changed the freezing rates of the liquids.

(d) The effect of neglecting the thermal capacity of ice was insignificant but the thermal capacity of water was an important factor in determining freezing rates.

(e) For all the liquids frozen; the subcooling and precooling stages occupied very little of the overall freezing time, the subcooling effect was small and the vast majority of the overall freezing time was taken up by the freezing stage.

8-1.2 Comparison of Freezing Distilled Water and Electrolyte Solutions.

(1) The freezing curves of grapefruit juice were very similar to distilled water, reasonable comparison between predicted freezing times by the modified Vasil'ev and

Uspenskii method and experimental freezing times obtained by readjustment of the temperature scales by the value of the freezing point of the juice. The freezing point was only a problem if it varied during the freezing process.

(2) The freezing rates of distilled water and 5 and 10 per cent solutions of sodium chloride were found to be the same under conditions of fast freezing rates (.005 mm/s) but different when slower freezing rates (.0012 mm/s) were used. Under these latter conditions the electrolyte solutions froze more slowly than the distilled water with the result that the theoretically predicted freezing times of the modified Vasil'ev and Uspenskii method underestimated the experimental freezing times.

8-1.3 Freezing of Electrolyte Solutions (5 and 10 per cent Sodium Chloride).

(1) The difference in freezing times between distilled water and the sodium chloride

solutions under conditions of slow freezing were explained by the migration of solute from the frozen phase to the unfrozen phase reducing the freezing point of the solution during the freezing process and hence the freezing rate.

(2) The degree of solute migration although found to be small in all experiments was higher at slower freezing rates.

(3) Experimental evidence supported the theory that a thin layer of high solute concentration was formed in the liquid adjacent to the advancing frozen-unfrozen interface, its thickness was inversely proportional to the freezing rate. The freezing temperature and hence the freezing rate of the solution was dependent on the liquid solute concentration at the interface.

(4) Incorporation of the solute effect into the modified Vasil'ev and Uspenskii method improved the prediction of the freezing rates of the sodium chloride solutions to within 15% (for H = 2000 W/m^2C).

8-2 RECOMMENDATIONS FOR FUTURE WORK.

This thesis has provided both an experimental and a theoretical basis for research into the freezing rates of aqueous solutions. Further areas of work for possible future research include :

1. Development of the Vasil'ev and Uspenskii finite difference method into a readily useable and simple form.

2. Study of solute migration in the freezing of electrolyte solutions, concentrating on determining the effects of the solute profiles in both the unfrozen and frozen phases particularly near the unfrozen-frozen interface.

3. Study of how the cellular structure of foodstuffs effects solute migration and determination of thermal properties of foodstuffs in order to be able to

predict freezing rates of food-stuffs.

(4) Theoretical development of the freezing rate methods to account for freezing of irregular shaped objects and evaluation of some of the most recent and complex theoretical freezing methods.

APPENDIX 1

RESULTS OF FREEZING RATE EXPERIMENTS

CARRIED OUT ON EXPERIMENTAL APPARATUS

Freezing times are given in minutes.

Frozen thicknesses are given in centimetres.

Temperatures are given in degrees C.

Heat transfer coefficients are given in W/m^2C.

APPENDIX 1-1 Distilled Water Results.

Run No. 47
Coolant temp. - 15.0
Initial temp. 20.0
Heat trans.coeff.2000

Time	Ice Thickness
1.0	0.05
2.0	0.15
3.0	0.24
5.0	0.37
9.0	0.66
15.0	0.90
20.0	1.11
28.0	1.36
32.0	1.48

Run No. 48
Coolant temp. -10.0
Initial temp. 20.0
Heat trans.coeff.2000

Time	Ice Thickness
1.0	0.05
2.0	0.12
4.0	0.26
7.0	0.41
9.0	0.49
15.5	0.77
20.0	0.90
30.0	1.16
43.0	1.42
53.0	1.57
61.0	1.66

Run No. 12
Coolant temp. -10.0
Initial temp. 3.5
Heat trans.coeff.2000

Time	Ice Thickness
4.0	.35
9.0	.64
12.0	.78
15.0	.89
18.0	.98
21.0	1.08
24.0	1.16
28.0	1.25
30.0	1.30
33.0	1.37
36.0	1.43
39.0	1.50
42.0	1.58
45.0	1.62
49.0	1.69
52.0	1.75
56.0	1.82
60.0	1.89

Run No. 9
Coolant temp. -13.0
Initial temp. 20.0
Heat trans.coeff.2000

Time	Ice Thickness
3.0	.24
6.0	.43
9.0	.57
12.0	.71
15.0	.82
18.0	.93
21.0	1.03
24.0	1.13
27.0	1.22
33.0	1.39
36.0	1.46
42.0	1.60
47.0	1.70
51.0	1.77
55.0	1.83
61.0	1.91
65.0	1.97
72.0	2.06
80.0	2.16

Run No. 49
Coolant temp. -10.0
Initial temp. 3.5
Heat trans.coeff.2000

Time	Ice Thickness
2.0	.19
5.5	.45
9.0	.65
14.0	.87
18.0	1.01
22.0	1.13
27.5	1.28
30.0	1.34
33.5	1.42

57.0	1.91
61.0	1.99

Run No. 50
Coolant temp. -10.0
Initial temp. 3.5
Heat trans.coeff.2000

Time	Ice Thickness
1.5	.16
3.0	.29
6.5	.53
12.5	.80
15.0	.89
20.0	1.03
27.0	1.23
43.0	1.61
52.0	1.80

Run No. 51
Coolant temp. -10.0
Initial temp. 25.0
Heat trans.coeff.2000

Time	Ice Thickness
2.0	.08
4.0	.21
8.0	.39
12.0	.53
15.0	.62
24.0	.86
35.0	1.11
43.0	1.27
51.0	1.41
59.0	1.52
67.0	1.62
86.0	1.81
93.0	1.88

Run No. 46
Coolant temp. -15.0
Initial temp. 20.0
Heat trans.coeff.2000

Time	Ice Thickness
1.0	.05
2.0	.15
3.0	.25
5.0	.39
9.0	.68
15.0	.89
20.0	1.12
28.0	1.36
32.0	1.48
35.0	1.58

Run No. 28
Coolant temp. -10.0
Initial temp. 3.5
Heat trans.coeff.2000

Time	Ice Thickness
3.0	.24
8.0	.58
16.0	.91
21.0	1.09
25.0	1.20
30.0	1.34
36.0	1.48
40.0	1.57
45.0	1.68
50.0	1.78
55.0	1.88
60.0	1.98

Run No. 29
Coolant temp. -10.0
Initial temp. 20.0
Heat trans.coeff.2000

Time	Ice Thickness
4.0	.26
8.0	.45
13.0	.63
18.0	.78
23.0	.91
28.0	1.03
33.0	1.22
43.0	1.34
51.0	1.49
60.0	1.66
65.0	1.75
72.0	1.79

Run No. 80
Coolant temp. -10.0
Initial temp. 15.0
Heat trans.coeff.2000

Time	Ice Thickness
4.0	.26
7.0	.44
13.0	.71
18.0	.83
25.0	1.01
30.0	1.13
35.0	1.24
40.0	1.33
45.0	1.43
50.0	1.53
55.0	1.63
61.0	1.73
68.0	1.86
73.0	1.94
81.0	2.07

Run No. 11
Coolant temp. -10.0
Initial temp. 20.0
Heat trans.coeff.2000

Time	Ice Thickness
3.0	.23
6.0	.39
9.0	.52
12.0	.64
15.0	.73
18.0	.83
21.0	.92
24.0	1.00
27.0	1.08
30.0	1.15
33.0	1.22
36.0	1.29
39.0	1.34
42.0	1.39
46.0	1.45
50.0	1.51
57.0	1.60
60.0	1.64
65.0	1.70
70.0	1.75
76.0	1.82
83.0	1.89

Run No. 10
Coolant temp. -10.0
Initial temp. 20.0
Heat trans.coeff.2000

Time	Ice Thickness
3.0	.19
6.0	.35
9.0	.49
12.0	.61
15.0	.71
18.0	.80
21.0	.89
24.0	.97
27.0	1.05
30.0	1.12
33.0	1.19
36.0	1.26
39.0	1.31
42.0	1.37
45.0	1.42
48.0	1.46
60.0	1.61
70.0	1.73
75.0	1.79

Run No. 23
Coolant temp. -10.0
Initial temp. 23.0
Heat trans.coeff.1700

Time	Ice Thickness
1.5	.04
2.0	.12
3.7	.25
5.5	.35
7.0	.43
11.7	.61
14.0	.68
17.0	.76
25.0	.97
31.0	1.10
36.5	1.22
42.0	1.31
48.0	1.41
54.7	1.52
60.0	1.61
65.0	1.69

Run No. 24
Coolant temp. -14.0
Initial temp. 20.0
Heat trans.coeff.1700

Time	Ice Thickness
2.2	.20
3.0	.28
5.0	.42
7.0	.54
10.0	.68
13.0	.83
17.2	.98
29.0	1.37
38.0	1.61
43.0	1.73
53.7	1.95

Run No. 22
Coolant temp. -10.0
Initial temp. 18.0
Heat trans.coeff.1700

Time	Ice Thickness
1.7	.09
3.0	.20
4.5	.30
6.5	.40
8.0	.47
11.0	.59
13.5	.68
19.0	.84
22.0	.93
28.0	1.08
38.0	1.29
48.0	1.47
54.5	1.59
58.7	1.66
65.0	1.76
68.0	1.80

Run No. 27
Coolant temp. -10.0
Initial temp. 6.0
Heat trans.coeff.1700

Time	Ice Thickness
1.7	.17
3.0	.31
5.0	.45
7.5	.59
10.0	.70
13.2	.85
16.2	.96
19.2	1.06
23.0	1.17
27.0	1.29
32.0	1.41

Run No. 25
Coolant temp. - 6.0
Initial temp. 16.4
Heat trans.coeff.1700

Time	Ice Thickness
3.5	.00
4.5	.09
5.7	.18
7.5	.27
10.0	.36
12.7	.45
23.5	.72
27.2	.79
45.7	1.09
51.7	1.17
55.5	1.23
60.0	1.28

Run No. 28
Coolant temp. -14.0
Initial temp. 15.4
Heat trans.coeff.1700

Time	Ice Thickness
2.0	.19
3.0	.29
5.0	.38
7.0	.55
10.0	.72
13.0	.84
19.0	1.07
32.2	1.45

Run No. 26
Coolant temp. -6.0
Initial temp. 5.0
Heat trans.coeff.1700

Time	Ice Thickness
3.0	.11
4.7	.22
6.5	.30
11.0	.49
18.5	.72
23.5	.84
30.0	.97
35.0	1.07
42.2	1.17

Run No. 3
Coolant temp. -11.0
Initial temp. 17.5
Heat trans.coeff. 900.0

Time	Ice Thickness
3.0	.13
6.0	.30
9.0	.42
12.0	.54
15.0	.64
18.0	.73
21.0	.82
25.0	.94
30.0	1.07
35.0	1.82
40.0	1.27
50.0	1.44
56.0	1.54
65.0	1.65

Run No. 4
Coolant temp. -10.0
Initial temp. 5.0
Heat trans.coeff. 900.0

Time	Ice Thickness
6.0	.44
9.0	.59
12.0	.71
16.0	.85
18.0	.92
22.0	1.04
25.0	1.12
28.0	1.19
32.0	1.28
41.0	1.48
47.0	1.59
52.0	1.69
60.0	1.83

Run No. 5
Coolant temp. -10.0
Initial temp. 15.5
Heat trans.coeff. 900.0

Time	Ice Thickness
3.0	.18
7.0	.31
9.0	.40
12.0	.51
15.0	.64
20.0	.77
25.0	.91
30.0	1.03
35.0	1.12
40.0	1.20
45.0	1.28
59.0	1.47
65.0	1.54
75.0	1.65

Run No. 6
Coolant temp. -10.0
Initial temp. 2.5
Heat trans.coeff. 900.0

Time	Ice Thickness
3.0	.26
7.0	.45
10.0	.59
13.0	.70
16.0	.79
19.0	.88
22.0	.96
26.0	1.07
30.0	1.16
35.0	1.23
40.0	1.37
46.0	1.49
51.0	1.59
55.0	1.66
60.0	1.99

Run No. 7
Coolant temp. -15.0
Initial temp. 16.0
Heat trans.coeff. 900.0

Time	Ice Thickness
3.0	.20
6.0	.37
9.0	.53
12.0	.67
15.0	.79
18.0	.91
21.0	1.02
25.0	1.16
27.0	1.23
30.0	1.32
33.0	1.41
36.0	1.48
39.0	1.54
42.0	1.60
48.0	1.72
52.0	1.79
56.0	1.86
60.0	1.93

Run No. 8
Coolant temp. -13.5
Initial temp. 15.5
Heat trans.coeff. 900.0

Time	Ice Thickness
3.0	.20
6.0	.37
12.0	.64
18.0	.87
21.0	.98
27.0	1.17
33.0	1.34
39.0	1.46
45.0	1.58
51.0	1.68
55.0	1.75
60.0	1.82
65.0	1.90

Run No. 1
Coolant temp. -10.0
Initial temp. 7.0
Heat trans.coeff. 900.0

Time	Ice Thickness
3.0	.19
6.0	.37
12.5	.65
17.0	.81
27.0	1.07
34.0	1.24
41.0	1.39
52.5	1.61
60.0	1.75

Run No. 35
Coolant temp. -10.0
Initial temp. 20.0
Heat trans.coeff. 900.0

Time	Ice Thickness
5.0	.17
14.5	.48
19.0	.58
30.0	.84
33.0	.90
39.0	1.02
45.5	1.14
70.0	1.52

Run No. 2
Coolant temp. -10.0
Initial temp. 20.0
Heat trans.coeff. 900.0

Time	Ice Thickness
9.5	.25
15.0	.49
34.0	1.01
43.0	1.18
51.0	1.29
55.0	1.35
81.0	1.64
95.0	1.78
103.0	1.85

Run No. 34
Coolant temp. -10.0
Initial temp. 20.0
Heat trans.coeff. 900.0

Time	Ice Thickness
2.0	.02
3.0	.07
11.0	.34
80.0	1.62
91.0	1.76
94.0	1.8

Run No. 31
Coolant temp. -15.0
Initial temp. 20.0
Heat trans.coeff. 900.0

Time	Ice Thickness
2.5	.07
3.5	.14
5.0	.24
7.5	.36
11.0	.52
15.0	.67
20.0	.84
25.0	.98
30.0	1.25
40.0	1.37
57.5	1.75
77.2	2.12
82.5	2.20

Run No. 32
Coolant temp. -15.0
Initial temp. 20.0
Heat trans.coeff. 900.0

Time	Ice Thickness
2.0	.09
3.0	.17
5.0	.28
8.0	.43
11.0	.56
16.0	.75
41.0	1.48
50.0	1.64
64.0	1.90
70.0	2.00

Run No. 33
Coolant temp. -15.0
Initial temp. 20.0
Heat trans.coeff. 900.0

Time	Ice Thickness
2.5	.09
7.5	.38
14.0	.67
18.0	.81
23.0	.97
55.0	1.69

Run No.
Coolant temp. -13.0
Initial temp. 20.0
Heat trans.coeff. 56.8

Time	Ice Thickness
52.0	.00
64.0	.13
69.0	.20
81.0	.33
91.0	.44
101.0	.54
132.0	.91
143.0	1.03
160.0	1.19
204.0	1.53
217.0	1.72
223.0	1.78
253.0	2.02

APPENDIX 1-2 Grapefruit Juice Results.

Run No. 74
Coolant temp. -10.0
Initial temp. 16.0
Heat trans.coeff. 900.0

Time	Ice Thickness
10.0	.26
20.0	.62
25.0	.77
30.0	.89
35.0	.99
40.0	1.10
45.0	1.20
55.0	1.40
60.0	1.49
66.0	1.60
71.0	1.68

Run No. 75
Coolant temp. -11.0
Initial temp. 15.0
Heat trans.coeff.2000

Time	Ice Thickness
9.0	.35
15.0	.59
21.0	.78
26.0	.91
34.0	1.11
41.0	1.26
48.0	1.40

Run No. 77
Coolant temp. -12.5
Initial temp. 10.0
Heat trans.coeff. 900.0

Time	Ice Thickness
5.0	.51
8.0	.70
13.0	.95
18.0	1.15
23.0	1.33
28.0	1.47
33.0	1.62
38.0	1.75
43.0	1.88
51.0	2.06
58.0	2.23
60.0	2.27

Run No. 72
Coolant temp. -10.0
Initial temp. 17.5
Heat trans.coeff. 2000

Time	Ice Thickness
7.0	.14
11.0	.37
15.0	.53
20.0	.70
25.0	.86
30.0	1.00
36.0	1.16
40.0	1.27
45.0	1.39
50.0	1.51
55.0	1.62
60.0	1.72

Run No. 73
Coolant temp. -10.0
Initial temp. 17.0
Heat trans.coeff. 900.0

Time	Ice Thickness
9.0	.14
14.0	.36
19.0	.49
22.0	.60
26.0	.69
31.0	.80
35.0	.88
40.0	.97
46.0	1.05
53.0	1.21
61.0	1.35
66.0	1.43
72.0	1.53
82.0	1.70
90.0	1.82

Run No. 71
Coolant temp. -10.0
Initial temp. 22.0
Heat trans.coeff. 900

Time	Ice Thickness
16.0	.16
20.0	.33
25.0	.49
30.0	.65
35.0	.73
40.0	.83
45.0	.92
50.0	1.01
60.0	1.17
70.0	1.39
80.0	1.51
90.0	1.67
101.0	1.83
110.0	1.96
123.0	2.14

APPENDIX 1-3 Five Per Cent Sodium Chloride Results

Run No. 54
Coolant temp. -13.0
Initial temp. 3.5
Heat trans.coeff. 2000

Time	Ice Thickness
2.0	.17
4.0	.32
10.0	.65
16.0	.90
21.0	1.06
33.0	1.41
44.0	1.66
50.0	1.81
60.0	2.10

Run No. 52
Coolant temp. -13.0
Initial temp. 17.0
Heat trans.coeff. 2000

Time	Ice Thickness
2.5	.12
4.0	.21
6.0	.31
11.0	.51
17.0	.68
23.0	.83
32.5	1.20
41.0	1.30
45.0	1.39
55.0	1.51

Run No. 55
Coolant temp. -13.0
Initial temp. 3.5
Heat trans.coeff. 2000

Time	Ice Thickness
1.5	.13
4.0	.32
7.0	.49
17.0	0.98
22.0	1.11
30.0	1.39
40.0	1.61
60.0	2.02

Run No. 53
Coolant temp. -13.0
Initial temp. 17.0
Heat trans.coeff. 2000

Time	Ice Thickness
2.0	.10
5.0	.31
12.0	.57
25.0	.98
44.0	1.32
50.0	1.45
58.0	1.62
65.0	1.76
80.0	2.00

Run No. 18
Coolant temp. -13.0
Initial temp. 17.0
Heat trans.coeff. 2000

Time	Ice Thickness
4.0	.28
6.0	.43
10.0	.57
12.0	.64
15.0	.72
18.0	.80
21.0	.88
26.0	.99
31.0	1.10
35.0	1.19
40.0	1.28
45.0	1.36
50.0	1.45
55.0	1.61
62.0	1.65
70.0	1.77
75.0	1.85
83.0	1.96
91.0	2.07
100.0	2.19
120.0	2.45
130.0	2.57

Run No. 17
Coolant temp. -13.0
Initial temp. 17.0
Heat trans.coeff. 2000

Time	Ice Thickness
6.0	.34
9.0	.42
15.0	.62
20.0	.76
25.0	.88
30.0	1.03
35.0	1.10
40.0	1.21
45.0	1.30
50.0	1.40
56.0	1.50
61.0	1.58
65.0	1.65
72.0	1.76
80.0	1.88
86.0	1.96
93.0	2.06
102.0	2.18
110.0	2.28
115.0	2.34

Run No. 19
Coolant temp. -13.0
Initial temp. 17.0
Heat trans.coeff. 900.0

Time	Ice Thickness
3.0	.04
6.0	.17
9.0	.28
12.0	.39
15.0	.48
19.0	.59
22.0	.66
25.0	.74
30.0	.85
35.0	.96
41.0	1.08
45.0	1.15
50.0	1.24
55.0	1.32
60.0	1.40
65.0	1.48
70.0	1.56
75.0	1.63
80.0	1.71
85.0	1.77
90.0	1.85
100.0	1.99
110.0	2.11
120.0	2.23

Run No. 20
Coolant temp.-13.0
Initial temp. 17.0
Heat trans.coeff. 900.0

Time	Ice Thickness
3.0	.04
6.0	.18
9.0	.28
12.0	.37
15.0	.45
18.0	.53
21.0	.60
25.0	.68
30.0	.79
35.0	.88
40.0	.97
45.0	1.06
50.0	1.15
55.0	1.24
60.0	1.32
65.0	1.41
70.0	1.49
75.0	1.57
80.0	1.66
85.0	1.73
90.0	1.81
100.0	1.97
110.0	2.10
120.0	2.23

Run No. 45
Coolant temp. -13.0
Initial temp. 17.0
Heat trans.coeff. 900.0

Time	Ice Thickness
7.0	.12
13.0	.37
21.0	.60
25.0	.70
45.0	1.13
47.0	1.17
58.0	1.37
60.0	1.43
75.0	1.62

Run No. 44
Coolant temp. -13.0
Initial temp. 17.0
Heat trans.coeff. 900.0

Time	Ice Thickness
4.5	.07
6.0	.15
9.0	.26
14.0	.41
18.5	.53
24.0	.65
29.0	.77
37.5	.93
43.0	1.04
50.0	1.14
54.0	1.21
75.0	1.56

Run No. 43
Coolant temp. -14.0
Initial temp. 18.0
Heat trans.coeff. 900.0

Time	Ice Thickness
3.5	.01
5.0	.16
8.0	.30
12.0	.47
18.0	.68
24.0	.85
31.0	1.02
38.0	1.22
44.0	1.32
50.0	1.46
60.0	1.67
95.0	2.39
109.0	2.65
112.0	2.70

Run No. 42
Coolant temp. -14.0
Initial temp. 18.0
Heat trans.coeff. 900.0

Time	Ice Thickness
2.5	.03
4.0	.11
7.5	.25
12.0	.41

18.0	.60
23.5	.73
32.5	.96
39.0	1.09
43.0	1.17

Run No. 41
Coolant temp. -15.0
Initial temp. 18.5
Heat trans.coeff. 900.0

Time	Ice Thickness
2.5	.03
4.0	.12
17.0	.65
28.0	.97

Run No. 40
Coolant temp. -15.0
Initial temp. 18.5
Heat trans.coeff. 900.0

Time	Ice Thickness
2.5	.02
3.0	.07
5.0	.17
11.0	.43
14.0	.56
29.0	.98
41.0	1.27
51.5	1.50
59.0	1.54

Run No. 16
Coolant temp. -13.0
Initial temp. 17.0
Heat trans.coeff. 350

Time	Ice Thickness
13.0	.00
15.0	.06
20.0	.14
25.0	.23
30.0	.30
34.0	.36
37.0	.40
46.0	.53
51.0	.60
56.0	.66
61.0	.76
67.0	.79
75.0	.85
80.0	.94
95.0	1.10
100.0	1.14
110.0	1.24
126.0	1.39
132.0	1.44

APPENDIX 1-4 Ten Per Cent Sodium Chloride Results

Run No. 56
Coolant temp. -16.0
Initial temp. 14.0
Heat trans.coeff. 2000

Time	Ice Thickness
2.0	.08
4.0	.25
6.5	.39
16.5	.77
20.0	.86
24.5	.98
39.0	1.28
43.0	1.36

Run No. 58
Coolant temp. -14.0
Initial temp. 14.5
Heat trans.coeff. 2000

Time	Ice Thickness
2.0	.05
4.0	.16
7.0	.27
12.0	.40
18.0	.53
28.5	.72
35.5	.83
45.0	.95
50.0	1.02

Run No. 57
Coolant temp. -16.0
Initial temp. 14.0
Heat trans.coeff. 2000

Time	Ice Thickness
1.5	.08
4.0	.28
7.0	.43
13.0	.64
21.0	.85
29.5	1.12

Run No. 59
Coolant temp. -13.0
Initial temp. 14.5
Heat trans.coeff. 2000

Time	Ice Thickness
2.0	.06
4.0	.16
41.5	.92
94.0	1.67

Run No. 60
Coolant temp. -14.0
Initial temp. 19.0
Heat trans.coeff. 2000

Time	Ice Thickness
3.0	.09
7.0	.23
14.0	.42
18.0	.49
22.0	.56
29.0	.67
35.0	.74
40.0	.82
45.0	.88

Run No. 61
Coolant temp. -14.0
Initial temp. 19.0
Heat trans.coeff.2000

Time	Ice Thickness
3.0	.12
8.0	.28
11.0	.36
17.0	.47
33.0	.72
62.5	1.18

Run No. 66
Coolant temp. -15.0
Initial temp. 13.0
Heat trans.coeff. 2000

Time	Ice Thickness
6.0	.29
22.0	.77
28.0	.90
35.0	1.03
47.0	1.27
70.0	1.68
83.0	1.92
86.0	1.97

Run No. 67
Coolant temp. -10.6
Initial temp. 16.5
Heat trans.coeff. 2000

Time	Ice Thickness
10.0	.15
42.0	.45
49.0	.48
63.0	.58
75.0	.69
82.0	.73
96.0	.85
100.0	.89
111.0	.97
120.0	1.04

Run No. 62
Coolant temp. -15.0
Initial temp. 21.0
Heat trans.coeff. 900.0

Time	Ice Thickness
4.0	.02
6.0	.07
10.0	.16
14.0	.22
29.0	.50

Run No. 63
Coolant temp. -15.0
Initial temp. 21.0
Heat trans.coeff. 900.0

Time	Ice Thickness
4.0	.02
6.0	.08
14.0	.27
20.0	.36
26.5	.47
36.0	.61
42.0	.70
51.5	.87
56.0	.93
66.0	1.09

APPENDIX 2.

FREEZING TIMES OF SOY BEAN CURD.

Comparison of experimental freezing times obtained by Komori (32) and predicted freezing times from four theoretical methods discussed in Chapter 4.

System conditions and physical properties of soy bean curd :-

	System 1.	System 2.
% moisture	83.0	89.2
K_1 (W/m C)	1.22	1.22
K_2 (W/m C)	0.42	0.42
C_1 (J/kg C)	2034.4	2034.4
C_2 (J/kg C)	3591.6	3687.9
L (J/kg)	$.27795 \times 10^6$	$.33488 \times 10^6$
H (W/m^2 C)	1402.3	3662.7
TC (C)	-28.0	-15.0
TI (C)	4.9	0.0
Tm (C)	0.0	0.0
ρ (kg/m^3)	1000.0	1000.0

RESULTS.

Frozen Thickness (mm)	Time to freeze frozen layer (h)				
	Experimental	Goodman	Modified Planck	Nagaoka	Vasil'ev and Uspenkii
System 1					
14	0.9	0.2	0.3	0.3	0.4
21	2.0	0.7	0.6	0.6	0.8
37	4.0	2.0	1.8	1.9	2.2
47	6.0	3.2	2.9	3.0	3.3
62	9.0	5.4	5.1	5.2	5.5
System 2					
15	0.9	0.7	0.6	0.6	0.7
21	2.0	1.4	1.2	1.2	1.4
32	4.0	3.2	2.8	2.8	3.1
40	6.0	4.8	4.3	4.3	4.6
54	9.0	8.4	7.8	7.8	8.1

APPENDIX 3.

DETERMINATION OF HEAT TRANSFER COEFFICIENT BETWEEN COOLANT AND FREEZING VESSEL.

NOMENCLATURE OF VARIABLES USED IN APPENDIX 3.

Physical properties of aluminium :

α = thermal diffusivity.

K = thermal conductivity.

Cp = specific heat.

ρ = density.

Temperatures :

TA = ambient temperature.

TI = initial temperature of aluminium bar.

Tc = coolant temperature.

TB = temperature of aluminium bar at $t = \infty$

TD = final offset temperature of heat transfer disc at $t = \infty$

H = heat transfer coefficient.

HG = heat gain coefficient.

---

k = time step length.

h = distance step length.

A3-1. INTRODUCTION.

The aims of appendix 3 are firstly to describe the evaluation of heat transfer coefficients, associated with the heat transfer discs used in the freezing rate experiments, for substitution into the theoretical methods described in chapter 4 and, secondly, to evaluate the accuracy of the optimised values of these coefficients.

The method of evaluation of the heat transfer coefficients used the same heat transfer apparatus as that used for the freezing experiments except that the freezing vessel was replaced by an aluminium bar. Determination of the coefficient was made by measuring the temperature transient in the aluminium bar brought into sudden contact with the coolant via the heat transfer disc and comparison with the heat transfer equation using a least squares minimization method.

The heat transfer coefficient to be determined was the coefficient between the coolant and the base of the aluminium bar. This coefficient was equal to the reciprocal value of the overall resistance between the base of the aluminium bar and coolant (which was equal to the sum of the coolant film resistance, disc resistance, and contact resistance between the disc and aluminium bar).

A3-2. EXPERIMENTS.

A3-2.1. Experimental Apparatus.

The essential elements of the apparatus were the coolant reservoir, heat transfer discs and aluminium bar. The coolant reservoir is described in Chapter 3, pp. 40-42.

The properties of the heat transfer discs are given in table A3-1 p 202

The aluminium bar, diameter 7.0 cm and length 5.08 cm, had the lower end machine smoothed to give good contact with the heat transfer discs. Two thermocouple holes were drilled to the axis of the aluminium bar at 0.635 and 3.18 cm distances from the smoothed surface of the bar. A copper-constantin thermocouple was inserted into each thermocouple hole and connected to the Honeywell temperature recorder.

All external surfaces of the apparatus were lagged.

Figure A3-1 shows the elements of the heat transfer apparatus. For experiments the apparatus was surrounded by a Dewar Flask.

Figure A3-1 Apparatus for heat transfer coefficient determination.

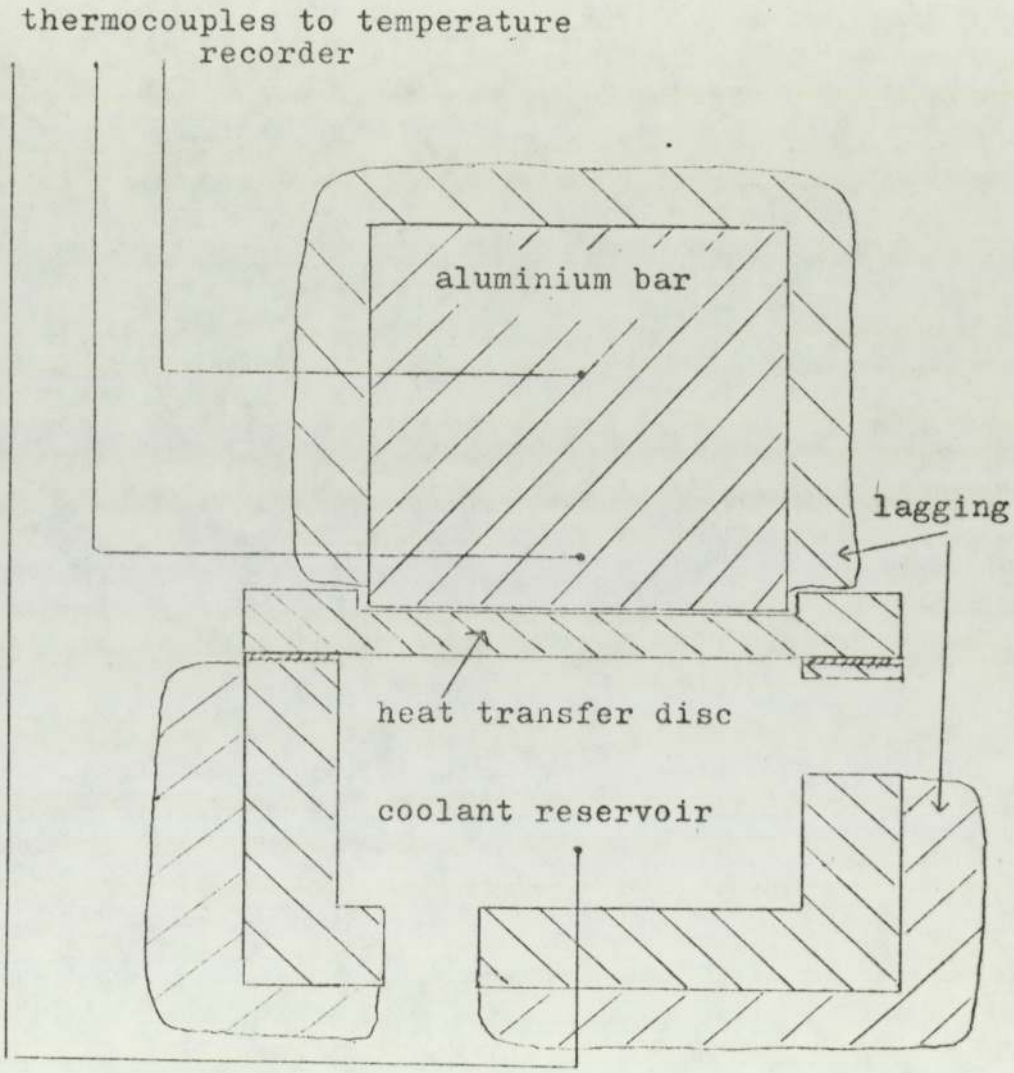

A3-2.2 Experimental Procedure.

With the aluminium bar and coolant at steady temperatures the bar was quickly brought into good thermal contact with the heat transfer disc, by pressing and turning the bar against the disc, and the temperature transients of the thermocouples in the bar recorded. Duplicate experiments with the two thermocouples interchanged minimized effects of thermocouple calibration errors.

A3-2.3 Experimental Variables.

Experiments were undertaken varying :

1. Coolant temperature between -3.6 C & -16.0 C

2. Initial aluminium bar temperature between 5.6 C & 26.4 C

3. Heat transfer disc : Number of experimental runs.

Perspex	10
Stainless steel	15
Copper & Polythene	5
Brass	20
Copper	20

A3-2.4 Experimental Results.

Reproducible results were only obtained when a good contact between the aluminium bar and heat transfer disc was made. Graphs A3-1 to A3-5 gives typical transient cooling curves of the aluminium bar for all five heat transfer discs.

Dimensionless temperatures : (T-Tc/TI-Tc),
(where T = aluminium bar temperature at a given time)

were used to eliminate differences in time-temperature profiles due to variation in coolant and initial bar temperatures.

For comparison of experimental and theoretical results the temperature profiles obtained from the thermocouple in the lower thermocouple position were used for each disc. The temperature profiles obtained from the experiments with each disc were smoothed to obtain the most accurate time temperature profiles.

A3-3. THEORY.

A3-3.1 Mathematical Model.

The assumptions of the model were : (see figure A3-2a).

Experimental Cooling Curves with Copper Disc

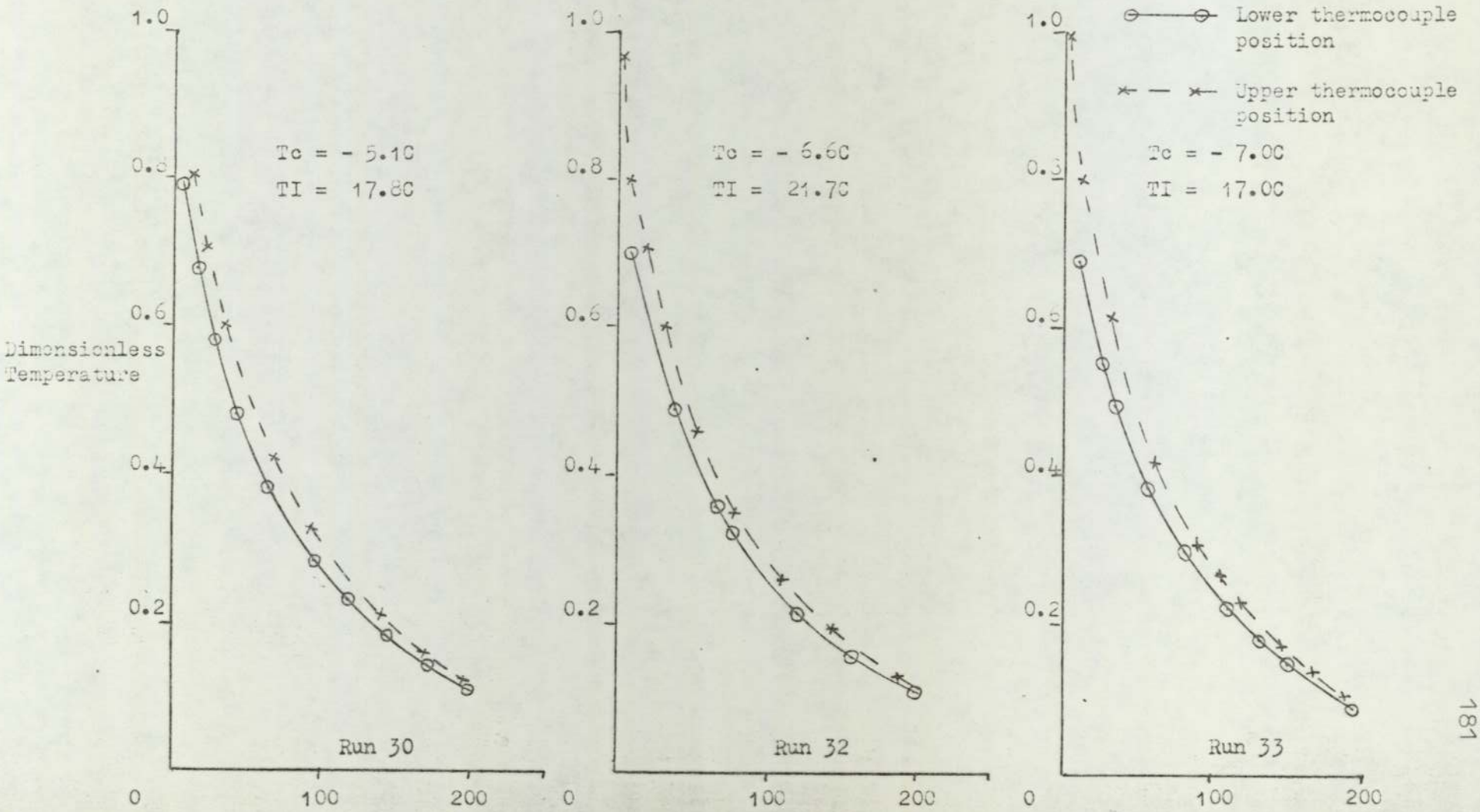

GRAPH A3 - 1

Experimental Cooling Curves with Brass Disc

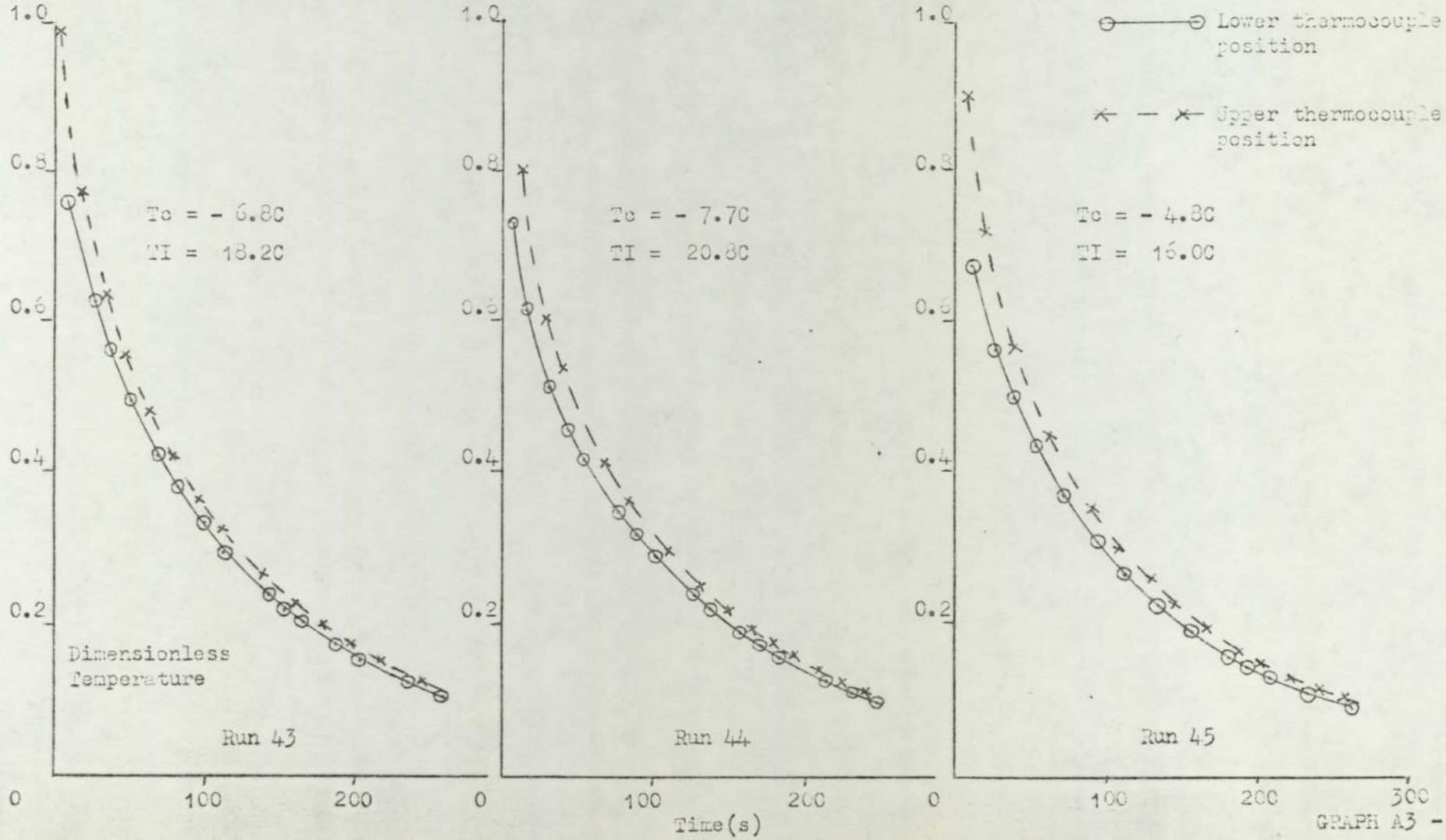

GRAPH A3 - 2

Experimental Cooling Curves with Stainless Steel Disc

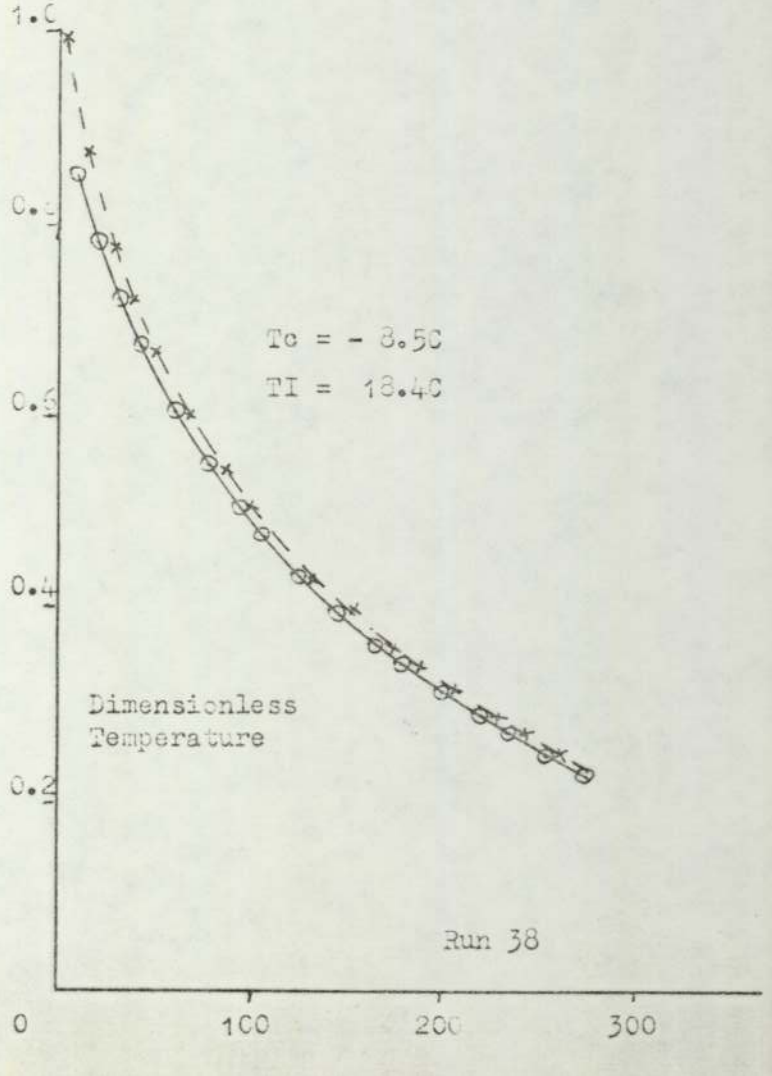

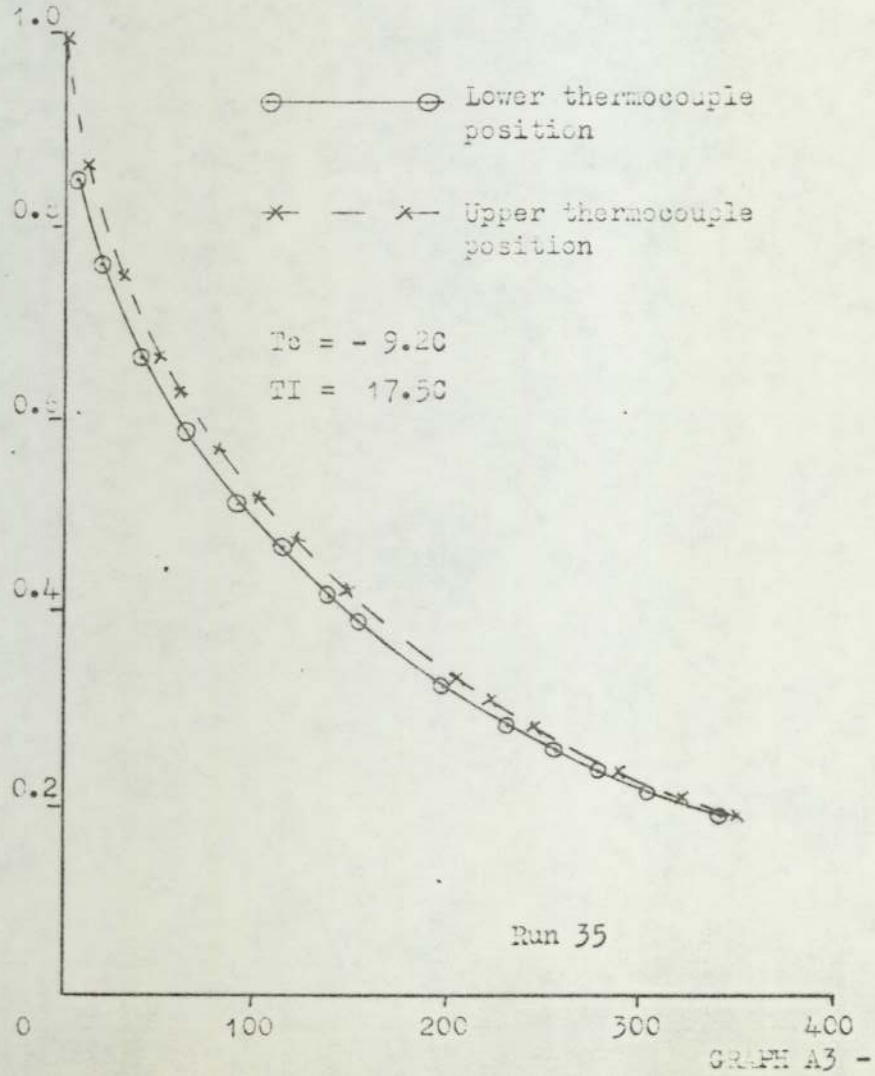

GRAPH A3 - 3

Experimental Cooling Curves with Copper plus Polythene Disc

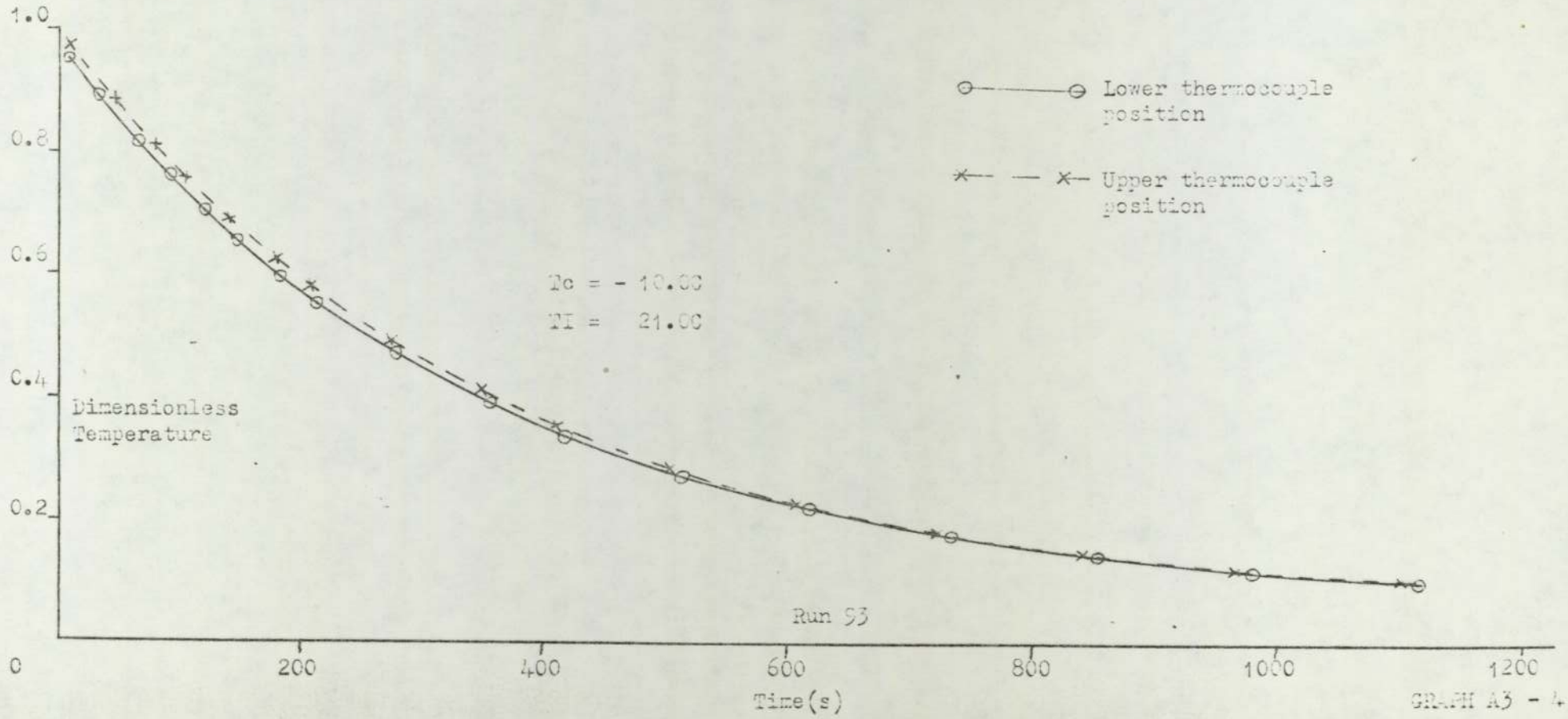

GRAPH A3 - 4

Experimental Cooling Curves with Perspex Disc

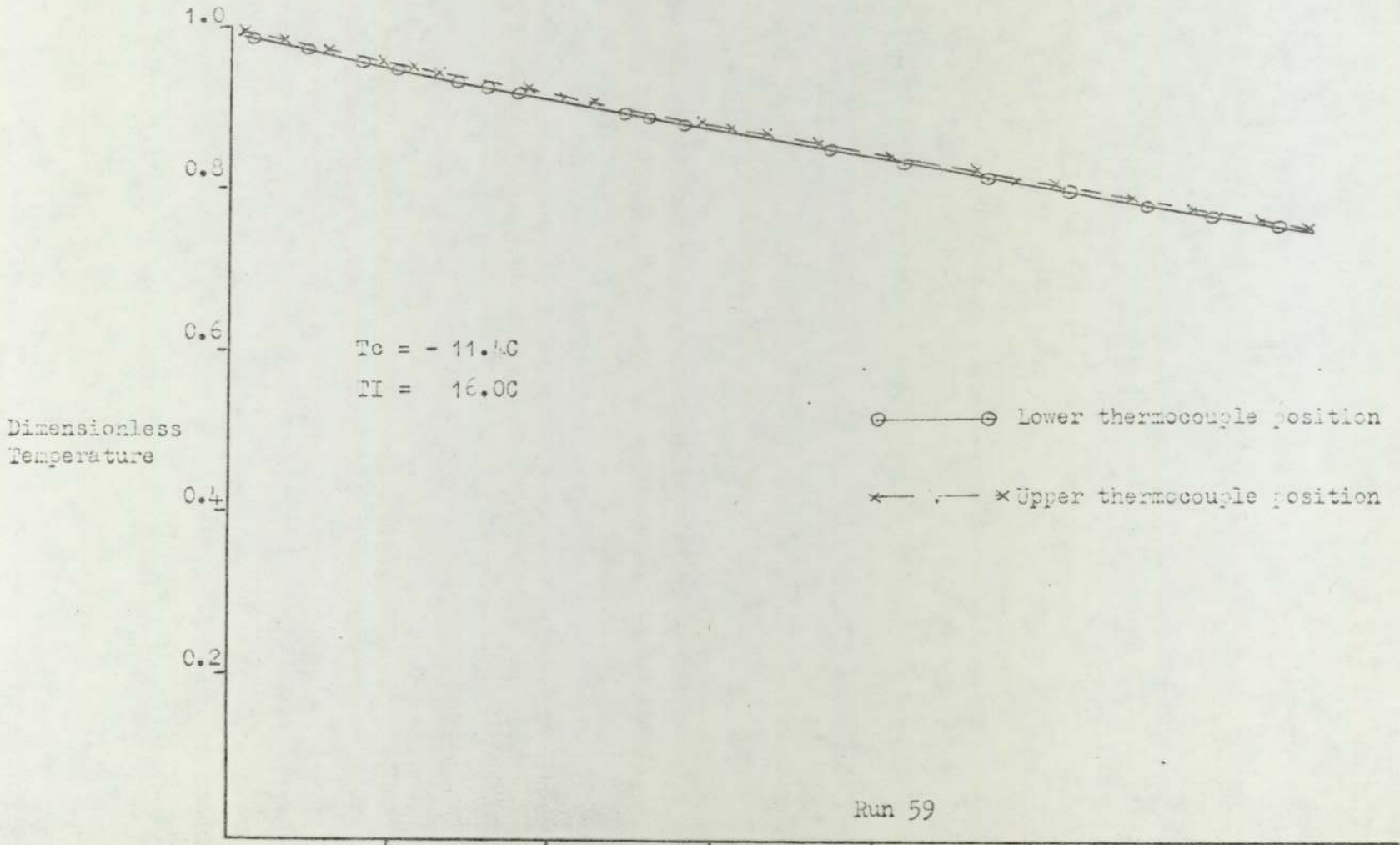

GRAPH A3 - 5

no radial heat flow (lagging and Dewar flask greatly reduced heat gain from the surroundings).

heat gain at x = L only.

constant physical properties.

Then the heat conduction equation becomes :

$$\frac{\partial T}{\partial t} = \alpha \frac{\partial^2 T}{\partial x^2} \quad (\text{where } \alpha = \frac{K}{\rho C_p}) \qquad (A3\text{-}1)$$

with initial condition : $T(x,t) = TI \quad 0 \leq x \leq L$

and boundary conditions :

at $x = 0$ for $t > 0$, heat conduction to coolant :

$$-K \left(\frac{\partial T}{\partial x} \right)_{x=0} = H(Tc - T(o,t)) \qquad (A3\text{-}2)$$

at $x = L$ for $t > 0$, $-K \left(\frac{\partial T}{\partial x} \right)_{x=L} = HG(T(L,t) - TA)) \qquad (A3\text{-}3)$

A3-3.2 Solutions to the Mathematical Model using Finite Difference Techniques.

For the solution of the mathematical model a fixed distance finite difference network was employed. The

Figure A3-2 Diagrams for determination of heat transfer coefficient

(a)

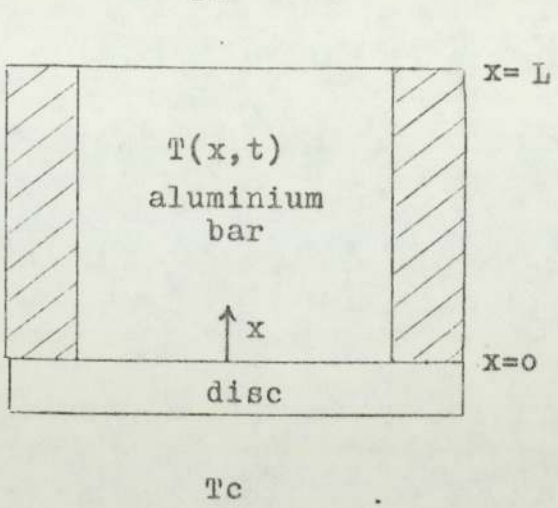

(b)

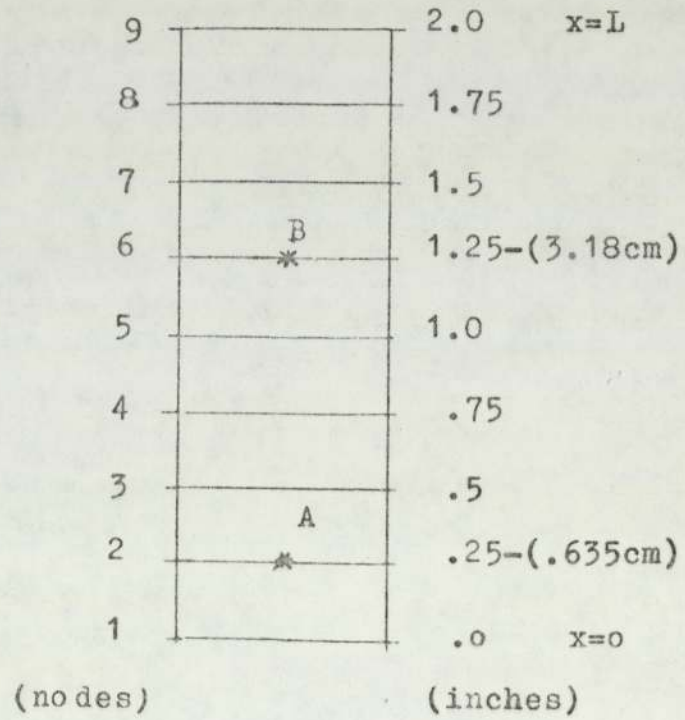

distance step length (HH in the computer programs) was fixed at 0.635 cm (0.25 in). The network involved eight steps (see figure A3-2b) covering the length of the aluminium bar (5.08 cm or 2.0 in) and nine nodes.

(A network involving sixteen step lengths was found to give no significant improvement in predicted aluminium bar temperatures compared to the eight step length network).

The temperatures at the nine nodes were calculated at each time step length. The theoretical temperatures calculated at node 2 (the lower thermocouple position, A in figure A3-2b) and node 6 (the upper thermocouple position, B in figure A3-2b) can be compared directly with experimental temperatures.

The finite difference approximation is now evaluated in detail both explicitly and implicitly with the differential coefficients $\partial T/\partial t$, $\partial T/\partial x$ and $\partial^2 T/\partial x^2$ defined as :

$$\frac{\partial T}{\partial t} = \frac{T_{n,m+1} - T_{n,m}}{k}$$

$$\frac{\partial T}{\partial x} = \frac{T_{n+1,m} - T_{n,m}}{h}$$

$$\frac{\partial^2 T}{\partial x^2} = \frac{T_{n+1,m} - 2T_{n,m} + T_{n-1,m}}{h^2}$$

A3-3.3 Explicit Finite Difference Approximation.

The heat conduction equation in 1 direction is :

$$\frac{\partial T}{\partial t} = \frac{K}{\rho C_p} \frac{\partial^2 T}{\partial x^2} \qquad \text{(A3-1)}$$

which can be expressed using an explicit finite difference approximation as :

$$\frac{T_{n,m+1} - T_{n,m}}{k} = \frac{K}{\rho C_p} \left(\frac{T_{n+1,m} - 2T_{n,m} + T_{n-1,m}}{h^2} \right) \qquad \text{(A3-4)}$$

where **k** = time step length

h = distance step length.

Equation A3-4 can be rearranged to give the relationship between the temperature at time step (m+1) and three temperatures at time step (m) :

$$T_{n,m+1} = BT_{n+1,m} + (1-2B)T_{n,m} + BT_{n-1,m} \qquad \text{(A3-5)}$$

where $B = \frac{kK}{\rho C_p h^2}$

Equation (A3-5) is used to calculate temperatures at all internal step length positions or nodes.

At x = 0, boundary condition equation (A3-2) can be expressed as :

$$\frac{-K\ (T_2 - (T_{-1})\ )}{2h} = H(Tc-T(o,t)\ )$$

By elimination of (T_{-1}), a fictitious node, the boundary equation at x=o, with $N = \frac{2hH}{K}$ becomes :

$$T_{1,m+1} = 2BT_{2,m} + (1-2B)T_{1,m} + B(N(Tc-T_{1,m})) \quad (A3-6)$$

At x = L, boundary condition equation (A3-3) can be expressed as :

$$\frac{-K\ (T_{10}-T_8)}{2h} = HG\ (T_9-TA)$$

By elimination of (T_{10}), a second fictitious node, the boundary equation at x = L, with NA = 2h HG/K becomes :

$$T_{9,m+1} = 2BT_{8,m} + (1-2B)T_{9,m} - B(NA(T_{9,m}-TA)) \quad (A3-7)$$

Since the temperatures for all values of n at zero time (initial temperatures) are known, the temperatures at successive time step lengths can be computed by equations A3-5, A3-6, and A3-7.

With the explicit finite difference procedure the stability criterion of no negative coefficients must be tested. In the above set of equations A3-5, A3-6 and A3-7 the value of B must comply with the following factor :

$$B \leq 1/2 \; (1/(_{1-N}) \;)$$

The flowdiagram and program listing are given on the next pages.

A3-3.4 Implicit Finite Difference Approximation.

Starting with the heat conduction equation (A3-1) in the following form :

$$\frac{T_{n,m+1} - T_{n,m}}{k} = \frac{K}{\rho C_p} \; \frac{(T_{n+1,m+1} - 2T_{n,m+1} + T_{n-1,m+1})}{h^2}$$

rearrangement with $B = \frac{kK}{h^2 \rho C_p}$ produces :

$$-1/B \; T_{n,m} = T_{n+1,m+1} - (2 + 1/B) \; T_{n,m+1} \qquad (A3\text{-}8)$$

as the general form of the implicit finite difference solution.

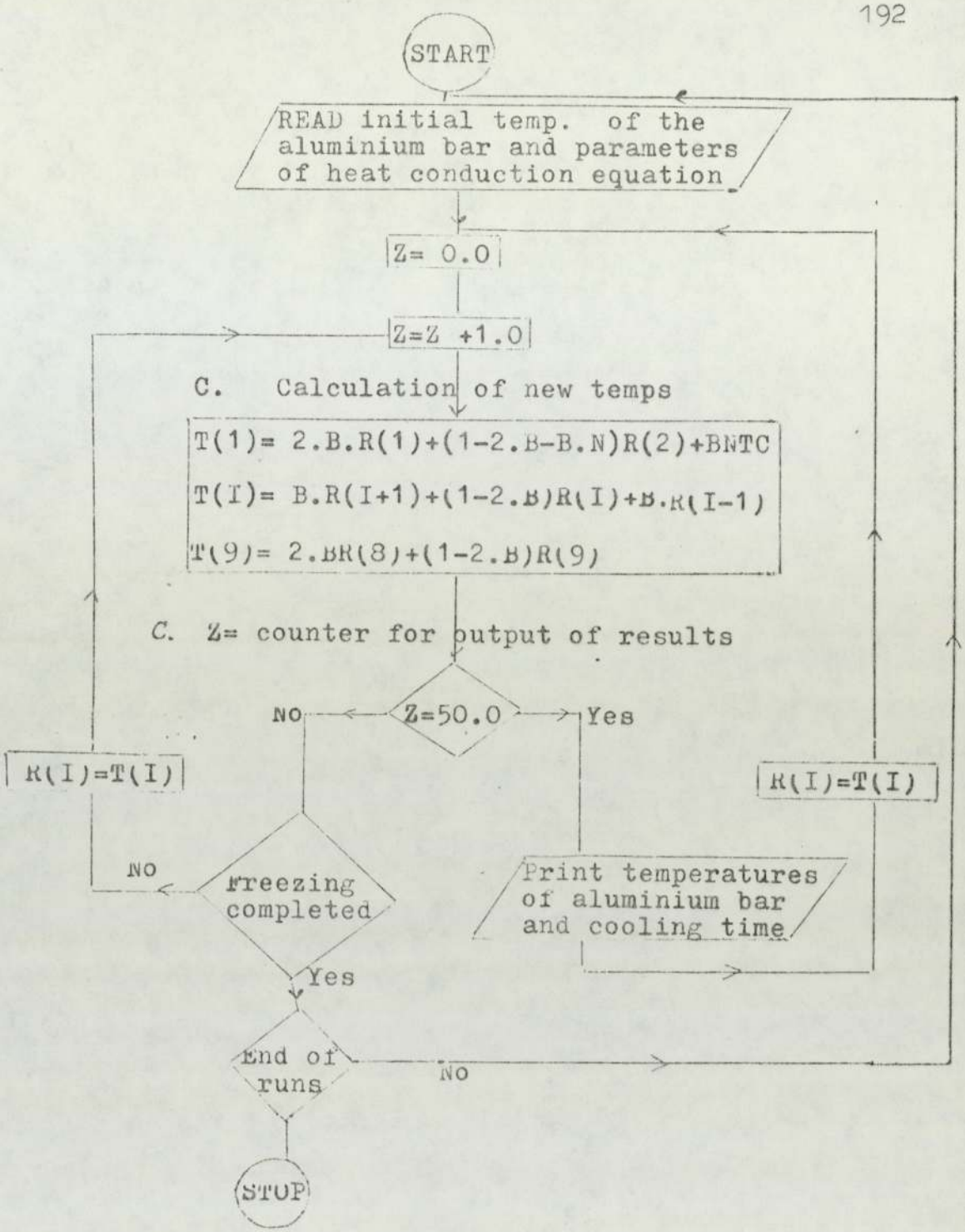

Flowdiagram for expicit finite difference solution

Computer program for explicit finite difference method for determining heat transfer coefficient

```
      PROGRAM NAME(INPUT,OUTPUT,TAPE1=INPUT,TAPE2=OUTPUT)
      DIMENSION RR(9)
      DIMENSIONR(9),T(9)
      READ(1,220)XK,P,CP
220   FORMAT(3F10.4)
      READ(1,60) TI,TC
60    FORMAT(2F10.4)
      NMK=0
      MBB=0
 520  DO 150 I=1,9
      R(I)=TI
 150  CONTINUE
      READ(1,230) YKK,H,HH
230   FORMAT(F10.7,F10.4,F10.2)
      TA=68.0
      AA=XK/(P*CP)
      BB=YKK/H**2
      B=AA*BB
      YXN=2.0*HH*H/XK
      REALT=0.0
      WRITE(2,62)YKK,H,HH
62    FORMAT(1H1,20X,'TIME STEP LENGTH IS',15X,F8.6,3X,'HRS'/20X,'DIST
     1CE STEP LENGTH IS',14X,F6.4,3X,'FT' /20X,'HEAT TRANSFER COEFFICI
     2NT IS',4X,F6.1,3X,'BTU/HR.F.FT**2'///)
48    WRITE(2,52)
52    FORMAT(3X,'TIME',25X,'DIMENSIONLESS TEMPERATURES'/ 3X,'(SECS)'
     123X,'     AT POINTS 1 TO 9'//)
666   Z=0.0
55    Z=Z+1.0
      REALT=REALT+(YKK*3600.0)
837   T(1)=2*B*R(2)+(1-2*B-B*YXN)*R(1)+  YXN*B*24.0
      DO 800 I=2,8
      T(I)=B*R(I+1)+(1-2*B)*R(I)+B*R(I-1)
800   CONTINUE
      T(9)=2.0*B*R(8)+(1.0-2.0*B)*R(9)
      IF(Z.EQ.50 .0) GO TO 450
777   DO 7 I=1,9
      R(I)=T(I)
7     CONTINUE
      GO TO 55
450   DO 57 I=1,9
      RR(I)=(T(I)-TC)/(TI-TC)
57    CONTINUE
      WRITE(2,50)REALT,RR(2),RR(6 )
50    FORMAT(2X,F8.3,5X,F6.5,2X,F6.5,5X,F6.5)
877   DO 9 I=1,9
      R(I)=T(I)
9     CONTINUE
      IF(REALT.LE.800 ) GO TO 5203
      GO TO 520
5203  CONTINUE
      GO TO 666
      END
```

The boundary condition equations are solved, by eliminating fictitious boundary temperatures, in the same way as for the explicit approximation to produce at :-

$$x = 0 : -1/B\ T_{1,m} = T_{2,m+1} - (2 + 1/B + N)T_{1,m+1} + NTC \qquad (A3\text{-}9)$$

where $N = \frac{2hH}{K}$

$$x = L : -1/B\ T_{9,m} = 2T_{8,m+1} - BAT_{9,m+1} + ANTA \qquad (A3\text{-}10)$$

where $BA = 2 + 1/B + AN$

and $AN = \frac{HG2h}{K}$

Equations (A3-8), (A3-9) and (A3-10) with the following substitutions :

$$BB = 2 + 1/B + N$$
$$RR = 1/B\ T_{1,m} - NTc$$
$$RB = 1/B\ T_{n,m}$$
$$C = 2 + 1/B$$

are used to determine the temperatures at the first time step length from the initial conditions and parameters of the equations. The process of evaluation of the

unknown temperatures involves calculating the parameters BB and C and the variables RR and RB and incorporating them into the two dimensional array given below :

-BB	2	0	0	0	0	0	0	0	-RR
1	-C	1	0	0	0	0	0	0	-RB
0	1	-C	1	0	0	0	0	0	-RB
0	0	1	-C	1	0	0	0	0	-RB
0	0	0	1	-C	1	0	0	0	-RB
0	0	0	0	1	-C	1	0	0	-RB
0	0	0	0	0	1	-C	1	0	-RB
0	0	0	0	0	0	1	-C	1	-RB
0	0	0	0	0	0	0	2	-C	-RB

The above array can be incorporated into the following tridiagonal matrix equation for the temperatures $T_1, T_2, \ldots\ldots T_n$

$$\begin{bmatrix} b_1 & C_1 & & & & \\ a_2 & b_2 & C_2 & & & \\ & a_3 & b_3 & C_3 & & \\ & & \ddots & \ddots & \ddots & \\ & & & a_{n-1} & b_{n-1} & C_{n-1} \\ & & & & a_n & b_n \end{bmatrix} \begin{bmatrix} T_1 \\ T_2 \\ T_3 \\ \vdots \\ T_{n-1} \\ T_n \end{bmatrix} = \begin{bmatrix} d_1 \\ d_2 \\ d_3 \\ \vdots \\ d_{n-1} \\ d_n \end{bmatrix} \quad \begin{matrix} \text{(A3-11)} \\ \text{(A3-12)} \\ \text{(A3-13)} \end{matrix}$$

The method of solving the temperatures in the tridiagonal matrix is one of elimination followed by back-substitution. The elimination process uses the following method :

$$b_1 T_1 + C_1 T_2 = d_1 \qquad \text{(A3-11)}$$

$$a_2 T_1 + b_2 T_2 + C_2 T_3 = d_2 \qquad \text{(A3-12)}$$

Elimination of $a_2 T_1$ from (A3-12) by multiplying equation (A3-11) by a_2/b_1 and then subtracting (A3-11) from (A3-12) produces :

$$\left(b_2 - \frac{a_2}{b_1} \cdot C_1\right) T_2 + C_2 T_3 = d_2 - \frac{a_2}{b_1} \cdot d_1$$

and if : $\beta_2 = b_2 - \frac{a_2}{b_1} \cdot C_1$ and $\delta_2 = d_2 - \frac{a_2}{b_1} \cdot d_1$

equation (A3-12) becomes : $\beta_2 T_2 + C_2 T_3 = \delta_2$

The process is continued for equations (A3-12) and (A3-13).

$$\beta_2 T_2 + C_2 T_3 = \delta_2 \qquad \text{(A3-12)}$$

$$a_3 T_2 + b_3 T_3 + C_3 T_4 = d_3 \qquad \text{(A3-13)}$$

to produce $\beta_3 T_3 + C_3 T_4 = \delta_3$ for equation (A3-12).

In general $\beta_r T_r + C_r T_r = \delta_r$

let $\beta_o = b_o$ and $\delta_o = d_o$

Therefore $$\beta_n = b_n - \frac{a_n C_{n-1}}{\beta_{n-1}}$$

and $$\delta_n = d_n - \frac{a_n \delta_{n-1}}{\beta_{n-1}}$$

for $n = 1, 2 \ldots . n$

At the end of the elimination process, by the above rearrangements equation n becomes $\beta_n T_n = \delta_n$, thus T_n can be found.

By back-substitution the values T_{n-1} to T_1 can be calculated :

$$\beta_{n-1}\, T_{n-1} + C_{n-1}\, T_n = \delta_{n-1}$$

therefore $$T_{n-1} = \frac{\delta_{n-1} - C_{n-1}, T_n}{\beta_{n-1}}$$

for n = n, n-1, n-2, ...1

This process is continued for future time steps.

The flow diagram is given on the next page, the program listing is incorporated into the optimisation program in subroutine FUNC (see pp210 -212)

A3-3.5 Theoretical Results.

In order to ensure correct results by the finite difference approximations comparison with an analytical solution (Carslaw and Jeager (10)) was made for the case of no heat gain (i.e. HG=0).

Graph A3-6 shows the time temperature profiles calculated at the lower thermocouple position in the aluminium bar, for various values of the heat transfer coefficient. The dotted lines represent the temperature profiles calculated by the explicit and implicit finite

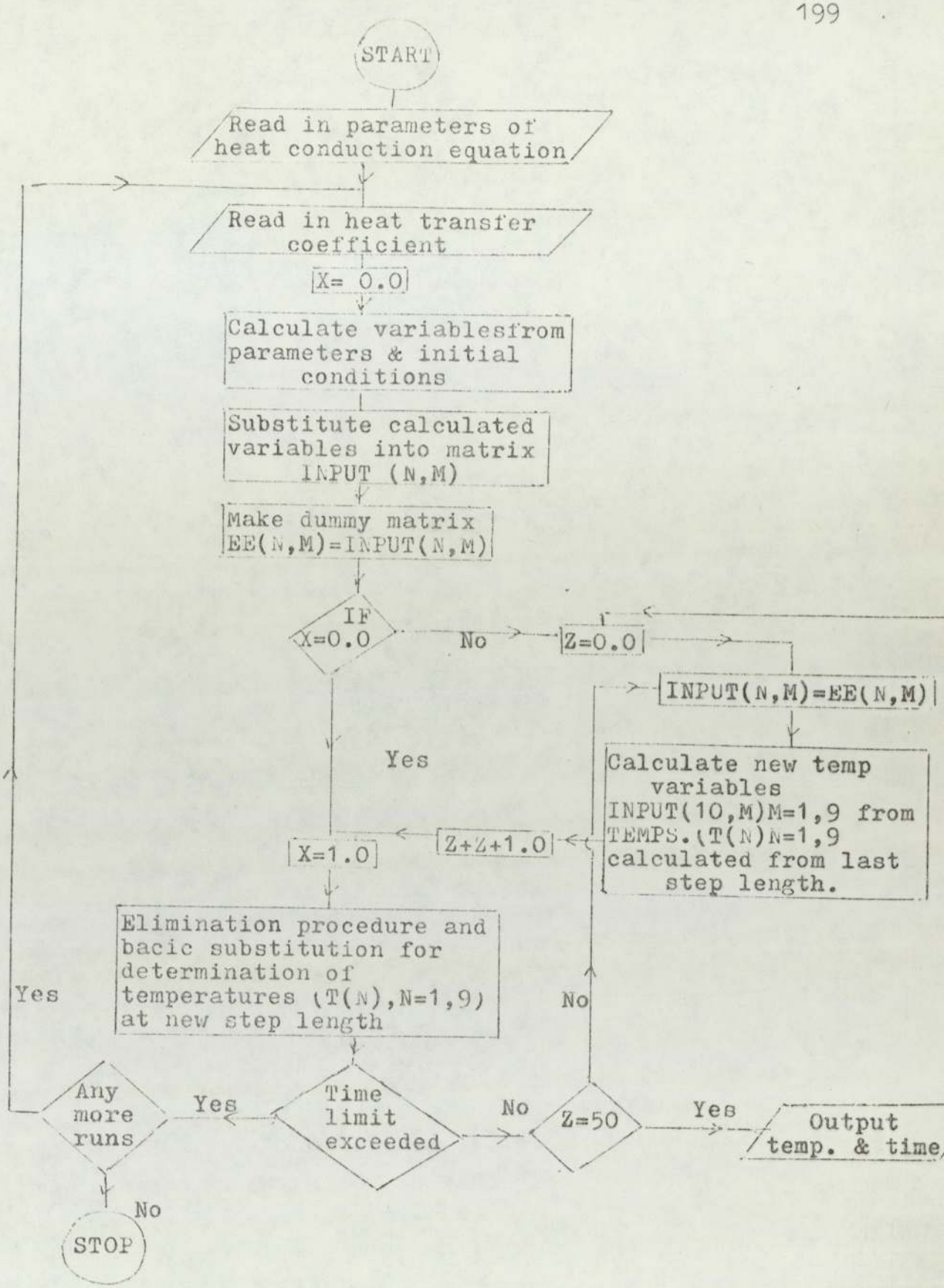

Flow diagram for implicit finite difference computer program

Theoretical Cooling Curves of Aluminium Bar (lower thermocouple position)

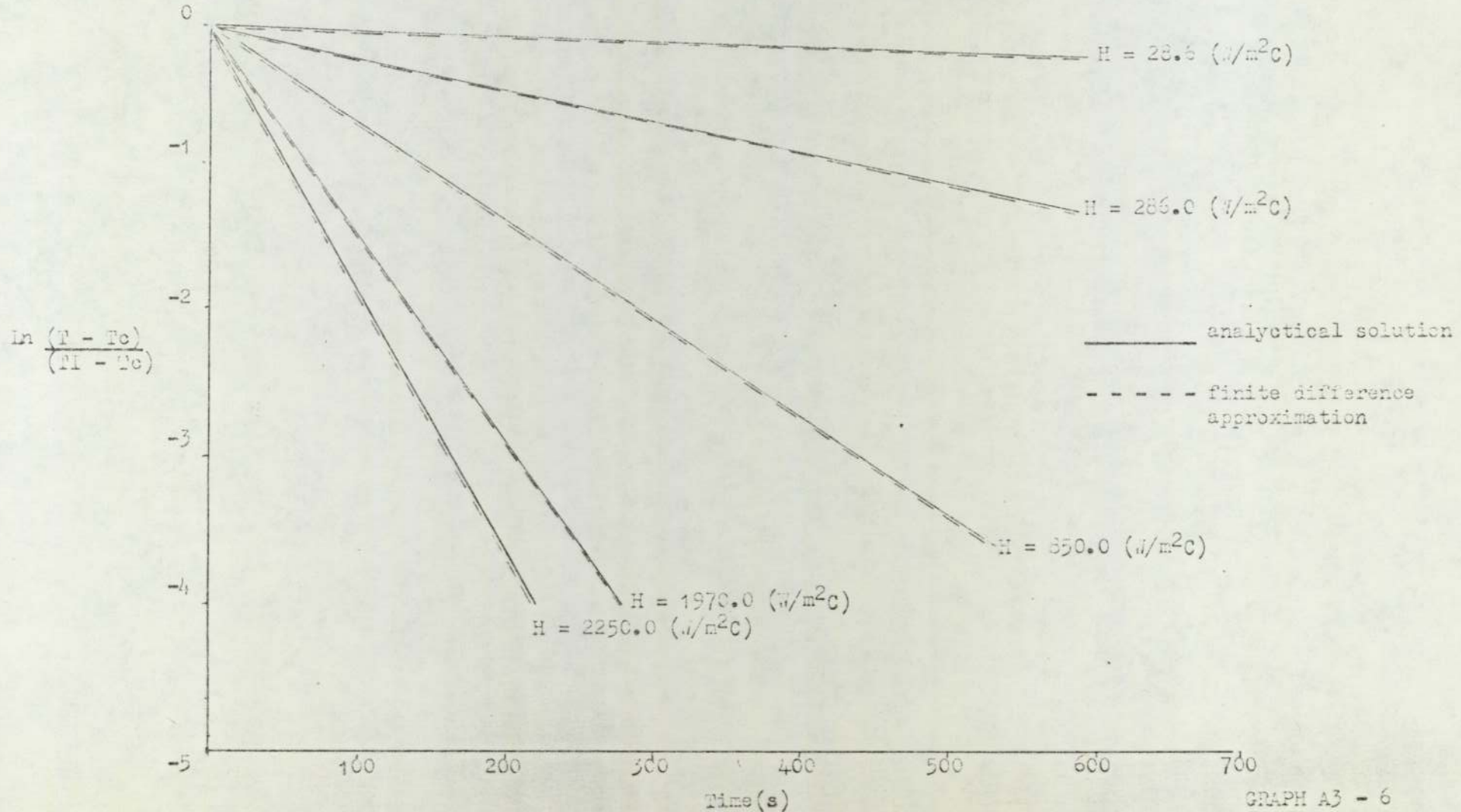

GRAPH A3 - 6

difference methods and the continuous lines show the temperature profiles calculated by the analytical solution. The predicted profiles obtained by both finite difference methods and by the analytical solution can be seen to agree well for all values of the heat transfer coefficient.

The difference in the theoretical cooling profiles between the two cases HG = 0 and HG $\neq$ 0 was that the cooling profiles did not attain steady state at the coolant temperature, but remained at a permanent offset temperature above the coolant temperature, when there was heat gain (i.e. HG $\neq$ 0).

Comparison of the finite difference solutions when HG $\neq$ 0 produced good agreement for the same values of the heat gain coefficient.

A3-4. DISCUSSION OF RESULTS.

A3-4.1 Offset Values.

Experimental aluminium bar cooling curves did not attain steady state at the coolant temperature but

remained, as with theoretical curves when HG≠ 0 at permanent offset values. The offset values were expressed by the dimensionless term (TB-Tc)/(TA-Tc) (Where TB = final state bar temperature). Table A3-1 lists the offset values.

TABLE A3-1 - Resistances and Offset Values of Heat Transfer Discs.

	TYPE OF DISC					
	PERSPEX	COPPER + POLY-THENE		STAINLESS STEEL	BRASS	COPPER
		(C)	(P)			
Thickness L (mm)	3.25	4.22	0.96	10.79	11.15	4.22
Thermal conductivity K (W/mC)	0.19	387.7	0.46	15.9	96.9	387.7
Disc resistance x 10^{-3}	17.1	.011 + 2.098		.68	.115	0.011
L/K (m^2C/W)		= 2.109				
Offset Value (dimensionless)	.08	.05		.03	.02	.02

The magnitude of the offset value was dependent on the heat transfer disc used. Using an electrical analogue of the system : - (see figure A3-4),

where R_1 = resistance of aluminium bar (constant value for all discs).

and R_3 = resistance of disc

Figure A3-4

the following formula was obtained :

$$\frac{TB - Tc}{R_3} = \frac{TA - Tc}{R_1 + R_3}$$

which on rearrangement produced :

$$TB = (TA - Tc)\ \frac{R_3}{R_3 + R_1} + Tc \qquad (A3\text{-}14)$$

Equation (A3-14) shows that the smaller R_3 (Disc resistance) is, the closer TB will be to Tc.

A3-4.2 Optimisation of Heat Transfer Coefficients

To obtain the most accurate values of the heat transfer coefficient between the base of the aluminium bar and the coolant the theoretical cooling curves obtained from the solution of the mathematical model were compared with experimental cooling curves using a least squares optimisation program. The program used was a Nelder and Mead optimisation routine (111).

The objective function to be minimised was:

$$\Sigma Y(I) = (EX(J) - EXPER(I,J))^{**2}$$

where $\Sigma Y(I)$ was the sum of squares function to be minimised over 10 points. The values of the array EXPER(I,J) were the experimentally recorded results for the temperature of the lower thermocouple position of the aluminium bar. Array EX(J) stored the calculated theoretical temperatures for the aluminium bar at the node corresponding to the lower thermocouple position from the finite difference solution in the mathematical model. Values of the heat gain and heat transfer coefficients were changed independently in the program to obtain theoretical cooling curves for comparison with the experimental results.

The optimised values of the coefficient are given in table A3-2. Comparison of the optimised

TABLE A3-2.

Heat Transfer Disc	Heat Transfer Coefficient (W/m^2C).	Heat Gain Coefficient (W/m^2C).
Perspex	56.8	2.7
Copper & Polythene	350.0	5.1
Stainless Steel	900.0	9.6
Brass	1700.0	9.6
Copper	2000.0	9.6

theoretical results are shown on graphs A3-7 to A3-11 and tables A3-3 to A3-7. The Flowdiagram and listing of the optimisation program are given after the graphs and tables.

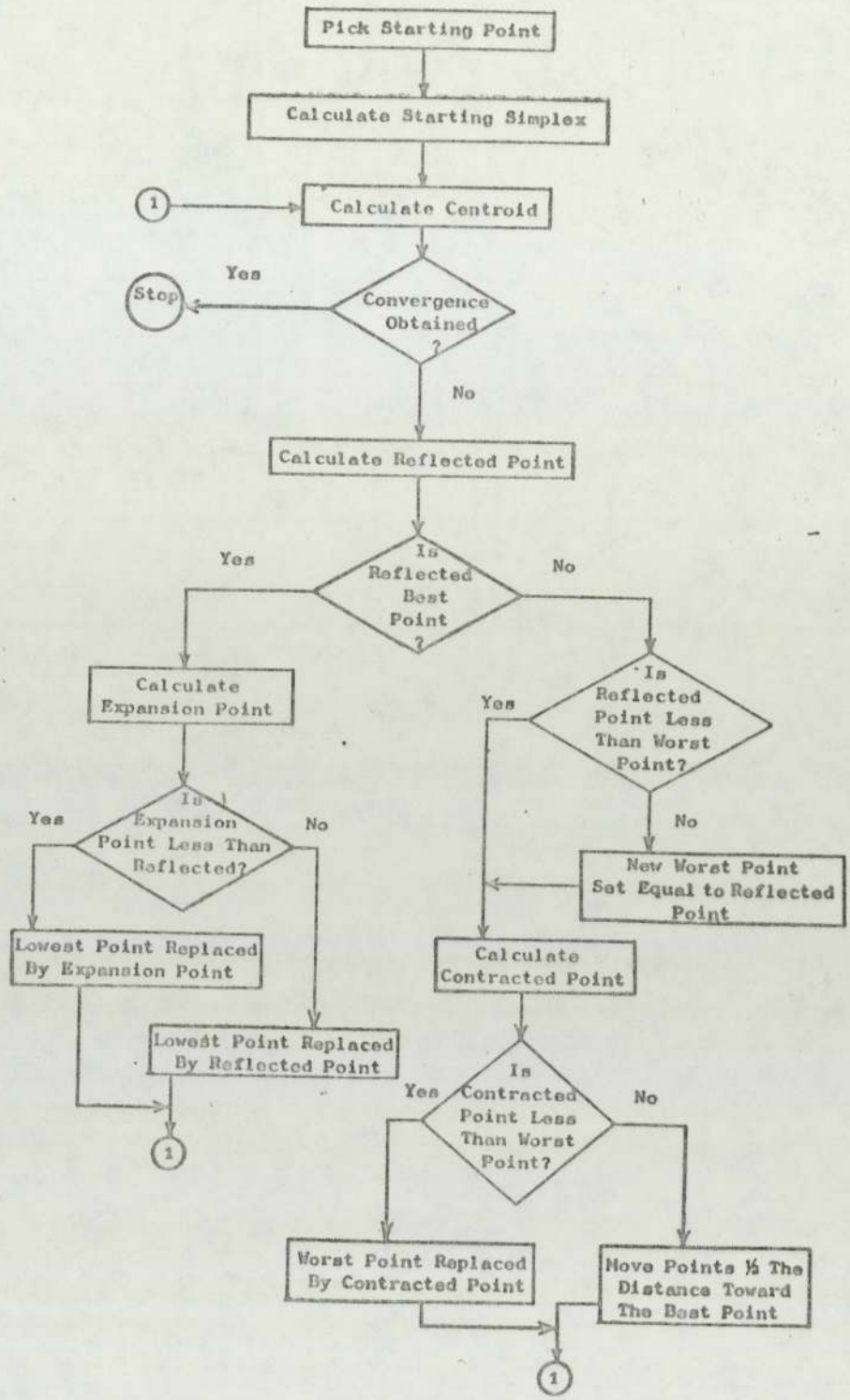

Nelder and Mead (NELDER ALGORITHM) Logic Diagram *(111)*

Optimisation (Nelder & Mead) program incorporating implicit finite difference method for determining heat transfer coefficient in subroutine FUNC. (111)

```
      PROGRAM NAME(INPUT,OUTPUT,TAPE1=INPUT,TAPE2=OUTPUT)
C
C     NELDER AND MEAD MINIMIZATION
C
      INTEGER W
      DIMENSION X(3,2),XCEN(3,2),XREF(3,2),XCON(3,2),XEX(3,2),Z(3)
      DIMENSION  EXPER(10,10)
      COMMON EXPER
      COMMON KZK
C
C
      KZK=0
C
C
      KAAJ = 0
      READ(1,101) N,ITMAX,IPRINT
  101 FORMAT(8I10)
      NP1 =N +1
      READ(1,102) ALFA, BETA, GAM, ACC, A
  102 FORMAT(8F10.0)
    7 READ(1,102) (X(1,J),J=1,N)
C
      KAAJ = KAAJ + 1
      READ(1,511)((EXPER(J,W),W=1,2),J=1,10)
  511 FORMAT(2 F10.0)
      Q =(A/N*(2.**.5))*((N+1.)**.5-1.)
      P =(A/N*(2.**.5))*((N+1)**.5+N-1.)
      M=N+1
      DO 130 I=2,M
      AP=1.
      DO 120 J=1,N
      AP =AP+1
      IF (I.EQ.AP) GO TO 135
      X(I,J) =X(1,J)+Q
      GO TO 120
  135 X(I,J)=X(1,J)+P
  120 CONTINUE
  130 CONTINUE
C
      IF(ALFA.EQ.0.) ALFA =1.
      IF(BETA.EQ.0.) BETA =.5
      IF(GAM.EQ.0.) GAM =2.
      IF(ACC.EQ.0.) ACC =.0001
C
      WRITE(2,103)
  103 FORMAT(1H1,10X,28HNELDER AND MEAD OPTIMIZATION)
      WRITE(2,104)
  104 FORMAT(/,2X,10HPARAMETERS)
C
      WRITE (2,105) N,ACC,ALFA, BETA,GAM
  105 FORMAT( /2X,3HN= ,I2,4X,'ACCURACY= ',E10.4 / 2X,'ALPHA= ',
     1E10.4,4X,'BETA = ',E10.4,4X,'GAMMA =',E10.4)
      DO 140 I=1,NP1
      WRITE(2,106)(I,J,X(I,J),J=1,N)
  106 FORMAT(/2(2X,2HX(,I2,1H,,I2,4H) = ,1PE12.5))
  140 CONTINUE
      ITR=0
```

```
  150 DO 155  I=1,NP1
      CALL FUNC(I,X,Z,N,NP1)
  155 CONTINUE
      ITR= ITR +1
      IF(ITR.GE.ITMAX)GO TO 145
      IF(IPRINT) 158,162,158
  158 WRITE(2,108) ITR
  108 FORMAT(///2X,'ITERATION NUMBER',I3)
      DO 160 J=1,NP1
  160 WRITE(2,106)(J,I,X(J,I),I=1,N)
      WRITE(2,109)(I,Z(I),I=1,NP1)
  109 FORMAT(/3(2X,2HF(,I2,4H) = ,F16.8))
  162 ZHI =AMAX1 (Z(1),Z(2),Z(3))
      ZLO =AMIN1 (Z(1),Z(2),Z(3))
      DO 165 I= 1,NP1
      IF (ZHI.EQ.Z(I)) GO TO 170
  165 CONTINUE
  170 K=I
      EN=N
      DO 180 J=1,N
      SUM= 0.
      DO 175 I=1,NP1
      IF(K.EQ.I) GO TO 175
      SUM =SUM +X(I,J)
  175 CONTINUE
  180 XCEN(K,J)= SUM/EN
      I=K
      CALL FUNC (I,XCEN,Z,N,NP1)
      ZCEN =Z(I)
      SUM =0.
      DO 185 I=1,NP1
      IF(K.EQ.I) GO TO 185
      SUM= SUM +(Z(I)-ZCEN)*(Z(I)-ZCEN)/EN
  185 CONTINUE
      EJ =SQRT(SUM)
      IF (EJ.LT.ACC) GO TO  998
      DO 190 J=1,N
      XREF(K,J)=XCEN(K,J) +ALFA*(XCEN(K,J)-X(K,J))
  190 CONTINUE
      I=K
      CALL FUNC (I,XREF,Z,N,NP1)
      ZREF =Z(I)
      DO 200 I=1,NP1
      IF(ZLO.EQ.Z(I)) GO TO 205
  200 CONTINUE
C
  205 L=I
      IF(ZREF.LE.Z(L))GO TO 240
      DO 207  I=1,NP1
      IF(ZREF.LT.Z(I)) GO TO 208
  207 CONTINUE
      GO TO 215
  208 DO 210 J=1,N
  210 X(K,J)= XREF(K,J)
      GO TO 150
  215 DO 220 J=1,N
  220 XCON(K,J)=XCEN(K,J)+BETA*(X(K,J)-XCEN(K,J))
```

```
      I=K
      CALL FUNC (I,XCON,Z,N,NP1)
      ZCON =Z(I)
      IF(ZCON.LT.Z(K))GO TO 230
      DO 225  J=1,N
      DO 225  I=1,NP1
  225 X(I,J) =(X(I,J)+X(L,J))/2.
      GO TO 150
  230 DO 235 J=1,N
  235 X(K,J) =XCON(K,J)
      GO TO 150
  240 DO 245 J=1,N
  245 XEX(K,J)=XCEN(K,J) +GAM *(XREF(K,J)-XCEN(K,J))
      I=K
      CALL FUNC (I,XEX,Z,N,NP1)
      ZEX =Z(I)
      IF (ZEX.LT.Z(L))GO TO 255
      DO 250  J=1,N
  250 X(K,J) =XREF(K,J)
      GO TO  150
  255 DO 260 J=1,N
  260 X(K,J) =XEX(K,J)
      GO TO 150
  145 WRITE (2,111) ITMAX
  111 FORMAT(///10X,'DID NOT CONVERGE IN',I5,'ITERATIONS')
  998 WRITE(2,112) ZLO
  112 FORMAT(//2X,'OPTIMUM VALUE OF F=', E16.8)
      WRITE(2,113)
  113 FORMAT(//2X,'OPTIMUM VALUES OF VARIABLES')
      DO 300 I=1,N
  300 WRITE(2,114) I,X(NP1,I)
  114 FORMAT(/2X,2HX(,I2,4H) = ,1PE16.8)
C
      GO TO (30,31,33,34,32), KAAJ
   30 WRITE(2,40)
   40 FORMAT(/'COPPER DISC ')
      GO TO 36
   31 WRITE(2,41)
   41 FORMAT(/'BRASS DISC')
      GO TO 36
   32 WRITE(2,42)
   42 FORMAT(/'STAINLESS STEEL DISC')
      GO TO 36
   33 WRITE(2,43)
   43 FORMAT(/'COPPER + POLYTHENE DISC')
      GO TO 36
   34 WRITE(2,44)
   44 FORMAT(/'PERPEX DISC')
   36 CONTINUE
      IF (KAAJ.GT.5) GO TO 3
      GO TO 7
    3 STOP
      END
```

```
      SUBROUTINE FUNC(I,X,Z,NA,NP1)
      REAL KK,K,NN,INPUT(10,10)    ,INNNN(10,10)
      INTEGER W
      DIMENSIONX(NP1,NA),Z(NP1)
      DIMENSION EX(10)
      DIMENSION EE(10,10)
      DIMENSION EXE(10,10) ,EXPER(10,10)
      DIMENSIONXR(10,10)    ,ZY(10)
      DIMENSION RN(10,10)
      DIMENSION E(10),T(10)
      COMMON EXPER
      COMMON KZK
      REALT=0.
      XX=0.
      YYY=0.
      NMAX=10
      IF(KZK.NE.0) GO TO 512
      READ(1,10) KK,HH,P,K,SP
10    FORMAT(F10.7,4F10.4)
C COOLANT TEMPERATURE IS TF
      READ(1,30)((INNNN(N,M),M=1,10),N=1,9)
30    FORMAT(10F5.2)
      WRITE(2,683)((EXPER(W,N),N=1,2),W=1,NMAX)
 683  FORMAT(/10X,2F10.3,5X,'EXPER'/)
 512  KZK=1
      DO 91 M=1,9
      DO 92 N=1,10
      EXE(M,N)=INNNN(M,N)
92    CONTINUE
91    CONTINUE
 844  TF=-10.
      TF=24.
      TA=68.
      TI=68.
      W=1
      DO 93 M=1,9
      DO 94 N=1,10
      INPUT(M,N)=EXE(M,N)
94    CONTINUE
93    CONTINUE
C
      TT=(TF+TI)/2.0
      B= K*KK/(SP*P*HH**2)
      NN=2.*X(I,1)*HH/K
      RR=1.0/B*TT+NN*TF
      XX=0.0
      C= 2.0 +1.0/B
      BB =2.0 +1.0/B+NN
      RB =1.0/B *TI
      INPUT(1,1)=-BB
      INPUT(1,10)=-RR
      DO 81 M=2,9
      INPUT(M,10)=-RB
81    CONTINUE
      AN=(2.*HH*X(I,2))/K
      WRITE(2,682) AN,NN,X(I,1),X(I,2)
 682  FORMAT(/10X,'VARS',4F15.7/)
```

```
      BA=(AN+2.0+1.0/B)
      DO 82 M=2,9
      INPUT(M,M)=-C
82    CONTINUE
      INPUT(9,9)=-BA
      DO 673 M=1,9
      DO 674 N=1,9
      EE(N,M)=INPUT(N,M)
674   CONTINUE
673   CONTINUE
      IF(XX.EQ.0.0)GO TO 70
618   ZZZ=0.
617   DO 77 M=1,9
      DO 78 N=1,9
      INPUT(N,M)=EE(N,M)
78    CONTINUE
77    CONTINUE
      INPUT(1,10)=-(1.0/B*T(1)+NN*TF)
      DO 12 N=2,8
      INPUT(N,10)=-1.0/B*T(N)
   12 CONTINUE
      INPUT(9,10)=-(1.0/B*T(9)+AN*TA)
   70 XX=1.0
      REALT=REALT+10.
      DO89 N=1,10
      RN(1,N)=INPUT(1,N)
89    CONTINUE
      DO 22 M=1,8
      DO 23 N=1,10
      XR(M,N)=RN(M,N)*INPUT(M+1,M)/RN(M,M)
      RN(M+1,N)=INPUT(M+1,N)-XR(M,N)
   23 CONTINUE
   22 CONTINUE
      DO 61 M=1,9
      DO 62 N=1,10
      INPUT(M,N)=RN(M,N)
62    CONTINUE
61    CONTINUE
      M=9
      T(M)=INPUT(M,M+1)/INPUT(M,M)
      DO 14  J=1,8
      N=M-J
      T(N)=(INPUT(N,M+1)-T(N+1  )*INPUT(N,N+1))/ INPUT(N,N)
   14 CONTINUE
      DO 71 N=1,9
      E(N)=T(N)
   71 CONTINUE
      IF(ABS(REALT-EXPER(W,1)).LT.0.02) GO TO 822
      GO TO617
 822  EX(2)=(E(2)-TF)/(TI-TF)
      ZY(W)=(EX(2)-EXPER(W,2))**2
      YYY=YYY+ZY(W)
      WRITE(2,661) EX(2),REALT,W,ZY(W),YYY ,E(2)
 661  FORMAT(//10X,'VALUES',2X,2F10.5,I6,4X,2F10.5,10X,F10.4//)
      W=W+1
      IF(W.GT.10) GO TO 859
      GO TO 618
```

```
859   CONTINUE
      Z(I)=YYY
      WRITE(2,667) Z(I)
667   FORMAT(//10X,'Z(I)',5X,F10.5//)
      RETURN
      END
```

Table A3-3

Copper Disc

Optimised heat transfer coefficient = 2000.0 W/m^2 C

Dimensionless temperatures		Time
Theoretical	Experimental	(s)
.760	.760	10
.383	.400	60
.197	.236	110
.106	.140	160
.062	.080	210
.040	.050	260
.029	.031	310
.024	.023	360
.022	.021	410
.203	.020	460
.020	.020	510
.019	.020	560

Comparison of Optimised and Experimental Cooling Curves with Copper Disc

(lower thermocouple position)

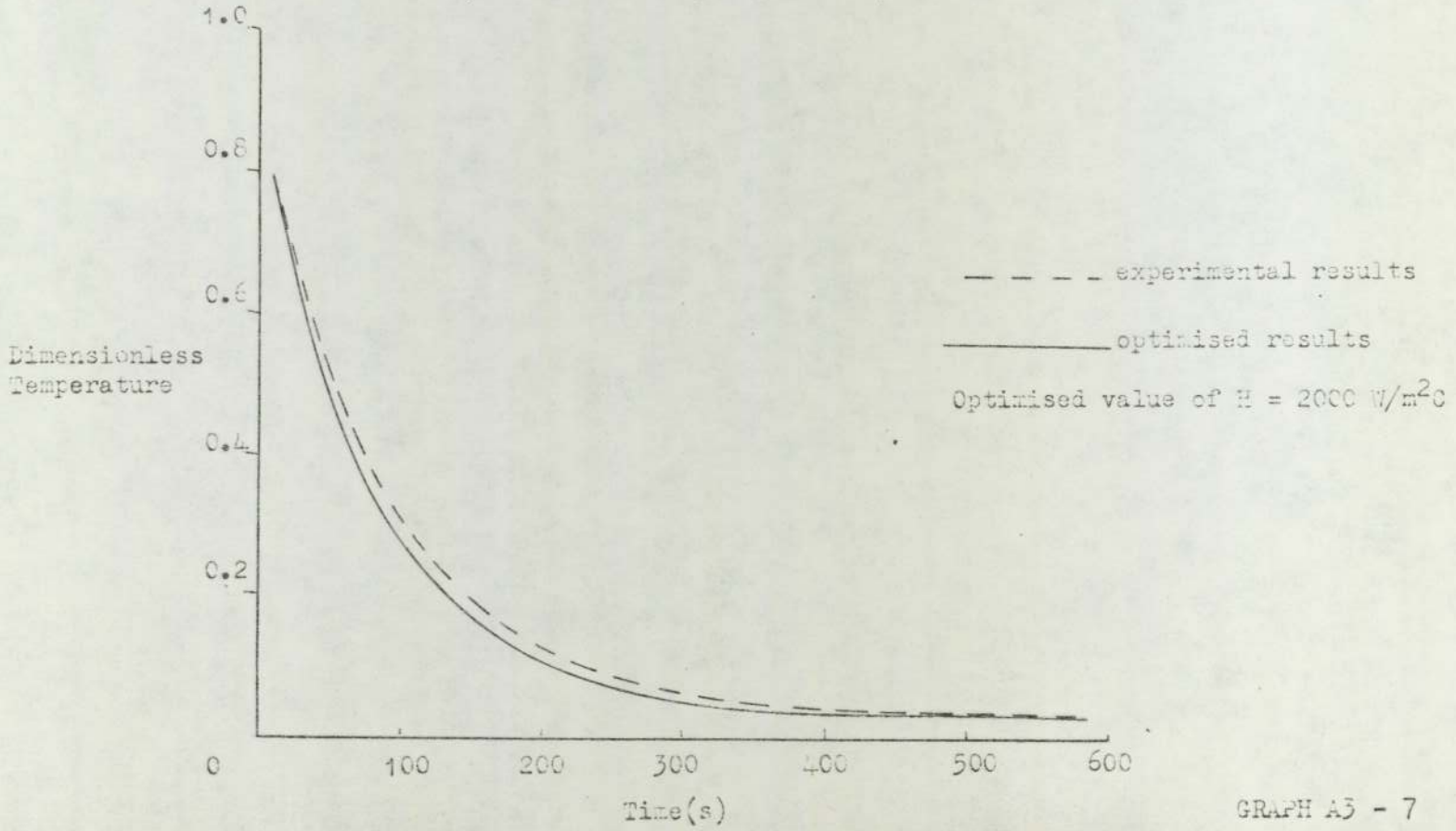

GRAPH A3 - 7

Table A3-4

Brass Disc

Optimised heat transfer coefficient = 1700.0 W/m^2 C

Dimensionless temperatures		Time
Theoretical	Experimental	(s)
.785	.785	10
.435	.435	60
.242	.262	110
.140	.176	160
.086	.121	210
.056	.090	260
.040	.069	310
.032	.058	360
.027	.042	410
.025	.038	460
.024	.029	510
.023	.024	560

Comparison of Optimised and Experimental Cooling Curves with Brass Disc

(lower thermocouple position)

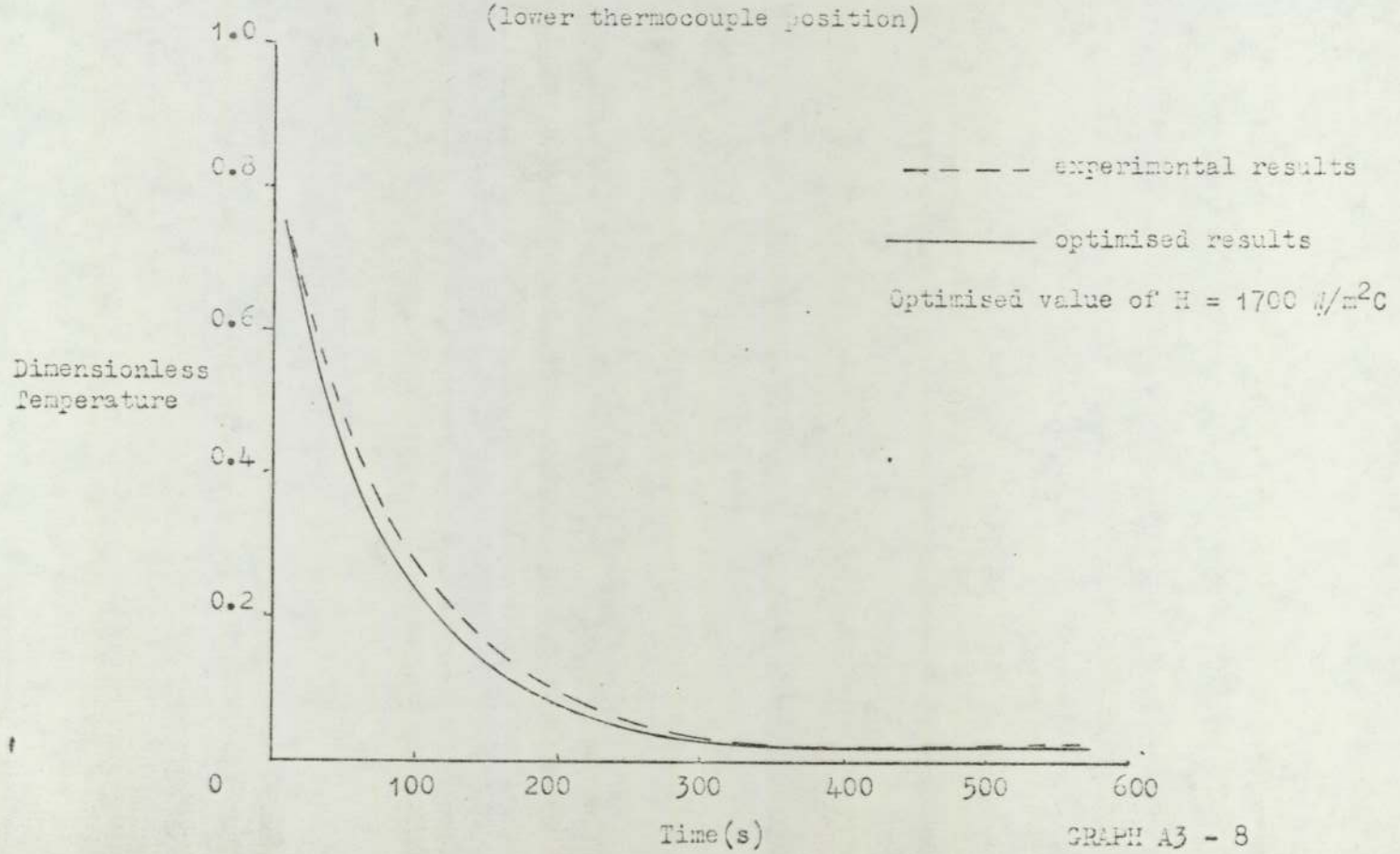

GRAPH A3 - 8

Table A3-5

Stainless Steel Disc

Optimised heat transfer coefficient = 900.0 W/m^2 C

Dimensionless temperatures		Time
Theoretical	Experimental	(s)
.860	.861	10
.612	.615	60
.442	.455	110
.321	.360	160
.236	.280	210
.177	.228	260
.136	.180	310
.107	.148	360
.087	.120	410
.073	.093	460
.063	.079	510
.056	.064	560

Comparison of Optimised and Experimental Cooling Curves with Stainless Steel Disc

(lower thermocouple position)

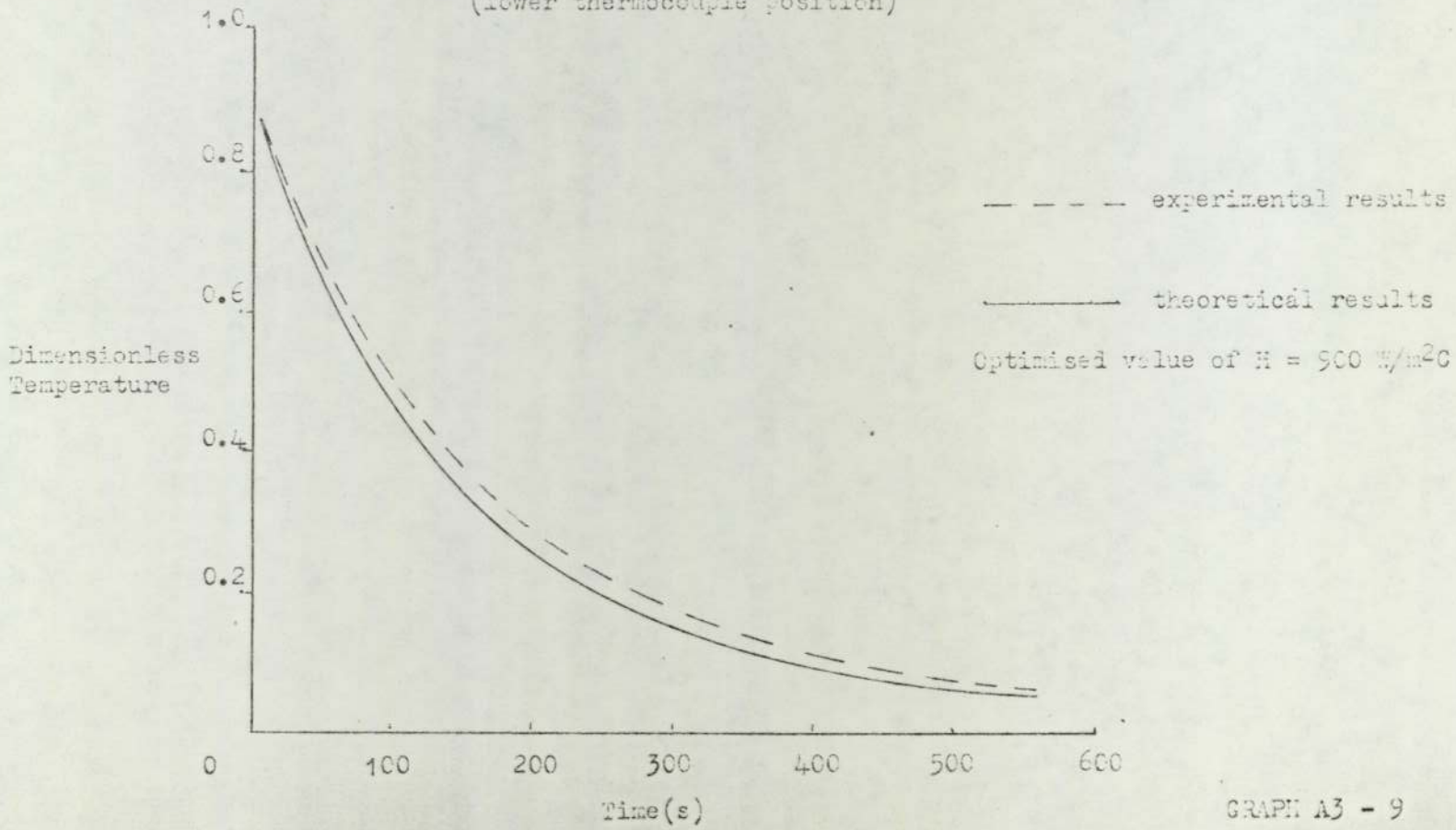

GRAPH A3 - 9

Table A3-6

Copper and Polythene Disc

Optimised heat transfer coefficient = 350.0 W/m^2 C

Dimensionless temperatures		Time
Theoretical	Experimental	(s)
.955	.958	10
.722	.725	110
.549	.550	210
.421	.428	310
.325	.338	410
.254	.265	510
.201	.220	610
.161	.180	710
.132	.140	810
.110	.110	910
.094	.100	1010
.082	.084	1110

Comparison of Optimised and Experimental Cooling Curves with Copper plus Polythene Disc

(lower thermocouple position)

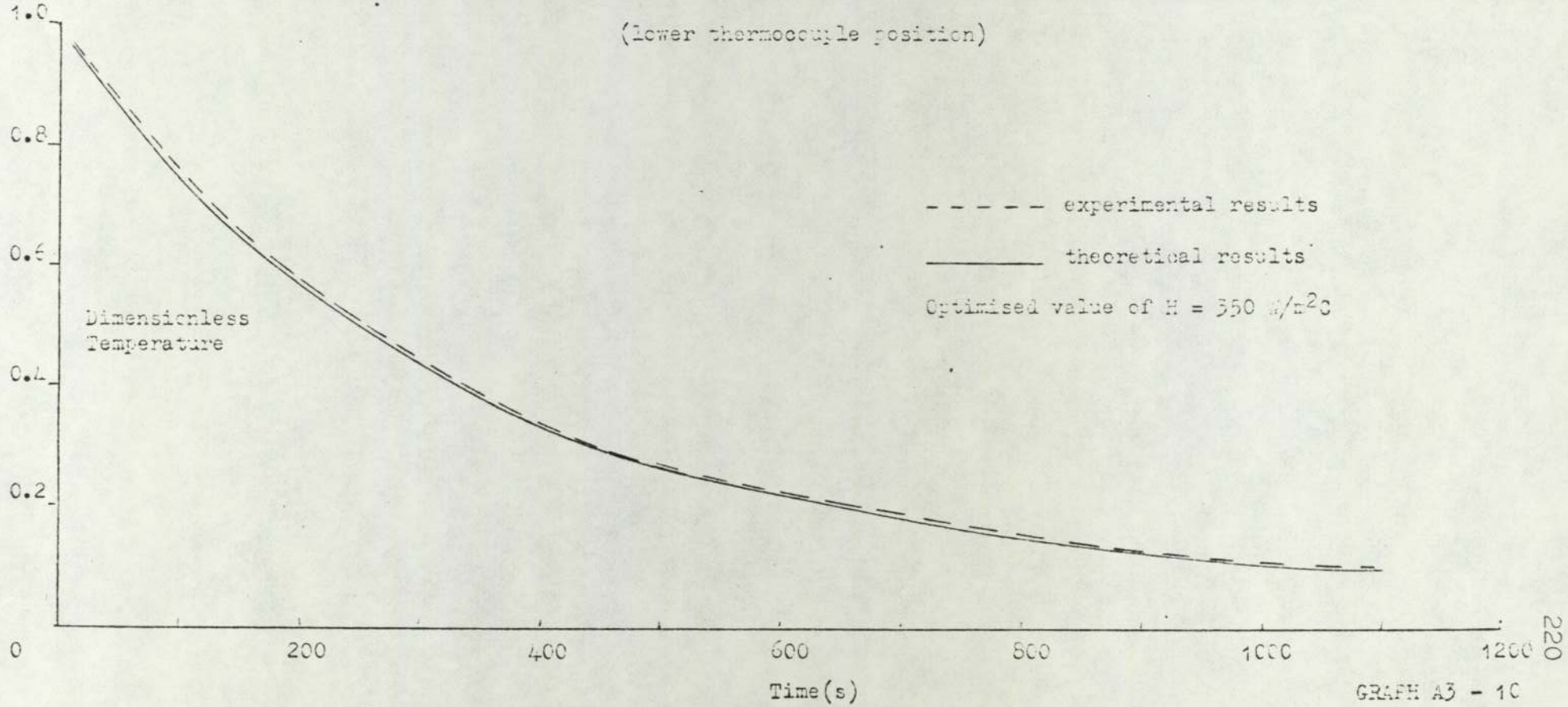

GRAPH A3 - 10

Table A3-7

Perspex Disc

Optimised heat transfer coefficient = 56.8 W/m^2 C

Dimensionless temperatures		Time
Theoretical	Experimental	(s)
.950	.951	100
.757	.760	600
.604	.620	1100
.486	.507	1600
.393	.412	2100
.321	.338	2600
.265	.278	3100
.221	.228	3600
.187	.192	4100
.160	.168	4600
.139	.149	5100
.123	.131	5600

Comparison of Optimised and Experimental Cooling Curves with Perspex Disc

(lower thermocouple position)

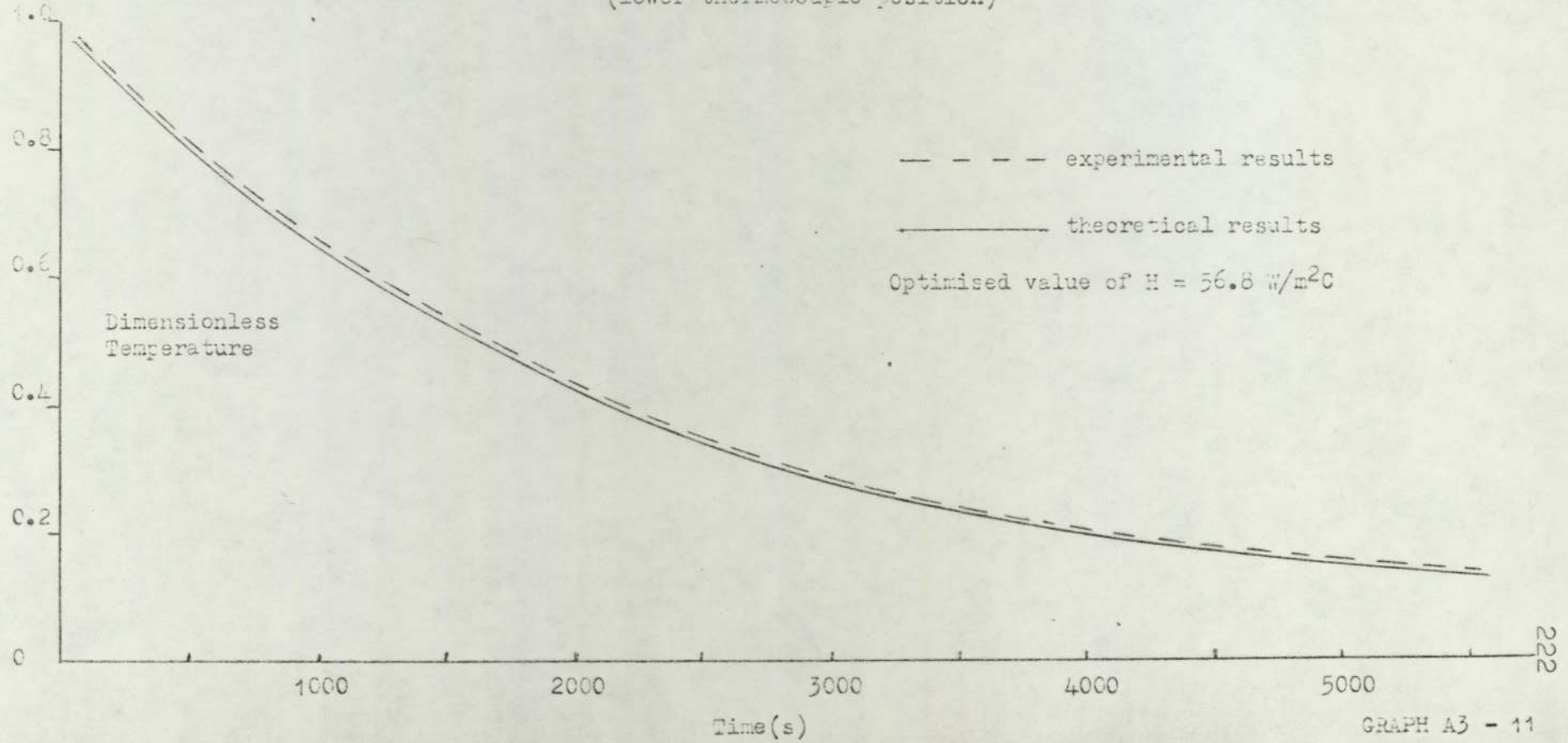

GRAPH A3 - 11

A3-4.3 Heat Gain Coefficients

An explanation of higher heat gain coefficients with the copper, brass, and stainless steel discs compared to the copper plus polythene and perspex discs could be found from stating that the initial assumption that all the heat gain was at $x = L$ was, although adequate, not true, and that heat gain may also have occurred at the discs. The radial heat transfer in the discs would increase as the disc conductivity increased, i.e. as the H value increased, and therefore be more significant with the metal discs.

It should be noted that the effect of the heat gain coefficient was very small compared with the heat transfer coefficient between the aluminium bar and coolant, and did not significantly alter the latter value. The heat gain coefficient explained the final offset values of the aluminium bar but had very little effect during the initial cooling period.

A3-4.4 Accuracy of Optimised Heat Transfer Coefficients.

The heat transfer conductance, H, for each disc depended on two quantities (1) the resistance of the disc, R, and (2) the coolant film and contact resistances Rc.

We may write

$$\frac{1}{H} = R + Rc \qquad \text{(A3-15)}$$

At constant coolant rate Rc should be constant and independent of the disc used. Changes in H resulted therefore from changes in R.

A check on the accurancy of the measurements of H was provided by a comparison of the Rc values from the runs with different discs. Rc was calculated from (A3-15) using the optimised H values (table A3-2) and the disc resistances (table A3-1).

Table A3-8 contains the values of 1/Rc found in this way.

TABLE A3-8

Heat Transfer Disc	Film and Contact Conductances (1/Rc)
	(W/m^2C)
Perspex	1996
Copper & Polythene	1370
Stainless Steel	2326
Brass	2110
Copper	2049

From table A3-8 values of (1/Rc) for the discs, omitting the copper plus polythene disc, can be seen to lie within a 16% range. With the latter disc the low conductance value was probably due to the extra resistance between the copper and polythene strip. The mean of (1/Rc) for the four discs (neglecting the copper plus polythene disc) was 2120.25. Using the t distribution for three degrees of freedom the 95% confidence limits of the mean were calculated to be:

$$2353 < \text{mean} < 1890$$

Using these confidence limits a confidence interval for the heat transfer coefficient for each disc was calculated. Table A3-9 compares the confidence limits for the coefficient with the optimised values for each disc.

TABLE A3-9

Heat Transfer Disc	95% confidence limits of heat transfer coefficient(W/m^2C)	Optimised heat transfer coefficients 'H' (W/m^2C)
Perspex	55.6 - 57.1	56.8
Stainless Steel	826.0 - 909.0	900.0
Brass	1565.0 - 1869.0	1700.0
Copper	1852.0 - 2294.0	2000.0

The error introduced by the variation of the film and contact resistances leading to uncertainties in experimental H values, in freezing formulas can be shown by predicting freezing times by the Modified Planck method. Times to freeze 1 cm. ice are given in table A3-10.

TABLE A3-10

Heat Transfer Disc	Heat Transfer Coefficient (W/m^2C)	Freezing times (secs)	Percentage difference in freezing times
Perspex	55.6 - 57.1	4972 4900	1.4
Stainless Steel	379.0 - 395.0	901 869	3.6
Brass	1565.0 - 1869.0	762 734	3.8
Copper	1852.0 - 2294.0	693 671	3.1

The maximum error in predicted freezing times can be seen to be small (4% for freezing 1 cm. ice).

The maximum effect of the variation of Rc on H, (however caused) produced no significant error in the freezing formulas since the discrepancies between theoretical formula and experimental freezing rates lie outside these limits, and were not explained by errors in the values of the heat transfer coefficients used, i.e. the coefficients have been determined accurately enough.

APPENDIX 4.

DETAILS OF MATHEMATICS AND COMPUTATION OF FREEZING RATE FORMULAS OUTLINED IN CHAPTER 4.

The assumptions used in the derivations of the freezing rate formulas outlined in chapter 4 and given in this appendix are :-

1. Initial uniform temperature of material being frozen.

2. Constant coolant temperature.

3. Material has constant thermal conductivity and specific heat (different for the two phases).

4. A density which does not vary with temperature or alter during the freezing process.

5. A definite freezing point at which latent heat is liberated.

6. Heat transfer is in 1-direction only.

7. Heat transfer within the watery solid is by conduction, with a convective boundary condition.

The governing equations of the mathematical model with the above assumptions are (see also chapter 1 and appendix 6) :

Conduction equations:

$$\frac{\partial T_1}{\partial t} = \alpha_1 \frac{\partial^2 T_1}{\partial x^2} \qquad (1\text{-}1)$$

$$\frac{\partial T_2}{\partial t} = \alpha_2 \frac{\partial^2 T_2}{\partial x^2} \qquad (1\text{-}2)$$

Boundary conditions: at frozen-unfrozen interface, $x = X(t)$.

$$-\frac{L\rho dx}{dt} = -K_1\left(\frac{\partial T_1}{\partial x}\right)_x + K_2\left(\frac{\partial T_2}{\partial x}\right)_x \qquad (1\text{-}3)$$

$$T_1 = T_2 = Tm \qquad (1\text{-}4)$$

at coolant surface, x = 0.

$$H(Tc - Ts) = -K_1 \left(\frac{dT_1}{dx} \right)_{x=0} \qquad (1\text{-}5)$$

at the axis of symmetry, x = a.

$$\left(\frac{\partial T_2}{\partial x} \right) = 0 \qquad (1\text{-}6)$$

Initial conditions :

$$X(t) = 0 \quad \text{at } t = 0 \qquad (1\text{-}7)$$

$$T_2 = f(x) \quad \text{at } t = 0 \qquad (1\text{-}8)$$

This appendix now derives in detail each theoretical formula outlined in chapter 4 in turn.

A4-1. PLANCK METHODS.

A4-1.1 PLANCK'S ORIGINAL METHOD.

The method assumes that the thermal capacities of

the frozen and unfrozen phases are negligible so that the unsteady conduction equations (1-1) and (1-2) reduce to the steady state equations :-

$$\left(\frac{\partial T_1}{\partial x}\right) = b_1 \quad \text{and} \quad \left(\frac{\partial T_2}{\partial x}\right) = b_2$$

where b_1 and b_2 are independent of x.

Inspection of figure A4-1 shows that :

$$b_2 = 0 \quad (\text{as } T_2 = Tm \text{ for all } t)$$

$$\text{and} \quad b_1 = \left(\frac{\partial T_1}{\partial x}\right) = \frac{Tm - Ts}{X(t)}$$

The resulting boundary condition equation at x=X(t) on substituting $(\partial T_1/\partial x)$ and $(\partial T_2/\partial x)$ into equation (1-3) is :

$$-L\rho \frac{dx}{dt} = K_1 \left(\frac{Tm - Ts}{X}\right) \qquad (A4\text{-}1)$$

At x = 0 the boundary condition equation on substituting $(\partial T_1/\partial x)$ into equation (1-5) becomes :

Figure A4-1 Assumed temperature profile of Plancks method.

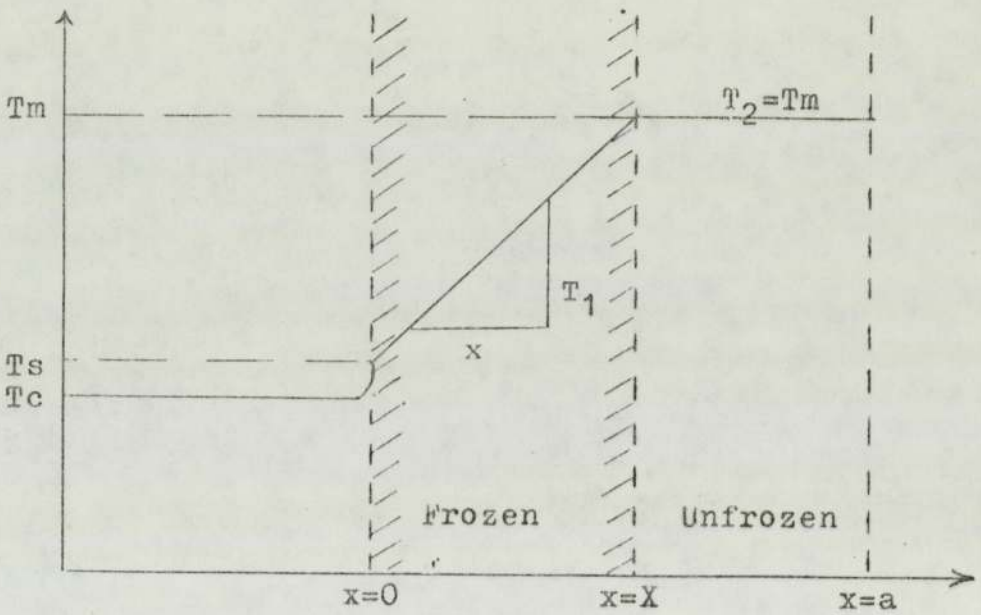

$$H(Tc - Ts) = -K_1 \left(\frac{Tm - Ts}{X} \right) \qquad (A4\text{-}2)$$

Elimination of Ts from (A4-1) and (A4-2) gives :

$$L\rho \frac{dx}{dt} = H(Tm - Tc) / (1 + HX/K_1) \qquad (A4\text{-}3)$$

Integration of equation (A4-3) between the limits $X = 0$ to $X = X(t)$ and $t = 0$ to $t = t$.

$$\int_{X=0}^{X=X(t)} \left(dx \left(1 + \frac{HX}{K_1} \right) \right) = \int_{t=0}^{t=t} \left(\frac{H}{L\rho} (Tm - Tc)\, dt \right)$$

$$X + \frac{HX^2}{2K_1} = \frac{H}{L\rho} (Tm - Tc)t$$

$$L\rho(2K_1X + HX^2) = 2K_1H (Tm - Tc)t$$

whence :

$$t = \frac{L\rho(2K_1X + HX^2)}{2K_1H(Tm-Tc)} \qquad (4\text{-}2)$$

A4-1.2 MODIFIED PLANCK METHOD.

Equation (4-2) which gives the time t to form a frozen thickness X will be most accurate for systems in which the sensible heat can reasonably be neglected. (i.e. when the initial liquid temperature is near the freezing point and the coolant temperature is not much below the freezing point). For higher initial temperatures, and lower coolant temperatures, the method can be improved by including the sensible heat to be removed as follows :

Let TI equal the original (uniform) temperature of the unfrozen solid and assume, for the purpose of calculating the heat supply to the solid, that the temperature profile during freezing is as in figure A4-2.

If we take T = 0 as the reference temperature for enthalpy, the enthalpy per unit mass of the frozen phase, whose average temperature is (Tm + Ts)/2, is C_1 (Tm + Ts)/2. The enthalpy per unit mass of the unfrozen phase, whose average temperature is (TI + Tm) /2 is C_1 Tm + L + C_2 ((TI + Tm)/2-Tm), where the first two terms are the enthalpy of the liquid at it's melting point, referred to as T = 0, and the third term is the enthalpy above the melting point, Tm.

Figure A4-2 Assumed temperature profile of the modified Planck method.

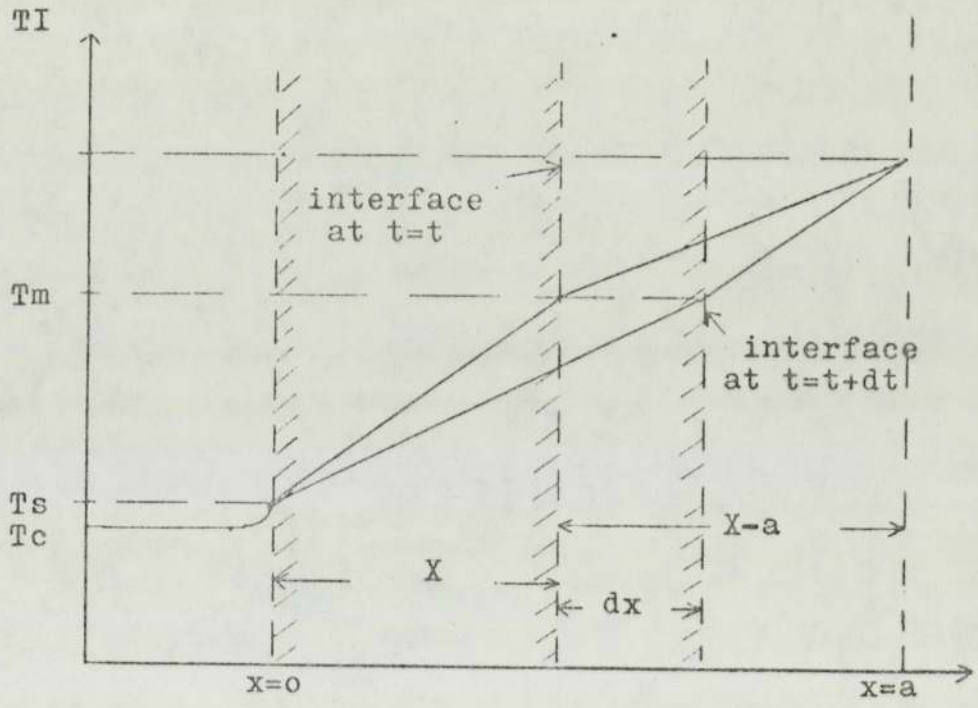

When the frozen-unfrozen interface is at X, the total enthalpy of a block of unit area normal to the x-direction, extending from x = 0 to x = a is :

$$X\rho C_1 \left(\frac{Tm + Ts}{2}\right) + (a-X)\rho \left(C_1 Tm + L + C_2\left(\frac{Tm+TI}{2}-Tm\right)\right)$$

When the interface is at X + dX, the total enthalpy per unit area is :

$$(X + dx)\rho C_1 \left(\frac{Tm + Ts}{2}\right) + (a-X-dx)\rho \left(C_1 Tm+L+C_2\left(\frac{Tm+TI}{2}-Tm\right)\right)$$

The total enthalpy supply, when the interface advances dX is thus :

$$\rho dX \left(C_1\left(\frac{Tm + Ts}{2}\right) - C_1 Tm - L - C_2 \left(\left(\frac{Tm + TI}{2}\right) - Tm\right)\right)$$

$$= \rho dX \left(C_1 \left(\frac{Tm - Ts}{2}\right) + L + C_2 \left(\frac{TI - Tm}{2}\right)\right)$$

The heat flux required to freeze unit mass thus changes from L when the specific heats are neglected to $C_1 \left(\frac{Tm - Ts}{2}\right) + L + C_2 \left(\frac{TI - Tm}{2}\right)$ when the specific heats are included.

The corresponding equation to (A4-1) by the first Planck method at X = X(t) becomes :

$$-\left(C_1 \frac{(Tm-Ts)}{2} + L + C_2 \frac{(TI-Tm)}{2}\right) \rho\left(\frac{dx}{dt}\right) = -K_1 \frac{(Tm-Ts)}{X} \qquad (A4-4)$$

Elimination of Ts between (A4-2) and (A4-4) and integration as with the previous method produces :

$$t = \left(\frac{\rho X^2}{(Tm-Tc)2\ K_1}\right)\left(C_1 \frac{(Tm-Tc)}{2}\right) + \left(\frac{1+2K_1}{HX}\right)\left(L+C_2\frac{(TI-Tm)}{2}\right)$$

A4-1.3 MODIFICATIONS TO PLANCKS METHODS BY NAGAOKA AND RUTOV.

Nagaoka (35) and Rutov (34) studying independently the freezing of fish and meat respectively, extended the Modified Planck method to account for the overall freezing time.

Their modifications take the form :

$$t_T = t_p\ (1 + A\ (TI - Tm)) \qquad (4-4)$$

where t_p = freezing time predicted by the Modified Planck formula (4-3).

t_T = total freezing time.

A = constant.

Rutov, like many Russian workers, developed the use of standard dimensionless groups (i.e. Fourier number, $\alpha\, t/X^2$ and Biot number, HX/K_1) for unsteady state heat transfer along with the Kossovitch number (L/C_1 (Tm-Tc)) for phase change. From experimentation he evaluated the correction factor, A, in equation 4-4 to be 0.0053 (4-4a).

Nagaoka working from the expression for the total enthalpy change over the whole process introduced his correction factor to take into account the precooling time and the density change on phase change. Nagaokas correction factor in equation (4-4) is given as 0.008. (4-4b).

A4-1.4 COMPUTATION OF METHODS BASED ON THE WORK OF PLANCK.

The main advantage of the methods of Planck, Rutov and Nagaoka is their ease of evaluation. The calculations

performed in the following computer program could quite easily be carried out on a hand calculator.

The program requires the input of the physical properties of the material being frozen and system conditions only. Evaluation of the extension to the method by Rutov and Nagoaka just require one extra line of calculation each.

A flowdiagram, listing and sample output are given on the next pages.

A4-2 GOODMAN'S INTEGRAL METHOD.

According to this method, the transient disturbance is assumed to have penetrated a distance X into the solid in question, and beyond X the original temperature persists. The original temperature is taken as being equal to the freezing temperature.

The method, with the above assumptions consists of :

(a) Multiplying equation 1 $\left(\frac{\partial T_1}{\partial t} = \alpha_1 \frac{\partial^2 T_1}{\partial x^2} \right)$

by dx and integrating it from x = 0 to x = δ to give :

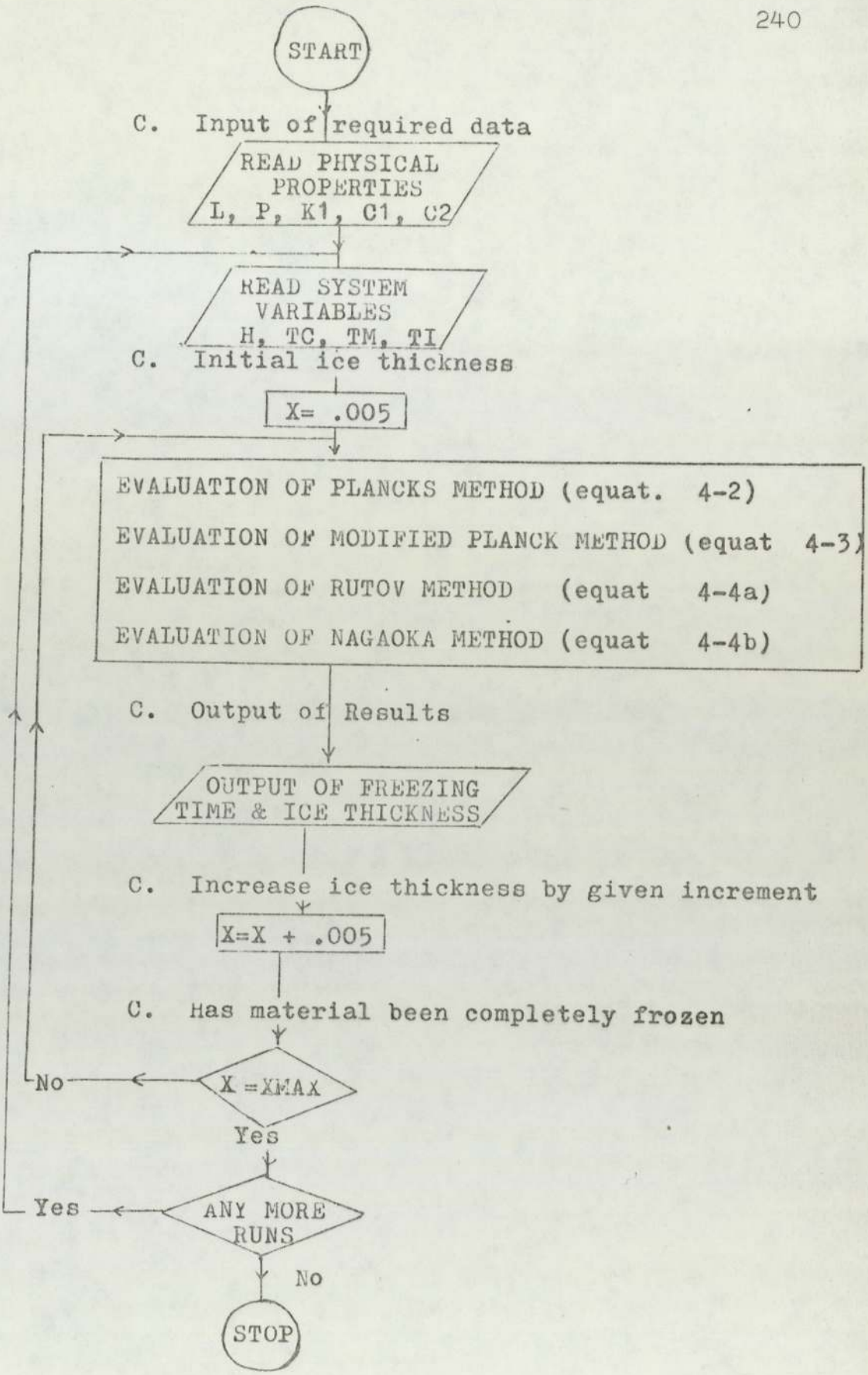

Flow diagram for the evaluation of Plancks method and extensions to the method.

```
      TRACE 1
      MASTER YYYY
      REAL L,K
C
C     FREEZING RATES PREDICTED BY PLANCK'S METHOD AND BY
C     MODIFICATIONS TO THE METHOD
C
C     DEFINITION OF VARIABLES
C
C     L = LATENT HEAT
C     C = SPECIFIC HEAT
C     P = DENSITY
C     K = THERMAL CONDUCTIVITY
C     H  = HEAT TRANSFER COEFFICIENT
C     TC = COOLANT TEMPERATURE
C     TM = FREEZING TEMPERATURE
C      TI = INITIAL TEMPERATURE
C
      NC=0
C
C
C
      READ ( 1,1000) L,P,K,C1,C2
 1000 FORMAT (5F10.0)
      IXI=12
      DO 485 KI=1,IXI
      READ(1,1010) H,TC,TM,TI
 1010 FORMAT (4F10.0)
C
C
      WRITE(2,3005) H,TC,TM,TI
 3005 FORMAT(1H1 ///// 20X,'FREEZING RATES PREDICTED BY',1X,
     1'PLANCKS APPROXIMATIONS' // 20X,'HEAT TRANSFER COEFFIC',
     2'IENT =',F7.1,2X,'(W/M**2*C)'//20X,'COOLANT TEMPERATURE ='
     3,F7.1,2X,'(C)'//20X,'FREEZING TEMPERATURE =',F7.1,2X,
     4'(C)'// 20X,'INITIAL TEMPERATURE =',F7.1,2X,'(C)')
C
      NC=NC+1
C
      WRITE(2,833)
  833 FORMAT(// 20X, 'FREEZING OF DISTILLED WATER' ///)
C
      WRITE(2,3445)
 3445 FORMAT(  15X,'THICKNESS OF ICE',8X,'PLANCK', 5X,
     1'MOD. PLANCK',5X ,'RUTOV',8X,'NAGOAKA'/20X,'  (CM)'
     2,15X,'(HRS)', 8X ,'(HRS)',9X ,'(HRS)',9X ,'(HRS)' //)
C
```

```
      X=0.
C
 50   X=X+.005
C
C     EVALUATION OF PLANCK'S METHOD
C
      TZ= L*P*(2.**K*X+H*X**2)/ (2.*K*H*(TM-TC))
      T1 = TZ
C
C     EVALUATION OF MODIFIED PLANCK'S METHOD
C
      T3= P*X**2/((TM-TC)*2.*K)
      T4= C1 * (TM-TC)/2.
      T5= 1. +2.*K/(H*X)
      T6=L+C2*(TI-TM)/2.
      TY= T3 *(T4 +(T5*T6))
      T2 = TY
C
C     EVALUATION OF RUTOV'S METHOD
C
      TR = TY*(1.+.0053*(TI-TM))
C
C     EVALUATION OF NAGAOKA'S METHOD
C
      TN = TY*(1.+.008*(TI-TM))
C
C
C
C     OUTPUT OF RESULTS
C
C
      X1 = X*100.0
      TB = T2/3600.
      TA = TR/3600.
      TF = TN/3600.
      TR=T2/3600.
      TP=T1/3600.
C
      WRITE(2,3315) X1,TP,TB,TA,TF
 3315 FORMAT (20X,F6.2, 12X,F5.2, 3(6X,F8.2))
C
      IF(X.LT..45E-01) GO TO 50
  485 CONTINUE
      STOP
      END
```

FREEZING RATES PREDICTED BY PLANCKS APPROXIMATIONS

HEAT TRANSFER COEFFICIENT = 56.7 (W/M**2*C)

COOLANT TEMPERATURE = -15.0 (C)

FREEZING TEMPERATURE = 0.0 (C)

INITIAL TEMPERATURE = 19.0 (C)

FREEZING OF DISTILLED WATER

THICKNESS OF ICE (CM)	PLANCK (HRS)	MOD. PLANCK (HRS)	RUTOV (HRS)	NAGOAKA (HRS)
0.50	0.66	0.74	0.82	0.86
1.00	1.40	1.58	1.74	1.82
1.50	2.23	2.51	2.76	2.89
2.00	3.13	3.53	3.88	4.07
2.50	4.11	4.64	5.11	5.35
3.00	5.17	5.85	6.44	6.74
3.50	6.31	7.15	7.87	8.23
4.00	7.53	8.54	9.40	9.84
4.50	8.83	10.02	11.03	11.55

$$\int_0^{\delta(t)} \left(\frac{\partial T_1}{\partial t}\right) dx = \alpha_1 \int_0^{\delta(t)} \left(\frac{\partial^2 T_1}{\partial x^2}\right) dx$$

$$\frac{d}{dt}\left[\int_0^{\delta(t)} T_1\, dx + T_1(\delta)\delta\right] = \alpha_1\left[\left(\frac{\partial T_1}{\partial x}\right)_\delta - \left(\frac{\partial T_1}{\partial x}\right)_0\right]$$

(b) Assuming that the temperature T_1 can be approximated by a polynomial in x. This procedure uses a quadratic equation :

$$T_1(x,t) = a(x-\delta) + b(x-\delta)^2 \qquad (4\text{-}5)$$

A quadratic polynomial was used instead of a linear one so that the effect of the thermal capacity of ice could be taken into account by the curved temperature profile. Goodman also used cubic polynomials (15). The choice of a quadratic polynomial was based on the fact that since by experimentation, the thermal capacity of ice was found to be a relatively insignificant factor in the freezing process the temperature profile in the frozen phase could be adequately described by a quadratic polynomial. (See figure A4-3).

Figure A4-3 Assumed temperature profile of Goodmans integral method.

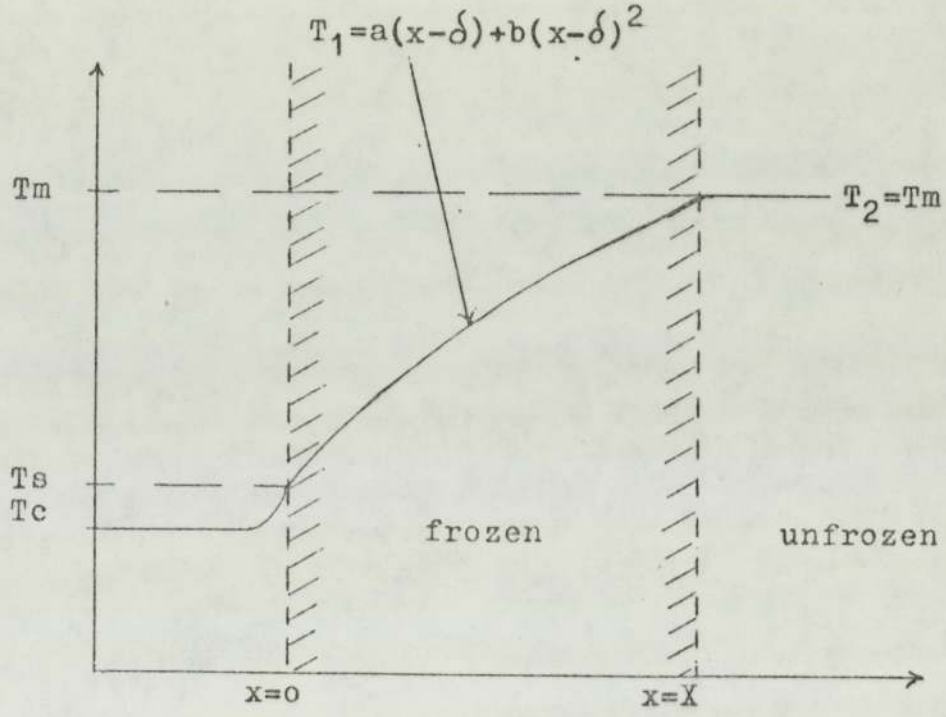

The values of T_1 and $\partial T_1/\partial x$ from equation (4-5) were substituted into (A4-7) to give an equation that can be integrated directly when constants a and b in (4-5) were known.

We found a and b from the boundary conditions at $x = 0$ and $x = \delta$. Following Goodman :

<u>At x = 0</u> $(T_1 \equiv Ts)$

$$H(Ts - Tc) = K_1 \left(\frac{\partial T_1}{\partial x} \right)_0 \qquad (1\text{-}5)$$

$$\therefore T_1 = Tc + K_1/H \left(\frac{\partial T_1}{\partial x} \right)_0$$

$$Tm - a\delta + b\delta^2 = Tc + K_1/H\,(a + 2b\delta) \qquad (A4\text{-}8)$$

<u>At x = δ</u> $$L\rho \frac{dX}{dt} = + K_1 \left(\frac{\partial T_1}{\partial x} \right)_X - K_2 \left(\frac{\partial T_2}{\partial x} \right)_X \qquad (1\text{-}3)$$

by the assumption that the liquid temperature T_2 was equal to the freezing temperature, this boundary condition was reduced to :

$$L\rho \frac{d\delta}{\delta t} = K_1 \left(\frac{\partial T_1}{\partial x} \right)_{\delta} \qquad \text{(A4-9)}$$

Again following the arguments of Goodman, this last boundary condition was transformed as follows :

Writing $T_1 = fn\ (x,t)$

$$dT_1 = \left(\frac{\partial T_1}{\partial x} \right) dx + \left(\frac{\partial T_1}{\partial t} \right) dt$$

if $x = fn(t)$ we may write

$$\frac{dT_1}{dt} = \left(\frac{\partial T_1}{\partial x} \right) \frac{dx}{dt} + \left(\frac{\partial T_1}{dt} \right)$$

and when $x(t) = \delta(t)$ with $T_1\ (\delta, t) = 0$

$$\left(\frac{\partial T_1}{\partial t} \right) = 0 = \left(\frac{\partial T_1}{\partial x} \right) \frac{d\delta}{dt} + \left(\frac{\partial T_1}{\partial t} \right)$$

substituting $(\partial T_1 / \partial t)$ from equation 1-1, we obtained :

$$\frac{d\delta}{dt} = \alpha_1 \left(\frac{\partial^2 T_1}{\partial x^2} \right) \Big/ \left(\frac{\partial T_1}{\partial x} \right) \qquad \text{(A4-10)}$$

Combining A4-9 and A4-10 we obtained :

$$\frac{\alpha_1 L \rho}{K_1}\left(\frac{\partial^2 T_1}{\partial x^2}\right) = -\left(\frac{\partial T_1}{\partial x}\right)^2$$

Which on substituting values from 4-5 gave :

$$\left(\frac{\alpha_1 L}{K_1}\right)(2b) = -(a)^2 \qquad \text{(A4-11)}$$

i.e. the second boundary condition at $x = \delta$.

Letting $n = \alpha_1 L\rho / K_1$ in equation (A4-11) we obtained the relationship between a and b as :

$$b = -a^2/2n \qquad \text{(A4-12)}$$

Rearrangement of (G-3A) with $m = H\delta/K_1$ together with (A4-12) gave a and b as :

$$a = \frac{Hn}{K_1 m}\left(\frac{1+m}{2+m}\right)\left[\sqrt{1 - \frac{2m\,Tc\,(2+m)}{n\,(1+m)^2}} - 1\right] \qquad \text{(A4-13)}$$

$$b = -\frac{H^2 n}{K_1 m^2}\left(\frac{1+m}{2+m}\right)^2\left[1 - \frac{m(2+m)\,Tc}{n\,(1+m)^2} - \sqrt{1 - \frac{2m(2+m)Tc}{n\,(1+m)^2}}\right] \qquad \text{(A4-14)}$$

In equation (A4-7) we substituted from (4-5)

$$(1) \qquad \int_0^{\delta(t)} T_1 \, dx = \int_0^{\delta(t)} \left(a\,(x-\delta) + b(x-\delta)^2 \right) dx =$$

$$(K_1{}^2/2H^2)\, am^2 + (K_1{}^3/3H^3) bm^3.$$

$$(2) \qquad T_1(\delta)\,\delta = Tm\,\delta$$

$$(3) \qquad \left(\frac{\partial T_1}{\partial x}\right)_\delta = a$$

$$(4) \qquad \left(\frac{\partial T_1}{\partial x}\right)_0 = a - 2b\delta = a - \left(\frac{2K_1}{H}\right) bm$$

to give :

$$\frac{d}{dt}\left[- \left(\frac{K_1{}^2}{2H^2}\right) am^2 + \left(\frac{K_1{}^3 b}{3H^3}\right) m^3 + Tm\delta \right] = 2\alpha_1 b$$

$$= \frac{2\alpha_1 K_1\, bm}{H}$$

whence :

$$t = \frac{K_1}{\alpha_1 H} \int_0^m \left[\frac{K_1}{H} \left(\frac{m}{2} + \frac{m^2}{6b} \frac{db}{dB} - \frac{a}{2b} - \frac{m}{4b} \frac{da}{dm} \right] dm \right.$$

(4-6)

Equation (4-6) gives t in terms of m, hence of δ and thus expresses the movement of the frozen-unfrozen interface with time.

To evaluate the integral in equation (4-6) we required values of a, b da/dm and db/dm for various values of m, and in particular at m = 0. The derivatives were found from the values of a and b. At m = 0, a and b are indeterminate, so we considered the limiting values as $m \longrightarrow 0$.

$$m \longrightarrow 0, \quad a \longrightarrow \frac{Hn}{2K_1 m}\left(\sqrt{1 - \frac{4m\,Tc}{n}} - 1\right)$$

$$= \frac{Hn}{2K_1 m}\left(1 - \frac{2\,Tcm}{n} - 1\right)$$

$$= -\frac{HTc}{K_1} \equiv ao$$

$$b \rightarrow \frac{-H^2 n}{4K_1{}^2 m^2}\left(1 - \frac{2Tcm}{n} - \sqrt{1 - \frac{4Tcm}{n}}\right)$$

$$= \frac{-H^2 n}{4K_1{}^2 m^2}\left(1 - \frac{2Tcm}{n} - 1 + \frac{2Tcm}{n} + \frac{2Tc^2 m^2}{n^2} \ldots\right)$$

$$= \frac{-H^2 Tc^2}{2K_1{}^2 n}$$

$$= - ao^2/2n \equiv b0$$

The numerical integration procedure consisted, essentially of the following steps :

(a) calculate the values of a and b at m = m.

(b) increase m by a suitable arbitrary step Δ m.

(c) calculate a and b for the new value of m = m Δm.

(d) approximate da/dm and db/dm at m by
$[a(m + \Delta m) - a(m)] \div \Delta m$ and
$[b(m + \Delta m) - b(m)] \div \Delta m$ respectively.

(e) evaluate the integral I(m) equation (4-6) at m from the values of a, b, da/dm, db/dm and m.

(f) repeat the calculations for m = m + Δ m to give I(m + Δ m).

(g) integrate by the trapezoidal approximation, to give: $t(m+\Delta m)-t(m) = \frac{1}{2}\,(I(m+\Delta m) + I(m))\times(\Delta m)$.

(h) continue this procedure over the range $m = 0$ (where a and b equal ao and $-ao^2/2n$ respectively) to $m = m_{max}$, a predetermined upper limit.

(i) tabulate $t(n.\Delta m)$ against $m = n.\Delta m$.

(j) as a check on the accuracy of the numerical integration procedure, repeat the calculations with a new increment of m, $m = m/2$. Repeatedly halve the increment and recalculate until sufficient accuracy is obtained.

A4-2.1 COMPUTATION OF GOODMAN'S METHOD.

In the computer program reduction of the increment value below X = .001, using the trapezoidal approximation, was found not to give improved accuracy. Since this

step length value of 10 mm (equivalent to x = .001) provided a useful incremental value for the ice thickness the use of other integration formulae such as Simpsons methods were not considered necessary.

The flowdiagram on the next page shows that the evaluation of the variables in the integral is carried out in subroutine JAWS. A sample listing and output are given on the pages after the flowdiagram.

A4-3 NEUMANN'S SOLUTION.

Neumann's solution assumes that the surface temperature (Ts) of the body being frozen is constant which corresponds in practical cases to the requirement of a high transfer coefficient, i.e. that Ts = Tc and most importantly that the unfrozen region is large compared to the frozen region for all times of interest, so that we may write :

$$T_2 \longrightarrow TI \text{ as } x \longrightarrow \infty$$

With the above restrictions equation (1-1) can be written as :

Flow diagram for Goodmans method

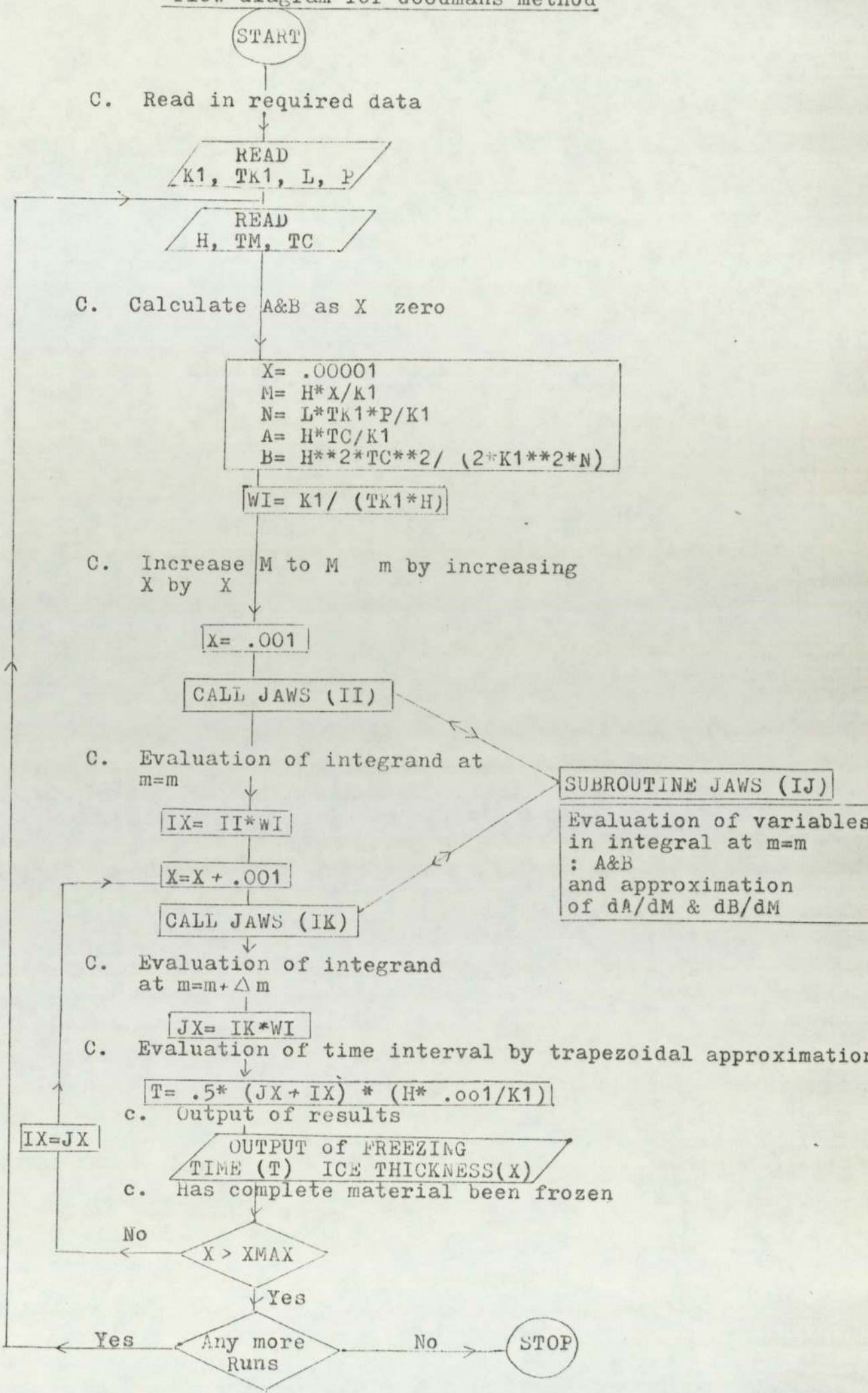

```
      PROGRAM NAME(INPUT,OUTPUT,TAPE1=INPUT,TAPE2=OUTPUT)
C
C     FREEZING RATES PREDICTED BY GOODMAN INTEGRAL METHOD
C
      REAL M,N,K1,L,NNEW,MNEW,II,III,IJ,IK,IX  ,JX ,MM
      COMMON H,X,TC,TM  ,MM
      COMMON M,N,K1,L,NNEW,MNEW,A,B,ANEW,BNEW
C
C     DEFINITION OF VARIABLES
C
C     X  = ICE THICKNESS
C     K1 = THERMAL CONDUCTIVITY OF ICE
C     L  = LATENT HEAT
C     P  = DENSITY
C     TM = FREEZING TEMPERATURE
C     TC = COOLANT TEMPERATURE
C     TK1= THERMAL DIFFUSIVITY OF ICE
C     H  = HEAT TRANSFER COEFFICIENT
C
      READ(1,1000) K1,TK1,L,P
 1000 FORMAT(4F10.0)
      DO 2113  IP =1,NC
      READ(1,1001) H,TM,TC
 1001 FORMAT(3F10.0)
C
C
C
      WRITE(2,2111 ) H,TM,TC
 2111 FORMAT(1H1 /// 20X,'FREEZING RATES PREDICTED BY',1X,
     2'GOODMANS INTEGRAL METHOD'/// 20X,'HEAT TRANSFER',1X,
     3'COEFFICIENT =',F8.1,2X,'(W/M**2*C)' //20X,'FREEZING',
     41X,'TEMPERATURE =',F8.1,2X,'(C)'// 20X,'COOLANT',1X,
     4'TEMPERATURE =',F6.1,2X,'(C)'///)
C
  105 WRITE(2,2500)
 2500 FORMAT (/20X,'FREEZING OF GRAPEFRUIT JUICE'/)
      WRITE(2,211 )
  211 FORMAT(/ 32X,'TIME',6X,'ICE THICKNESS'/
     222X,'(SECS',10X,'(HRS)',10X,'(CMS)'/)
C
C
C     VALUES OF VARIABLES A AND B AS ICE THICKNESS (X)
C     APPROACHES ZERO
      X = .00001
      XN=0.
      M= H*X/ K1
      MM=M
      N= L*TK1*P/ K1
C
C     A AND B  EVALUATED AS AO AND BO
C
      A = -H*TC / K1
      B = -H**2*TC**2 / (2.*K1**2*N)
      WI= K1/(TK1*H)
C
      TT=0.
C
```

```
PROGRAM NAME        76/76    OPT=1 TRACE                    FTN 4.5+420
2

C
C       INCREASE X AND HENCE M
C
        X=X+.001
C
        CALL JAWS (II)
C
C       EVALUATION OF INTEGRAL AT M =M
C
        IX=II*WI
        A =ANEW
        B =BNEW
        MM=MNEW
C
  500   X=X+.001
C
        CALL JAWS(IK)
C
C
C       EVALUATION OF INTEGRAL AT M =M +DM
C
        JX=IK* WI
C
C       EVALUATION OF TIME FOR ICE THICKNESS TO INCREASE BY
C       ONE STEP LENGTH - CALCULATED BY TRAPEZOIDAL APPROXIMATION
C
        TIME = 0.5*(JX+IX)*(H*.001/K1)
        TT=TT+TIME
C
C       OUTPUT OF TIME AND ICE THICKNESS
        XN=XN+.001
        XZZ=XN*100.
        TYP = TT/3600.
        WRITE(2,2000) TT,TYP,XZZ
 2000   FORMAT(20X,F10.3,10X,F6.3,10X,F6.1)
C
C
C       EXCHANGE OF VARIABLE VALUES FOR EVALUATION OF TIME OVER
C       NEXT STEP INTERVAL
C
        A=ANEW
        B=BNEW
        MM=MNEW
        ZX=X
        IX=JX
        IF(X.GT.0.04) GO TO 999
        GO TO 500
    999 CONTINUE
   2113 CONTINUE
        END
```

```
      SUBROUTINE JAWS(IJ)
C
C     SUBROUTINE JAWS FOR EVALUATION OF VARIABLES IN INTEGRAL
C
      REAL M,N,K1,L,NNEW,MNEW,II,III,IJ,IK,IX  ,JX ,MM
      COMMON H,X,TC,TM  ,MM
      COMMON M,N,K1,L,NNEW,MNEW,A,B,ANEW,BNEW
      MNEW =  H*X/ K1
      M=MNEW
C
C     EVALATION OF NEW VALUESOF A AND B AS ANEW AND BNEW
C
      AB= H*N*(M+1.)/(K1*M*(M+2.)  )
      AC=SQRT ((1.-2.*TC*M*(M+2) / (N*(M+1.)**2)))-1.
      ANEW= AB*AC
      BC= -H**2*N*(M+1.)**2/(K1**2*M**2*(M+2.)**2)
      BD= TC*M*(M+2.)/(N*(M+1.)**2)
      BE= 1.-BD-SQRT(1.-2.*BD)
      BNEW= BC*BE
C
C     APPROXIMATION OF DERIVATIVES OF A AND B
C
      AM =(ANEW-A)/(MNEW-MM)
      BM =(BNEW-B)/(MNEW-MM)
      M=MM
      RI =TM/(2.*M*B*K1)*H
      XI =M/2.+M**2/(6.*B)*BM
      YI = -A/(2.*B)+M/(4.*B)*AM
      IJ = K1/H*XI+YI+RI
      RETURN
      END
```

FREEZING RATES PREDICTED BY GOODMANS INTEGRAL METHOD

HEAT TRANSFER COEFFICIENT = 900.0 (W/M**2*C)

FREEZING TEMPERATURE = -1.0 (C)

COOLANT TEMPERATURE = -10.0 (C)

FREEZING OF GRAPEFRUIT JUICE

TIME (SECS)	TIME (HRS)	ICE THICKNESS (CMS)
520.705	.145	.1
607.115	.169	.2
714.003	.198	.3
843.432	.234	.4
996.042	.277	.5
1172.135	.326	.6
1371.880	.381	.7
1595.386	.443	.8
1842.726	.512	.9
2113.953	.587	1.0
2409.106	.669	1.1
2728.216	.758	1.2
3071.304	.853	1.3
3438.391	.955	1.4
3829.492	1.064	1.5
4244.619	1.179	1.6
4683.783	1.301	1.7
5146.993	1.430	1.8
5634.256	1.565	1.9
6145.580	1.707	2.0
6680.969	1.856	2.1
7240.428	2.011	2.2
7823.963	2.173	2.3
8431.576	2.342	2.4
9063.272	2.518	2.5
9719.052	2.700	2.6
10398.921	2.889	2.7
11102.880	3.084	2.8
11830.932	3.286	2.9
12583.078	3.495	3.0
13359.320	3.711	3.1
14159.660	3.933	3.2
14984.100	4.162	3.3
15832.641	4.398	3.4
16705.284	4.640	3.5
17602.030	4.889	3.6
18522.881	5.145	3.7
19467.836	5.408	3.8
20436.899	5.677	3.9

$$T_1 = A \text{ erf } \frac{X}{2(\alpha_1 t)^{\frac{1}{2}}} \quad \text{where A is a constant}$$

(A4-15)

For the unfrozen section a standard solution is given by :

$$T_2 = TI - B \text{ erfc } \frac{X}{2(\alpha_2 t)^{\frac{1}{2}}} \quad \text{where B is a constant}$$

(A4-16)

Substituting (A4-15) and (A4-16) into (1-4) a boundary condition at $x = X(t)$ we obtain :

$$A \text{ erf } \frac{X}{2(\alpha_1 t)^{\frac{1}{2}}} = TI - B \text{ erfc } \frac{X}{2(\alpha_2 t)^{\frac{1}{2}}} = Tm \quad \text{(A4-17)}$$

As this has to be true for all values, both

$$\frac{X}{2(\alpha_1 t)^{\frac{1}{2}}} \text{ and } \frac{X}{2(\alpha_2 t)^{\frac{1}{2}}}$$ must be equal to a constant

so we may write :

$$X = 2 \lambda (\alpha_1 t)^{\frac{1}{2}} \quad \text{(A4-7)}$$

where λ is defined by the following equation obtained from (1-3) (A4-17) and (4-7).

$$\frac{\exp(-\lambda^2)}{\text{erf}} - \frac{(K_2^2 \alpha_1)^2}{(K_1^2 \alpha_2)} \frac{(TI-Tm)\exp(-\alpha_1 \lambda^2 / \alpha_2)}{(Tm-Ts)\text{erfc}(\lambda^2 \alpha_1 / \alpha_2)^{\frac{1}{2}}}$$

$$= \frac{\lambda L \pi^{\frac{1}{2}}}{C_1 (Tm-Ts)} \qquad (4\text{-}8)$$

Once λ has been determined and corresponding values of time and ice thickness evaluated from (4-8) the temperatures in the two phases can be rewritten by combining (A4-15), (A4-16), (A4-17) and (4-7) in the following two equations :

$$T_1 = \frac{TI}{\text{erf}\lambda} \frac{\text{erf } x}{2(\alpha_1 t)^{\frac{1}{2}}}$$

$$T_2 = TI - \frac{(TI-Tm)}{\text{erfc}\,\lambda (\alpha_1/\alpha_2)^{\frac{1}{2}}} \text{erfc} \frac{x}{2(\alpha_2 t)^{\frac{1}{2}}}$$

A4-3.1 COMPUTATION OF NEUMANN'S SOLUTION.

In the computer program the error function, ERFA, is calculated by the formula :

$$ERFA = 1 (A_1 TZ + A_2 TZ^2 + A_3 TZ^3) * EXP(-A**2)$$

(A4-18)

where A = first estimate of the error coefficient.

A_1= .34802

A_2= -.09587

A_3= .74785

P = .47047

TZ= 1/(1 + P*A)

The error coefficient ERFAC is then obtained from the expression (1-ERFA).

The values of ERFA and ERFAC are then substituted into equation (4-8) and a value of ANEW calculated. The value of ANEW is compared to the initial value of A, an iterative process is used until A equals ANEW to a sufficient accuracy.

A flow diagram, program listing and sample output are given on the next pages.

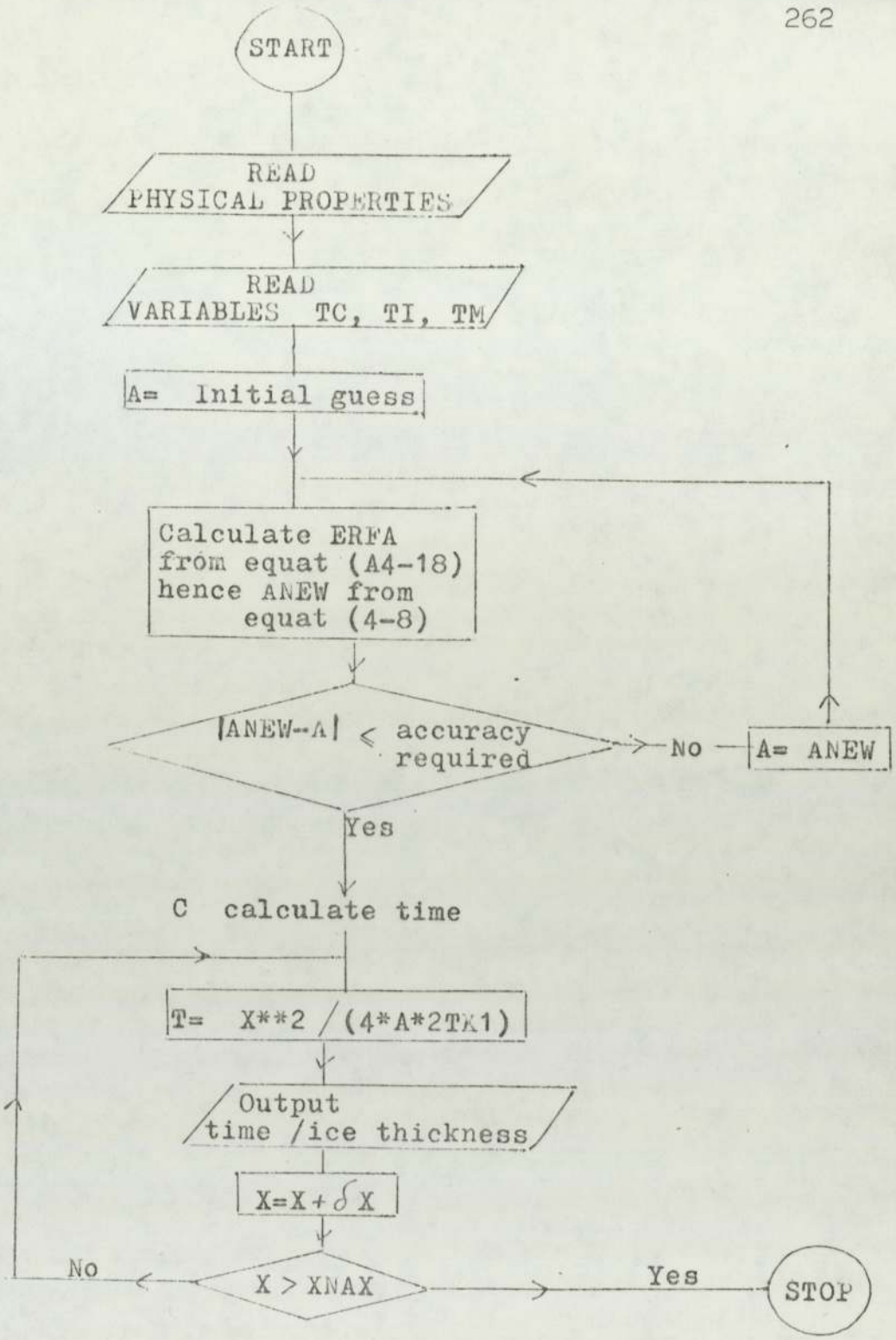

Flow diagram for Neumanns method

```
      PRØGRAM NAME(INPUT,ØUTPUT,TAPE1=INPUT,TAPE2=ØUTPUT)
C     NEUMANN'S SØLUTIØN TØ FREEZING PRØBLEM - INFINITE HEAT TRANSFE
C    ·CØEFFICIENT  -  TS =TC
C
      REAL L,K1,K2
      READ(1,1000) K1,K2,TK1,TK2,L,P,C1
 1000 FØRMAT(10F10.0)
      IP =10
      DØ 8 IZ =1,IP
      READ(1,1010) TC,TI,TM
 1010 FØRMAT(10F10.0)
C
C
C     DEFINITIØN ØF VARIABLES
C
C     K1 = THERMAL CØNDUCTIVITY ØF ICE
C     K2 = THERMAL CØNDUCTIVITY ØF WATER
C     TK1= THERMAL DIFFUSIVITY ØF ICE
C     TK2= THERMAL DIFFUSIVITY ØF WATER
C     L  = LATENT HEAT
C     C1 = SPECIFIC HEAT ØF ICE
C    P= CØNSTANT
C     TM = FREEZING TEMPERATURE
C     TI = INITIAL TEMPERATURE
C     TC = CØØLANT TEMPERATURE
C
      WRITE(2,2510) TC   ,TI,TM
 2510 FØRMAT(1H1 /// 20X,'FREEZING RATE AS PREDICTED BY NEUMANNS',
     1'SØLUTIØN' // 20X,'CØØLANT TEMPERATURE =',F6.2,2X,'(C)' //
     220X,'INITIAL TEMPERATURE =',F6.2,2X,'(C)'//20X,
     3'FREEZING TEMPERATURE =',F5.2 ,2X,'(C)'///)
C
C
C
      WRITE(2,2525)
 2525 FØRMAT( 36X,'TIME',21X,'THICKNESS ØF ICE' / 24X,'(HRS)',15X,
     1'(SECS)',16X,'(CMS)'/)
C
      A=.05
      PY =.47047
   50 TZ =1./(1.+PY*A)
      AA= SQRT(K2**2*TK1 / (K1**2*TK2))
      AB= EXP(-TK1*A**2 /TK2) * (TI -   TM)
      AD=TM-TC
      AE= EXP(-A**2)
      AF= L*SQRT(P)
      AG= C1*(TM-TC)
      A1 =.34802
      A2 =-.09587
      A3 =.74785
      AC=SQRT(A**2*TK1/TK2)
      TZZ=1./(1.+PY*AC)
      ERFAC= 1.-(A1*TZZ+A2*TZZ**2+A3*TZZ**3)*EXP(-AC**2)
      ERFA=1.-(A1*TZ +A2*TZ**2 +A3*TZ**3)*EXP(-A**2)
C
      ANEW = AG/AF*(AE/ERFA -(AA*AB/(AD*(1.-ERFAC))))
C
```

```
      IF(ABS(ANEW-A).LE.0.00001) GØ TØ 200
      A=ANEW
      GØ TØ 50
C
  200 X=.001
      A=ANEW
  250 TIME =  X**2 / (4.*A**2*TK1)
C
      X1=X *100.
      TT= TIME /3600.
      WRITE(2,2530) TT,TIME,X1
 2530 FØRMAT(20X,F10.3,10X,F10.5,10X,F10.2)
C
      X=X +.001
      IF(X.GE..03) GØ TØ 600
      GØ TØ 250
  600 CØNTINUE
    8 CØNTINUE
      STØP
      END
```

FREEZING RATE AS PREDICTED BY NEUMANNS SØLUTIØN

CØØLANT TEMPERATURE =-15.00 (C)

INITIAL TEMPERATURE = 20.00 (C)

FREEZING TEMPERATURE = 0.00 (C)

TIME (HRS)	TIME (SECS)	THICKNESS ØF IC (CMS)
.001	3.07317	.10
.003	12.29269	.20
.008	27.65855	.30
.014	49.17075	.40
.021	76.82930	.50
.031	110.63419	.60
.042	150.58542	.70
.055	196.68300	.80
.069	248.92692	.90
.085	307.31719	1.00
.103	371.85379	1.10
.123	442.53675	1.20
.144	519.36604	1.30
.167	602.34168	1.40
.192	691.46367	1.50
.219	786.73200	1.60
.247	888.14667	1.70
.277	995.70768	1.80
.308	1109.41504	1.90
.341	1229.26874	2.00
.376	1355.26879	2.10
.413	1487.41518	2.20
.452	1625.70791	2.30
.492	1770.14699	2.40
.534	1920.73241	2.50
.577	2077.46418	2.60
.622	2240.34228	2.70
.669	2409.36674	2.80
.718	2584.53753	2.90

A4-4 VASIL'EV AND USPENSKII FINITE DIFFERENCE METHOD

A4-4.1 Introduction to the method

This section first discusses the principle of a backward- difference finite difference approximation to the heat conduction equation, and then gives details of, and extensions to, the Vasil'ev and Uspenskii method to the moving boundary problem of one-dimensional freezing which include finite difference approximations to calculate the precooling and tempering stages of a freezing process.

The finite difference methods are based on substituting finite difference approximations into the heat conduction equations (1-1) and (1-2).

With the differential coefficients $\partial T/\partial t$, $\partial T/\partial x$ and $\partial^2 T/\partial x^2$ approximated by

$$\frac{\partial T}{\partial t} = \frac{(T_{i,n} - T_{i,n-1})}{\Delta n}$$

$$\frac{\partial^2 T}{\partial x^2} = \frac{(T_{i+1,n} - 2T_{i,n} + T_{i-1,n})}{h^2}$$

(in the case of boundary conditions, eg. equation A4-22 p.268 $\partial T/\partial x$ may be approximated over two distance step lengths eg.

$$\frac{\partial T}{\partial x} = \frac{(T_{i+1,n} - T_{i-1,n})}{2h} \qquad)$$

the conduction equation :

$$\frac{\partial T}{\partial t} = \alpha \frac{\partial^2 T}{\partial x^2}$$

on substitution of the differential coefficients becomes :

$$\frac{T_{i,n} + T_{i,n-1}}{2n} = \alpha \frac{(T_{i+1,n} - 2T_{i,n} + T_{i-1,n})}{h^2}$$

(A4-19)

equation A4-19 on algebraic manipulation forms two sets of implicit finite difference equations for the frozen and unfrozen phases of the form :

$$-\frac{1}{B} T_{i,n-1} = T_{i+1,n} - (2 + \frac{1}{B}) T_{i,n} + T_{i-1,n}$$

$$n = 1,2 \text{ ---- } N \qquad \text{(A4-20)}$$

where $B = \alpha \frac{2n}{h^2}$

Boundary conditions for one dimensional freezing problem

The boundary conditions to be considered are at

(i) the limit of the liquid (furthest from the coolant surface),

(ii) at the coolant surface and (iii) at the interface.

(i) At the limit of the liquid (i = N for computation)

Alternative conditions are considered. The first condition assumes that there is no heat flow ie $\partial T/\partial x = 0$. In this case the temperatures $T_{N+1,n}$ and $T_{N-1,n}$ in equation (A4-20) are assumed to be equal, the resultant boundary condition equation is

$$\frac{1}{B} T_{N,n-1} = 2T_{N-1,n} - (2 + \frac{1}{B}) T_{N,n} \qquad \text{(A4-21)}$$

The alternative condition at the limit of the liquid assumes that there is heat gain to the system, characterised by the heat transfer coefficient, HG, between the liquid and its surroundings.

The boundary condition

$$-K \left(\frac{\partial T}{\partial x}\right)_{x = a} = HG\ (T_N - TA) \qquad \text{(1-6b)}$$

where T_N = temperature at limit of liquid

is written in finite difference form as :

$$-K\frac{(T_{N+1,n} - T_{N-1,n})}{2h} = HG\,(T_{N,n} - TA) \qquad (A4\text{-}22)$$

Evaluation of the fictitious boundary node $T_{N+1,n}$

in (A4-22) produces :

$$T_{N+1,n} = \frac{-2hHG}{K}\,(T_{N,n} - TA) + T_{N-1,n} \qquad (A4\text{-}23)$$

Substitution of equation (A4-23) into (A4-20)produces the alternative boundary condition at the limit of the liquid as :

$$-\frac{1}{B}\,T_{N,n-1} = -(AN + 2 + \frac{1}{B})\,T_{N,n} + 2\,T_{N-1,n} + ANTA \qquad (A4\text{-}24)$$

where $AN = \frac{2hHG}{K}$

(ii) At the coolant surface (i = 1 for computation)

By an identical procedure to that used to produce equation A4-24 the boundary condition equation is :

$$-\frac{1}{B}\ T_{1,n-1} = T_{2,n} - \left(2 + \frac{1}{B} + N\right)\ T_{1,n} + PTC$$

(A4-25)

where $P = \frac{2hH}{K}$

(iii) At the interface (i = n for computation)

In the method of Vasil'ev and Uspenskii the freezing point, Tm, is defined to be zero. The interface temperatures in both phases, by equation (1-4) are defined $T_1 = T_2 = T_m$ as equal to 0.

The boundary equation at the interface :

$$-L\rho\frac{dX}{dt} = -K_1\left\{\frac{\partial T_1}{\partial x}\right\}_X + K_2\left\{\frac{\partial T_2}{\partial x}\right\}_X \quad (1\text{-}3)$$

can be approximated in finite difference form as :

$$-L\rho\frac{h}{n} = -K_1\ \frac{(T_{n,n} - T_{n-1,n})}{h} + K_2\ \frac{(T_{n+1,n} - T_{n,n})}{h}$$

(A4-26)

But since $T_{n,n}$ for both the frozen and unfrozen phase is equal to 0 equation (A4-26) reduces to :

$$-L\rho \frac{h^2}{Zn} = K_1 (T_{n-1,n}) + K_2 (T_{n+1,n}) \qquad (A4\text{-}27)$$

Equation (A4-27) can be rearranged to give Zn as :

$$Zn = -L\rho h^2/(K_1 (T_{n-1,n}) + K_2 (T_{n+1,n}) \qquad (A4\text{-}28)$$

Equation (A4-28) is used in the computer program to calculate the time interval for the interface to travel from node n-1 to node n, (see figure A4-4) in place of equation (A4-53) as proposed by Vasil'ev and Uspenskii (see p. 282)

Extensions to Vasil'ev & Uspenskii Method

The implicit finite difference scheme outlined above requires a starting temperature profile for initial conditions. This temperature profile is supplied by incorporating a second finite difference scheme to calculate the precooling time. The precooling time in this case is taken as the time required to reduce the temperature, at the first internal node (i.e. i = 2) of the body being frozen from its initial temperature to 0°C. The temperatures calculated at the end of the precooling time are then used as the initial conditions for the freezing period. The freezing period starts by calculating the time for the unfrozen-frozen interface to traverse

Figure A4-4 Assumed temperature profiles of Vasil'ev & Uspenskii finite difference method

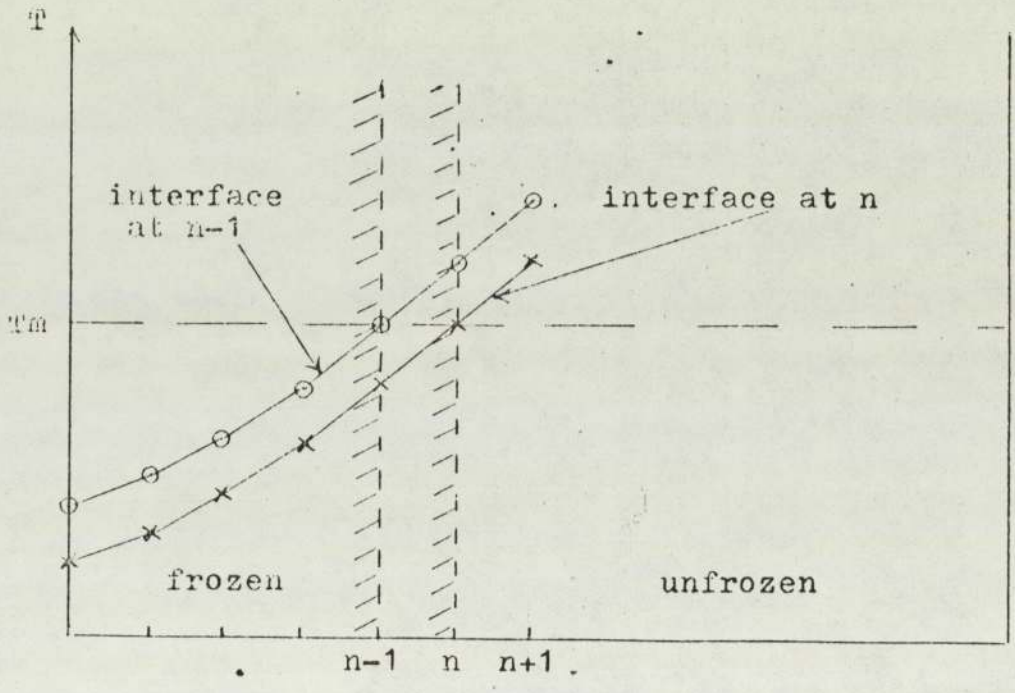

the first step length with the material being at 0 , but unfrozen, at the first internal node. The first estimate of the time for the interface to traverse the first step length is obtained from equation (A4-54) p 284. Using this estimated time the temperature profiles in both phases are calculated for the end of the step length and the time recalculated by equation (A4-28). Recalculation of the time interval is continued iteratively by recalculation of temperature profiles until successive times agree to within the required accuracy. The process is continued across all the distance step lengths until the material is completely frozen. At the end of the freezing period of third finite difference scheme calculates the time to reduce the temperature of the thermal centre of the body to its storage temperature.

The procedure used for the additonal finite difference schemes, which were worked out implicitly, was the same as that used to determine the temperature profile of the aluminium bar in the determination of the heat transfer coefficient given in appendix 3 (section A3-3.4).

For the materials not having a freezing point of 0, the temperature scales must be changed to bring the freezing point back to 0. Thus for 5 per cent sodium chloride the temperature scales must be adjusted by 3 C, (freezing point of 5% NaCl is -3 C). Further details of the use of the Vasil'ev and Uspenskii program for the freezing of electrolyte solutions is given in Chapter 6, section 6-3.

The method of Vasil'ev and Uspenskii is now given.

According to this method we divide the region $0 \leq x \leq a$ into (N-1) equal parts with points x_i, such that $x_i = ih$, for $i = 1,2 \ldots N$. Here h equals the spacing between adjacent points. The basic computation of the method calculates the time interval, Δn, required for the frozen-unfrozen interface to advance from x_i to x_{i+1}. Denoting the temperature at the mesh point i at time n by $W_{i,n}$ in the frozen phase, and $V_{i,n}$ in the unfrozen phase, the implicit iterative finite difference scheme is :

$$\delta t\,(W_{i,n}) = \alpha_1\ \delta xx\,(W_{i,n});\ i = 2,3 \ldots, n-1 \qquad n>2 \qquad (A4\text{-}29)$$

$$\delta t\,(V_{i,n}) = \alpha_2\ \delta xx\,(V_{i,n});\ i = n+1, n+2 \ldots, N-1 \qquad n<N-1. \qquad (A4\text{-}30)$$

$$-L\rho\,\frac{h}{\Delta n} = K_1\,\delta x\,(W_{n-1,n}) - K_2\,\delta x\,(W_{n,n}) \qquad (A4\text{-}31)$$

$$W_{n,n} = V_{n,n} \equiv 0 \qquad (A4\text{-}32)$$

$$-q_1\,(t_{n-1}) = K_1\ \delta x\,(W_{i,n}) \qquad (A4\text{-}33)$$

$$-q_2\,(t_{n-1}) = K_2\,\delta x\,(W_{N-1,n}) \qquad (A4\text{-}34)$$

$$V_{i,1} = \phi\,(ih);\ i = 1,2,\ldots\ldots, N \qquad (A4\text{-}35)$$

Where the differential coefficients $\delta t, \delta xx, \delta x$ are defined by :

$$\delta t\,(W_{i,n}) = \frac{1}{Z_n}\,(W_{i,n} - W_{i,n-1})$$

$$\delta x\,(W_{i,n}) = \frac{1}{h}\,(W_{i+1,n} - W_{i,n})$$

$$\delta xx\,(W_{i,n}) = \frac{1}{h^2}\,(W_{i-1,n} - 2W_{i,n} + W_{i+1,n})$$

The numbers of equations *(A4-29)* to *(A4-35)* correspond to the analagous equations (1-1) to (1-8) of the original problem (See appendix 6). Note that, acccrding to equation *(A4-32)* the melting point of the solid is defined as $Tm \equiv 0$. Equations *(A4-33)* and *(A4-34)* are less specific than the corresponding equations (1-5) and (1-6) with the heat fluxes q_1 and q_2 yet to be defined. It will be appreciated that equations *(A4-29)* and *(A4-30)* each represent a set of equations one for each mesh point, and that the number of points to which each applies changes as the freezing interface advances (see figure A4-5).

When we have computed the temperatures at time n-1 ($W_{i,n-1}$ and $V_{i,n-1}$) we determine the unknowns, $W_{i,n}$, $V_{i,n}$ and Z_n as follows:

Figure A4-5 Diagrams for Vasil'ev & Uspenskii method

(a) Region $0 \leq x \leq a$ divided into 10 sections:

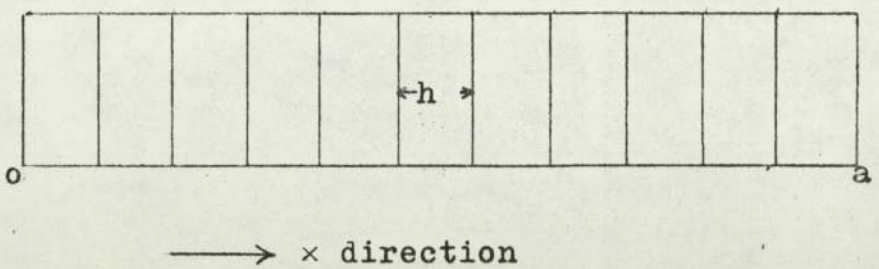

(b) Situation when interface is at 4th node:

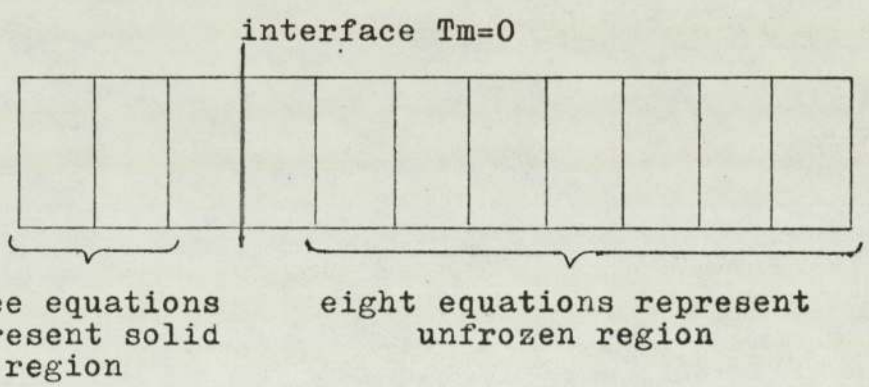

(c) Situation when interface is at 7th node:

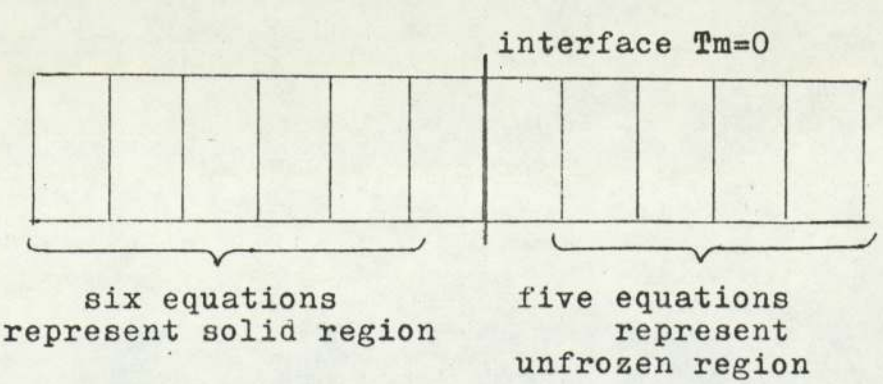

(I) Make a first estimate of Z_n as $Z_n^{(0)}$.

(II) Substitute $Z_n^{(s)} = Z_n^{(0)}$ in the finite difference scheme :

$$\delta t\,(W_{i,n}^{(s)}) = \lambda_1\,\delta xx(W_{i,n}^{(s)}) \qquad (A4\text{-}36)$$

$$\delta t\,(V_{i,n}^{(s)}) = \lambda_2\,\delta xx(V_{i,n}^{(s)}) \qquad (A4\text{-}37)$$

$$W_{n,n}^{(s)} = V_{n,n}^{(s)} \qquad (A4\text{-}38)$$

$$-q_1\,(t_{n-1}) = K_1\,\delta x\,(W_{i,n}^{(s)}) \qquad (A4\text{-}39)$$

$$-q_2\,(t_{n-1}) = K_2\,\delta x\,(W_{N-1,n}^{(s)}) \qquad (A4\text{-}40)$$

$$V_{i,1}^{(s)} = \phi\,(ih) \qquad (A4\text{-}41)$$

$$Z_n^{(s+1)} = \left(\frac{h}{q_1(t_{n-1}) - q_2(t_{n-1})}\right)\left\{L\rho + \frac{\dot{Z}_n^{(s)}}{h}[\,Q]\right\} \qquad (A4\text{-}42)$$

where $Q = q_1(t_{n-1}) - q_2(t_{n-1}) + K_1\,\delta x W_{n-1,n}^{(s)} - K_2\,\delta x\,V_{n,n}^{(s)}$

(III) Compute the values of $W_{i,n}^{(S)}$ and $V_{i,n}^{(S)}$ in equations (A4-36, A4-37, A4-38, A4-39 and A4-40 and A4-35 when n = 2) and hence determine $Z_n^{(S+1)}$.

(IV) Resubstitute $Z_n^{(S)} = Z_n^{(S+1)}$, recompute $W_{i,n}^{(S)}$ and $V_{i,n}^{(S)}$ hence $Z_n^{(S+1)}$ again.

(V) Continue until $Z_n^{(S)} \longrightarrow Z_n^{(S+1)}$ to the required accuracy.

A4-4.2 Computation of Vasil'ev and Uspenskii Method.

The computations of step (III) require the solution of two sets of linear algebraic equations, A4-36, A4-38 and A4-39 and A4-37, A4-38 and A4-40. The following pages describe a Fortran program to calculate the rate of progress of the freezing interface and discusses the method of incorporating the heat fluxes q_1 and q_2 into the boundary conditions.

Equation (A4-36) gives, on expansion, a set of algebraic equations of the form :

$$\frac{W_{i,n}^{(S)} - W_{i,n-1}}{\Delta n^{(S)}} = \frac{\alpha_1}{h^2}\left(W_{i-1,n}^{(S)} - 2W_{i,n}^{(S)} + W_{i+1,n}^{(S)}\right)$$

or $$W_{i-1,n}^{(S)} - (2 + h^2/\alpha_1 \Delta n^{(S)}) = (h^2/\alpha_1 \Delta n^{(S)})W_{i,n-1}$$

for $i = 2,3, \ldots\ldots, n-1$ (A4-43)

Similarly, (A4-37) gives :

$$V_{i-1,n}^{(S)} - (2 + h^2/\alpha_2 \Delta n^{(S)})V_{i,n}^{(S)} + V_{i+1,n}^{(S)} = (h^2/\alpha_2 \Delta n^{(S)})\, V_{i,n-1}$$

for $i = n+1, n+2, \ldots\ldots, N-1$ (A4-44)

In these equations, the i suffixes refer to points in space, the n suffixes to points in time, the superfix S to variables to be calculated in the current computation.

At $i = 1$, and $i = N$, there are additional equations (A4-39) and (A4-40). At $i = 1$, writing $-q_1 (t_{n-1})$ as $H (W_{1,n}^{(S)} - WC)$, where WC is the external coolant

temperature, (A4-39) becomes :

$$(K_1/h\ (W_{2,n}^{(S)} - W_{1,n}^{(S)}) = H\ (W_{1,n}^{(S)} - WC\ )$$

or $$(1 + Hh/K_1)\ W_{1,n}^{(S)} - W_{2,n}^{(S)} = (Hh/K_1)WC \qquad (A4-45)$$

At i = N, we use the *no heat flux condition at the boundary*:

$V_{N-1,n} = V_{N+1,n}$, equivalent to $q_2 = 0$ in to give, from

$$2\ V_{N-1,n}^{(S)} - (2 + h^2/\alpha_2\ Z_n^{(S)})V_{N,n} = (h^2/\alpha_2\ Z_n^{(S)})V_{N,n-1} \qquad (A4-46)$$

A second boundary condition at i = N takes into account the effect of heat gain. Equation (A4-23) has evaluated the fictitious temperature node as :

$$V_{N+1,n} = -AN\ (V_{N,n} - TA) + V_{N-1,n} \qquad (A4-23)$$

where AN = -2h HG/K

This temperature is substituted into (A4-37) to give

$$2V_{N-1,n}^{(S)} - (2 + h^2/\alpha_2\ Z_n^{(S)} + AN)\ V_{N,n} + ANTA$$
$$= -(h^2/\alpha_2\ Z_n^{(S)})V_{N,n-1} \qquad (A4-47)$$

Finally, the interface condition, (A4-38) is, with the melting point = 0,

$$W_{n,n} = V_{n,n} = 0 \qquad \text{(A4-48)}$$

At the S^{th} iteration of n^{th} time step, the temperatures W_i and V_i are thus found by solution of the following two sets of simultaneous algebraic equations. (From which the suffix (n) and superfix (S) are dropped for simplicity).

(I) Phase 1. Equations (A4-43) (A4-45) & A4-48)

$$W_1 (1 + Hh/K_1) - W_2 = (Hh/K_1) WC \qquad (i = 1) \quad \text{(A4-49)}$$

$$W_1 - (2 + h^2/\alpha_1 \Delta n) W_2 + W_3 = -(h^2/\alpha_1 \Delta n) W_{2,n-1} \qquad (i = 2) \quad \text{(A4-50)}$$

$$W_2 - (2 + h^2/\alpha_1 \Delta n) W_3 + W_4 = -(h^2/\alpha_1 \Delta n) W_{3,n-1} \qquad (i = 3)$$

$$W_{i-1} - (2 + h^2/\alpha_1 \Delta n) W_i + W_i + 1 = (h^2/\alpha_1 \Delta n) W_{i,n-1} \qquad (i = i)$$

$$W_{n-2} - (2 + h^2/\alpha_1 \mathcal{Z}n)W_{n-1} = -(h^2/\alpha_1 \mathcal{Z}n)W_{n-1,n-1} \qquad (i=n-1)$$

$$W_n = 0 \qquad (i=n)$$

(II) Phase 2 equations (A4-44), (A4-46), (A4-48).

$$V_n = 0 \qquad (i=n)$$

$$-(2 + h^2/\alpha_2 \mathcal{Z}n)V_{n+1} + V_{n+2} = -(h^2/\alpha_2 \mathcal{Z}n)\, V_{n+1,\, n-1} \qquad (i=n+1)$$

$$V_{i-1} -(2 + h^2/\alpha_2 \mathcal{Z}n)V_i + V_{i+1} = -(h^2/\alpha_2 \mathcal{Z}n)V_{i,n-1} \qquad (i=i) \quad (A4\text{-}51)$$

$$2\, V_{N-1} -(2 + h^2/\alpha_2 \mathcal{Z}n)V_N = -(h^2/\alpha_2 \mathcal{Z}n)V_{N,n-1} \qquad (i=N) \quad (A4\text{-}52)$$

The method of solution of these equations is the same as used for the evaluation of the implicit finite

difference scheme for the determination of the heat transfer coefficient between the coolant and base of the aluminium bar. (See appendix 3, section A3-3.4).

When we know W_{n-1} and V_{n+1} from the procedure outlined in appendix 3, we can apply equation (A4-42) to recalculate z_n, as follows in (A4-42):

$$-q_1' (t_{n-1}) = H(W_{1,n} - WC)$$

$$-q_2 \equiv 0$$

$$K_1 \delta x (W_{n-1,n}) = K_1 (W_{n,n} - W_{n-1,n}) / h$$
$$= (-K_1/h) W_{n-1,n} \text{ since } W_{n,n} = 0$$

$$K_1 \delta x (W_{n,n}) = (K_2/h) W_{n+1,n}$$

hence, in (A4-42)

$$z_n^{(S+1)} = \frac{(hL\rho + z_n^{(S)}(H(WC - W_{1,n}^{(S)}) - (K_1/h)W_{n-1,n}^{(S)} - (K_2/h)V_{n+1,n}^{(S)})}{H(WC - W_{1,n}^{(S)})} \qquad (A4-53)$$

Equation (A4-53) is as given by Vasil'ev and Uspenskii but

was found on computation to sometimes give negative times for $Z_n^{(S+1)}$. The reason for negative freezing times is that the numerator attains a positive value under certain freezing conditions while the denominator $H(WC-W_{1,n}^{(S)})$ always retains a negative value.

Modifications to Vasil'ev & Uspenskii Method

An alternative to (A4-53) results from a direct application of equation (1-3).

$$-L\rho \frac{dx}{dt} = -K_1 \left(\frac{\partial T_1}{\partial x}\right)_X + K_2 \left(\frac{\partial T_2}{\partial x}\right)_X \qquad (1\text{-}3)$$

whose finite difference approximation written as :

$$-L\rho \frac{h}{Z_n^{(S+1)}} = -K_1 \delta x\,(W_{n-1,n}^{(S)}) + K_2 \delta x (V_{n,n}^{(S)})$$

produces on arrangement : (see also p. 270)

$$Z_n^{(S+1)} = -L\rho h^2/(K_1 W_{n-1,n}^{(S)} + K_2 V_{n+1,n}^{(S)}) \qquad (A4\text{-}28)$$

Equation (A4-28) was used in place of (A4-53) in all computations. The corrected value of Z_n, from (A4-53), is substituted back into equations (A4-43), (A4-44), (A4-45) and (A4-46), and the computations

repeated. We evaluate W_{n-1} and W_{n+1} for resubstitution into (A4-28). When $z_n^{(S+1)}$ agrees with $z_n^{(S)}$ to a sufficient accuracy we evaluate all the temperatures and proceed to the next grid point setting $W_{i,n} \equiv W_{i,n-1}$, for use in equations (A4-43), (A4-44), (A4-45) and (A4-46).

For the first estimate of $z_n^{(S)}$, $z_n^{(0)}$ we use an approximation of equation (1-3) at the first mesh point :

$$-L\rho \frac{dx}{dt} = -q_1 + q_2$$

where $q_1 = -H(W_{1,1} - WC\ )$ and $q_2 = 0$

to give

$$z_n^{(0)} = L\rho\, h/H(W_{1,1} - WC\ ) \qquad (A4\text{-}54)$$

In the early and late stages of the computation, when n = 2 or 3 and n = N or N-1 the method of solution of the linear sets of equations outlined in appendix 3-3.4 is inefficient since the solid and liquid phases respectivity are represented by one or two equations only. Instead the equations, with the following substitutions:

$$B1 = 1 + Hh/K_1$$

$$AR1 = Hh/K_1$$

$$S1 = -h^2/(\alpha_1 Z n)$$

$$XT1 = -2 + h^2/(\alpha_1 Z n)$$

$$XT2 = -2 + h^2/(\alpha_2 Z n)$$

$$S2 = h^2/(\alpha_2 Z n)$$

used to determine new temperatures are, firstly, in the solid phase :

(I) when n = 2 equation (A4-49) is rearranged to give :

$$W_{(1,n)} = AR1\ WC/B1 \qquad (A4\text{-}55)$$

(II) when n = 3 equations (A4-49) and (A4-50) are rearranged to give :

$$W_{(2,n)} = (S1\ W(_{2,n-1}) - AR1\ WC/B1)/XT1 + 1/B1)$$

$$W(_{1,n}) = (AR1\ WC + W(_{2,n-1})/B1$$

and secondly in the liquid phase :

(I) When n = N-1 equations (A4-51) and (A4-52) are rearranged to give :

$$W(_{N-1,n}) = \frac{S2(W(_{N-1,n-1}) - W(_{N,n-1}) / XT2}{(XT2 - 2/XT2)}$$

$$W(_{N,n}) = \frac{S2W(_{N,n-1})}{XT2} - \frac{2W(_{N-1,n-1})}{XT2}$$

(II) when n = N equation (A4-52) is rearranged to give :

$$W(_{N,n}) = S2\ W(_{N,n-1}) / XT2$$

A flow diagram, computer and sample output, for the program for freezing distilled water, are given on the next pages.

In the program it is assumed that there is no heat gain from the surroundings. The frozen ice is reduced in temperature to -5 C.

For details of extension of Vasil'ev and Uspenskii method to account for the freezing of materials with freezing points not equal to 0 C see Chapter 6.

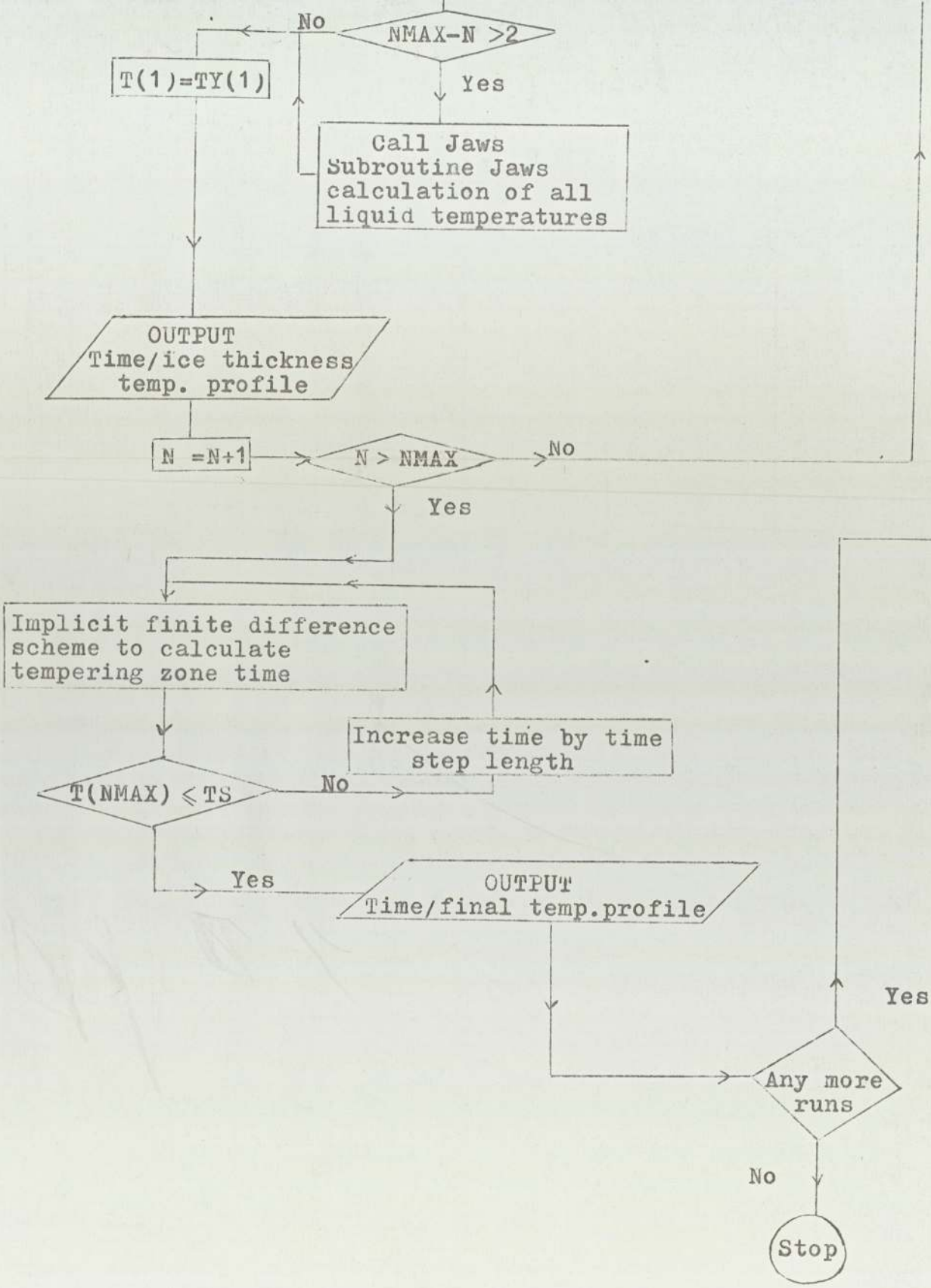

Flow diagram for modified Vasil'ev & Uspenskii method

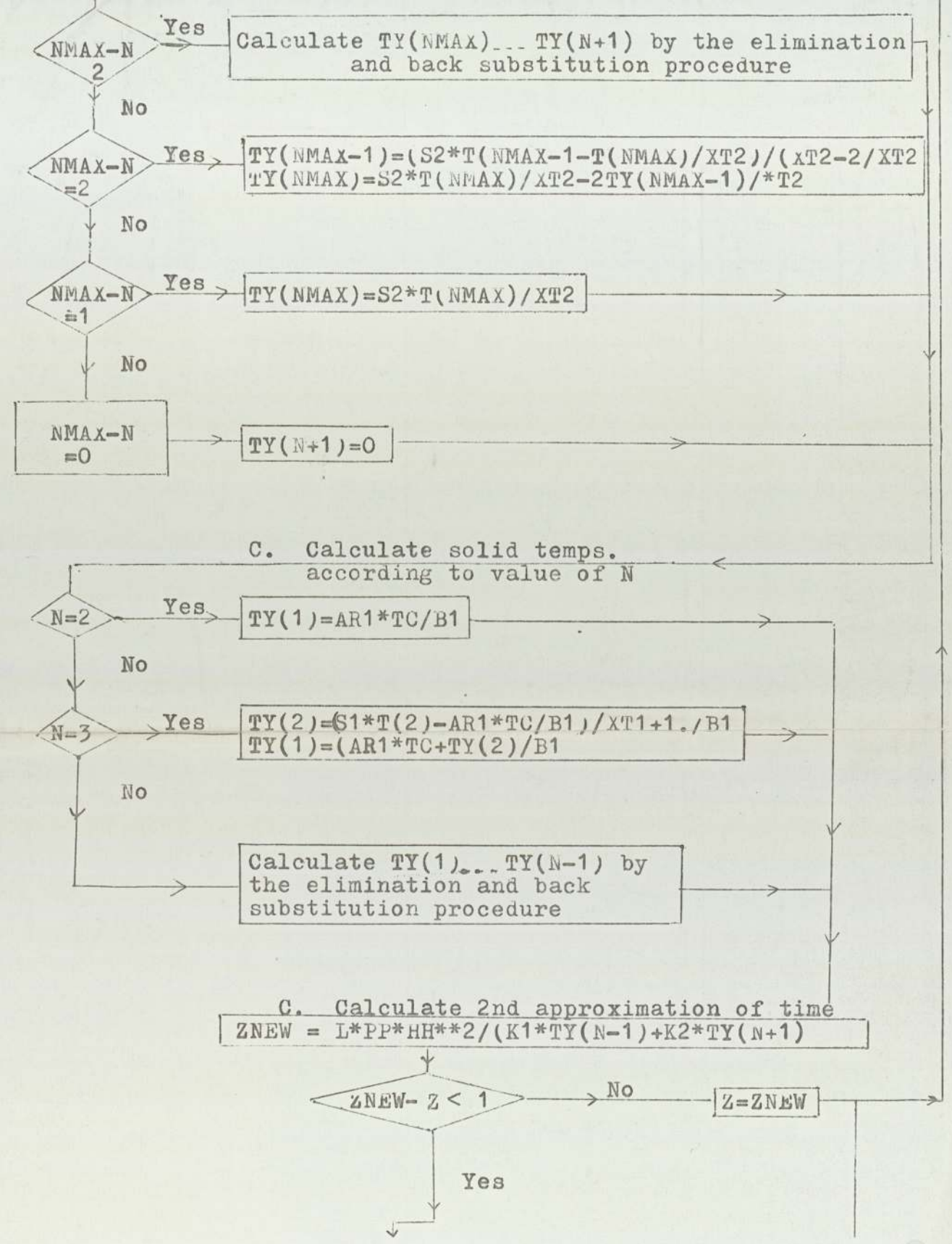
NMAX-N 2
Yes
Calculate TY(NMAX)... TY(N+1) by the elimination and back substitution procedure
No
NMAX-N =2
Yes
TY(NMAX-1)=(S2*T(NMAX-1-T(NMAX)/XT2)/(xT2-2/XT2
TY(NMAX)=S2*T(NMAX)/XT2-2TY(NMAX-1)/*T2
No
NMAX-N =1
Yes
TY(NMAX)=S2*T(NMAX)/XT2
No
NMAX-N =0
TY(N+1)=0
C. Calculate solid temps. according to value of N
N=2
Yes
TY(1)=AR1*TC/B1
No
N=3
Yes
TY(2)=(S1*T(2)-AR1*TC/B1)/XT1+1./B1
TY(1)=(AR1*TC+TY(2)/B1
No
Calculate TY(1)... TY(N-1) by the elimination and back substitution procedure
C. Calculate 2nd approximation of time
ZNEW = L*PP*HH**2/(K1*TY(N-1)+K2*TY(N+1)
ZNEW- Z < 1
No
Z=ZNEW
Yes

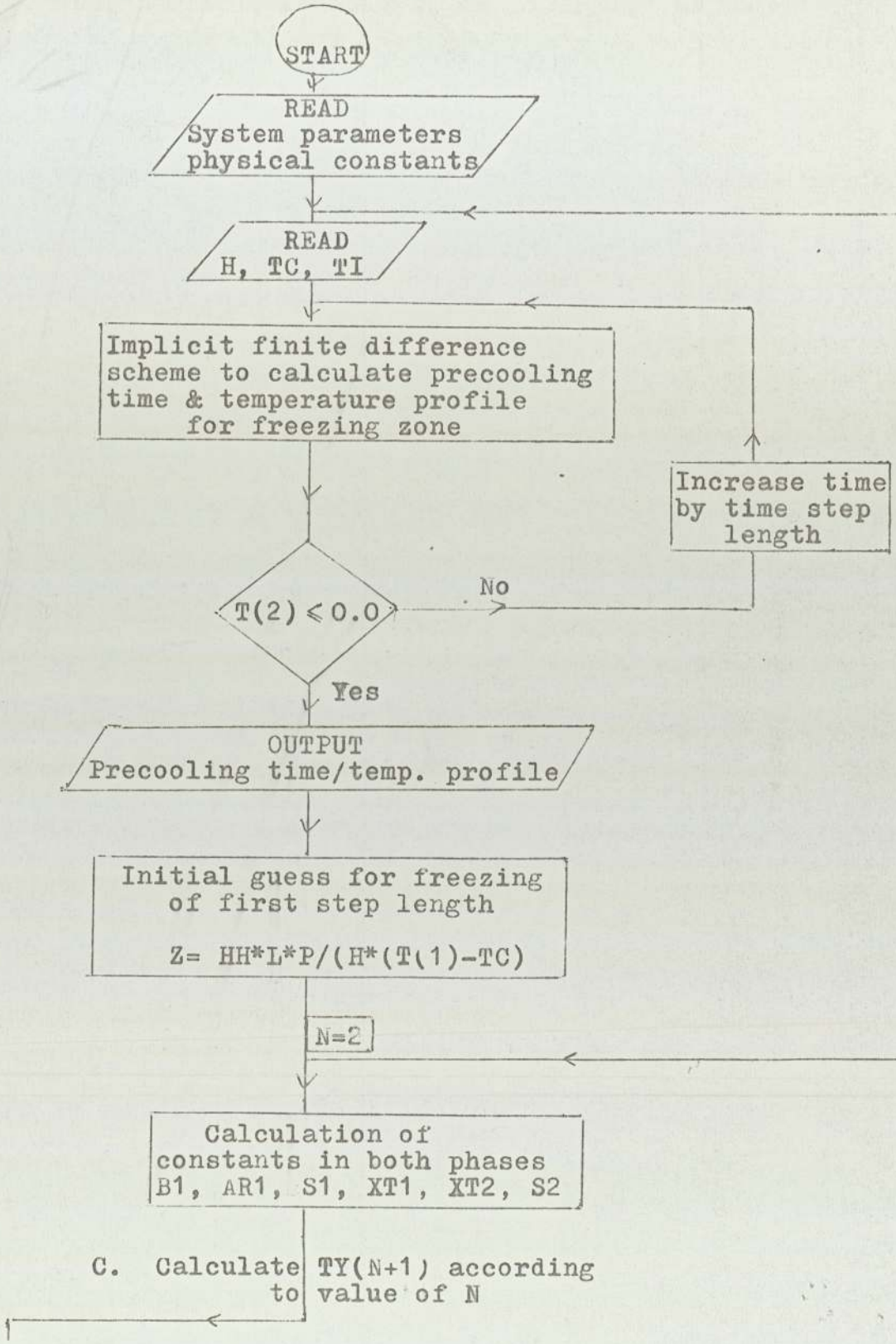
START
READ
System parameters
physical constants
READ
H, TC, TI
Implicit finite difference
scheme to calculate precooling
time & temperature profile
for freezing zone
Increase time
by time step
length
T(2) ⩽ 0.0
No
Yes
OUTPUT
Precooling time/temp. profile
Initial guess for freezing
of first step length
Z= HH*L*P/(H*(T(1)-TC)
N=2
Calculation of
constants in both phases
B1, AR1, S1, XT1, XT2, S2
C. Calculate TY(N+1) according
to value of N

```
PRØGRAM NAME        76//6    ØPT=1 TRACE                    FTN 4.6+433
1
      PRØGRAM NAME(INPUT,ØUTPUT,TAPE1=INPUT,TAPE2=ØUTPUT)
C
C     PRØGRAM FØR SØLUTIØN ØF FREEZING PRØBLEMS USING
C     VASIL'EV AND USPENSKII FINITE DIFFERENCE METHØD
C
C
C     DEFINITIØN ØF VARIABLES
C
C     YKK = TIME STEP LENGTH
C     HH  = DISTANCE STEP LENGTH
C     K   = THERMAL CØNDUCTIVITY
C     TK  = THERMAL DIFFUSIVITY
C     P   = DENSITY
C     C   = SPECIFIC HEAT
C     L   = LATENT HEAT
C     TI  = INITIAL BØDY TEMPERATURE
C     TC  = CØØLANT TEMPERATURE
C     H   = HEAT TRANSFER CØEFFICIENT
C
C     SUBSCRIPT 1 REFERS TØ FRØZEN PHASE
C     SUBSCRIPT 2 REFERS TØ UNFRØZEN PHASE
C
C     ********************
C
      INTEGER W
      REAL INCØØL,L,K1,K2,NN,INPUT(50,50),ICE(50,50)
      REAL LIQUID(50,50)
      DIMENSIØN SØL(50,50),SØLID(50,50),WATER(50,50)
      DIMENSIØN UNFRØZ(50,50),RR(50),R(50),T(50)
      DIMENSIØN SS(50),RY(50),TY(50)
      CØMMØN TY,NMAX,N,WATER
      CØMMØN JJJJ
      READ(1,1000) K1,P,C1,YKK,HH
 1000 FØRMAT(5F10.0)
       READ (1,1020) K2,L,C2
 1020 FØRMAT(3F10.0)
      READ(1,4111) NMAX
 4111 FØRMAT(110)
C
      TK2=K2/(P*C2)
      TK1=K1/(P*C1)
      IX1=5
      DØ 2610 IZIP =1,IX1
C
C
      TS=-5.
C
C
C
      READ(1,1010) H,TC,TI
 1010 FØRMAT(3F10.0)
C
      WRITE(2,9001)
 9001 FØRMAT(1H1/// 20X,'FREEZING RATES USING VASIL EV AND',
     11X,'USPENSKII FINITE',/35X,'DIFFERENCE METHØD'//)
C
      WRITE(2,2500)
```

```
PROGRAM NAME        /0/70   OPT=1 TRACE                    FTN 4.0+433
2

 2500 FORMAT (/ 20X,'FREEZING DISTILLED WATER'/)
      TZ = TI
      PZ = TC
C
      WRITE(2,9003) TZ,TS,PZ,H
 9003 FORMAT(// 20X,'INITIAL TEMPERATURE =',F6.1,2X,'(C)' //
     220X,'STORAGE TEMPERATURE =',F6.1,2X,'(C)'//
     320X,'COOLANT TEMPERATURE =',F6.1,2X,'(C)'///
     420X,'HEAT TRANSFER COEFFICIENT =',F7.1,2X,'(W/M**2*C)')
C
      HZ=.1
      NPZ=1
C
C
C
C     INITIAL SECTION TO PREDICT PRECOOLING ZONE TIME AND TO
C     PROVIDE A TEMPERATURE PROFILE FOR START OF FREEZING
C     AT START OF FREEZING - USING EXPLICIT FINITE DIFFERENCE SCHE
C
      JJJJ = 0
      ZZ = 0.
      REALT = 0.
C
      WRITE(2,3005)
 3005 FORMAT(///// 35X,'INITIAL COOLING PERIOD'///)
      WRITE(2,5010)
 5010 FORMAT(20X,'TEMPERATURE PROFILE',10X  , 'TIME' //
     111X,'T(1)',3X ,'T(16)' ,3X,'T(31)',3X,'T(NMAX)'
     2         // 11X,'0CM',4X, '1.5CM', 3X,'3CM',5X,'MAX(M',
     34X,'TOTAL', 6X ,'PRECOOLING'/
     443X,'TIME',7X,'TIME' //)
C
C
C
      DO 150 I=1,NMAX
      R(I)=TI
  150 CONTINUE
C
      AA=HK2
      BB= YKK /HH**2
      B =AA*BB
      YXN =2.*HH*H/K2
   50 T(1) =2.*B*R(2)+      (1.-2.*B-B*YXN)*R(1)+ YXN*B*TC
      JZZ=NMAX-1
      DO 800 I=2,JZZ
      T(I)= B*R(I+1)+(1.-2.*B)*R(I)+B*R(I-1)
  800 CONTINUE
      T(NMAX) =2.*B*R(NMAX-1) +(1.-2.*B)*R(NMAX)
      REALT = REALT + YKK
      RZR = REALT
      IF(T(2).LT.0.01) GO TO 80
      IF(NPZ.EQ.100) GO TO 79
      GO TO 78
   79 WRITE(2,2000) T(1),T(16),T(31),T(NMAX),REALT,RZR
 2000 FORMAT( 8X,F6.1,3(2X,F6.1),2X,F7.1,5X,F5.1)
C
      NPZ = 1
```

```
PRØGRAM NAME      76/76   ØPT=1 TRACE                    FTN 4.6+433
3
C
   78 NPZ = NPZ + 1
      DØ 7 I=1,NMAX
      R(I)=T(I)
    7 CØNTINUE
      GØ TØ 50
C
   80 WRITE(2,2000) T(1),T(16),T(31),T(NMAX),REALT,RZR
C
C
C
C     SECTIØN FØR DETERMINING ACTUAL FREEZING TIME
C
      WRITE(2,3006)
 3006 FØRMAT(/////35X,'FREEZING PERIØD'///)
      WRITE(2,3009)
 3009 FØRMAT(15X,' TEMPERATURE PRØFILE',13X,'TIME      ',7X,
     1' ICE'/ 12X,'T(1)',3X,'T(16',3X,'T(31)',2X,'T(NMAX)'
     25X,'TØTAL',2X,'FREEZING',7X,'LAYER'/)
      WRITE(2,3999)
 3999 FØRMAT(8X,F4.1,3X,F4.1,3X,F4.1,3X,F4.1,10X,'(SECS)',
     1 4X,'(CMS)' //)
C
C
C     INITIAL GUESS FØR TIME
C
C
      PAA = 0.
      Z = HH*L*P/(H*(T(1)-TC))
C
C     EVALUATIØN ØF CØNSTANTS IN BØTH PHASES
C
C
      N= 2
  400 B1 = 1.+H*HH/K1
      AR1= H*HH/K1
      S1 = -HH**2/(TK1*Z)
      XT1= -(2.+HH**2/(TK1*Z))
      XT2= -(2.+HH**2/(TK2*Z))
      S2 = -HH**2/(TK2*Z)
C
      DØ 351 I= 1,NMAX
      KKK = NMAX+1
      DØ 352 J =1,KKK
      LIQUID(I,J) =0.
      UNFRØZ(I,J) =0.
      WATER(I,J) =0.
      SØLID(I,J) =0.
      ICE(I,J) =0.
      SØL(I,J)=0.
  352 CØNTINUE
  351 CØNTINUE
      IF(NMAX-N.GT.2) GØ TØ 207
      IF(NMAX-N.EQ.2) GØ TØ 609
      IF(NMAX-N.EQ.0) GØ TØ 1100
C
      TY(NMAX) = S2*T(NMAX)/XT2
```

```
PRØGRAM NAME        7o/76    øPT=1 TRACE                    FTN 4.6+433
4
      GØ TØ 201
 1100 TY(N+1) =0.
      GØ TØ 203
  609 TY(NMAX-1)=(S2* (T(NMAX-1)-T(NMAX)/XT2))/(XT2-2./XT2)
      TY(NMAX) = S2*T(NMAX) /XT2-2.*TY(NMAX-1)/XT2
      GØ TØ 201
C
C
C     CALCULATE TEMPERATURES IN LIQUID PHASE
C
C
  207 CØNTINUE
      LIQUID(1,2)=2.
      LIQUID(1,1)= XT2
      LLL = NMAX-N
      DØ 70 M =2,LLL
      LIQUID(M,M)=XT2
      LIQUID(M,M-1)=1.
   70 CØNTINUE
C
C
      NNN = NMAX-N-1
      DØ 71 M =2,NNN
      LIQUID(M,M+1)=1.
   71 CØNTINUE
C
      DØ 72 I = 1,LLL
      SS(I) = T(NMAX+1-I)*S2
      LIQUID(1,NMAX-N+1) =SS(I)
   72 CØNTINUE
C
      JJJ =NMAX-N+1
      DØ 73 LL =1,JJJ
      WATER(1,LL) = LIQUID(1,LL)
   73 CØNTINUE
C
      DØ 74 K=1,NNN
      DØ 75 LL=1,JJJ
      UNFRØZ(K,LL) = WATER(K,LL)*LIQUID(K+1,K)/WATER(K,K)
      WATER(K+1,LL)= LIQUID(K+1,LL) - UNFRØZ(K,LL)
   75 CØNTINUE
   74 CØNTINUE
C
C
      TY(N+1) = WATER(NMAX-N,NMAX-N+1)/WATER(NMAX-N,NMAX-N)
C
C
C     CALCULATE TEMPERATURES IN FRØZEN PHASE
C
C
  201 CØNTINUE
      IF(N.EQ.2) GØ TØ 2016
      IF(N.EQ.3) GØ TØ 202
      GØ TØ 203
 2016 TY(1)= AR1*TC/B1
      GØ TØ 204
C
```

```
PROGRAM NAME        76/76   OPT=1 TRACE                    FTN 4.6+433
5
      202 TY(2) =(S1*T(2)- AK1*TC/B1)/(XT1+1./B1)
          TY(1) =(AK1*TC + TY(2))/B1
          GO TO 204
C
      203 NYP =N-1
          DO 60 I=2,NYP
          WY(I) = S1*T(I)
       60 CONTINUE
          WY(1)=AK1*TC
C
          DO 61 I=1,NYP
          SOLID(I,N) = WY(I)
       61 CONTINUE
C
          SOLID(1,1) = B1
          SOLID(1,2) = -1.
          NXX=N-1
          DO 62 M =2,NXX
          SOLID(M,M)= XT1
          SOLID(M,M-1)=1.
       62 CONTINUE
          JKL =N-2
          DO 63 M=2,JKL
          SOLID(M,M+1)=1.
       63 CONTINUE
C
          LKK = N+1
          DO 64 J=1,N
          ICE(1,J) =SOLID(1,J)
       64 CONTINUE
C
          DO 65 K=1,JKL
          DO 66 J=1,N
          SOL(K,J) = ICE(K,J)*SOLID(K+1,K)/ICE(K,K)
          ICE(K+1,J) =SOLID(K+1,J) - SOL(K,J)
       66 CONTINUE
       65 CONTINUE
C
          TY(N-1) =ICE(N-1,N)/ICE(N-1,N-1)
          DO 8 I = 2,NYP
          APH =ICE(N-I,N-I)
          TY(N-I)=(ICE(N-I,N)-TY(N-I+1)*ICE(N-I,N-I+1))/ APH
        8 CONTINUE
C
      204 CONTINUE
C
C         DETERMINATION OF ACCURACY OF TIME FOR FREEZING
C
          ZNEW = -L*P *HH**2 /(K1*TY(N-1) + K2*TY(N+1))
C
C
          IF(ABS(Z-ZNEW),LT,1.) GO TO 298
          Z =ZNEW
          GO TO 400
      298 CONTINUE
          IF((NMAX-N),LE,2) GO TO 5171
          CALL JAWS
```

```
PRØGRAM NAME        76/76    ØPT=1 TRACE                    FTN 4.6+433
0
 5171 CØNTINUE
      REALT = REALT+Z
      ZZ =ZZ+Z
      TY(N) =0.
      DØ 600 I=1,NMAX
      T(I) = TY(I)
  600 CØNTINUE
C
      WRITE (2,2002)T(1),T(15),T(21),T(NMAX),REALT,ZZ,HZ
 2002 FØRMAT(10X,F6.1,3(2X,F6.1),          3(3X,F7.1))
      HZ=HZ+.1
      N=N+1
C
      IF(N.GT.NMAX) GØ TØ 401
      GØ TØ 400
  603 KGB = 0
  401 CØNTINUE
      PAA =0.
      WRITE(2,6001)
 6001 FØRMAT(////35X,'TEMPERING PERIØD'///)
      WRITE(2,6110)
 6110 FØRMAT(20X,'TEMPERATURE PRØFILE',10X ,'TIME'  //
     111X,'T(1)',3X,'T(16)', 3X,'T(31)',3X ,'T(NMAX)', 9X
     2          // 11X,'0CM',4X,'1.5CM',3X ,'3CM',4X ,'MAXCM'
     3,/X,'INITAL', 6X ,'TEMPERING'/
     445X,'TIME',/X, 'TIME' //)
      CZ=BB*TK1
      CXN=2.*HM*H/K1
 7003 DØ 804 I=1,NMAX
      R(I)=T(I)
  804 CØNTINUE
 7004 T(1) = 2.*CZ*R(2) +(1.-2.*CZ-CZ*CXN)*R(1) +CXN *CZ*TC
      DØ 802 I=2,JZZ
      T(I)= CZ*R(I+1)+ (1.-2.*CZ) * R(I) +CZ*R(I-1)
  802 CØNTINUE
      T(NMAX ) = 2.*CZ*R(NMAX-1) +(1.-2.*CZ)*R(NMAX)
C
      KGB=KGB+1
      PAA=PAA+YKK
      REALT=REALT+YKK
C
      IF(KGB.EQ.100) GØ TØ          409
      DØ 7005 I=1,NMAX
 7005 R(I)=T(I)
      GØ TØ 7004
  409 WRITE(2,2009)T(1),T(16),T(31),T(NMAX),REALT, PAA
 2009 FØRMAT( 8X,F6.1,3(2X,F6.1),7X,F7.1,5X,F5.1)
      KGB= 0
      IF(T(NMAX).LE.TS) GØ TØ 403
      GØ TØ 7003
  403 CØNTINUE
C
 2610 CØNTINUE
      END
```

SUBROUTINE JAKS 76/76 OPT=1 TRACE FTN 4.6+433

```
      C
            SUBROUTINE JAKS
            DIMENSION TY(50),WATER(50,50)
            COMMON TY,NMAX,N,WATER
            COMMON JJJJ
      C
            JJJJ = JJJJ+1
            NNNN = NMAX-JJJJ+1
            LLL  = NMAX-N
      C
            DO 6  I=2,LLL
            TIT = WATER(NNNN-I+1,NMAX-N+1)
            TTT = -TY(N+I-1)* WATER(NNNN-I+1,NNNN-I)
            TY(N+I)=(TIT +TTT)/ WATER(NNNN-I+1,NNNN -I+1)
          6 CONTINUE
      C
            RETURN
            END
```

FREEZING RATES USING VASIL EV AND USPENSKII FINITE DIFFERENCE METHOD

FREEZING DISTILLED WATER

INITIAL TEMPERATURE = 20.0 (C)

STORAGE TEMPERATURE = -5.0 (C)

COOLANT TEMPERATURE = -10.0 (C)

HEAT TRANSFER COEFFICIENT = 900.0 (W/M**2*C)

INITIAL COOLING PERIOD

TEMPERATURE PROFILE				TIME	
T(1)	T(10)	T(31)	T(NMAX)		
0CM	1.5CM	3CM	MAXCM	TOTAL TIME	PRECOOLING TIME
-2.4	20.0	20.0	20.0	10.0	10.0
-4.3	20.0	20.0	20.0	19.9	19.9
-5.2	20.0	20.0	20.0	29.8	29.8
-5.8	20.0	20.0	20.0	39.7	39.7
-6.2	20.0	20.0	20.0	49.6	49.6
-6.3	20.0	20.0	20.0	52.6	52.6

FREEZING PERIOD

TEMPERATURE PROFILE				TIME		ICE
T(1)	T(10)	T(31)	T(NMAX)	TOTAL	FREEZING	LAYER
-2.9	19.6	19.9	20.0	124.6	72.0	.1
-4.5	18.5	19.7	20.0	222.4	169.8	.2
-5.5	16.9	19.1	20.0	344.0	291.4	.3
-6.2	14.9	18.2	20.0	488.8	436.2	.4
-6.7	12.9	16.9	20.0	656.6	604.0	.5
-7.1	10.9	15.5	19.9	847.3	794.7	.6
-7.4	9.0	14.0	19.7	1061.0	1008.4	.7
-7.6	7.3	12.5	19.4	1297.4	1244.8	.8

-8.0	4.3	9.0	18.4	1838.8	1788.2	1.0
-8.2	3.1	8.3	17.7	2143.4	2090.8	1.1
-8.3	1.9	7.0	16.8	2470.0	2417.4	1.2
-8.4	.9	5.8	15.8	2818.0	2765.4	1.3
-8.5	0.0	4.7	14.7	3186.3	3133.7	1.4
-8.6	-.6	3.7	13.5	3573.6	3521.0	1.5
-8.7	-1.1	2.8	12.3	3978.0	3925.4	1.6
-8.7	-1.5	1.9	11.0	4397.7	4345.1	1.7
-8.8	-1.9	1.2	9.8	4830.7	4778.1	1.8
-8.8	-2.3	.5	8.6	5275.0	5222.4	1.9
-8.9	-2.6	0.0	7.5	5729.9	5677.3	2.0
-8.9	-3.0	-.4	6.4	6192.5	6139.9	2.1
-9.0	-3.2	-.8	5.4	6661.9	6609.3	2.2
-9.0	-3.5	-1.2	4.4	7137.1	7084.5	2.3
-9.1	-3.7	-1.5	3.6	7617.7	7565.1	2.4
-9.1	-4.0	-1.8	2.9	8103.4	8050.8	2.5
-9.1	-4.2	-2.1	2.3	8594.5	8541.9	2.6
-9.2	-4.4	-2.3	1.7	9091.2	9038.6	2.7
-9.2	-4.6	-2.6	1.3	9594.1	9541.5	2.8
-9.2	-4.7	-2.8	.9	10103.9	10051.3	2.9
-9.2	-4.9	-3.0	.6	10621.7	10569.1	3.0
-9.3	-5.0	-3.2	.4	11148.5	11095.9	3.1
-9.3	-5.2	-3.4	.3	11685.3	11632.7	3.2
-9.3	-5.3	-3.6	.2	12233.3	12180.7	3.3
-9.3	-5.4	-3.8	.1	12793.5	12740.9	3.4
-9.3	-5.6	-4.0	.0	13366.8	13314.2	3.5
-9.4	-5.7	-4.1	.0	13953.9	13901.3	3.6
-9.4	-5.8	-4.3	.0	14555.5	14502.9	3.7
-9.4	-5.9	-4.4	.0	15171.9	15119.3	3.8
-9.4	-6.0	-4.5	.0	15803.3	15750.7	3.9
-9.4	-6.1	-4.7	.0	16449.9	16397.3	4.0
-9.4	-6.2	-4.8	.0	17111.7	17059.1	4.1
-9.4	-6.3	-4.9	.0	17788.7	17736.1	4.2
-9.5	-6.3	-5.0	.0	18480.9	18428.3	4.3
-9.5	-6.4	-5.1	.0	19188.3	19135.7	4.4
-9.5	-6.5	-5.2	.0	19910.9	19858.3	4.5
-9.5	-6.6	-5.3	.0	20648.8	20596.2	4.6
-9.5	-6.6	-5.4	.0	21401.9	21349.3	4.7
-9.5	-6.7	-5.5	0.0	22170.2	22117.6	4.8

TEMPERING PERIOD

TEMPERATURE PROFILE				TIME	
T(1)	T(16)	T(31)	T(NMAX)		
0CM	1.5CM	3CM	MAXCM	TOTAL TIME	TEMPERING TIME
-9.5	-6.5	-3.5	-.7	22180.2	10.0
-9.5	-6.5	-3.5	-1.0	22190.2	20.0
-9.5	-6.5	-3.5	-1.2	22200.2	30.0
-9.5	-6.5	-3.6	-1.4	22210.2	40.0
-9.5	-6.5	-3.6	-1.6	22220.2	50.0
-9.5	-6.5	-3.6	-1.8	22230.2	60.0
-9.5	-6.5	-3.7	-1.9	22240.2	70.0
-9.5	-6.5	-3.7	-2.0	22250.2	80.0
-9.5	-6.5	-3.8	-2.2	22260.2	90.0
-9.5	-6.5	-3.8	-2.3	22270.2	100.0

-9,5	-6,6	-3,9	-2,5	22290,2	120,0
-9,5	-6,6	-4,0	-2,6	22300,2	130,0
-9,5	-6,6	-4,1	-2,7	22310,2	140,0
-9,5	-6,6	-4,1	-2,8	22320,2	150,0
-9,5	-6,6	-4,2	-2,9	22330,2	160,0
-9,5	-6,6	-4,2	-3,0	22340,2	170,0
-9,5	-6,7	-4,3	-3,1	22350,2	180,0
-9,5	-6,7	-4,3	-3,1	22360,2	190,0
-9,5	-6,7	-4,4	-3,2	22370,2	200,0
-9,5	-6,7	-4,5	-3,3	22380,2	210,0
-9,5	-6,8	-4,5	-3,4	22390,2	220,0
-9,5	-6,8	-4,6	-3,5	22400,2	230,0
-9,5	-6,8	-4,6	-3,5	22410,2	240,0
-9,5	-6,8	-4,7	-3,6	22420,2	250,0
-9,5	-6,9	-4,7	-3,7	22430,2	260,0
-9,5	-6,9	-4,8	-3,8	22440,2	270,0
-9,5	-6,9	-4,8	-3,8	22450,2	280,0
-9,6	-6,9	-4,9	-3,9	22460,2	290,0
-9,6	-7,0	-4,9	-4,0	22470,2	300,0
-9,6	-7,0	-5,0	-4,0	22480,2	310,0
-9,6	-7,0	-5,0	-4,1	22490,2	320,0
-9,6	-7,0	-5,1	-4,2	22500,2	330,0
-9,6	-7,1	-5,1	-4,2	22510,2	340,0
-9,6	-7,1	-5,2	-4,3	22520,2	350,0
-9,6	-7,1	-5,2	-4,3	22530,2	360,0
-9,6	-7,1	-5,3	-4,4	22540,2	370,0
-9,6	-7,2	-5,3	-4,5	22550,2	380,0
-9,6	-7,2	-5,4	-4,5	22560,2	390,0
-9,6	-7,2	-5,4	-4,6	22570,2	400,0
-9,6	-7,3	-5,5	-4,6	22580,2	410,0
-9,6	-7,3	-5,5	-4,7	22590,2	420,0
-9,6	-7,3	-5,6	-4,7	22600,2	430,0
-9,6	-7,3	-5,6	-4,8	22610,2	440,0
-9,6	-7,4	-5,7	-4,9	22620,2	450,0
-9,6	-7,4	-5,7	-4,9	22630,2	460,0
-9,6	-7,4	-5,7	-5,0	22640,2	470,0
-9,6	-7,4	-5,8	-5,0	22650,2	480,0

APPENDIX 5.

THERMAL PROPERTIES.

This chapter shows the temperature variation of the important physical properties of water and ice. The unfrozen thermal properties can be seen to remain largely constant over the temperature range 0 C to 30 C while the frozen thermal properties vary only slightly (maximum of 9%) between 0 C to -30 C. It seems that variation in thermal properties is more important in systems involving large temperature differences and in non aqueous solutions where there is greater physical property variation with temperature.

A5-1 Physical Properties of Solutions Used for Freezing Experiments.

(1) Freezing temperatures (Tc, (C)) (125)

5% NaCl	10% NaCl	Grapefruit Juice
-3.01	-6.56	-1.0

(2) Thermal properties (90, 124, 125).

Latent heat, $L = .330292 \times 10^6$ (J/kg)

Thermal conductivity ice, K_1 = 2.215 (W/mC)

Thermal conductivity, water, K_2	= 0.5112	(W/mC)
Specific heat, ice, C_1	= 2093.4	(J/kgC)
Specific heat, water, C_2	= 4186.8	(J/kgC)

These properties were used for distilled water, 5% and 10% NaCl and grapefruit juice.

(3) Densities (ρ (kg/m^3))

	Distilled Water	5% NaCl	10% NaCl	Grapefruit Juice
ρ_1 (Perry, 125)	997	1036	1073	-
ρ_1 (expt)	997	1037	1073	1035
ρ_2 (expt)	906	977	1037	975

A5-2 Variation of Thermal Properties with Temperature.

(1) Density (ρ (kg/m^3))

Published data (125) shows only a negligable percentage decrease in water density between 0 C and 30 C.

A maximum increase in ice density of 4% between -30 C and 0 C was reported (128).

(2) Specific heat (C (J/kgC))

Water specific heat is quite constant between 0 C and 100 C (90, 125, 124).

Ice specific heat decreases steadily with temperature, a 10% variation between -30 C and 0 C (128).

(3) Thermal conductivity (K (W/mC))

Water thermal conductivity remains quite constant over the temperature range 0 C to 50 C.

Ice thermal conductivity decreases with temperature. Thermal conductivity values of ice must however be accepted with some caution since agreement between reported values is rather poor. The largest variation (Jacob and Erk) gives a variation of 9% between 0 C and -30 C (129).

(4) The most important point to note with the thermal properties is their change in value on phase change.

	Phase 1 (frozen)	Phase 2 (Unfrozen)	Ratio phase 1/phase 2
K(W/mC)	2.215	.5112	3-4
C(J/kgC)	2093.4	4186.8	0.5
$\alpha(m^2/s)$	$.111 \times 10^{-5}$	$.12 \times 10^{-6}$	9-10

A5-3 PHYSICAL PROPERTIES OF FOODSTUFFS.

(1) Freezing temperature.

Freezing points of foods decrease with increase in soluble solid content. Table A5-1 give freezing points of selected foods.

(2) Thermal trends of properties.

There is, as with water, a marked difference between unfrozen and frozen values of specific heat, thermal conductivity and thermal diffusivity. Table A5-2 gives specific heats of selected foods.

Table A5-1 Freezing Temperatures of Selected Foods.

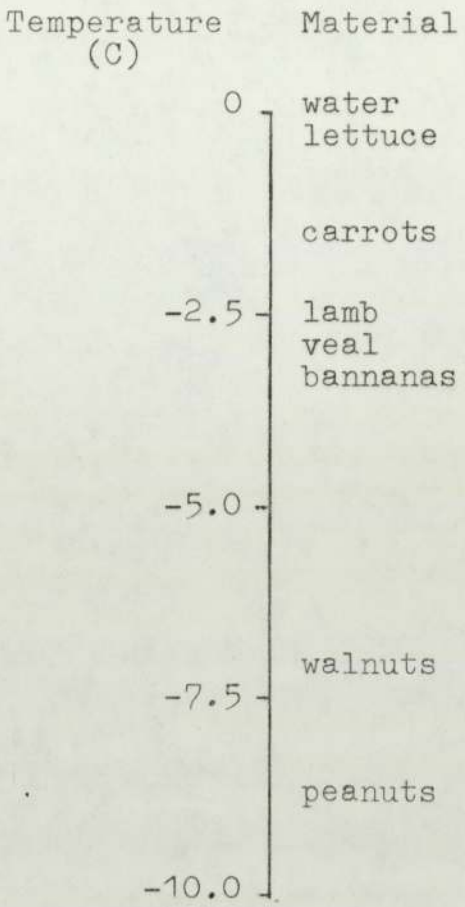

Table A5-2 Specific Heats of Foods (J/kgC)

Food	Specific Heat above freezing C_2	Specific Heat below freezing C_1
Liver	0.72	0.40
Apples	0.71	0.39
Carrots	0.87	0.47
Eggs	0.76	0.40
Milk	0.90	0.46

a) Specific Heat.

Many of the published lists (130) of specific heat values are calculated rather than observed. An equation with the following general form is frequently used for calculating specific heat :

$$\mathcal{Z} = \sum_{1}^{n} S_1 C_1 + S_2 C_2 + S_3 C_3 \ldots\ldots S_n C_n$$

where $\mathcal{Z}$ = the calculated specific heat of the food.

S = the specific heat of a food component.

C = the mass fraction of a food component.

n = the total number of components being considered in the calculation.

The accuracy of this method is obviously heavily dependent on knowing accurately the individual specific heats of all the components.

A second, simpler formula for estimating specific heats is given as : (87)

$$C = 0.005M + 0.2$$

where M = % by wt of water in the foodstuff.

b) Latent Heat.

Latent heats of foodstuffs are usually calculated by Woolrich's and Siebal's equation (87).

$$Lf = LH_2O \cdot M$$

where Lf = latent heat of food

LH_2O = latent heat of water

M = % by wt of water in the foodstuff.

c) Thermal conductivities.

Earle (132) gives two correlations for determining thermal conductivities, one for the frozen phase and one for the unfrozen phase.

In Btu/hr ft F

above 32 F $K = \frac{1.4M}{100} + \frac{.15}{100}(100-M)$

below 32 F $K = \frac{0.32M}{100} + \frac{.15}{100}(100-M)$

Maxwell (1904) and Eucken (1940) (131) have developed a formula for estimating frozen thermal conductivities of heterogeneous materials as:

$$K = kc \left[\frac{1 - (1 - a \frac{kd}{kc}) b}{1 + (a-1) b} \right]$$

where K = thermal conductivity of the heterogeneous material.

kc = thermal conductivity of continuous phase.

kd = thermal conductivity of the dispersed phase, such as ice crystals, fat etc.

$$a = \frac{3kc}{2kc + kd}$$

$$b = \frac{Vd}{Vc + Vd}$$

Vd = volume of the dispersed phase.

Vc = volume of the continuous phase.

Charm (127) gives a method for calculating the thermal conductivity of frozen foods and the heat transfer coefficient associated with freezing systems employing the heat penetration curve. Charm states the calculated values by his method lie within the range of values found in the literature. Further references on thermal properties of foodstuffs are given (133-135).

APPENDIX 6.

MATHEMATICAL STATEMENT OF 1-DIMENSIONAL FREEZING PROBLEM.

(Subscript 1 refers to the frozen phase, subscript 2 to the unfrozen phase).

In general, the physical properties of the solid differ from those of the unfrozen liquid so that the conduction equations for the two phases are not the same. As heat transfer proceeds the unfrozen phase shrinks and is replaced by frozen solid. Calculation of freezing rates thus involves the simultaneous solution of two conduction equations with a moving boundary.

The conduction equations in 1 direction are :

Phase 1
$$\frac{\partial T_1}{\partial t} = \alpha_1 \frac{\partial^2 T_1}{\partial x^2} \qquad (1\text{-}1)$$

Phase 2
$$\frac{\partial T_2}{\partial t} = \alpha_2 \frac{\partial^2 T_2}{\partial x^2} \qquad (1\text{-}2)$$

The rate of advance of the frozen-unfrozen interface is found as follows : Let the interface be at X(t). When the interface advances a distance dx the quantity of latent heat absorbed per unit interfacial area is $-Lx\rho dx$ (The use of this equation assumes that the density of the frozen and of the unfrozen phases are the same, and for this reason ρ has no suffix. If there is a significant change in density on freezing, the freezing interface may move as a result of the expansion or contraction and may even be broken up. When this effect becomes significant analysis becomes impossible). If the time for this advance is dt, then the rate of heat supply to the interface becomes $-L\rho\frac{dx}{dt}$. This rate for heat supply equals the net flow per unit area to the interface by conduction :

$$\text{i.e.} \quad -L\rho\frac{dx}{dt} = -K_1\left(\frac{\partial T_1}{\partial x}\right)_X + K_2\left(\frac{\partial T_2}{\partial x}\right)_X \qquad (1\text{-}3)$$

Equation 1-3 is a boundary condition at x=X(t). A second boundary condition at X(t) is that the temperature of the two phases is the same :

$$\text{i.e.} \quad T_1 = T_2 = Tm \quad \text{at} \quad x = X(t) \qquad (1\text{-}4)$$

The remaining boundary conditions necessary for the solution of equations (1-1) and (1-2) are :

(a) The value of the surface temperature Ts. This temperature may be known and fixed -as for example in plate freezing -or, more generally, may be expressed in terms of the surface heat transfer coefficient, H, by equating the heat fluxes on either side of the solid boundary to give :

$$H(Tc - Ts) = -K_1\left(\frac{\partial T_1}{\partial x}\right)_{x=0} \qquad (1\text{-}5)$$

where Tc is the temperature of the coolant, when H is large we may simplify (1-5) to :

$$Ts = Tc \qquad (1\text{-}5a)$$

b) At the axis of symmetry we have no heat flow, i.e.

$$\frac{\partial T_2}{\partial x} = 0 \text{ at } x=a \qquad (1\text{-}6)$$

A second boundary condition at the axis of symmetry takes into account heat gain from the surroundings. By equating the heat fluxes on either side of the boundary we derive :

$$-K \left(\frac{\partial Ta}{\partial x} \right)_{x = a} = HG \quad (Ta - TA) \qquad (1\text{-}6b)$$

where Ta is the temperature at the axis of symmetry.

c) The initial conditions are :

$$X \ (t) = 0 \quad \text{at} \quad t = 0 \qquad (1\text{-}7)$$

and $$T_2 = f(x) \quad \text{at} \quad t = 0 \qquad (1\text{-}8)$$

Equation (1-7) states that the solid is wholly unfrozen at the start of the freezing operation, and (1-8) defines the temperature distribution in the unfrozen solid.

APPENDIX 7.

FREEZING PRESERVATION OF FOODS.

A7-1. INTRODUCTION

Storage in cold places has been a traditional method of preserving foods since ancient times. It was not however until 1930 when Clarence Birdseye in the U.S.A. developed the fast freezing process, which was subsequently introduced to the U.K. after the second world war, that the process of freezing as a method of food preservation really started to be of commercial importance. The food freezing process is now one of the three main methods, with canning and dehydration, of food preservation. All three preservation methods have the common objective of reducing microbiological spoilage of the foodstuff. Since bacteria generally require water and air (except anaerobes e.g. clostridium botulinum) as basic necessities for life and are temperature sensitive the preservation processes aim to reduce bacterial growth by (a) elimination of water (dehydration), or (b) elimination of air (vacuum packaging of dehydrated foods and canning) or (c) application of, high temperatures (sterilization in canning causes the death of the bacteria e.g. clostridium botulinum) or, low temperatures (freezing prevents multiplication of bacteria) (87, 88).

Freezing to date has largely concentrated on meat, fish, fruit and vegetables, all of which have a high water content (113). Fruits and vegetables tend to suffer less from the attack of micro-organisms than from the continuation of their own life processes after harvesting. These life processes can be slowed down by reduction of temperature (112).

In order for freezing to compete commercially with canning and dehydration as a preservation process the product must have a shelf life of at least 6 months (88). Thus in order to produce an edible product the freezing process not only involves correct freezing procedure but good storage and thawing techniques as well. The three processes are now considered in turn.

A7-2. FREEZING OF FOODSTUFFS.

It is generally agreed that the final quality of the frozen foodstuff is improved by increased freezing rate (88). It is during the freezing stage that structural damage may occur to foodstuffs. See figure A7-1. (The

Figure A7-1 Comparison between slow and quick freezing.

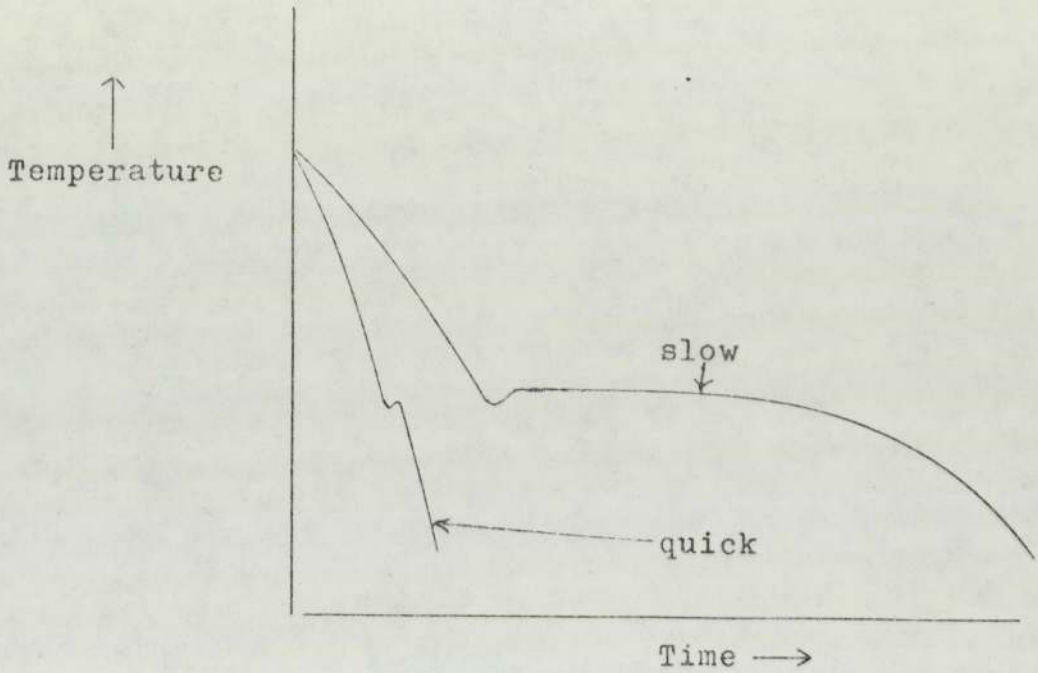

length of the freezing stage is dependent on the rate the frozen interface traverses the body being frozen). The damage is due to the rupturing of cell walls by large ice crystals formed during slow freezing operations (86) causing water loss or 'drip' on thawing, while under fast freezing conditions smaller crystals form either within or between cells and cause little cell rupture.

Experiments by Kalruhe on green beans (88) showed improvements in colour, flavour, texture and vitamin C content with quick freezing (air blast freezer) compared to slow freezing (still air) operations.

Specific problems encountered with predicting the freezing rates of foodstuffs are found due to the following factors :

1. The lack of knowledge of the thermal properties of foodstuffs (6,8).

2. The marked variability in the thermal properties of individual foodstuffs resulting from varietal differences, agricultural practices, seasonal variations and growth locations (112).

3. The existance of unfreezable or 'bound' water produces difficulties in determining the end of the freezing stage and the beginning of the tempering stage. With meat, for example, about 10% of the water content does not appear to freeze even at -40 C, and it is generally assumed to be too tightly bound to protein, while the remaining 90% of the water is readily freezable. (126).

A7-3. STORAGE OF FROZEN FOODS.

For many years -10 C was specified as the 'safe' temperature for storage of frozen foods even though it was recognised that the quality of the product gradually deteriorated at this temperature.

During storage with temperatures fluctuating around -10 C the size of the ice crystals gradually increases and textural damage may occur causing drip on thawing. Apart from the textural changes, the loss of water caused by drip reduces the weight of the final product

and reduces the margin of profit to the processer (112).

With the advent of quick freezing lower storage temperatures were advocated. Generally -18 C is now recommended although with fish, which have a natural low temperature environment, lower storage temperatures may be needed since the bacteria they support may still reproduce at -18 C. (115).

Gortner et al (116) stored pork roasts, strawberries, beans and peas for 12 months at -17.7 C and -12.2 C. Results showed that the quality of the foods stored at -17.7 C was definitely superior to that of the foods stored at -12.2 C and therefore supported the evidence of better quality with storage temperatures of about -18 C.

A7-4. THAWING OF FROZEN FOODSTUFFS.

Industrial thawing processes must be carried out under specified and controlled physical conditions otherwise there is a risk of appreciable bacterial growth, weight loss and deterioration in appearance (114).

Thawing takes place in three stages :

a) Temperature rise to melting point.

b) Melting.

c) Rise in temperature to ambient temperature (88).

There is still considerable argument about the optimum conditions for thawing although the principle, given on commercial frozen food packages, of slow thawing for relatively thick articles (e.g. chickens) and no thawing before cooking for small items (e.g. peas) is fairly well established.

The experimental apparatus used for carrying out freezing experiments could not be adapted for thawing experiments. No comparison between experimental and theoretical thawing rates was therefore possible. However, for the thawing of water the freezing rate formulas, by just inter-changing the position and properties of the frozen and unfrozen phases, can in theory be used for predicting thawing rates.

For the thawing of electrolyte solutions study

of solute migration should be investigated to find out how it affects the thawing temperature and hence thawing rate.

The thermal diffusivity of ice is approximately nine times, and the conductivity four times, that of water. The result of these differences in physical properties between ice and water is that the time-temperature profiles of freezing and thawing systems, under identical system conditions, differ, with thawing overall being a slower process.

The result of the variation in physical properties is shown in figure A7-2. The temperature rise to melting point in the thawing process will be faster than the corresponding precooling phase in freezing systems since heat is being transferred to the coolant via ice instead of water as in freezing systems.

However, the melting stage and rise in temperature to ambient stage in thawing processes take substantially longer than the corresponding freezing and tempering phases since the heat released at the interface must be transferred across a water layer instead of an ice layer as in freezing systems. Further references on food preservation are given (117-123).

Figure A7 - 2

Comparison of Freezing and Thawing Curves

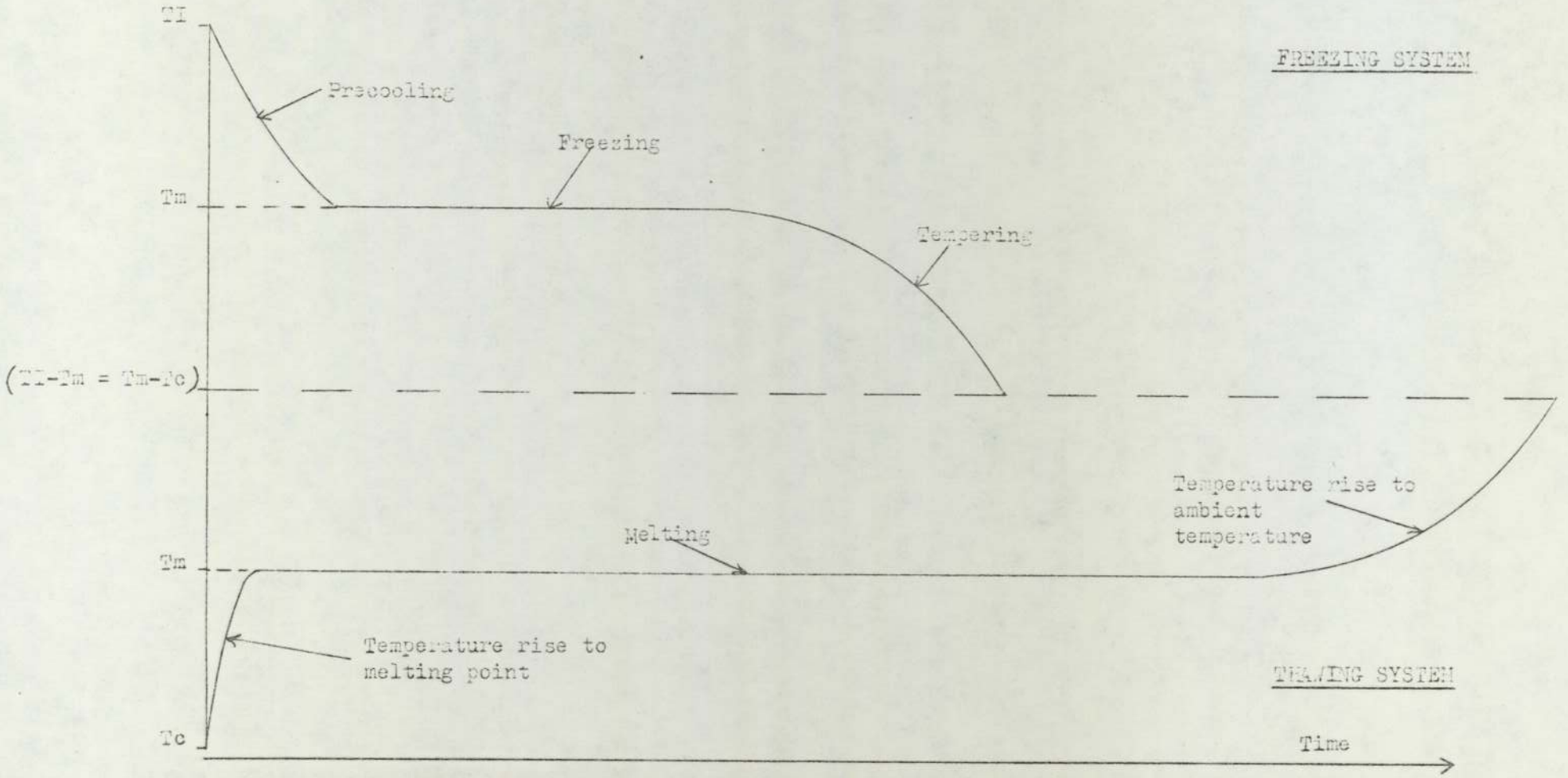

APPENDIX 8.

COMPARISON OF EXPERIMENTAL AND THEORETICAL RESULTS.

Units.

Ice thicknesses : mm

Freezing times: s

Heat transfer coefficient : W/m^2 C

Freezing points of liquids.

Grapefruit juice -1C

5% Sodium chloride -3C

10% Sodium chloride -6.6C

TABLE A8-1.

FREEZING OF DISTILLED WATER.

FREEZING TIMES.

Ice Thickness	Experimental	Theoretical					
		PLANCK	MODIFIED PLANCK	RUTOV	NEUMANN	GOODMAN	VASIL'EV & USPENSKII.
		System conditions Tc = -15 TI = 20 H = 2000					
2	150	42	48	53	12	51	88
6	480	245	284	315	111	330	405
10	1030	607	708	783	307	853	961
14	1750	1128	1317	1457	602	1619	1751
20	-	2208	2583	2856	1229	3227	3299
		System conditions Tc = -10 TI = 20 H = 2000					
2	182	63	72	79	17	75	141
6	680	367	422	467	155	487	639
10	1475	911	1050	1161	431	1256	1507
14	2570	1692	1953	2160	845	2385	2719
20	-	3312	3826	4232	1725	4755	4949

TABLE A8-1 (Continued)

Ice Thickness	Experimental	Theoretical					
		PLANCK	MODIFIED PLANCK	RUTOV	NEUMANN	GOODMAN	VASIL'EV & USPENSKII.
		System conditions Tc = 10 TI = 3.5 H = 2000					
2	120	63	65	66	27	75	89
6	480	367	384	391	241	487	457
10	1115	911	954	972	669	1256	1088
14	2020	1692	1776	1809	1312	2385	1980
20	3750	3312	3480	3545	2678	4755	3787
		System conditions Tc = -10 TI = 25 H = 2000					
2	215	63	74	83	15	75	161
6	850	367	434	492	133	487	705
10	1800	911	1078	1221	370	1256	1655
14	3050	1692	2007	2273	726	2385	2967
20	-	3312	3932	4453	1481	4755	5293

TABLE A8-1 (Continued)

Ice Thickness	Experimental	Theoretical					
		PLANCK	MODIFIED PLANCK	RUTOV	NEUMANN	GOODMAN	VASIL'EV & USPENSKII
		System conditions Tc = -15 TI = 20 H = 900					
2	245	69	78	87	12	79	138
6	730	326	375	415	111	416	538
10	1500	742	859	950	307	997	1174
14	2425	1317	1530	1692	602	1822	2041
20	4150	2477	2886	3192	1229	3518	3683
		System conditions Tc = -10 TI = 20 H = 900					
2	375	103	117	130	17	117	234
6	1180	489	559	618	155	615	851
10	2250	1113	1277	1413	431	1470	1843
14	3500	1975	2272	3177	845	2685	3163
20	-	3716	4282	4736	1725	5184	-

TABLE A8-1 (Continued)

Ice Thickness	Experimental	Theoretical	
		Modified Planck	Vasil'ev & Uspenskii
	System conditions Tc = -13 TI = 19 H = 56.8		
2	4800	1031	3066
6	6300	3252	6269
10	8520	5687	9133
14	12120	8335	11878
20	14760	12706	15322
	System conditions Tc = -10 TI = 23 H = 1700		
2	180	-	164
5	525	-	537
8	1100	-	1130
12	2150	-	2252
16	3525	-	3672
	System conditions Tc = -10 TI = 18 H = 1700		
2	170	-	144
6	660	-	643
10	1480	-	1498
14	2640	-	2685
18	4080	-	4118

TABLE A8-2 FREEZING OF GRAPEFRUIT JUICE

FREEZING TIMES

Ice Thickness	Experimental	Theoretical	
		Modified Planck	Vasil'ev & Uspenskii
	System conditions Tc = -10 TI = 22 H = 900		
2	1020	132	278
6	1700	630	1027
10	3000	1440	2209
14	4350	2561	3746
20	6840	4826	6365
	System conditions Tc = -11 TI = 15 H = 2000		
2	300	114	201
6	900	547	786
10	1740	1249	1711
14	2880	2222	2953
20	-	4188	-
	System conditions Tc = -10 TI = 16 H = 900		
2	540	128	241
6	1146	610	923
10	2088	1393	2001
14	3300	2477	3428
16	3960	-	4233

TABLE A8-3 FREEZING OF FIVE PER CENT SODIUM CHLORIDE.
FREEZING TIMES.

Ice Thickness	Experimental	Theoretical	
		Modified Planck	Vasil'ev & Uspenskii
	System conditions Tc = -13 TI = 3.5 H = 2000		
2	130	66	96
6	528	391	486
10	1100	972	1159
14	1920	1808	2113
20	3505	3543	4016
	System conditions Tc = -13 TI = 17 H = 2000		
2	189	71	141
6	700	422	641
10	1500	1050	1513
14	2640	1953	2729
20	5040	3827	4967
	System conditions Tc = -13 TI = 17 H = 900		
2	350	117	224
6	1150	559	854
10	2400	1277	1850
14	3550	2272	3175
20	6040	4282	5527
	System conditions Tc = -15 TI = 18.5 H = 900		
2	360	99	187
6	930	471	714
10	1785	1077	1550
14	2880	1916	2676
15	3090	-	2995

TABLE A8-4 FREEZING OF TEN PER CENT SODIUM CHLORIDE FREEZING TIMES

Ice Thickness	Experimental	Theoretical	
		Modified Planck	Vasil'ev & Uspenskii
	System conditions Tc = -16 TI = 14 H = 2000		
2	200	76	152
4	430	224	369
6	725	445	687
8	1080	740	1103
10	1500	1107	1618
	System conditions Tc = -14 TI = 19 H = 2000		
2	336	98	234
4	792	291	547
6	1450	578	1007
8	2354	959	1608
10	3060	1434	2341
	System conditions Tc = -15 TI = 21 H = 900		
2	720	143	338
4	1295	371	708
6	2100	683	1208
8	2804	1080	1834
10	3520	1561	2573
	System conditions Tc = -10.6 TI = 16.5 H = 2000		
2	882	176	477
4	2268	522	1083
6	3780	1035	1974
8	5400	1717	3108
10	7110	2568	4411

APPENDIX 9.

DILATOMETER CALIBRATION AND OPERATION OF THE APPARATUS FOR ACCURATE MEASUREMENT OF THE ICE THICKNESS.

A9-1. DILATOMETER CALIBRATION.

The bore of the dilatometer tube was measured to be 4.28 mm. From this measurement a graph of tube volume against length of tube was drawn (Graph A9-1).

Since the volume difference obtained from the phase change depends on the difference in densities of the two phases independent density determinations, using specific gravity bottles, were performed to obtain densities of all freezing solutions in both the frozen and unfrozen state. The results, with values from Perry (125) are given in table A9-1.

The thickness of ice, X, calculated from the dilatometer rise (Δ) and the liquid and solid densities (ρ_2 and ρ_1) by the expression :

$$X = \frac{Rt^2}{Rv^2} . \Delta . \left(\frac{\rho_2}{\rho_2 - \rho_1} \right) \qquad \text{(A9-1)}$$

Graph of Length of Dilatometer Tube against it's Volume

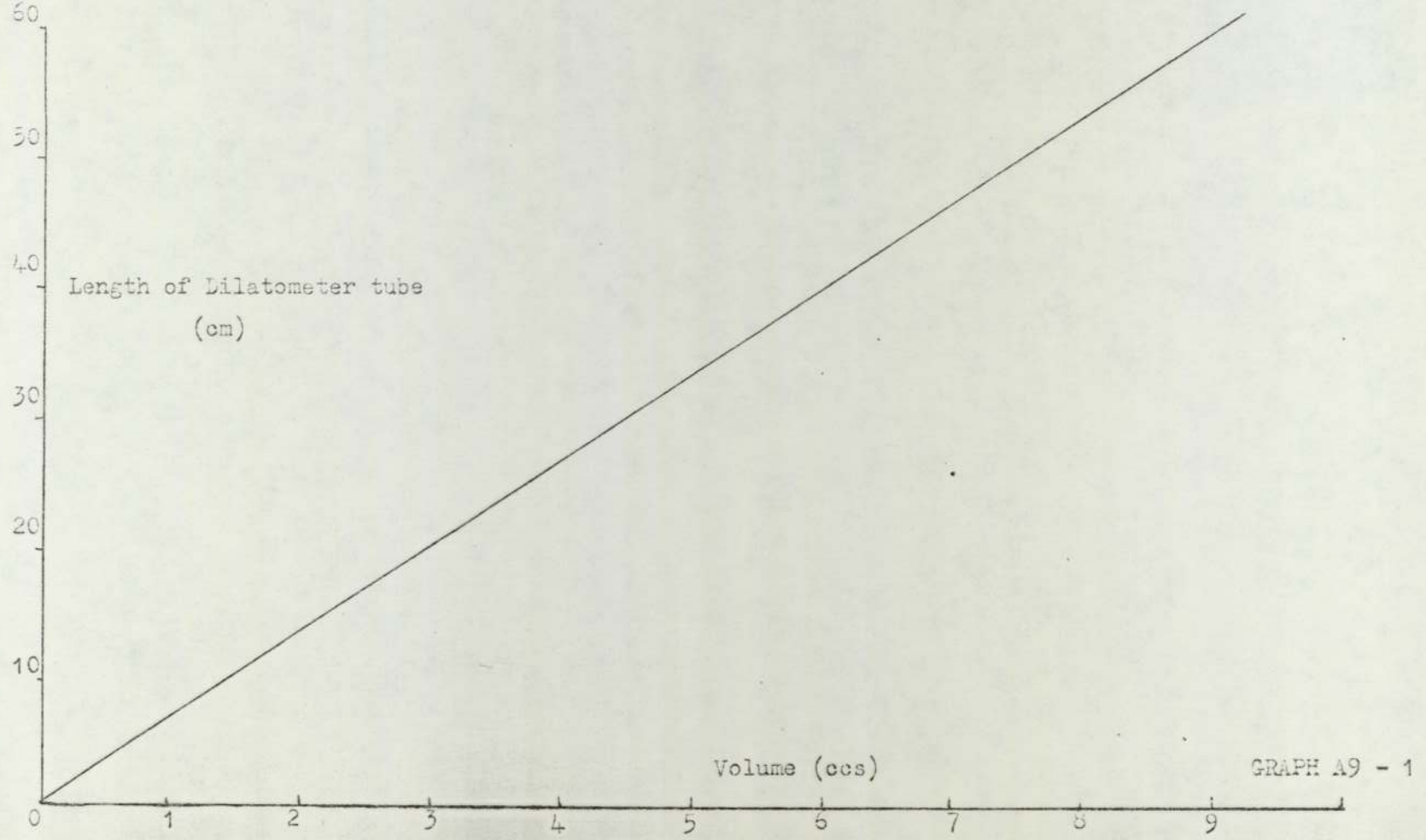

GRAPH A9 - 1

where Rv = radius of freezing chamber

Rt = radius of dilatometer tube.

was compared with the visual measurement of the frozen layer using the travelling telescope.

TABLE A9-1 DENSITIES (Kg/m^3)

SOLUTION	Experimental Results		Literature Densities
	liquid (15 C to 20 C)	frozen (-10 C to 15 C)	Liquid (20 C)
Distilled Water.	997	906	997
5% NaCl	1037	977	1036
10% NaCl	1073	1037	1073
Grape-fruit Juice	1035	975	-

The continuous lines on graph A9-2 represent, for distilled water, theoretical relationships between thickness of ice and increase in length of fluid in the dilatometer tube for assumed ice densities of 900, 920, 940 and 960 Kg/m^3.

Graph A9-2 Comparison of height of distilled water in dilatometer tube with varying theoretical ice densities (kg/m^3) and experimental visual observations.

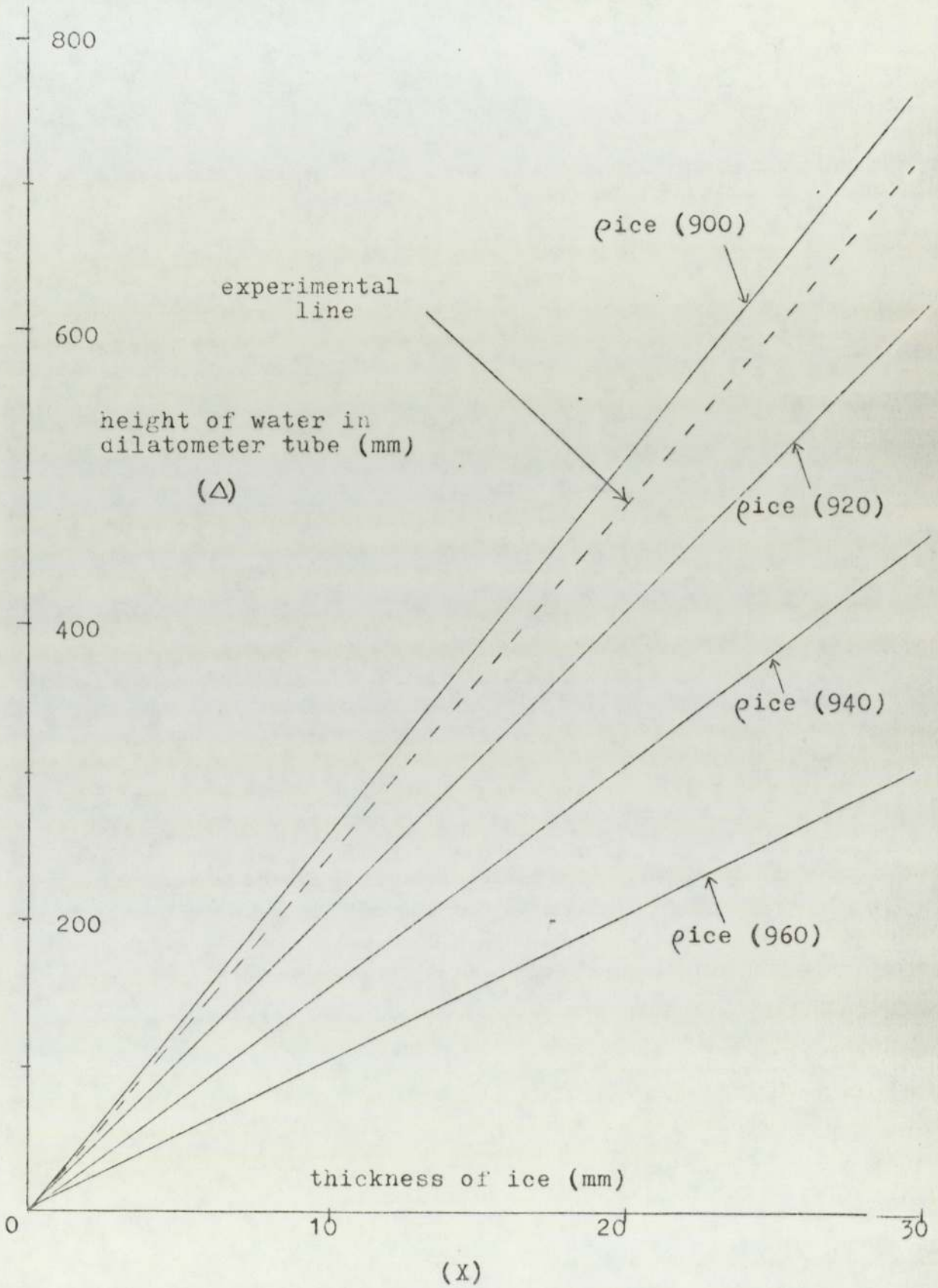

The dotted line on graph A9-2 represents the best fit straight line through the experimental points obtained from measuring ice thicknesses by the travelling telescope under experimental conditions. The dotted experimental line lies between the theoretical densities of 900 and 920 Kg/m^3 and agrees closely with the independent ice density determination of 906 Kg/m^3 (see table A9-1). From the slope of the dotted line the 'dilatometer scale factor', $\triangle /X$, was calculated. The dilatometer scale factor related the increase in liquid tube height to frozen layer thickness. The frozen thickness was equal to the change in height of the liquid in the dilatometer tube divided by the dilatometer scale factor. Similar calibrations were carried out for all the liquids frozen and the dilatometer scale factors are given in table A9-2.

To determine whether the dilatometer scale factors changed according to the density change ($\rho 2-\rho 1$) the experimental dilatometer scale factors were compared with the theoretical scale factors calculated by the following procedure :

In the freezing vessel :

Mass of ice in thickness $X = X \pi R v^2 \rho_1$ (A9-2)

Mass of ice in thickness X $= X \pi Rv^2 \rho_1$ (A9-2)

Mass of liquid in thickness X $= X \pi Rv^2 \rho_2$ (A9-3)

Therefore mass displaced by change of phase $= X \pi Rv^2 (\rho_2 - \rho_1)$ (A9-4)

Volume of displaced mass $= X \pi Rv^2 \frac{(\rho_2 - \rho_1)}{\rho_2} = V = \pi \Delta Rt^2$ (A9-5)

(A9-5) can be rewritten as :

$$X = \frac{\Delta Rt^2}{Rv^2} \cdot \left(\frac{\rho_2}{\rho_2 - \rho_1} \right) \qquad \text{(A9-1)}$$

The displaced volume of liquid increased the liquid height in the dilatometer tube. The increase in height in the dilatometer tube was obtained directly from graph A9-1 or by the expression : $\Delta = \frac{V}{\pi Rt^2}$ from (A9-5)

TABLE A9-2

SOLUTION	Experimental Dilatometer Scale Factor	$\frac{(\rho_2 - \rho_1)}{\rho_2}$	Theoretical Dilatometer Scale Factor
Water	23.6	.0913	23.3
5% NaCl	13.9	.0578	14.6
10% NaCl	8.0	.0335	8.5
Grapefruit Juice	13.7	.0580	13.2

Table A9-2 compares the theoretical and experimental dilatometer scale factors and shows close agreement between the results for all the liquids, therefore, the dilatometer scale factors can be said to have changed according to the density change ($\rho_2 - \rho_1$). The slight variation in the results (up to 6%) between the theoretical and experimental dilatometer scale factors was probably due to the experimental ice densities determined by the specific gravity bottle experiments, which were used in the theoretical dilatometer scale factor determination, being slightly different to the ice densities formed in the freezing vessel.

A9-2 OPERATION OF THE APPARATUS FOR ACCURATE MEASUREMENT OF THE ICE THICKNESS.

A9-2.1 Temperature control.

Maintaining the coolant at a constant temperature.

A controlled variable of the freezing experiments was the coolant temperature. This temperature was regulated by the three cooling units, the heater, contact thermometer and relay switch to an accuracy of $\pm$ 0.2 C.

Temperature recording and calibration of thermocouples.

The copper-constantin thermocouples used in all experiments were calibrated over the range of experimental temperatures to an accuracy of 0.05 C. The Honeywell temperature recorder, with a twelve point 72 second cycle, was used to record the thermocouple temperatures.

A9-2.2 Precautions to ensure good contact between heat transfer discs and freezing vessel.

To ensure reproducible results in the freezing experiments, and in the heat transfer coefficient measurements, it was essential to bring the heat transfer disc into consistently good thermal contact with the freezing vessel or aluminium test bar.

As mentioned (pp 40,41) the contact surfaces of the heat transfer discs and freezing chamber were machine smoothed to help achieve good contact. In all experiments a thin layer of oil was smeared over the disc and a rotating motion, turning the freezing vessel over the disc which was firmly held, produced a satisfactory contact.

A9-2.3 Experimental confirmation of uniform heat flow through the heat transfer discs.

Uniform heat flow through the heat transfer discs was essential for providing an even temperature driving force and hence conditions for even ice formation. (With the dilatometer method of measuring ice thickness error due to uneven ice formation would be undetected).

A second copper heat transfer disc with three axial thermocouple holes drilled into it was used to determine uniform heat flow through the disc. As can be seen from figure A9-1 the thermocouple holes reached different depths into the copper disc. By rotating the copper disc (by use of the four screws, figure A9-1) by 90degrees the thermocouples recorded their temperatures at different positions relative to the inlet and outlet pipes of the coolant. This process of rotation by 90 degrees was carried out three times. In all cases the same temperatures were recorded in the copper disc thus providing conditions for even ice formation.

Figure A9-1

Thermocouples in Copper Disc

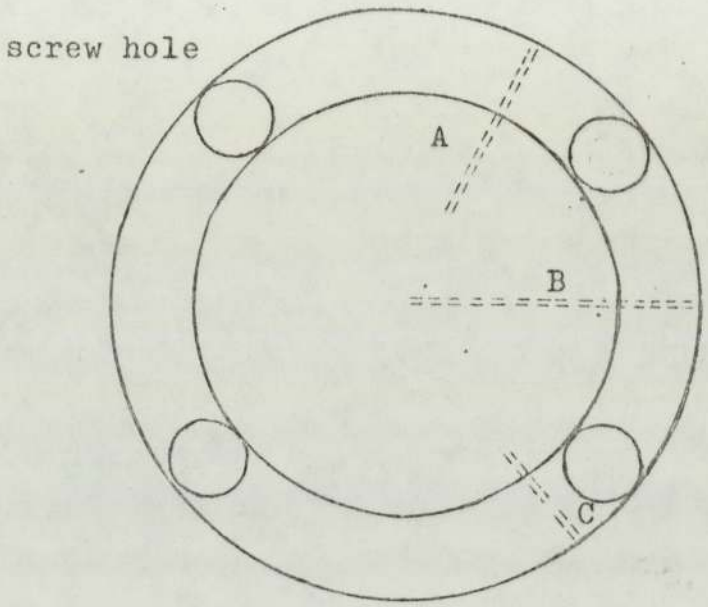

A = 25.4mm

B = 38.1mm

C = 12.7mm

APPENDIX 10.

APPENDIX 10-1.

DATA FOR PRODUCING EXPERIMENTAL AND VASIL'EV AND USPENSKII RESULTS INTO SIMPLE CORRELATION.

TABLE A10-1 FREEZING OF DISTILLED WATER.

Thickness of ice (mm)	Vasil'ev & Uspenskii.	FREEZING TIMES (S)	
		Experimental	(Experimental)$^{\frac{1}{2}}$
SET 1	H = 2000 W/m^{2}C	TI = 20 C	Tc = -15 C
2	88	150	12.2
6	405	480	21.9
10	961	1030	32.1
14	1751	1750	41.8
20	3299		
SET 2	H=2000 W/m^{2}C	TI = 20 C	Tc = -10 C
2	141	182	13.5
6	639	680	26.1
10	1507	1475	38.4
14	2719	2570	50.7
20	4949		
SET 3	H=2000 W/m^{2}C	TI = 3.5 C	Tc = -10 C
2	89	120	11.0
6	457	480	21.9
10	1088	1115	33.4
14	1980	2020	44.9
20	3787	3750	61.2
SET 4	H=2000 W/m^{2}C	TI = 25 C	Tc = -10 C
2	161	215	14.7
6	705	850	29.2
10	1655	1800	42.4
14	2967	3050	55.2
20	5293		

Thickness of ice (mm)	Vasil'ev & Uspenskii.	FREEZING TIMES (S)	
		Experimental	(Experimental)$^{\frac{1}{2}}$
SET 5	H=1700 W/m^{2}C	TI = 20 C	Tc =-15 C
2	164	180	13.4
5	537	525	22.9
8	1130	1100	33.2
12	2252	2150	46.4
16	3672	3525	59.4
SET 6	H=1700 W/m^{2}C	TI = 18 C	Tc =-10 C
2	144	170	13.0
6	643	660	25.7
10	1498	1480	38.5
14	2685	2640	51.4
18	4118	4080	63.9
SET 7	H= 900 W/m^{2}C	TI = 20 C	Tc = -15 C
2	138	245	15.7
6	538	730	27.0
10	1174	1500	38.7
14	2041	2425	49.2
20	3683	4150	64.4
SET 8	H= 900 W/m^{2}C	TI = 20 C	Tc = -10 C
2	234	375	19.4
6	851	1180	34.4
10	1843	2250	47.4
14	3163	3500	59.2
SET 9	H =56.8 W/m^{2}C	TI = 19 C	Tc = -13 C
2	3066	4800	69.3
6	6269	6300	79.4
10	9133	8520	92.3
14	11878	12120	110.1
20	15322	14760	121.5

VASIL'EV AND USPENSKII COMPUTATIONS OF X(t) VS t FOR RANGE OF H, TI & Tc VALUES.

TABLE A10-2.

APPENDIX 10-2.

SET	H	TI	Tc	X = 5mm	10	15	20	25	30
A	900	20 Time by (7-4)	-15 (% diff)	416 565(36)	1174 1374(17)	2301 2538(10)	3766 4054(8)	5467 5325(8)	7278 8148(12)
B	1698	18 Time by (7-4)	-10 (% diff)	485 612(26)	1498 1669(11)	3057 3245(6)	5070 5341(5)	7350 7957(8)	9790 11090(13)
C	1698	23 Time by (7-4)	-10	536 642(20)	1647 1753(6)	3350 3408(2)	5500 5609(2)	7857 8357(6)	10326 11650(13)
D	900	5	-14	338 459(36)	975 1116(14)	1917 2060(7)	3160 3292(4)	4681 4811(3)	6440 6616(3)
E	900	24.7	-14	490	1373	2683	4358	6234	8182
F	900	11.2	-14	378	1081	2123	3496	5140	6374

VASIL'EV AND USPENSKII COMPUTATIONS OF X(t) VS t FOR RANGE OF H, TI & Tc VALUES.

TABLE A10-2 (Continued)

SET	H	TI	Tc	X = 5mm	10	15	20	25	30
G	900	15.0 Time by (7-4)	-14 (% diff)	408 572 (40)	1159 1390 (20)	2274 2567 (13)	3730 4101 (10)	5448 5993 (10)	7322 8242(13)
H	1658	15.4	-14	318 425 (33)	988 1157 (17)	2026 2245 (11)	3414 3701 (8)	5075 5511 (9)	6898 7682 (11)
I	2001.5	25	-10	531 611 (15)	1657 1711 (3)	3395 3367(-1)	5581 5577 (0)	7952 8341 (5)	10418 11661(12)
J	2001.5	20	-10	479	1508	3102	5154	7454	9895
K	2001.5	20 Time by (7-4)	-15 (% diff)	304 389 (28)	961 1091 (13)	1588 2147 (8)	3364 3556 (6)	4994 5318 (6)	6749 7434 (10)
L	2001.5	3.5	-10	340 412 (21)	1088 1155 (6)	2245 2272 (1)	3807 3763 (-1)	5744 5629 (-2)	8019 7870 (-2)

REFERENCES.

1. J.C. Muehlbauer, J.E. Sunderland. Heat conduction with freezing or melting. Applied Mechanics Review, 1965, 8 (No.12), 951-959.

2. S.G. Bankoff. Heat conduction or diffusion with a change of phase. Advances in Chem. Eng., 1964, 5, 75-143. Academic Press, New York.

3. E. Kinder, E. Lamb. The prediction of freezing times of foodstuffs. Meat Freezing - Why and How. Agricultural Research Council MRI Symposium No.3 April 1974. Meat Research Inst. - Langford. Section 17.1.

4. A.J. Ede. Temperature distribution during freezing and thawing. Proc. 1X Int. Congress Refrig., 1955, 2-029.

5. Malton. Observations of temperatures in commercial freezing and storage of meat and meat products. Ref. 3. section 35.1.

6. S.E. Charm, D.H. Brand, D.W. Baker. A simple method for estimating freezing and thawing times of cylinders and slabs. ASHRAE Journal 1972 (Nov.), 39-44.

7. R.L. Earle, W.B. Earle. Freezing rates in blocks of meat of simple shape. 3rd Int. Heat Transfer Conference, Illinois, 1966, 153-158.

8. A. Bakal K.I. Hayakawa. Heat transfer during freezing and thawing of foods. Advances in Food Research, 1973, 20, 218.

9. Riemann-Weber. Die Partiellen Differential gleichungen der Mathematischen Physki, 1912, 2, 121.

10. H.S. Carslaw, J.C. Jaeger. Conduction of heat in solids 2nd Ed., Oxford, Clarenden Press, 1959.

11. A.V. Luikov. Analytical heat diffusion theory. Academic Press, New York, 1968.

12. J. Stefan. Uber die theories der eisbildung, insobesondere uber die eisbilding in polarmaere. Annalen der Physik und Chemie, 1891, 42, 269.

13. R. Planck. Freezing time of ice-blocks. Zeit. ges Kalte-Ind, 1913, 20, 109.

14. T.R. Goodman. The heat-balance integral and its application to problems involving a change of phase. Trans. ASME 1958, 80, 335-342.

15. T.R. Goodman. Applications of integral methods to transient non-linear heat transfer. Advances in Heat Transfer, 1964, 1, 52-120, (New York Academic).

16. H. Schlicting. Boundary Layer Theory (Ch.12) Mc Graw-Hill, 1955.

17. T.R. Goodman, J.J. Shea. The melting of finite slabs. J. Applied Physics, 1960, 82, 16-24.

18. O.M. Griffin. On the melting of solids to non-Newtonian fluids. Chem. Eng. Science, 1970, 25, 109-117.

19. M. Altman. Some aspects of the melting solution for a semi-infinite slab. Chem. Eng. Progress Symposium Series, No. 32, 1961, 57, 16-23.

20. Chi Tien, Yin-Chao Yen. Approximate solution of a melting problem with natural convection. Chem. Eng. Progress Symposium Series No. 64, 1966, 62, 166-172.

21. W.J. Green. An expansion method for parabolic partial differential equations. J. Research of National Bureau of Standards, 1953, 51, 127.

22. G. Poots. On the applications of integral-methods to the solution of problems involving the solidification of liquids initially at fusion temperature. Int. J. Heat & Mass Transfer, 1962, 5, 525-531.

23. S.H. Cho., J.E. Sunderland. Heat conduction problem with melting or freezing. Trans. ASME, Series C, J. Heat Transfer 1969, 36, 421-426.

24. R.H. Tein, G.E. Geiger. The unidimensional solidification of a binary eutectic system with a time-dependent surface temperature. ASME Trans. Series C, J. Heat Transfer, 1968, 36, 27-31.

25. R.A. Seban, A.L. London. Rate of ice formation. Trans ASME 1943, 65, 771-778.

26. F. Kreith, F.E. Romie. A study of the thermal diffusion equation with boundary conditions corresponding to solidification or melting of materials initially at the fusion temperature. Proc. London Physical Soc. 1955, 68, 277-291.

27. D.L. Cochran. Solidification application and extension of theory. Technical Report 24, Navy Contract N6-orr-251, Stanford University, Standford, Calif. 1955.

28. S.R. Robertson. H. Schenck Jr. Correcting the London and Seban equation for the case of molten metal solidification. Trans. ASME, 1967, 89, 118-119.

29. H. Schenck. FORTRAN method in heat flow, Ch. 4. The Ronald Press, New York, 1963.

30. N.D. Cowell. The calculation of food freezing times. Proc. XII Int. Congress Refrig., Madrid, 1967.

31. S. Charm. J. Slavin. A method for calculating freezing time of rectangular packages of food. Annexe Bull., Int. Inst. Freezing, 1962, 1, 567-578.

32. T. Komori.E. Hirai. Solutions of heat conduction problem with change of phase - a slab. J. Chem. Eng. Japan 1972, 5, (3), 242-8.

33. R. Planck. Contribution to the calculation and evaluation of the freezing rate for food. Beihefte Zeit ges. Kalte-Ind., 1941, 3, No. 10, UDI-Verlag, Berlin.

34. D.G. Rutov. Calculation of the time of cooling of food products. Annexe Bull. Int. Inst. Refrig. 1958, 2, 415-421.

35. J. Nagaoka, S. Takagi, S. Hotani. Experiments on the freezing of fish in an air-blast freezer. Proc. 9th Int. Congress Refrig., 4, 105.

36. A.J. Ede. The calculation of the rate of freezing and thawing of foodstuffs. Modern Refrig., 1949, 52, 52-55.

37. V.A. Teider. Determination of the freezing time with different conditions of heat exchange at the body surface. Proc. in Refrig. and Sci. Tech. 1963, 2, 953.

38. R.B. Walker. Heat transfer in precooked frozen food. 1970, M. Phil Thesis, Leeds University.

39. A.K. Fleming. Immersion freezing of small meat products. Proc. 12th Int. Cong. Refrig. 1967, 2, 683 (Madrid).

40. R.A. Seban, A.L. London. Experimental confirmation of predicted water freezing rates. Trans. ASME 1945, 67, 39-44.

41. G. Liebmann. A new electrical analog method for the solution of transient heat conduction problem. Trans. ASME, 1956, 78, 655.

42. P.V. Danckwerts. Unsteady-state diffusion or heat conduction with moving boundary. Trans. Faraday Soc. 1950, 46, 701-712.

43. D. Rosenthal. The theory of moving sources of heat and its application to metal treatments. Trans. ASME 1946, p. 849.

44. S.D. Holdsworth. Mathematical procedures for calculating freezing times for foodstuffs and methods of determining temperature distributions in frozen products. Chem. Engineer, 1970, No.238, 127.

45. H.M.N. Lightfoot. The solidification of molten steel. Proc. London Math. Soc., 1229 Series 2, 97.

46. P.A. Longwell. A graphical method for solution of freezing problems. AICHE Journal, 1958, 4, 53-57.

47. H.G. Landau. Heat conduction in a melting solid. Quarterly of Applied Maths., 1950, 8, 81-94.

48. D. Langford. The freezing of spheres. Int. J. Heat and Mass Transfer, 1966, 9, 827-828.

49. F.P. Vasil'ev, A.B. Uspenskii. A finite difference method for the solution of a two phase Stefan problem with a Quasi-linear equation. Zh. Vych. Mat., 1963, 3, 874.

50. L.W. Ehrlich. A numerical method of solving a heat flow problem with moving boundary. J. Association for Computing Machinery, 1958, 5, 161-176.

51. J. Crank, P. Nicholson. A practical method for numerical evaluation of solutions of partial differential equations of the heat conduction type. Proc. Cambridge Philosophical Soc., 1947, 43, 50-67.

52. G.M. Dusinberre. Numerical methods for transient heat flow. Trans., ASME, 1945, 67, 703-772.

53. N.R. Eyres, D.R. Hartlee, J. Ingham, R. Jackson, R.J. Sargent, J.B. Wagstaff. The calculations of variable heat flow in solids. Philosophical Trans. Royal Soc. London, 1947, Series A, 240, 1-57.

54. P.H. Price, M.R. Slack. Stability and accuracy o numerical solutions of the heat flow equation. Brit. J. Applied Physics, 1952, 3, 379-384.

55. W.D. Murray, F. Landis. Numerical and Machine Solutions of transient heat-conducting problems involving melting or freezing. Part 1 - Method of analysis and sample solutions. Trans. ASME, Series C, J. Heat Transfer 1959, 81, 95-105.

56. D.G. Rutov. Calculation of the duration of refrigeration for food products. Dokl. at SSSR nauchn. konf. komissii 3, 4 and 5 Mezhdunar in-ta kholoda, Komissiya, 1958,4, 89-98.

57. M. Lotkin. The numerical integration of heat conduction equations. J. Mathematical Physics, 1958, 37, 178-187.

58. M. Lotkin. The calculation of heat flow in melting solids. Quarterly of Applied Mathematics, 1960, 18, 79-85.

59. J. Douglas, T.M. Gallie. On the numerical integration of a parabolic differential equation subject to a moving boundary condition. Duke Mathematical Journal, 1955, 22, 557-571.

60. C.A. Forster. Finite difference approach to some heat conduction problems involving change of state. Luton, England, English Electric Company, 1954.

61. L.R. Ingersoll, O.S. Zobell, A.C. Ingersoll. Heat conduction with engineering and geological applications. Mc. Graw-Hill, New York, 1948.

62. K.T. Yang. Transient conduction in a semi-infinite solid with variable thermal conductivity. J. Applied Mech., 1958, 25, 146.

63. L.C. Tao. Generalised numerical solutions of freezing a saturated liquid in cylinders and spheres. A.I. Ch.E. J. 1967, 13, 165.

64. S.J. Citron. Heat conduction in a melting slab. J. Aerospace Sciences, 1960, 27, 219.

65. F.C. Lockwood. Simple numerical procedure for the digital computer solution of non linear transient heat conduction with changes of phase. J. Mech. Eng. Sc., 1966, 8, 259-263.

66. R.H. Tein, V. Koump. Effect of density change on the solidification of alloys. ASME Trans Series C, J. Heat Transfer, 1970, 92, 11-16.

67. C.M. Adams. Thermal consideration in freezing. Liquid Metals and Solidification, Am. Soc. for Metal, 1958 p.187.

68. K.L. Clark. Methods employed to obtain rates of solidification. Trans. Am. Foundryman's Soc. 1945, 53, 88.

69. J.H. Weiner. Transient heat conduction in multiple media. Brit. J. Applied Physics, 1955, 6, 361.

70. J.P. Terwilliger, S.F. Dizio. Salt Rejection Phenomena in the freezing of saline solutions. Chem. Eng. Sci. 1970, 25, 1331-49.

71. B.W. Grange, R. Viskanta, W.H. Stevenson. Diffusion of heat and solute during freezing of salt solutions. Int. J. Heat and Mass Transfer 1975, 19, (No.4) 373-383.

72. T. Hayakawa, M. Matsouka. Effect of heat transfer on crystal growth for inorganic salt-water systems. Heat Transfer-Japan Res., 1972, 2, 104-115.

73. T. Hayakawa, M. Matsouka. Studies of unidirectional crystal growth as the basis of normal freezing. J. Chem. Eng. Japan 1974, 7, 180-186.

74. J.W. Mullin. Crystallisation. CRC Press, Cleveland 1972.

75. A. Kramer, K. Wani. The effect of freezing rate on temperature of freezing and solids movement of foods. Proc. 12th. Int. Congress Refrig. 2, Madrid.

76. R. Heiss. The course of temperature in meat cubes during freezing and thawing. Bull. Int. Inst. Refrig. Annex. 1958-2, p.429.

77. G.J. Keller, J.H. Ballard. Predicting temperature changes in frozen liquids. Ind. Eng. Chem., 1956, 48, (2), 188.

78. S. Lin. The optimal freezing time for the formation of ice intakes. Kaltetechnik, 1965, 17, (No.12), 378-381.

79. T.C. Patton. Graphical methods for temperature distribution with unsteady heat flow. Ind. Eng. Chem. 1944, 36, 990.

80. H. Pfriem. Graphical technique for solving temperature distribution in freezing. ZVDI, 1942, 86, 703-709.

81. J.A. Bailey, A. Dula. Acoustic technique for use in some solidification rate studies. The Review of Scientific Instruments 1967, Vol. 38, No. 4.

82. C. Elbaum, B. Chambers. Can. J. Phys. 1955, 33, 196.

83. R.W. Ruddle. Solidification of castings. Inst. Metals, 1957, London.

84. L.J. Thomas, J.W. Westwater. Chem. Eng. Prog. Symp. Ser. 59, 1963, No. 41.

85. M.C. Jones. Unpublished research project.

86. S.D. Holdsworth. Current aspects of preservation by freezing. 1968, 43, 38-42.

87. J.G. Brennan, J.R. Butters, N.D. Cowell, A.E.V. Lilly. Food engineering operations. Elsevier, 1969.

88. A.J. Ward. Final year food science - lecture course Leeds University 1971/2. Leeds 2.

89. C. Emerson, D.E. Brady, L.N. Tucker. The effect of certain packaging and storage treatments on the acceptability of frozen beef. Missouri State Agr. Ext. Sta., Tech. Bull, 470, 1951.

90. F. Kreith. Principles of Heat Transfer. 2nd Ed., International Textbook Company. 1965.

91. W.H. Mc Adams. Heat Transmission. 3rd. Ed., Mc Graw-Hill, New York, 1954.

92. O. Fennema, W.D. Powrie. Low Temperature food preservation. Advances in Food Research, 1964, 13, 238-289.

93. D.K. Tressler, W.B. Van Arsdel, M.J. Copley. The Freezing Preservation of Foods, Vol. 1, Vol 11, Vol 111, Vol 1V. A.V.I. 1968.

94. W.B. Van Arsdel, M.J. Copley, R.L. Olson. Quality and Stability of Frozen Foods. Wiley International 1969.

95. J.L. Rogers, R. Binstead. Quick-Frozen Foods. Food Trade Press, 1972.

96. J. Hawthorn, E.J. Rolfe. Low temperature biology of Foodstuffs. Pergamon Press, 1968.

97. G. Glew. Cook/Freeze catering. Aber, 1973.

98. R.L. Earle. Unit operations in food processing. Pergamon, 1966.

99. S. Charm. The Fundamentals of Food Engineering. Elsevier (1971).

100. J.H. Stocking, C.J. King. Secondary nucleation of ice in sugar solutions and fruit juices. A.I. Ch. E. Journal, 1976, 22, (No. 1), 131-140.

101. J.G. Muller. Freeze concentration of food liquids, theory practice and economics. Food Technol., 1967, 21, (No. 1), 49-61.

102. P.M. Heertjes, Ir. Ong Tsing Gie. Crystallisation of water by unidirectional cooling. Brit. Chem. Eng., (June) 1960, 413-420.

103. P.M. Heetjes, J.A. de Leeuw den Bouter. Subcooling effects in a crystallisation system. Chem. Process Eng., (Dec.) 1965, 654-658.

104. Commercial grapefruit juice - Cyprus - Marks and Spencer.

105. J. Rutter, B. Chalmers. Can. J. Phys., 1953, 31, 15.

106. W. Morris, W.A. Tiller, J. Rutter, W.C. Winegard. Trans. Am. Soc. Met., 1955, 47, 463.

107. N.G. Johnson. Svenska hydrogr. biol. Kommm. Skr. 1943, 18, 1.

108. C.M. Adams, D.E. French, W.D. Kingery. In Ice and Snow, M.I.T. Press, Cambridge, Mass. 1963, p.277.

109. Ref. 70 p.1332.

110. Ref. 71 p.376.

111. J.L. Kuestr, J.H. Mize. Optimisation Techniques in Fortran. Mc Graw-Hill.

112. E.C. Bate-Smith. Progress in the chilling and Freezing of foods. J. Food Technol., 1967, 2, 191-206.

113. J.A. Nicholas, J.S. Perry. Basic behaviour of freezing and thawing of six foods. Agric. Eng. 1951, 32, (2), 102-105.

114. S. Vanichseni, D.P. Haughey, P.M. Nottingham. Water and air-thawing of frozen lamb shoulders. J. Food Technol, 1972, 7, 259-270.

115. J.D. Winter, A. Hustrulid, I. Noble, E. Sater-Ross. The effect of fluctuated storage temperatures on the quality of stored frozen foods. Food Technol. 1952, 6, 311-318.

116. W.A. Gortner. Effect of fluctuating storage temperatures on quality of frozen foods. Ind. Eng. Chem. 1948, 40, 1423.

117. J.G. Woodroof, E. Shelor. Effect of freezing storage on strawberries, blackberries, raspberries and peaches. Food Freezing, 1947, 2, 206.

118. S.R. Pottinger. Effect of fluctuating storage temperatures on quality of frozen fish fillets. Com. Fisheries, Rev., 1951, 13 (2), 19.

119. J. Clemmensen, P. Zeuthen. Physical factors influencing the quality of unwrapped pork sides during freezing 253.

120. R.J. Mc Colloch, R.G. Rice, M.B. Bandurskii, B. Gentili. The time temperature tolerance of frozen foods. Food Technol., 1957, 11, 444-449.

121. A. Hustrulid, J.D. Winter. The effect of fluctuating storage temperatures on frozen fruits and vegetables. Agr. Eng., 1943, 24, 416.

122. C.S. Pederson, H.G. Beattie. Concentration of fruit juices by freezing. New York State Agricultural Experimental Station, Bull. No. 727 Sept. 1947.

123. R.L. Earle, A.K. Fleming. Cooling and Freezing of lamb and mutton carcasses. Food Technol, 1967, 21 (1), 79-84.

124. C.D. Hodgman. Handbook of Chemistry and Physics. Chem. Rubber Publishing Co., Cleveland, Ohio.

125. J.H. Perry. Chemical Engineers Handbook. Mc Graw-Hill.

126. Ref. 3 section 13.1 M.J. Morley. Thermophysical properties of frozen meat.

127. S. Charm. A method for experimentally evaluating heat transfer coefficients in freezers and thermal conductivity of frozen foods. Food Technol., 1963, 17 (10), 93-96.

128. Ref. 92. p.240.

129. Ref. 92. p.242.

130. Ref. 92. p.280.

131. Ref. 92. p.283.

132. Holdsworth.S.D. Heat transfer in the freezing of fruit and vegetables. J. Chem. Eng. 1970, No. 238, 127-34.

133. C.P. Lents. Thermal conductivity of meats, fats, gelatin gels, and ice. Food Technol., 1961, 15, 243.

134. A.C. Jascon, R.A.K. Long. The specific heat and thermal conductivity of fish muscle. Proc. Intern. Congr. Refrig. 1, 2100, 1955.

135. F.G. Smith, A.J. Ede, R. Gane. The thermal conductivity of frozen foodstuffs. Modern Refrig. 1956, 55,254.